UNIVERSITY OF CALIFORNIA
RIVERSIDE

Next Generation Intelligent Driver-Vehicle-Infrastructure Cooperative System for Energy Efficient Driving in Connected Vehicle Environment

A Dissertation submitted in partial satisfaction
of the requirements for the degree of

Doctor of Philosophy

in

Electrical Engineering

by

Xuewei Qi

December 2016

Dissertation Committee:
Dr. Matthew J. Barth, Chairperson
Dr. Hamed Mohsenian-Rad
Dr. Guoyuan Wu

The Dissertation of Xuewei Qi is approved:

Committee Chairperson

University of California, Riverside

Acknowledgements

First of all, my gratitude would absolutely be first given to my parents. Without their support during the countless long days and nights in my pursuit of two master degrees and one doctoral degree, I could not have made any achievement thus far. Their continuous support and sacrifice are always my motivation and encourage me to be diligent during the years of my Ph.D. study.

Of course, this dissertation would not be possibly completed without the help from the following individuals who have worked with me at University of California, Riverside:

First and foremost, I would like to thank my major advisor, the head of the dissertation committee, Prof. Matthew J. Barth for his continuous mentoring, encouragement and inspirations over the years of doctoral study. Thank him for providing me sufficient funding for my research work including many conference travels over the years when I was participating with the research projects at CE-CERT. He is always willing to help me in successfully applying many different research fellowships and awards. He provided me many opportunities of training in participating the funding applications which is usually not available for a student. In addition, Prof. Barth has always been very generous with his time and wisdom for providing me advice on how to choose a right direction and how to dive deep in one specific area I was so fortunate to be always challenged by him to think about new methods to solve the problems within the realm Environmental ITS and expanding the concepts with various new applications. I believe what I have learned from him during the past years will be invaluable for my future academic career.

In addition, I would also give my gratitude to another dissertation committee member: Dr. Guoyuan Wu, who has been leading most of the research projects that I participated in at CE-CERT. His experience in the subject area has been incredibly helpful, and inspiring. I am so lucky to be able to work with him during my time at UCR and so grateful that he is always

ready to talk, discuss and provide very helpful advice for the problems that I encountered. His attitude towards life and scientific research always inspires me a lot. He is very generous in taking much time to help me revise and improve my draft manuscripts. The research method and academic attitude learned from him will be a beneficial experience in my life and also a good foundation for my future academic career.

I also would love to show my sincere thanks to Dr. Kanok Boriboonsomsin for his guidance and help provided to me during my doctoral study. Dr. Kanok Boriboonsomsin is always willing to help whenever I have a question. I was always able to learn from the conversation with him. In addition, I could not go without acknowledging all my lovely colleagues who have also contributed to this desertion by various forms, specifically want to mention Peng Hao, Jill Luo, Alex Vu, Chao Wang, and Fei Ye. They all made contributions to the research projects included in this dissertation, tremendously helpful and supportive. A great deals of credit is owed to their support.

Finally, the author would also like to acknowledge several agencies for partially funding the research projects on which this dissertation work is built: the U.S. Department of Transportation, The National Center for Sustainable Transportation (NCST), and the California Energy Commission (CEC).

ABSTRACT OF THE DISSERTATION

Next Generation Intelligent Driver-Vehicle-Infrastructure Cooperative System for Energy Efficient Driving in Connected Vehicle Environment

by

Xuewei Qi

Doctor of Philosophy, Graduate Program in Electrical Engineering
University of California, Riverside, December 2016
Dr. Matthew J. Barth, Chairperson

Transportation-related fossil fuel consumption and greenhouse gas emissions have received increasing public concern in recent years. To reduce energy consumption and mitigate the environmental impact of transportation activities, this dissertation research work aims at providing technical solutions by taking advantage of recent technology development in vehicle automation, vehicle connectivity and vehicle electrification.

More specifically, a driver-vehicle-infrastructure(DVI) cooperative framework for energy efficient driving of plug-in electric vehicles (PEVs) is proposed in this dissertation. Within this framework, this research improves energy efficiency of PEVs in the following ways: vehicle dynamics optimization and powertrain optimization, as well as co-optimization between them.

For vehicle dynamics optimization, a connected ecodriving system has been designed for PEVs to optimize their speed profiles when travelling through signalized intersections, by receiving real-time signal phase and timing information obtained through wireless communications. The calculated optimal speed trajectory (in terms of energy efficiency) is provided to the driver through an in-vehicle display in real-time. The performance of this connected ecodriving system is implemented and evaluated at different automation levels: human driving without considering the driver error, human driving considering the driver error, and partial automated (longitudinal) driving. Numerical analysis with real-world driving data shows that there is 12%,

14% and 21% potential energy savings that can be achieved by these proposed strategies respectively.

For powertrain operation optimization, an evolutionary algorithm based power-split control system for plug-in hybrid electric vehicle has been designed and evaluated with real-world traffic data. The designed model is used to optimally control the power-split between two different power sources (i.e., battery and gas tank) by considering various traffic conditions to achieve the minimum fuel consumption when satisfying total power-demand. In addition, a reinforcement-learning based autonomous learning strategy is also proposed for learning the optimal power-split decision based on historical driving data. Approximately 14% and 12% energy savings are identified by these two different powertrain operation strategies respectively.

For co-optimization of the vehicle dynamics and powertrain optimization, a bi-level optimization strategy has been designed and tested with real-world driving data to achieve augmented energy benefits from the compound effect of vehicle dynamics and powertrain operations optimization. An average of 29% improvement of fuel efficiency for the tested PHEV is identified by combining the vehicle dynamics and powertrain operation optimization.

The main contribution of this dissertation research is the design and validation of a DVI framework for PEV energy efficient driving. To the best of our knowledge, this is one of the first efforts to systematically investigate the potential energy benefits of both vehicle dynamics and powertrain operation optimization as well as its compound effect with real-world driving data for PEVs. The designed connected ecodriving system and power-split control model are quite promising in improving PEV energy efficiency.

Table of Contents

List of Tables

Table Page

List of Figures

Figure Page

1 Introduction

This chapter provides an overview of the proposed dissertation research work, in terms of the motivation, objectives, contributions and organization of this dissertation.

1.1 Motivation

1.1.1 Transportation related energy consumption and GHG emission

In recent years, a significant amount of transportation-related fossil fuel consumption and greenhouse gas emissions have created an increasing amount of public concern. Tailpipe emissions from vehicles are the single largest human-made source of carbon dioxide, nitrogen oxides, and methane in transportation related activities. Vehicles that are stationary, idling, and traveling in a stop-and-go pattern due to congestion in urban areas emit more pollutant emissions and greenhouse gases (GHGs) than those traveling in free-flow conditions. The resulted air quality degradation is very serious in some major cities of U.S. as well as other developing countries (e.g., China). For example, Los Angeles on the west coast of U.S. has a significant amount of transportation-based emissions, in part due to the large sea ports and freight movement (see Fig. 1-1a). Beijing, the capital of China, also suffers from severe air quality problems, in part due to its high population and very serious traffic congestion (see Fig. 1-2b).

a. Smoggy morning downtown Los Angeles (2010) b. Smoggy morning downtown Beijing (2015)

Figure 1-1 Air pollution in major citeis in U.S. and China

In addition to improving air quality, reducing transportation-related energy consumption and greenhouse gas (GHG) emissions has been a common goal of public agencies and research institutes for many years. In 2014, the total energy consumed by the transportation sector in the United States was as high as 23.70 Quadrillion BTU which is 28% share of the total energy [1] (see Fig. 1-2). The U.S. Environmental Protection Agency (EPA) reported that nearly 26% of GHG emissions resulted from fossil fuel combustion for transportation activities in 2014 [2] (see Fig. 1-3 and 1-4).

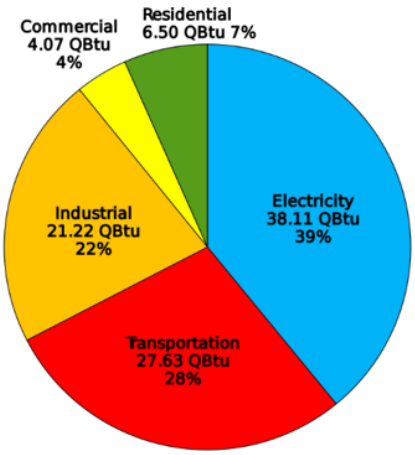

Figure 1-2 U.S. Energy Consumption by Economic Sector 2014
(source: http://www.eia.gov/forecasts/aeo/)

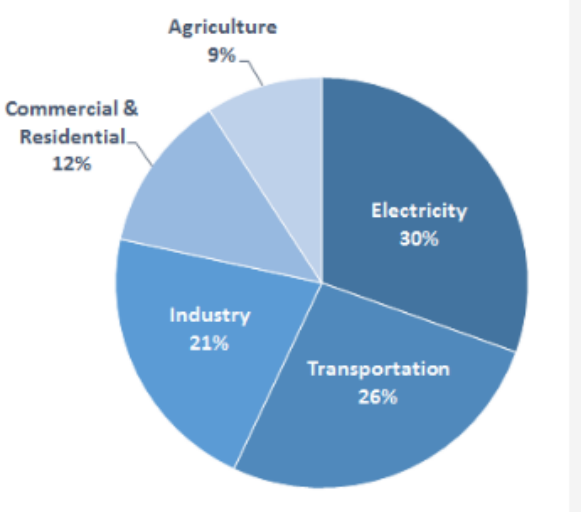

Figure 1-3,Total U.S. Greenhouse Gas Emissions by Economic Sectors in 2014
(Source: US EPA: www.epa.gov)

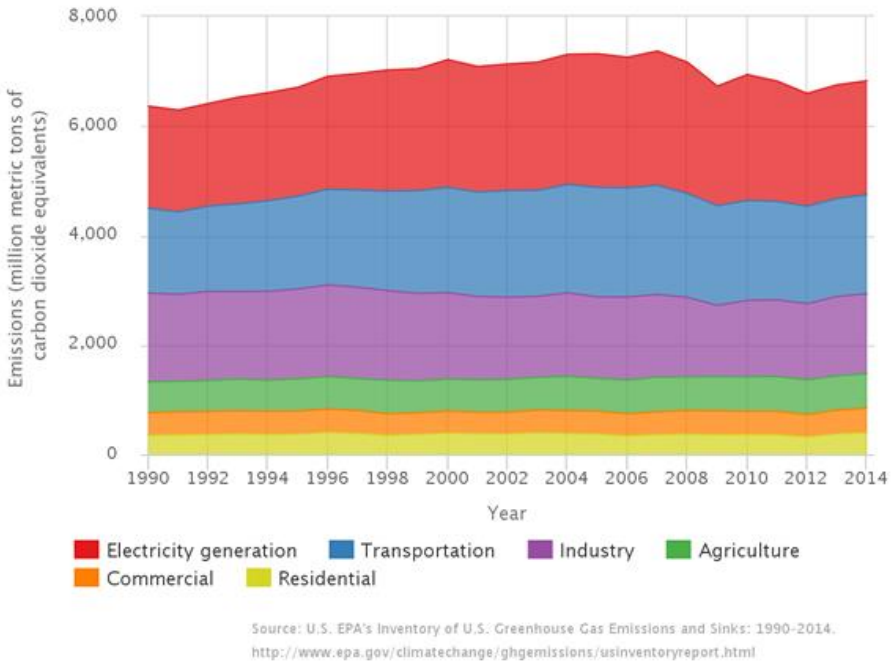

Figure 1-4,U.S. Greenhouse Gas Emissions by Economic Sector, 1990-2014
(Source: US EPA: www.epa.gov)

All together, the transportation-related impacts on air quality, climate change, and energy consumption have motivated researchers from different technical backgrounds to develop different ways to reduce vehicle emissions and energy consumption. In recent years, with the rapid development of vehicle related technologies, such as connected vehicle (CV) technology as well as automation technology, there is now a common vision for future vehicles that will be *automated, connected, electrified* and *shared*. As can be seen in Fig 1-5, for each of those features, multiple benefits can be identified (as listed in the figure) in terms of safety, mobility and environmental impact. However, reducing energy consumption and emissions are the only benefits can be achieved in all four of these features. This is explained in more detail below:

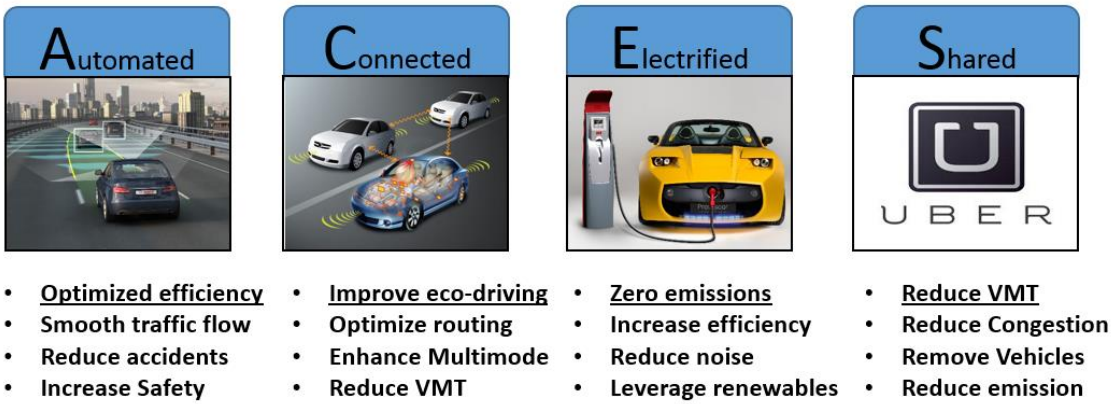

Figure 1-5 Key features of future vehicles.

1) *Automated*: Vehicle automation including automated vehicle dynamics control (i.e., adaptive cruise control (ACC)) and automated powertrain operations (i.e., power-split control for PHEVs), can be used to improve vehicle energy efficiency and reduce emissions. For example, eco-friendly adaptive cruise control (Eco-ACC) is designed to automatically control the vehicle speed profile when following a preceding vehicle smoothly to reduce unnecessary accelerations so that energy efficiency can be improved. In addition, designing future powertrain systems will also allow for higher energy efficiency, which is especially important for plug-in hybrid electric vehicles (PHEVs). In comparison to conventional hybrid electric vehicles (HEVs), the energy management system (EMS) for PHEVs are more complex due to their extended electric-only propulsion and battery chargeability via external electric power sources. The power-split ratio between these two different energy sources can be optimized according to different traffic conditions so that the fuel consumption can be minimized. Numerous efforts have been made in developing a variety of EMS for PHEVs [3, 4].

2) *Connected*: Connected vehicle (CV) technology has recently emerged with the development of wireless communications that has brought a new revolution for the modern

intelligent transportation system. In a CV environment, all the vehicles in the transportation network can be connected by wireless communications (vehicle-to-vehicle or V2V), as well as connectivity between the vehicle and road infrastructure (vehicle-to-infrastructure or V2I or I2V). These types of communications enables unlimited potential applications. For example, connected ecodriving technology is designed in a CV environment to encourage more energy efficient driving, such as reducing traffic congestion and unnecessary stop-and-go maneuvers at signalized intersections. It is reported that nearly 7 billion hours of delay and more than 3 billion gallons of fuel were wasted in 2015 due to traffic congestion in U.S. [5], a significant portion of which resulted from getting stuck at traffic signals. Therefore, a specific type of connected ecodriving technology called Eco-approach and departure (EAD) system [6] was developed to help vehicles travel through the signalized intersection smoothly and to avoid unnecessary idling and acceleration/deceleration with the knowledge of signal phase and timing (SPaT) information.

3) *Electrified*: In recent years, researchers have been trying to develop and use cleaner alternative energy sources for vehicles to replace fossil fuels, such as electricity from renewable resources (e.g., solar, wind) and hydrogen. With these alternative fuels, many new powertrain types can be developed, such as, plug-in electric vehicles (PEVs) and fuel cell vehicles. Transportation electrification is one of the more promising ways to reduce transportation related fossil fuel consumption and emissions; however, the massive adoption of PEVs is currently impeded by the limited charging infrastructure and the perceived limited driving range per charge (i.e., the so-called “range anxiety”) [7]. Groundbreaking advances have been witnessed in powertrain electrification in the past decade, such as the development of hybrid electric vehicles (HEVs) and battery electric vehicles (BEVs). HEVs are able to achieve higher fuel efficiency than internal combustion

engine (ICE)-powered vehicles by taking advantage of electric energy. BEVs eliminate the need for fossil fuels by using only electricity.

4) *Shared*: Shared Vehicle Systems have emerged in the last two decades provide a variety of shared mobility options. Shared vehicle systems have had this tremendous growth due to advances in electronic and wireless technologies that made sharing assets easier and more efficient. Automobile manufacturers, rental car companies, venture-backed startups and city-sponsored programs have sprung up with new mobility solutions ranging from large physical networks to mobile applications designed to alter routes, fill empty seats and combine fare media and real-time arrival and departure information. The main benefits of shared vehicle systems is to reduce vehicle miles travelled (VMT), thereby reducing vehicle energy consumption and tailpipe emissions.

In this dissertation, the main focus has been combining three of these four features: automation, connectivity, and electrification. Specifically, this dissertation focuses on a *connected* and *automated* ecodriving system is developed and evaluated for plug-in *electric* vehicles. The goal is to maximize the energy efficiency of PEVs by taking advantage of vehicle automaton and connectivity, as illustrated in Figure 1-6. Therefore, this dissertation research work only involves the first 3 features:

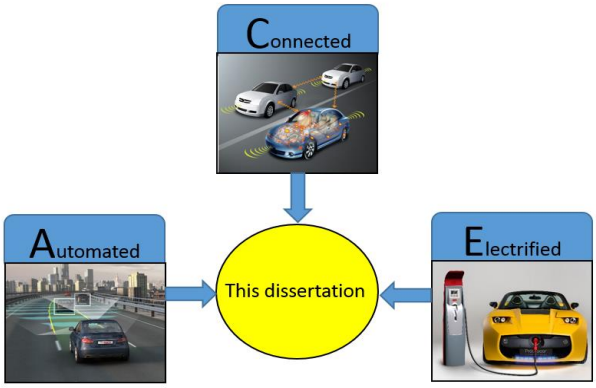

Figure 1-6 The three features involved in this dissertation research.

1.1.2 Increasing PEV Popularity and Penetration Rate

As previously described, the adoption of electric-drive vehicles has the potential to play a significant role in addressing both energy and environmental impacts brought by on by today's transportation systems. Using electricity as a transportation fuel has a number of benefits. Electricity has a strong potential for GHG reduction, as long as it is generated from renewable sources such as solar and wind. Electric vehicles themselves have zero direct emissions, although generating the electricity to power the vehicle often results in indirect emissions at the power plants. If electricity is generated from the current U.S. average generation mix, EVs can reduce GHG emissions by about 33%, compared to today's ICE powered vehicles [8]. If we assume 56% light-duty vehicle (LDV) penetration by 2050, this could provide a total reduction in transportation emissions of 26–30% [8].

The huge potential benefits of EVs have already attracted significant interest and investment in EV technology. Since late 2010, more than 20 automakers have introduced BEVs or PHEVs. Within the United States, the government has allocated considerable stimulus funding to promote the use of alternative fuels [9]. The American Recovery and Reinvestment Act (ARRA) of 2009 provided over $2 billion for electric vehicle and battery technologies, geared toward achieving a goal of one million electric vehicles on U.S. roads by 2018 [10]. Many states also have committed themselves to promoting EVs. For example, California has taken a number of legislative and regulatory steps to promote electric vehicle deployment and adoption, such as the Zero Emission Vehicle and Low Carbon Fuel Standard regulatory programs and rebates for purchasing electric vehicles [11]. With this momentum, it is not difficult to see that in the near future EVs may gain significant market penetration, particularly in densely populated urban areas with systemic air quality problems.

1.1.3 Increasing Vehicle Automation and Vehicle Connectivity

It is possible to improve efficiency of electric vehicles by introducing vehicle connectivity and automation. The majority of current EV research is focused on how to overcome technical barriers such as battery technology limitations [12] and charging infrastructure problems [13]. However, very little research has been focused on improving the efficiency of the EV driving through intelligent transportation and intelligent vehicle technologies.

In recently years, interest in vehicle automation is at an all-time high, with many recent real-world demonstrations from a variety of companies and research groups. The key fundamental building blocks for automating vehicles have been in development for many years, making vehicle automation a near-term reality. Also in recent years, there have been significant efforts to make vehicles more energy efficient and less polluting, through the development of advanced vehicle control system and powertrains operations. However, most of the relevant studies are focused on ICE vehicles recently. Only a few have realized that vehicle automation is highly amenable to electric-drive vehicles: greater synergies with automation are possible in terms of how automation can assist with providing electric energy to the vehicles [14]. Furthermore, the on-board energy management strategies of electric-drive vehicles (e.g., plug-in hybrid electric vehicles) can be specifically designed to take advantage of different automation regimes, including freeway driving, driving through automated arterial roadway infrastructure, and routing to known destinations [15]. It is envisioned that vehicle electrification and vehicle automation will go hand-in-hand in future developments.

In addition, connected vehicle technology enables the vehicle-to-vehicle and vehicle-to-infrastructure wireless communications, so that vehicle and infrastructure can be considered and modeled holistically in one system to achieve additional augmented efficiency improvement of EVs. Many recent research have proved that connected vehicle technologies are able to significantly improve the fuel efficiency of ICE vehicle by sharing the information

between vehicles and road infrastructure. It is also envisioned that vehicle connectivity will be capable of further improving EV efficiency through the combination of vehicle automation and connectivity, by considering and modeling the unique characteristics of EVs that different from ICE vehicles.

1.1.4 Co-optimizations of Vehicle Dynamics and Powertrain Operations

It is also important to note that the recently connected and automated vehicle applications are mostly focused on the vehicle dynamics optimization which aims at improving the vehicle efficiency by only controlling the vehicle as whole. However, for some PEVs, such as plug-in hybrid electric vehicles, it is also possible to improve the efficiency though the optimal powertrain operations. Therefore, it is quite promising to augment the efficiency improvement by developing an integrated vehicle/powertrain eco-operation system for plug-in hybrid electric vehicles through co-optimization of vehicle dynamic and powertrain (VD&PT) controls by taking advantage of vehicle connectivity and automation technologies as well as advanced machine learning techniques.

Inspired and motivated by the above mentioned problems and possible technical solutions, in this proposed dissertation research, a holistic driver-vehicle-infrastructure cooperative system is designed and tested for PEVs to improve vehicle energy efficiency and reduce GHG emission. The proposed system has the following characteristics:

a. *Integrated:* the designed system integrates and models all the major components in the transportation system that impact energy consumption, including the human driver, the vehicles, and the roadway infrastructure.

b. *Cooperative*: by taking advantage of connected vehicle technology, human driver, vehicles and road infrastructure are connected with each other and also cooperate with each other to maximize the energy efficiency.

c. *Optimal*: the control of vehicle dynamics and powertrain operation are optimized individually and also co-optimized together.

d. *Intelligent*: machine learning and deep learning techniques are used to learn the optimal control strategies from the historical driving behavior so that the designed system is able to adapt to continuously changing driving conditions.

1.2 Objectives

The goal of this dissertation study is to design, model, test, and evaluate a driver-vehicle-infrastructure cooperative system for energy efficient driving of PEVs, which integrates a human driver, the vehicle, its powertrain, and the road infrastructure, consisting of different functional components to achieve the maximum energy efficiency when driving in real-world traffic conditions. To achieve this goal, there are multiple sub-objectives that are defined according to different functional components; they also corresponding to different chapters in this dissertation.

1.2.1 Objective 1: Design of Overall System Framework

A system framework for connected ecodriving of PEVs that includes different function blocks has been designed. The proposed system framework defines the functional blocks (e.g., vehicle dynamics and powertrain operations optimization) and the relationships between different blocks as well as the information flow from and into each component. The designed system framework encompasses the human driver, vehicle, powertrain and road infrastructure to form a cooperative system that aims at improving PEV driving efficiency and reducing energy consumption.

1.2.2 Objective 2: Design of a Power-split Control System for PHEV

This subcomponent is designed to optimize the powertrain operations of a PHEV. More specifically, the designed model is able to optimally control the power-split between two different power sources: an electric motor and an ICE engine for a parallel hybrid electric powertrain. The designed model is able to take into consideration of various traffic conditions to achieve the minimum fuel consumption when satisfying total power-demand. In this model, we assume that the electricity (possibly from renewable sources such as wind and solar) is much cleaner and cheaper than fossil fuel and therefore the it only aims at reducing the fuel consumption for a PHEV.

1.2.3 Objective 3: Design of a Connected Ecodriving System for EVs

This component is designed to optimize the vehicle dynamics, more specifically, the velocity when PEV travelling through the signalized intersections, by being given the real-time signal phase and timing information through wireless communications. The calculated optimal speed is advised to the driver through an in-vehicle display in real-time. Two different versions of this driving assistance system have been designed, one that does not consider the driver error when following the advised speed, and the other one that does consider the driver error. The proposed system has been designed, prototyped and field-tested in real-world driving.

1.2.4 Objective 4: Design of an EV Energy Consumption Estimation Model

One of the core functional blocks for the ecorouting system that helps the driver choose the most energy efficient route to the destination, is the roadway link-level energy consumption estimation model. This subcomponent is designed to estimate the link-based energy

consumption for EVs by considering the unique characteristics of EV that are different ICE vehicles such as the regenerative braking power collection.

1.2.5 Objective 5: Design of a Co-optimization Framework

After the previous objectives 2 and 3 are achieved for powertrain optimization and vehicle dynamics optimization, a model for co-optimization of vehicle dynamics and powertrain operations has been designed and tested with real-world driving data. The augmented energy benefits from the compound effect of vehicle dynamics optimization and powertrain operations optimization has been analyzed numerically.

1.2.6 Objective 6: Design of an Autonomous Learning System

In objectives 2, 3 and 4, all the energy efficiency improvement for PEVs result from the fact the optimization utilizes predicted future driving conditions. In some situations, the predicted future driving conditions are not reliable or even not available. Hence, a machine learning based optimal power-split control system has been designed to learn the optimal control strategy autonomously with its own historical driving behavior record. The designed system does not rely on the expected driving conditions but only uses recorded historical driving behaviors.

1.3 Contributions of the Dissertation Research

This primary goal of this dissertation is to develop and evaluate an advanced connected ecodriving assistance system for PEVs that incorporates the human driver, vehicle, powertrain and road infrastructure in a holistic framework. During the 3 years and 3 months of the doctoral study and research period, the following procedures were carried out to achieve the goal of this dissertation research work.

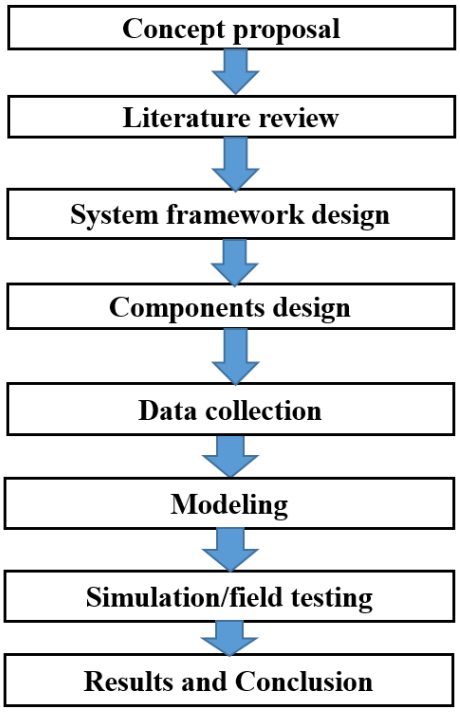

Figure 1-7 The flowchart of research steps

This dissertation research created several key contributions to the areas of intelligent transportation systems, connected and automated vehicle technologies, and advanced driving assistance systems in terms of methodology, performance evaluation and numerical analysis. These contributions correspond to the defined different objectives and are listed as follows:

- A novel driver-vehicle-infrastructure cooperative framework for PEV energy efficient driving considering PEV characteristics is proposed and implemented. Most of the existing technologies only focuses on vehicle and infrastructure side, no similar framework has been proposed for PEV energy efficient driving.
- Three different versions of evolutionary algorithms based real-time power-split control of PHEVs were designed and tested with real-world driving data. The designed systems have been proven to be able to achieve 14% of fuel savings comparing the baseline control strategies.

- A connected ecodriving assistance system for EVs is proposed and evaluated with real-world driving data at different automation levels (level 0 and level 1 or in-vehicle advising and automatic longitudinal control respectively). The energy benefits are analyzed comprehensively. A 12% and 22% of average energy savings are achieved by the level 0 and level 1 automation level in real-world driving.
- This connected ecodriving assistance system also considers the human driver error when displaying the driving advice. The performance is validated by comparing to the real-world advising driving without considering human error. An additional 6% energy savings has been achieved compared to the connected Ecodriving system without considering the driver error.
- A new mathematical formulation of the co-optimization of vehicle dynamics and powertrain operations has been defined. A bi-level optimization model was designed to obtain the near optima solution of the defined co-optimization problem. The proposed model has been tested on the real-world driving data with different technology combinations (i.e., different vehicle automaton and powertrain control strategies). A maximum of 29.38% average fuel efficiency improvement for the tested PHEV was identified with the combination of automatic longitudinal speed optimal control and online energy management system (i.e., online optimal power-split control). To the best of my knowledge, this is the first-of-its-kind model that aims at co-optimizing vehicle dynamics and powertrain operations together.
- A novel reinforcement learning based energy management system has been designed and tested with real-world driving data. The designed model is capable of learning the optimal control strategy from historical driving data, rather than relying on the predicted future driving conditions. About 12% of fuel savings is achieved after the model is well trained.

1.4 Organization of Dissertation

The organization of this dissertation is provide in the following figure:

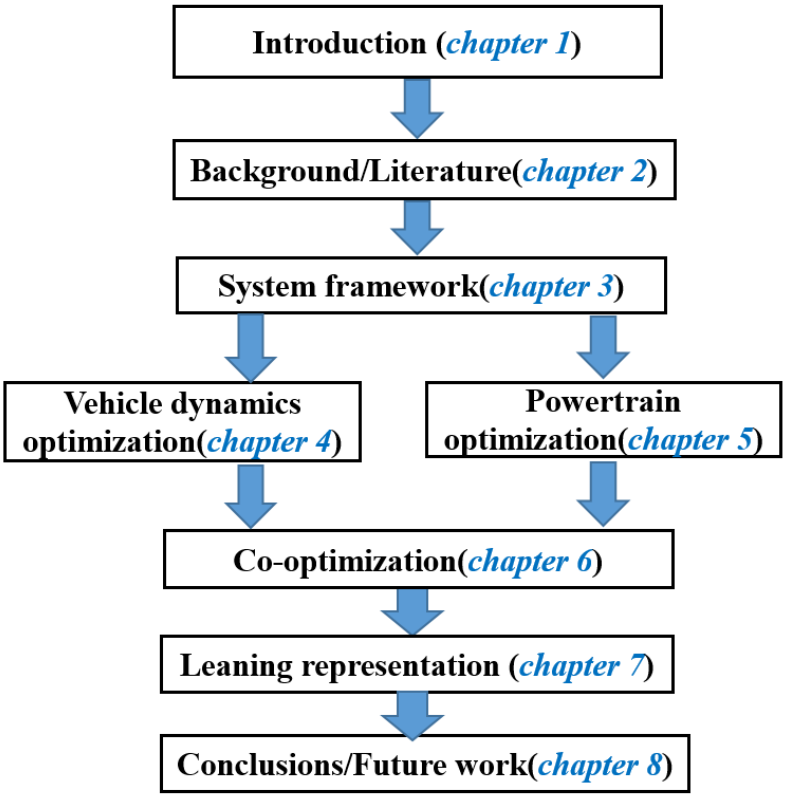

Figure 1-8 Organization of this dissertation

2 Background & Literature Review

This chapter includes all the relevant background knowledge and literature review. The major topics are environmental ITS, connected and automated vehicles (CAV) and connected ecodriving. The relation between these concepts are depicted in the following Fig.2-1.

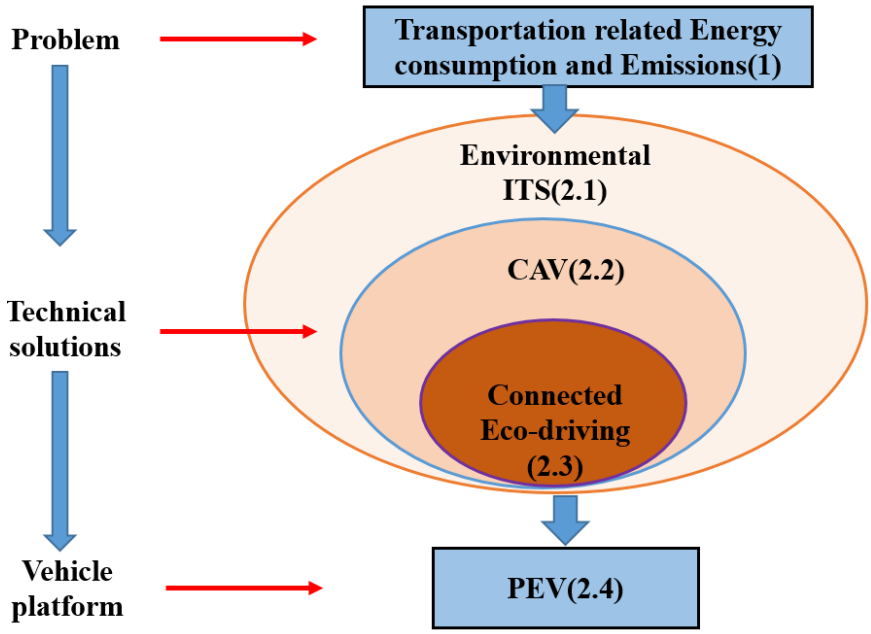

Figure 2-1 Areas of literature review

2.1 Environmental Intelligent Transportation Systems (Eco-ITS)

As reported in [65], Intelligent Transportation Systems (ITS) has been significantly improved in recent years, with the application of modern control, communications, and information technology to vehicles, roadway infrastructure, and traffic information systems. In the past, the primary objectives of ITS have been focused primarily on improving safety and increasing mobility. However, recently, ITS technology is now a popular way to reduce transportation-related environmental impacts, which includes pollutant emissions that lead to poor air quality, as well as energy consumption and greenhouse gas (GHG) emissions.

As described in the U.S. National Intelligent Transportation System Architecture [17]. In general, ITS can be categorized into three major target areas: V*ehicle Systems, Traffic Management Systems, and Travel Information Systems*. We briefly introduce these general areas below, describing how they potentially can reduce GHG emissions:

2.1.1 Vehicle Onboard Systems

The onboard vehicle system is now using modern control systems, faster on-board processors, and wireless communications to provide features that greatly improve their performance and safety. Examples of emerging vehicle systems include: ***Longitudinal Collision Avoidance Systems***, which are designed to monitor headways between vehicles, and by providing feedback to the vehicle's braking system, collisions can be reduced. ***Lateral Collision Avoidance Systems*** are being designed to avoid collisions that occur during lane changes, merges, or any kind of turning movement. Computer vision technology and other sensors coupled with wireless communications are being deployed to provide lane departure warnings and to warn drivers of pending lateral collisions. The majority of these ITS-related vehicle systems are primarily focused on safety, resulting in a reduction of the number of accidents that occur on our roadways. But actually this should result in a significant GHG emissions benefit due to the fact that the reduction of uncessary stop-and-go behavior can significantly reduce vehicle energy consumption [18].

2.1.2 Traffic Management Systems

In the past several decades, the total amount of driving (as measured in vehicle-kilometers-traveled or VKT) has grown significantly, contributing to severe roadway congestion in many urban areas. Building additional infrastructure to handle the increase in travel demand is not always possible. However, there are a number of ITS-based Traffic Management System solutions that can help mitigate congestion, two examples are: ***Traffic Monitoring Systems*** are improving with better sensor technology, more reliable communication channels, and more

advanced information processing capability. it is designed to transportation managers with real-time traffic information that can be used for better traffic system management and for individual drivers choosing alternative routes, resulting in a reduction of congestion. ***Integrated Corridor Management*** techniques are designed to keep traffic flowing as smoothly as possible through the corridor, greatly reducing the amount of idling by applying cooperatively to both freeway networks (e.g., innovative ramp metering) and to signalized arterial networks (e.g., advanced signal timing algorithms). The general goal of traffic management is to take full advantage of capacities of existing roadway infrastructure, thus keeping traffic flowing smoothly which will have a large impact in reducing energy consumption and GHG emissions.

2.1.3 Travel Information Systems

To make things more convenient to drivers, a wide variety of information systems for travelers have recently evolved. Examples of this technology include: ***Route Guidance Systems*** is designed to use geographic and real-time traffic information and can select optimal routes in a roadway network from specific origins to specific destinations. These systems attempt to minimize some criteria, such as travel time, travel distance, or even GHG emissions. ***Geo-Location Systems*** are typically coupled with route guidance systems to allow users to find specific locations, cutting down on excessive driving (e.g., searching for a gasoline filling station, open parking space, etc.). All of these different systems are also have a significant benefit in reducing GHG emissions.

All of these ITS areas have the potential for indirectly reducing GHG emissions through improvements in safety, mobility, and driver convenience. In addition, a number of ITS research programs have emerged that have been specifically designed to minimize transportation GHG emissions. The remainder of this chapter describes several of these recent ITS programs that are targeting the energy and environmental impacts of transportation.

2.1.4 Recent Major Environmental ITS Research Programs World-wide

In the last decade, the U.S. Department of Transportation (USDOT) has initiated a variety of environmentally-focused ITS research programs. Many of these are part of the Federal Highway Administration Exploratory Advanced Research program [19]. As an example in the ITS vehicle systems area, researchers at the University of California (UC) Berkeley have investigated both ACC and CACC and their impacts on mobility and the environment [20]. Furthermore, as an example in the area of traffic management systems, there is an on-going EAR project on Advanced Traffic Signal Control Algorithms, where several algorithms have been developed specifically for reducing energy use and emissions [21].

In addition to the EAR program, the USDOT has a major University Transportation Centers program (UTC, see [22], where university faculty, staff and students across the U.S. work on a number of advanced transportation research projects. There are now a number of UTCs that have a focus on sustainability, and several of those are investigating the environmental impacts of ITS [23] and [24] . Some example projects from these centers include examining Ecodriving techniques and freight signal priority for heavy-duty vehicles [25], and how variable speed limits can be used to reduce transportation energy consumption and improve vehicle mobility [26].

As another major effort, the U.S. DOT has a long-term research program in connected vehicles. One of the foundational elements of the connected vehicle research effort in the environment area is the Applications for the Environment: Real-Time Information Synthesis (AERIS) program [27]. The overall AERIS program vision is to create “Cleaner Air through Smarter Transportation”. To meet the vision, the AERIS program studies how generation, capture and

analysis of vehicle-to-vehicle (V2V), vehicle-to-infrastructure (V2I) and infrastructure-to-vehicle (I2V) data, along with implementing important environmental applications, will reduce the environmental impacts of surface transportation system users and operators. Making up the key elements of the AERIS program are operational concepts and applications that have the potential to significantly reduce environmental impacts of surface transportation systems.

Besides, there were several initial exploratory research projects carried out by a variety of researchers in the U.S. These projects investigated a number of new concepts across the different areas of ITS, which is listed in table 2-1:

Table 2-1 Environmental ITS projects in US

Type	**Projects**	**Leading organization**	**reference**
Onboard System	Eco-Drive application	Virginia Tech	[28]
	Assessment, Fusion, and Modeling of Commercial Vehicle Engine Control	Calmar Telematics UC Riverside	[29]
Traffic Management System	Eco-Speed Control	Virginia Tech	[30]
	Eco-Friendly Intelligent Transportation Systems (ECO-ITS)	UC Riverside	[31]
Travel information system	Lowest Fuel Consumption Route Guidance	University at Buffalo	[32]
Eco-Traffic Signal Operations	Eco-Approach and Departure at Signalized Intersections	UC Riverside	[33]
	Eco-Traffic Signal Timing	UC Riverside	[34]
	Eco-Traffic Signal Priority	UC Riverside	[34]
Eco-speed control	eco-speed harmonization and	UC Riverside	[35]
	eco-cooperative adaptive cruise control	UC Riverside	[35]

There are also many projects that are carried out in the EU, these projects investigated a number of new concepts across the different areas of ITS, as listed in table 2-2:

Table 2-2 Environmental ITS projects in EU.

Projects	**Leading organization**	**reference**
iMobility Forum	WG4CEM	[36]
eCoMove	EU	[37]
ECOSTAND	joint EU - Japan - US task force	[38]
Compass4D	EU	[39]
COSMO	EU	[40]
ConCERTO	EU	[41]
CARBOTRAF	EU	[42]
AMITRAN	EU	[43]
EcoGem	EU	[44]

2.2 Connected & Automated Vehicles (CAV)

In recent years, various connected and automated vehicle concepts have been described very frequently in research papers, government reports and media coverages. Terminology such as connected vehicles, autonomous vehicles, automated vehicles, and connected and automated vehicles have been used in different context. It is important to provide the detailed definitions and explanations on the difference between these concepts. Therefore, this chapter attempts to provide the formal definitions and intentional meaning of each concept. This is helpful for the readers to better understand the methodologies proposed in the following sections.

2.2.1 Connected Vehicles

The concept of *connected vehicles*—previously known as IntelliDrive or Vehicle Infrastructure Integration—uses advanced wireless communications, global positioning systems (GPS), vehicle sensors, and smart infrastructure to allow vehicles and the infrastructure to communicate wirelessly. In a connected vehicle environment, a vehicle equipped with the

technology can share its location, speed, heading, and many other data in real time with nearby equipped vehicles and the surrounding infrastructure via wireless communications.

Connected vehicle is an emerging technology with the development of wireless communicate that brings a new revolution for the modern intelligent transportation system. With vehicle connectivity including vehicle-to-vehicle(V2V) communication as shown in Fig.2-2 and vehicle-to-infrastructure (V2I) communication as shown in Fig.2-3, unlimited potential applications are enabled to improve vehicle energy efficiency.

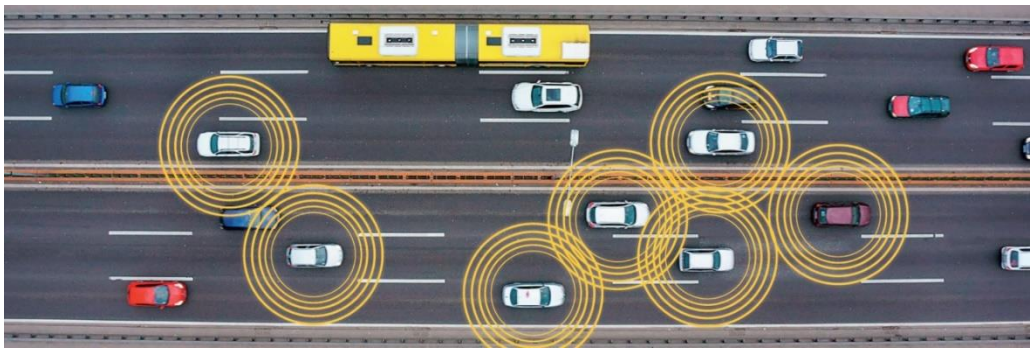

Figure 2-2 Connected vehicle technology (V2V)
(sourece: https://www.sogeti.com/explore/reports/cybersecurity-for-the-connected-vehicle/)

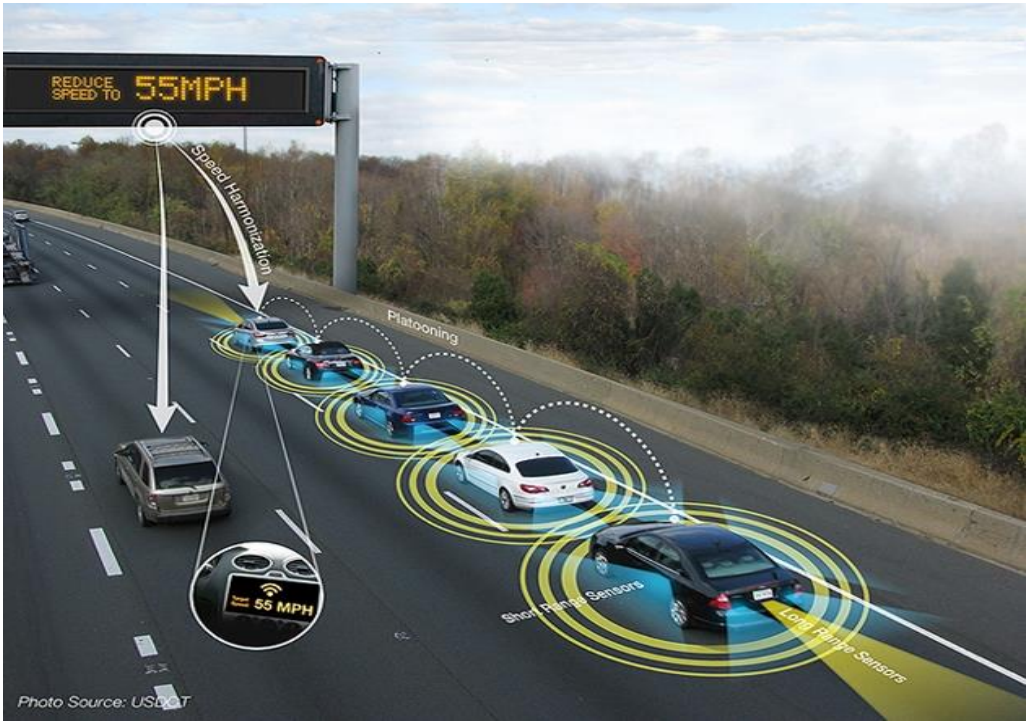

Figure 2-3 Connected vehicle technology(V2I/I2V)
(source: http://www.montana.edu/news/16120/msu-researchers-to-collaborate-on-automated-and-connected-vehicle-research-opportunities)

A good description of the classifications of connected vehicle applications can be found in the website of *Connected Vehicle Reference Implementation Architecture (CVRIA):* https://www.iteris.com/cvria/html/applications/applications.html)

2.2.2 Automated/Autonomous Vehicles

Autonomous Vehicle

An *autonomous car* (driverless car [45], self-driving car [46], robotic car [47]) is a vehicle that is capable of sensing its environment and navigating without human input [48].

Autonomous vehicles can detect their surroundings using a variety of techniques such as radar, lidar, GPS, odometry, and computer vision (see Fig.2-4). Advanced control systems interpret sensory information to identify appropriate navigation paths, as well as obstacles and

relevant signage[49,50] . Autonomous cars have control systems that are capable of analyzing sensory data to distinguish between different cars on the road, which is very useful in planning a path to the desired destination[51].

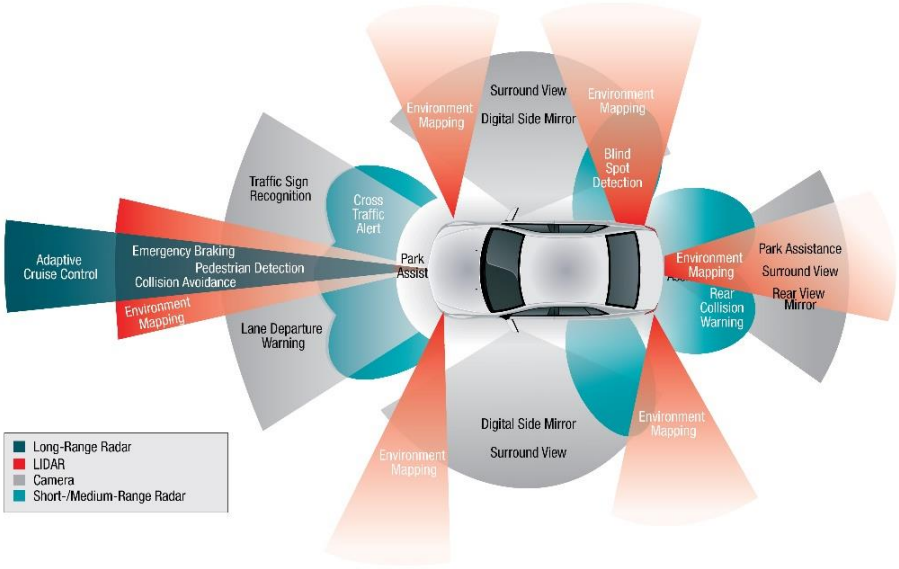

Figure 2-4 Functional blocks of autonomous vehicle(source: https://community.cadence.com/cadence_blogs_8/b/breakfast-bytes/archive/2015/11/12/automotive-ethernet).

Autonomous vs. Automated

Literally, *automated* means have the power of achieving automatic control and the *autonomous* means having the power for self-governance [52]. *Autonomous vehicle* is higher level of *automated* v*ehicle*, which relies more on artificial intelligent for perceptual and cognitive recognition of driving environment. In most of the medial coverage, Articles generally use the term "autonomous," instead of the term "automated". "autonomous" was chosen because it is the term that is currently in more widespread use (and thus is more familiar to the general public). From technology perspective, the term “Automated” connotes control or operation by a machine, while "autonomous" connotes acting alone or independently. Most of the vehicle concepts (that we are currently aware of) have a person in the driver’s seat, utilize

a communication connection to the Cloud or other vehicles, and do not independently select either destinations or routes for reaching them. Thus, the term "automated" might be more accurately describe these vehicle concepts[53].

Level of Vehicle Automation

A classification system for vehicle automaton levels was published in 2014 by Society of Automotive Engineers (SAE), an automotive standardization body.[54] This classification system is based on the amount of driver intervention and attentiveness required, rather than the vehicle capabilities, although these are very closely related. SAE automated vehicle classifications (see Table 2-3):

- Level 0: Automated system has no vehicle control, but may issue warnings.
- Level 1: Driver must be ready to take control at any time. Automated system may include features such as Adaptive Cruise Control (ACC), Parking Assistance with automated steering, and Lane Keeping Assistance (LKA) Type II in any combination.
- Level 2: The driver is obliged to detect objects and events and respond if the automated system fails to respond properly. The automated system executes accelerating, braking, and steering. The automated system can deactivate immediately upon takeover by the driver.
- Level 3: Within known, limited environments (such as freeways), the driver can safely turn their attention away from driving tasks.
- Level 4: The automated system can control the vehicle in all but a few environments such as severe weather. The driver must enable the automated system only when it is safe to do so. When enabled, driver attention is not required.
- Level 5: Other than setting the destination and starting the system, no human intervention is required. The automatic system can drive to any location where it is legal to drive.

Table 2-3 Vehicle automaton level by SAE[54]

SAE level	Name	Narrative Definition	Execution of Steering and Acceleration/ Deceleration	*Monitoring* of Driving Environment	Fallback Performance of *Dynamic Driving Task*	System Capability *(Driving Modes)*
***Human driver* monitors the driving environment**						
0	**No Automation**	the full-time performance by the *human driver* of all aspects of the *dynamic driving task*, even when enhanced by warning or intervention systems	Human driver	Human driver	Human driver	n/a
1	**Driver Assistance**	the *driving mode*-specific execution by a driver assistance system of either steering or acceleration/deceleration using information about the driving environment and with the expectation that the *human driver* perform all remaining aspects of the *dynamic driving task*	Human driver and system	Human driver	Human driver	Some driving modes
2	**Partial Automation**	the *driving mode*-specific execution by one or more driver assistance systems of both steering and acceleration/ deceleration using information about the driving environment and with the expectation that the *human driver* perform all remaining aspects of the *dynamic driving task*	**System**	Human driver	Human driver	Some driving modes
***Automated driving system* ("system") monitors the driving environment**						
3	**Conditional Automation**	the *driving mode*-specific performance by an *automated driving system* of all aspects of the dynamic driving task with the expectation that the *human driver* will respond appropriately to a *request to intervene*	System	**System**	Human driver	Some driving modes
4	**High Automation**	the *driving mode*-specific performance by an automated driving system of all aspects of the *dynamic driving task*, even if a *human driver* does not respond appropriately to a *request to intervene*	System	System	**System**	Some driving modes
5	**Full Automation**	the full-time performance by an *automated driving system* of all aspects of the *dynamic driving task* under all roadway and environmental conditions that can be managed by a *human driver*	System	System	System	**All driving modes**

2.2.3 Connected and Automated Vehicle Applications

As introduced in the previous section, autonomous vehicles are usually operating in isolation from other vehicles using onboard sensors (e.g., lidar and radar). The traffic operations with autonomous vehicles will not likely change much because mobility and environmental impacts will remain the same or could be even worse. For example, single vehicle based partial automaton such as the automated cruise control (ACC) has been shown to have negative traffic mobility impacts. However, when autonomous vehicle enabled with connectivity, connected and automated vehicles (CAVs) are built to leverages compound benefits from vehicle automaton and vehicle connectivity (see Fig.2-5). Traffic operations with CAVs will have an improved safety, mobility and environmental impacts.

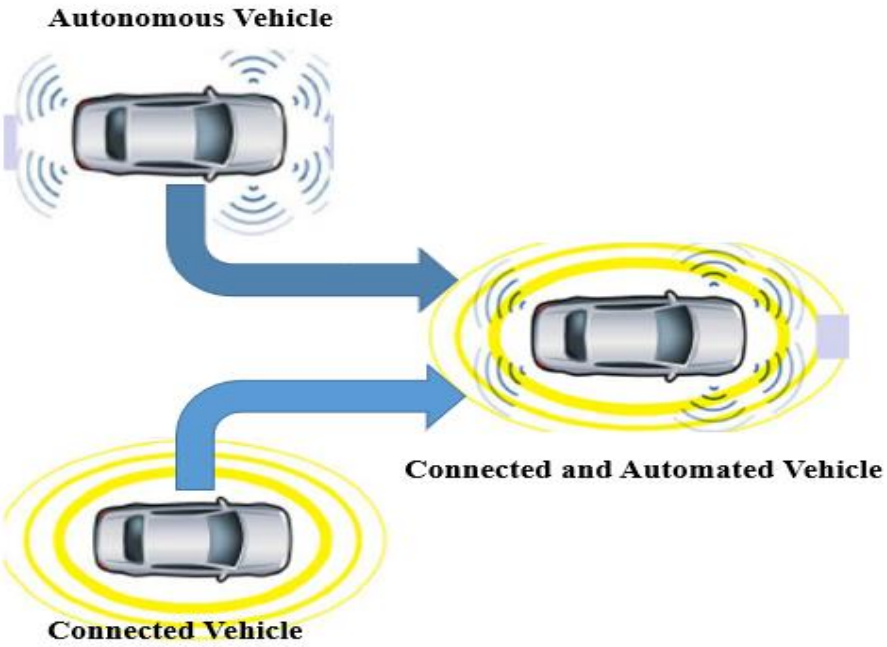

Figure 2-5 The relationship between autonomous vehicle, automated vehicle and connected& automated vehicles (source: http://slideplayer.com/slide/4589633/)

2.3 Connected Ecodriving Technology

Some CAV application are called connected Ecodriving applications, which provides customized real-time driving advice to drivers so that they can adjust their driving behavior to save fuel and reduce emissions. Ecodriving advice includes recommended driving speeds, optimal acceleration, and optimal deceleration profiles based on prevailing traffic conditions, interactions with nearby vehicles, and upcoming road grades. The application also provides feedback to drivers on their driving behavior to encourage drivers to drive in a more environmentally efficient manner. Finally, the application may include vehicle-assisted strategies where the vehicle automatically implements the Ecodriving strategy (e.g., changes gears, switches power sources, or reduces its speed in an eco-friendly manner).

2.4 Plug-in Electric Vehicle (PEV)

A plug-in electric vehicle (PEV) is any motor vehicle with rechargeable battery packs that can be charged from the electric grid, and the electricity stored on board drives or contributes to drive the wheels for propulsion[56-57]. Plug-in electric vehicles are also sometimes referred to as grid-enabled vehicles (GEV) and also as electrically chargeable vehicles.[58]

PEV is a subcategory of electric vehicles that includes battery electric vehicles (BEVs), plug-in hybrid vehicles, (PHEVs), and electric vehicle conversions of hybrid electric vehicles and conventional internal combustion engine vehicles[56-57]. Even though conventional hybrid electric vehicles (HEVs) have a battery that is continually recharged with power from the internal combustion engine and regenerative braking, they cannot be recharged from an off-vehicle electric energy source, and therefore, they do not belong to the category of plug-in electric vehicles.

2.4.1 Plugin Hybrid Electric Vehicle (PHEV)

PHEV is a hybrid vehicle which utilizes rechargeable batteries, or another energy storage device, that can be restored to full charge by connecting a plug to an external electric power source (usually a normal electric wall socket). A PHEV shares the characteristics of both a conventional hybrid electric vehicle, having an electric motor and an internal combustion engine (ICE).

PHEVs have great potential in reducing energy consumption and pollutant emissions, due to the use of electric batteries as another energy source. The cost for electricity to power plug-in hybrid EVs for all-electric operation has been estimated at less than one quarter of the cost of gasoline in California.[57] Compared to conventional vehicles, PHEVs reduce air pollution

locally and dependence on petroleum. PHEVs may reduce greenhouse gas emissions that contribute to global warming, compared with conventional vehicles.

2.4.2 Battery Electric Vehicle (BEV)

A battery electric vehicle (BEV), battery-only electric vehicle (BOEV) or all-electric vehicle is a type of electric vehicle (EV) that uses chemical energy stored in rechargeable battery packs. BEVs use electric motors and motor controllers instead of internal combustion engines (ICEs) for propulsion. They derive all power from battery packs and thus have no internal combustion engine, fuel cell, or fuel tank. BEVs include bicycles, scooters, skateboards, rail cars, watercraft, forklifts, buses, trucks and cars.

Gradually replacing conventional vehicles with electric vehicles (EVs) is a promising way to reduce fossil fuel consumption and pollutant emissions in transportation sector. There have been many efforts to improve the performance of EVs such as better component and battery sizing. However, the market share of EVs is still hindered by the limited all-electric range and charging facilities.

EV adoption has a great potential to play a significant role in addressing both energy and environmental crises brought by the current transportation system. For instance, electricity has a strong potential for GHG reduction. Electric vehicles themselves have zero emissions, although generating the electricity to power the vehicle is likely to create air pollution. If electricity is generated from the current U.S. average generation mix, EVs can reduce GHG emissions by about 33%, compared to today's ICE powered vehicles [8]. If we assume 56% light duty vehicle (LDV) penetration by 2050, this could provide a total reduction in transportation emissions of 26–30% [8].

The huge potential benefits of EVs have already attracted significant interest and investment in EV technology. Since late 2010, more than 20 automakers have introduced BEVs or PHEVs. Within the United States, the government has allocated considerable stimulus funding to promote the use of alternative fuels [9]. With this momentum, it is not difficult to see that in the near future EVs may gain significant market penetration, particularly in densely populated urban areas with systemic air quality problems. We will soon face one of the biggest challenges: How to improve efficiency for the whole EV transportation system? (Here the EV transportation system includes any EV related applications of technologies and policies to the planning, functional design, operation and management of facilities and infrastructure in order to provide for the safe, efficient, economical, and environmentally compatible movement of people and goods.)

3 Driver-vehicle-infrastructure Cooperative System Framework

In this chapter, a system level driver-vehicle-infrastructure cooperative framework is designed and described. This framework integrates three different parties that impact the energy consumption of PEVs: Human driver, vehicle and infrastructure. It is designed for PEV energy efficient driving and can be used to maximize the energy efficiency of PEVs. To implement this proposed framework, an integrated co-optimization system is also designed for the connected Ecodriving of PEVs.

3.1 Driver-vehicle-infrastructure cooperative system

In the connected vehicle environment, a vehicle equipped with wireless communication devices can share its location, speed, heading, and many other data in real-time with nearby equipped vehicles and the surrounding infrastructure via wireless communications. Therefore, in the designed cooperative system, the vehicle and infrastructure are tightly integrated by taking advantage of advanced wireless communications, high accuracy positioning, and onboard sensing technology. In addition, the impact of driving behavior is also integrated into the framework by modeling and estimating the driver error in the in-vehicle advising driving. Human driver is involved in this framework; hence it is designed for assisted driving rather than fully autonomous driving.

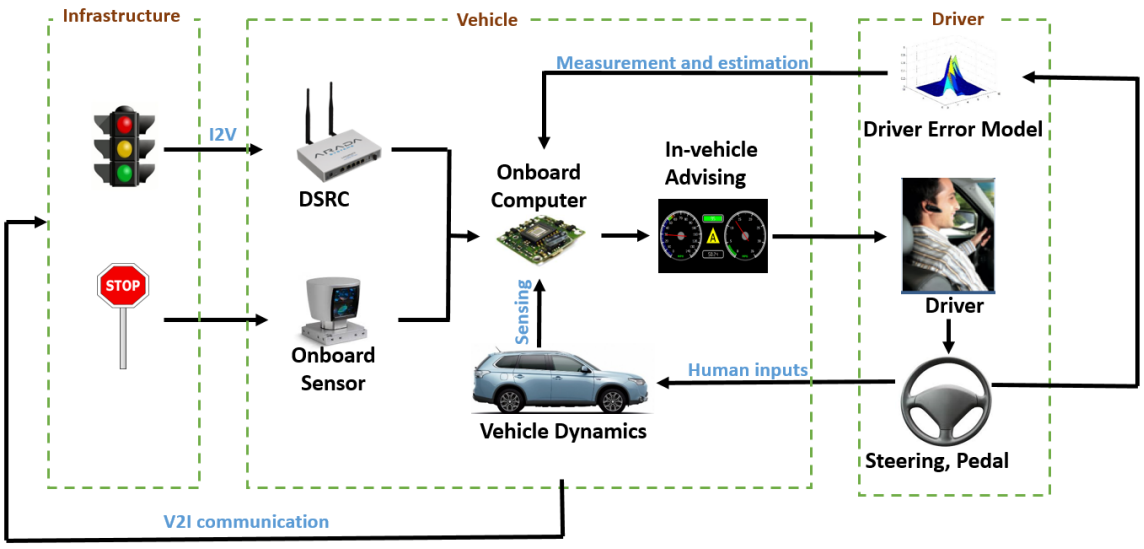

Figure 3-1 Driver-Vehicle-Infrastructure cooperative system

In the designed cooperative system, the interaction among the three objects or between every two objects (e.g., between infrastructure and vehicle) are all bidirectional (see Fig.3-1). For example, vehicles can adjust its speed according to the signal phase and timing. The traffic signal is also able to adjust its signal phase and timing according to the vehicle states at the intersection (e.g. traffic signal priority).

Based on this proposed cooperative system framework, this dissertation work aims at designing a driver-in-the-loop adaptive connected Ecodriving assistance system that considering the driver error for PEVs. As a baseline for comparison, an open-loop Ecodriving assistance system without considering driver error is also designed and discussed.

3.2 Integrated Co-optimization System for Connected Ecodriving

To achieve the maximum energy efficiency, besides the consideration of the interaction between driver, vehicle and infrastructure, this dissertation further proposes an integrated co-optimization system for connected Ecodriving of PEVs. It aims at optimize the PEV driving from three different levels: route level, vehicle dynamics level and powertrain level to reduce energy consumption. As shown in Fig.3-2, the system architecture consists of 3 different levels.

The information flow is in top-down direction but the design follows bottom-up direction. Within each of the dashed square box in the figure is a functional component that is responsible for the optimization of one specific type of task: vehicle routing, vehicle speed or powertrain operations. More details are provided as follows:

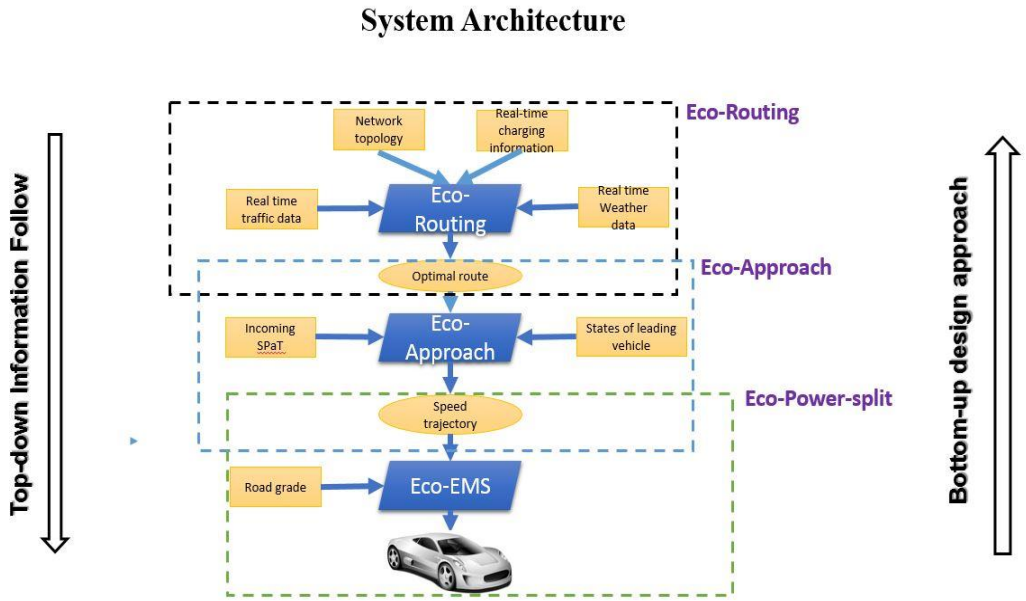

Figure 3-2 System architecture of integrated co-optimization for connected Ecodriving

3.2.1 Functional component 1: Eco-routing for PEVs

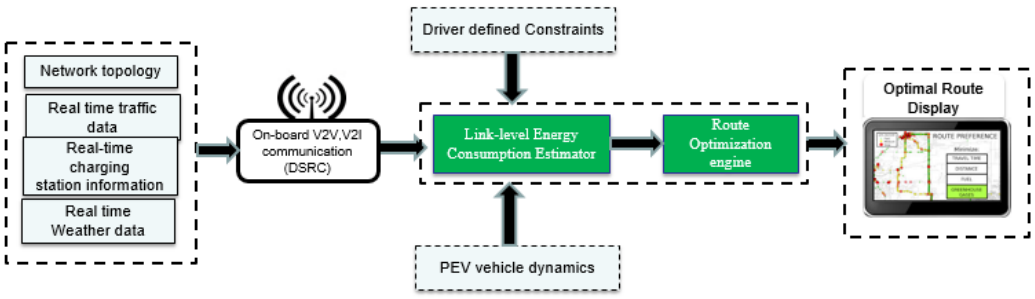

Figure 3-3 Eco-routing system for PEVs

This functional component aims at optimizing the route for PEVs that can minimize the energy consumption according to the different driving conditions. It is capable of choose the best route that consume the least energy for PEVs based on the real-time information such as the average

speed on each road link. This selected route is used as the input for the next functional components: connected Ecodriving. The prerequisite of an Eco-routing system is the accurate estimation of PEV energy consumptions based on the real-time traffic information. This functional block is shown in the Fig. 3-3 with a green box. Hence, in this dissertation study, a novel link-based energy consumption estimation model for EVs are designed and tested with real-world driving data.

3.2.2 Functional component 2: Connected Ecodriving for PEVs

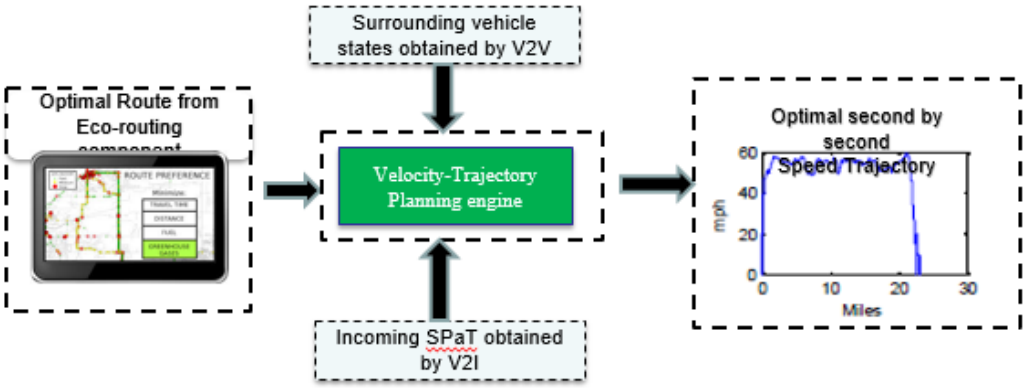

Figure 3-4 Connected Ecodriving for PEVs

The optimal route selected by the abovementioned Eco-routing component is input to this functional component: connected Ecodriving which aims at optimizing the vehicle speed profile when traveling through signalized intersections in urban driving. As shown in Fig.3-4, the core part of this component is the velocity trajectory planning algorithm (VTPA) which is designed to calculate the optimal speed (second-by-second) according to the signal phase and timing information that is obtained from single controller via vehicle-to-infrastructure wireless communication in connected vehicle environment. The details of VTPA will be given in the following sections. The calculated optimal speed trajectory is used as the input for the last functional component: powertrain optimal control.

3.2.3 Functional component 3: Powertrain optimal control

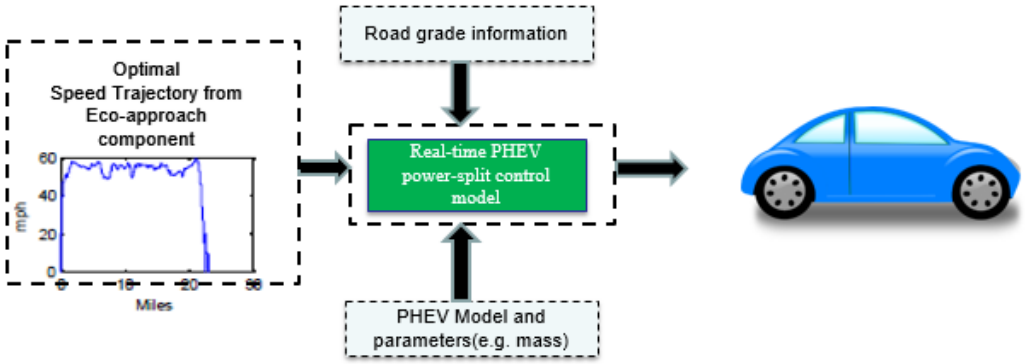

Figure 3-5 Powertrain optimal control

This functional component is designed to optimize the power-split control for parallel PHEVs. With the input optimal second by second speed profile, this model is capable of obtaining the best power-split ratio at each time step to achieve the minimal fuel consumption and therefore reduce the GHG emissions. In this dissertation study, several different power-split model are proposed, tested and compared. More details are provided in the following sections.

4 Vehicle Dynamics Optimization: Connected Ecodriving

In this chapter, vehicle dynamics optimization is implemented in the form of connected ecodriving at signalized intersections. Three different connected ecodriving assistance sytem for PEVs are designed and compared by evaluating with real-world driving data. In the following sections of this chapter, EV energy consumption estimation model is developed with real-world driving data (section 4.3). Three different connected ecodriving strategies are proposed developed and evaluated with real-world driving data: (1) EAD assistance without considering driver error (section 4.4); (2) EAD assistance with considering driver error (section 4.5); and (3) EAD assistance with partial automaton (longitudinal automatic control). The performance of these proposed models evaluated individually and also summarized in section 4.6. This chapter provides a full set of numerical evidence for energy saving potentials of different connected Ecodriving strategies for PEVs.

4.1 Connected Ecodriving at Signalized Intersections

Vehicular Movements at Isolated Intersections

Basically, there are 4 different "passing scenarios" for a vehicle to travel through an isolated signalized intersection. The velocity profiles of these 4 different scenarios are shown by the green, blue, red, and yellow lines in Figure 4-0. It is also noted that all these trajectories have the same initial and final velocities, and same traveled distance (e.g., within the dedicated short range communication range). More specifically, these scenarios can be described as follows:

- Scenario 1 (cruise): the vehicle cruises through the intersection at a constant speed (green line);
- Scenario 2 (speed-up): the vehicle speeds up to pass the intersection and then gets back to the initial speed after the intersection (blue line);

- Scenario 3 (coast-down with stop): the vehicle slows down and stops at the intersection (red line);
- Scenario 4 (coast-down without stop or glide): the vehicle slows down and passes the intersection at a mid-range speed, and then speeds up to its initial speed (yellow line).

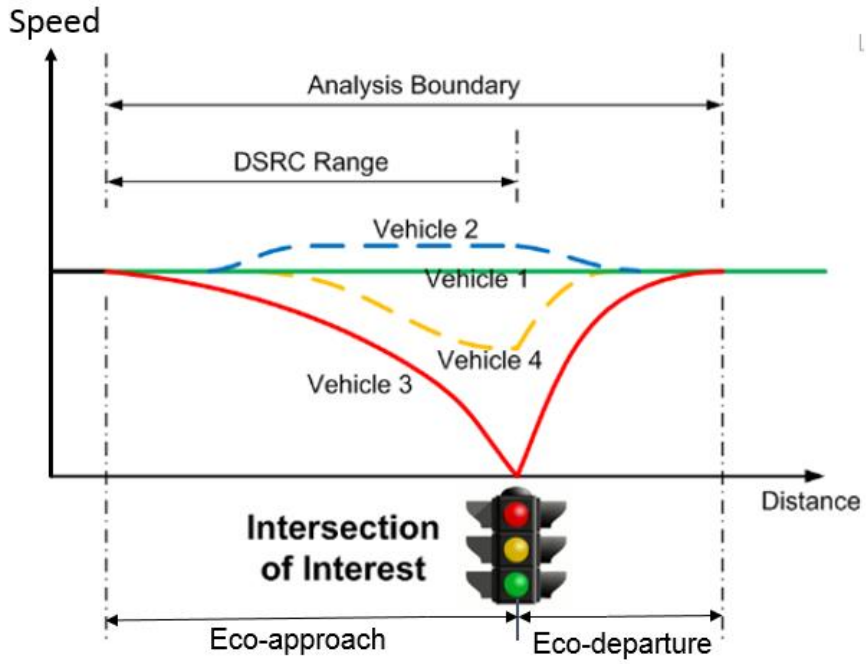

Figure 4-0 Illustration of different vehicle trajectories traveling across an intersection. (from [ref])

For conventional gasoline vehicles, our previous research [65] has shown that, even though all these scenarios cover the same distance with the identical initial and final velocities, the associated fuel consumption and emissions may vary greatly. Vehicle 1 (or Scenario 1) uses the least fuel since it does not need to accelerate or make unnecessary deceleration. Vehicle 2 (or Scenario 2) consumes more fuel than vehicle 1 since there is a slight acceleration and deceleration before and after the intersection. Vehicle 3 (or Scenario 3) might use the most amount of fuel since it has to decelerate to a full stop, idle for a certain period, and then accelerate from a stop to a desired final speed. Finally, Vehicle 4's (or Scenario 4's) fuel consumption may be comparable to Vehicle 2's since both vehicles have a slight speed up and slow down during their trips, although the acceleration occurs at a relatively lower speed.

Therefore, when a gasoline vehicle is traveling through a signalized intersection, its velocity profile could be optimized to achieve minimum fuel consumption for each of the 4 scenarios. Similarly, the velocity profile of an EV can also be optimized to achieve minimum energy consumption by taking into consideration of its distinctive characteristics (e.g., regenerative braking). This is the basic idea behind the vehicle trajectory planning algorithm described in the following.

Optimal Vehicle Trajectory Planning

In this study, a vehicle trajectory planning algorithm (VTPA) is designed for generating an optimal velocity profile based on real-time SPaT information. Among all the possible velocity profiles with which a vehicle can safely travel through an intersection, the VTPA can choose the velocity profile that has minimum tractive power requirements, in order to minimize energy consumption. The required tractive power of a vehicle depends on the instantaneous velocity and acceleration under the point mass assumption, as given by:

$$P_{tract.} = Av + Bv^2 + Cv^3 + M(0.447a + gsin\theta)v * 0.4471000 \qquad (1)$$

where M is vehicle mass with appropriate inertial correction for rotating and reciprocating parts (kg); v is instantaneous speed (miles/hour or mph); a is acceleration (mph/second); g is gravitational acceleration (9.81 meters/second2 or m/s2); and θ is road grade angle in degree. Here, the coefficients $A, B,$ and C are associated with rolling resistance, speed-correction to rolling resistance, and aerodynamic drag, respectively, which can be determined empirically.

As suggested in our previous work [65], there are numerous ways to accelerate or decelerate from one speed to another, such as constant acceleration and deceleration rates, linear acceleration and deceleration rates, and constant power rates. A family of piecewise trigonometric-linear functions is selected as the target velocity profiles (for both approach and

departure portions), due to its mathematical tractability and smoothness. For more details of the algorithm, please refer to [65].

4.2 Real-world Driving Data Collection

In this dissertation study, two different real-world driving data sets are collected: one set is the real-world EV driving data that is used to build the energy consumption model of EVs; the other set is the real-world driving data of connected Ecodriving at signalized intersections with different technology stages, which is used for performance evaluation of the designed technologies in this dissertation work.

4.2.1 Real-world EV Driving Data for Energy Consumption Estimation

A 2013 NISSAN LEAF was used as the test EV for data collection in this study (see Fig.4-1). To obtain second-by-second vehicle states (e.g., speed), energy consumption, and road topology (e.g., road grade) data, the following two data acquisition systems were used simultaneously:

A high-resolution professional diagnostic tool specifically designed for all NISSAN vehicle models (Including LEAF), called CONSULT III plus kit, was used to access data from the test vehicle's CAN bus, including vehicle speed, battery pack current (positive for charging while negative for discharging) and voltage, air conditioner (A/C) power, and accessory power. Therefore, the net propulsion power, P^{prop}, can be estimated as:

$$P^{prop} = -\left(I^{bp} \times V^{bp}\right) - \left(P^{AC} + P^{acc}\right) \quad (4-1)$$

where I^{bp} and V^{bp} represent the instantaneous current (in ampere) and voltage (in volt), respectively, from/to the battery pack. P^{AC} and P^{acc} are the power consumed by A/C and other accessories (e.g., radio), respectively.

a. Test EV b. CONSULT III plus Kit (OBD reader) c. GPS data logger

Figure 4-1 Data collection equipment

It is well known that road grade is one of the major factors affecting a vehicle's energy consumption. We used a GPS data loggers to collect latitude and longitude data, which are then map matched with a 3D map to acquire the road grade of each data point.

Using the data acquisition systems described above, two types of experiment were conducted to collect EV driving and energy consumption data in the field: *Driving under real-world conditions and Driving under controlled environment:*

To cover a variety of traffic conditions, road types and road grades, we carefully chose three pairs of origin-destination (shown in Fig. 4-2) and routes in Riverside, CA to conduct real-world driving data collection for about four months. The vehicle was driven by different drivers at different traffic conditions during the field driving test. In total, more than 100 hours of driving under real-world conditions were conducted, yielding a substantial amount of data.

Besides the real-world driving experiment, we also collected data under a controlled environment (i.e., no interaction with other traffic) to better understand the energy consumption

of the test EV at different cruise speeds. The cruise speeds vary from 5 mph to 50 mph with a 5-mph increment. These data will be used to build the baseline scenarios case for comparison.

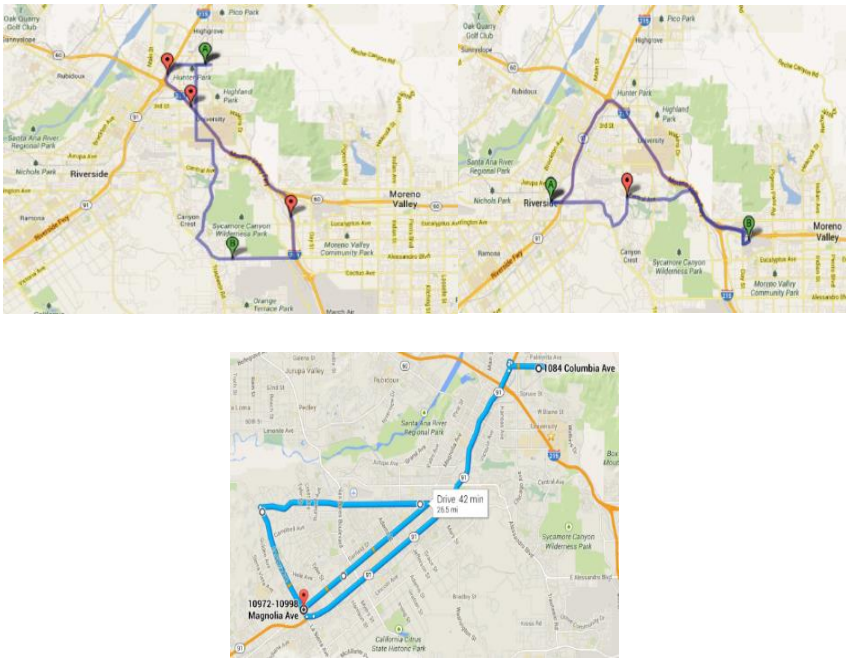

(a) Loop between CE-CERT and Alessandro Blvd., Riverside, CA
(b) Loop between Riverside Plaza and Towngate Circle, Moreno Valley, CA
(c) Loop between CE-CERT and Magnolia Ave., Riverside, CA

Figure 4-2 Routes for real-world driving data collection

Before the field data from the CONSULT III Plus kit and the GPS data logger can be used for analysis, they have to be time synchronized first (see Fig.4-3). The synchronized data then have to be associated with road grade values of road segments through map matching. More specifically, there are two steps of data fusion.

The raw data files from the GPS data logger are not aligned with the ones from the CONSULT III Plus kit in terms of updating rate. Hence, all raw data files were processed into 1 Hz, which is suitable for the data synchronization as well as the energy consumption estimation to be done later.

It is noted that the GPS data logger reports the Coordinated Universal Time (UTC) as a temporal reference. However, the CONSULT III Plus kit only reports the relative time stamp (i.e., each run always starts from time "0") for each run. To fuse these two data sources, a common feature needs to be identified. In this study, we selected the vehicle speed and applied the cross-correlation technique [82] to synchronize these two data sources. Fig. 4-4 presents an example of speed trajectories after synchronization. The following steps are taken:

- Conduct map matching onto the fused dataset, where each data point is matched to the associated roadway link on the digital map that has the least orthogonal distance to the data point(see Fig. 4-5).
- Break down the fused data stream into short driving snippets based on roadway link.
- Group link-based snippets by roadway type, average speed and grade etc.
- Calculate the average speed and energy consumption rate (per mile) for each real-world driving snippet

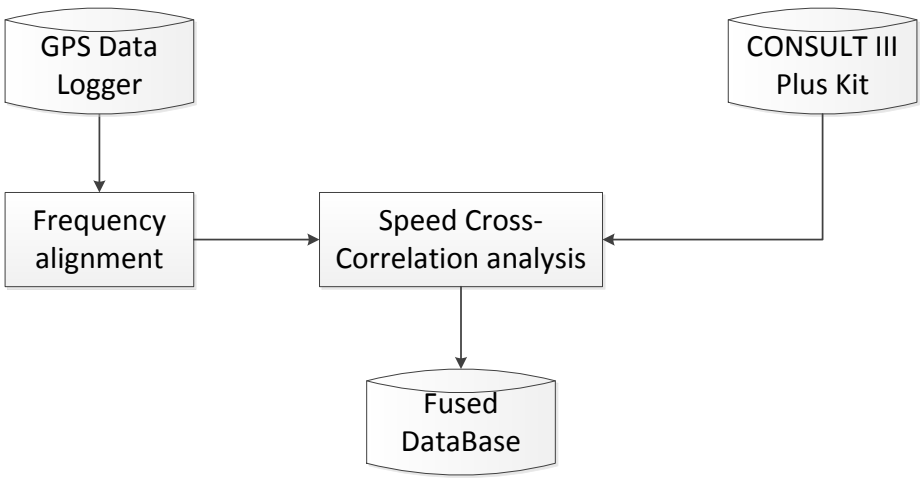

Figure 4-3 Flowchart for fusing data from the CONSULT III Plus kit and the GPS data loggers

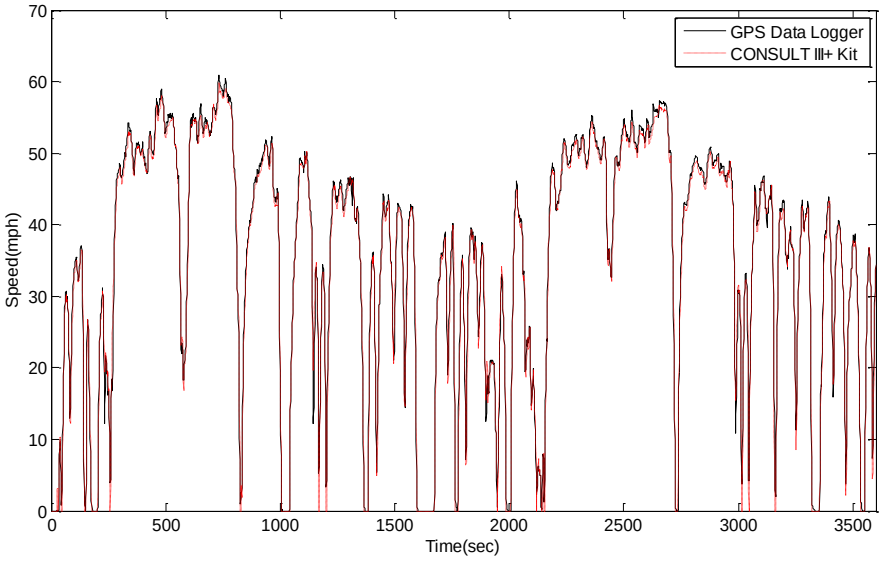

Figure 4-4 An example of synchronized speed trajectories

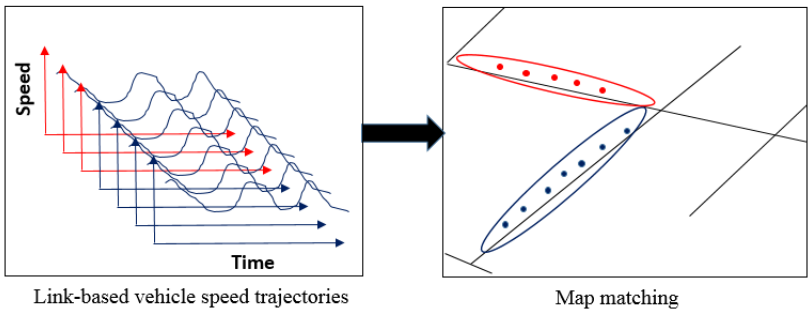

Figure 4-5 Trajectory snippets and map matching

4.2.2 Real-world Ecodriving Data for Performance Evaluation

To fully investigate the performance of the proposed driver-in-the-loop connected ecodriving system by comparing with the exiting systems, real-world driving data with the designed open-loop EAD assistance system was conducted and data are collected. The field test was conducted at the Turner-Fairbank Highway Research Center (TFHRC) in McLean, Virginia using the Saxton Lab Intelligent Intersection, which offered a sheltered traffic environment where the connected ecodriving prototype was able to be tested with minimal safety risk and without

disrupting live traffic operations. Figure 4-6 provides an overview of the field test site, specifying starting point where the vehicle will begin test runs from a stop and travel westbound towards the intersection and relevant roadside infrastructure (including an Econolite 2070 controller, Windows PC to encode SPaT and MAP messages, and Arada Locomate DSRC Roadside Unit). The test zone covers a range from 190 meters to the east of the intersection to 116 meters to the west, which allows a maximum traveling speed of up to 30 mph. The traffic signal controller was set up for fixed timed signal plan: 27-seconds green, 3-seconds yellow, followed by 30-seconds of red, which has removed excess all red clearance timings and all loop detector triggers from actuating the signal.

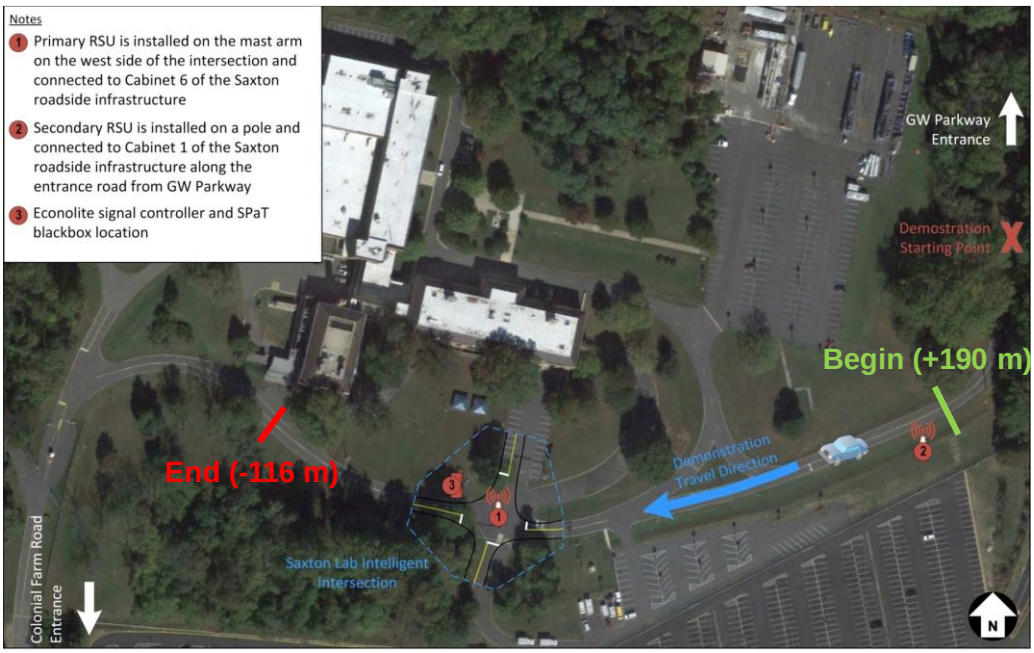

Figure 4-6. Field study site in Turner Fairbank Highway Research Center in McLean, VA.

In order to comprehensively investigate the energy benefits of the proposed system for EVs, we collected real-world driving data with 3 different technological as elaborated in the following:

- *Uninformed driving*. In this stage, the driver approached and traveled through the intersection in a normal fashion without guidance or automation, stopping as needed

without any guidance. The vehicle is fully controlled by the human driver. This stage is used as lower bound performance technological stage.

- *Advising driving without consider driver error*. In this stage, the driver was assisted by an open-loop EAD system as described in Fig. 4. An enhanced dashboard presenting a recommended range of driving speed is provided (see Figure 5). This information can assist the driver to approach and depart the intersection in an environmentally friendly manner while obeying the traffic signal. This driving assistance system does not consider human driver error.

- "*Partially automated" driving.* At this stage, an automatic controller was responsible for longitudinal control of the vehicle, allowing it to speed up or slow down while the driver steered for lateral control. The vehicle automatically controlled the brake and throttle based on the calculated eco-friendly velocity profile according to signal state and distance to the stop-bar.

To investigate different scenarios with respect to when a vehicle enters a signalized intersection and get an average performance of the proposed system at various traffic conditions, the field experiment was designed to have the test vehicle approach the intersection at different time instances throughout the entire signal cycle (i.e., every 5 seconds in the 60-second cycle). We call these different entering cases as "*entry case*" in the rest of this paper. Furthermore, the test vehicle approached the intersection at different operating speeds (i.e., 20 mph and 25 mph). Therefore, a test matrix was designed, consisting of the operating speed along the vertical axis, and the *entry case* across the horizontal access. In this matrix, there are a total of 12 *entry cases* × 2 speed levels = 24 test cells. For the Stage I and Stage II experiments, a total of four drivers were recruited to conduct test runs. Each driver completed each of the test cells in the test matrix. Therefore, a total of 24 test cells × 3 stages × 4 drivers = 288 test runs were conducted. For each test run, data such as speed and distance to the stop bar were logged at 10 Hz and post-processed to determine energy consumption and other performance measures. It is noted that a

hybrid vehicle (2012 Ford Escape) was used for the field study. The energy consumption was estimated by the EV energy consumption model based on the collected driving speed trajectories for different cases.

4.3 Macroscopic EV Energy Consumption Estimation Model

As described in chapter 2, in the past decade, Ecodriving technology has attracted interest as a way to improve vehicle energy efficiency not only for conventional internal combustion engine (ICE) vehicles, but also for electric vehicles. Recent research shows that these Ecodriving technologies are capable of improving the energy (i.e., electricity) efficiency of EVs so that the all-electric range can be extended [83]. For example, in one of our previous work, an Eco-approach and departure (EAD) system [65] was developed to help vehicles travel through the signalized intersection smoothly and avoid unnecessary idling and acceleration/deceleration with the knowledge of signal phase and timing (SPaT) information.

However, accurate estimation of EV energy consumption using real-world driving condition data (e.g., provide by ITS traffic management systems) is an essential prerequisite for applying these Ecodriving technologies. For example, in an eco-routing system for EVs, the EV energy consumption on each road segment or link has to be estimated prior to select the most energy-efficient route. Thus far, several researchers have investigated different factors that impact EV energy consumption and built different estimation models upon these impact factors (see Table 1). These existing models can be classified by the following features:

a. *Granularity:* For different application purposes, EV energy consumption estimation models can be developed at a different granularity. For instance, for some applications that involve second-by-second vehicle velocity profile planning, such as EAD applications, the estimated energy consumption must be instantaneous and capable of estimating the

second-by-second energy consumption [83, 84,87,90,93,94,95]. On the other hand, for applications like eco-routing systems, the estimation model is used to estimate the total energy consumption over the entire trip. And this model can be aggregated from the previously mentioned second-by-second mode [85, 88, and 92]. For some sophisticated applications, both two types model are required to form a hybrid estimation model that is capable of estimating energy consumption at different granularity simultaneously [86,89,91].

b. *Impact factors:* Various factors have been proved to influence EV energy consumption (Figure 4-7). Those reported factors can be classified into the following categories: 1) the factors from traffic conditions that ultimately influence vehicle dynamic parameters such as speed, acceleration [83-97] etc; 2) infrastructure related factors such as road grade, road surface rolling resistance [86]; 3) ambient environment factors such as the ambient temperature and weed speed [86]; and 4) driving behaviors related factors, such as acceleration/deceleration profile [90] etc. Thus far, all the above mentioned factors are regarded as raw factors that can be obtained by measurement. In most cases, it is quite difficult to measure and obtain all these types of factors due to the limited resources. Therefore, there should be a new type of factors that can be constructed to aggrade the compound influences of several different types of raw factors. As shown in Fig 1, this new type of impact factors: constructed compound factors is identified at the intersections of all types of raw impact factors, which will be defined and discussed in this study.

c. *Type of model:* An EV energy consumption model explains the quantitative relationship between EV energy consumption rate and various impact factors. Both analytical and data-driven models can be used to capture such relationship (Fig. 4-8).

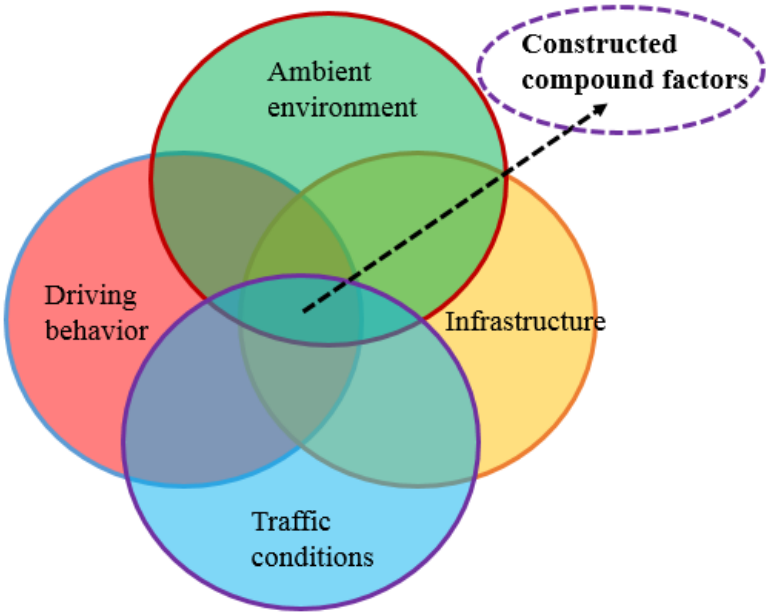

Figure 4-7 Impact factors of EV energy consumption

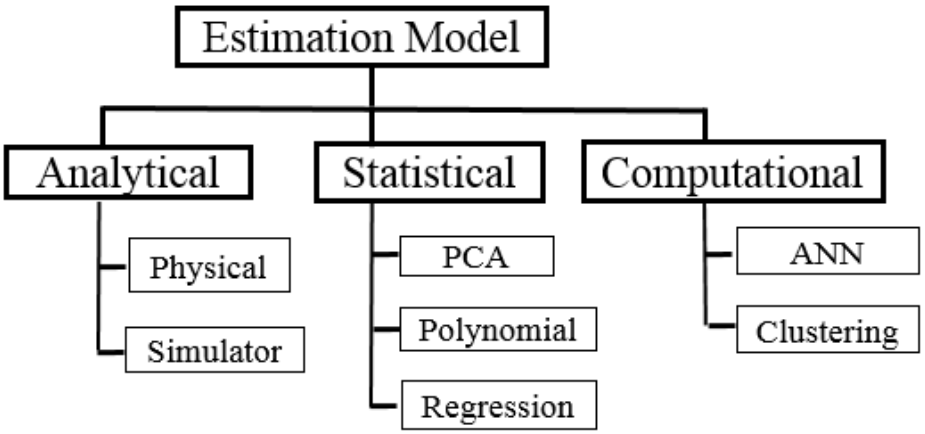

Figure 4-8 Categories of EV energy consumption estimation models

Among all the above reviewed existing work, there are only a few focused on the link-level EV energy consumption estimation. Link-based EV energy consumption estimation model is built and compared for different road types in [96], the proposed model is based on vehicle specific power(VSP) which mainly consider the average speed and accelerations. A flexible link-level energy consumption estimation model is proposed in [97] with different degrees of accuracy and various requirements in respect of complexity, computing time and necessary input

features. The energy consumption estimation is based on the crowd-sourced energy consumption data from other vehicles on the road network, which might be not accurate due to the different vehicle models and energy efficiency. More than 18 link-based features are extracted for estimating the energy consumption on each link, such as the average speed, mean and standard deviation of accelerations and etc. the major drawbacks of these existing works are the lack of analyzing the impact of regenerative braking power of EV when running in the real-world traffic congestion.

In this work, the EV energy consumption on a road link in real-world traffic congestion is first decomposed based on fundamental physics. Then, with the real-world EV driving data, a data-driven energy consumption decomposition analysis is conducted by analyzing two newly constructed compound factors: positive kinetic energy (PKE), and negative kinetic energy (NKE). The NKE is analyzed and related to the regenerative braking power collection characteristics. The energy consumption rate curve along the average speed is constructed and a "W" shape curve is discovered and explained with real-world driving data. An accurate and simple EV energy consumption estimation model is built upon this decomposition and the feature selection analysis also prove the significant effectiveness of these two constructed factors. The comparison to the existing models are also conducted to validate the outperformance of the proposed model. It shows that a good energy consumption estimation model does not have to be very complicated as long as it is derived from the fundamental physics and verified by the real-world test driving data.

There are the several major contributions of this proposed model:

- NKE is used as a variable for capturing the regenerative braking effect in a link-level EV energy consumption estimation model;

- A systematic data-driven EV energy consumption decomposition analysis is conducted;
- A novel link-level EV energy consumption estimation model is built upon the decomposition analysis; and
- A "W"-shaped relationship between link-level EV energy consumption rate and link average speed is discovered and explained with the real-world EV driving data.

4.3.1 EV Energy Consumption Analysis

Analytical Model of EV Energy Consumption

An understanding of vehicle energy consumption is important for building a vehicle energy consumption estimation model. Figure 8 shows an example of a vehicle moving from point A to point B on a road segment with length L_{link} and road grade Θ. The vertical displacement is H_{link}. According to physics fundamentals and the law of energy conservation, the total energy consumption (from a power source) of a vehicle with mass *m* traveling from point A to point B (see Figure 4-9) is calculated as:

$$E_{total} = E_{tractive} + E_{A/C} + E_{accessory} \quad (4\text{-}2)$$

$$E_{tractive} = \Delta E_{kinetic} + \Delta E_{potential} + E_{rolling} + E_{aerodynamic} + E_{loss} \quad (4\text{-}3)$$

and,

$$\Delta E_{kinetic} = \frac{1}{2} m v_t^2 - \frac{1}{2} m v_0^2 \quad (4\text{-}4)$$

$$\Delta E_{potential} = m g H_{link} = m g L_{link} \tan(\Theta) \quad (4\text{-}5)$$

where $E_{tractive}$ is the energy consumed for traction; $E_{A/C}$ and $E_{accessory}$ represent the energy consumed by air conditioner and other accessories, respectively; $\Delta E_{kinetic}$ and $\Delta E_{potential}$ represent the changes in vehicle kinetic energy and potential energy between point A and point B, respectively; $E_{rolling}$ represents the energy consumed to overcome the friction on road surface; $E_{aerodynamic}$ denotes the energy consumed to overcome the air friction; and E_{loss} is the internal energy loss due to e.g., friction in the transmission system or heat loss from the motor and mechanical brake during the travel from point A to point B;

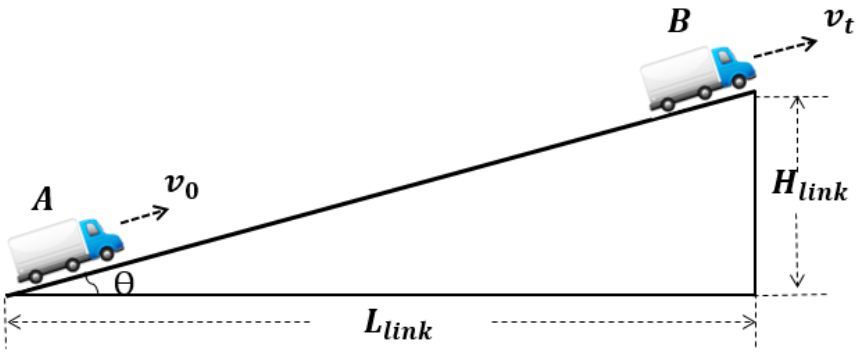

Figure 4-9. Change of mechanical energy of vehicle movement.

In this study, the tractive energy is of the major interest, while the energy consumption from air conditioner and other accessories are measured and excluded from the total energy consumption as shown in Equation (2). It is also noted that for a specific road segment (or link), $\Delta E_{potential}$ and $E_{rolling}$ are independent of speed trajectories (under traffic conditions). For a passenger vehicle (i.e., NISSAN LEAF in this study), the energy consumed to overcome the air resistance, $E_{aerodynamic}$ is not so significant (around 5% [99]), especially when the vehicle is affected by the other traffic and the speed is not so high. It is very challenging to accurate model the internal energy loss, E_{loss}. For simplicity, we assume that it is proportional to the tractive energy. Furthermore, the sum of $E_{aerodynamic}$ and E_{loss} is written as

$$E_{aerodynamic} + E_{loss} \approx \mu \cdot E_{tractive} \quad (4\text{-}6)$$

where μ is a constant, independent of the driving cycle.

Along a specific road segment, therefore, the tractive energy can be approximated as

$$E_{tractive} \approx \Delta E_{kinetic} + \delta + \mu \cdot E_{tractive} \tag{4-7}$$

or,

$$E_{tractive}(v) \approx \alpha + \beta \cdot \Delta E_{kinetic}(v) \tag{4-8}$$

where $\delta \approx \Delta E_{potential} + E_{rolling}$, $\alpha = \delta/(1-\mu)$, and $\beta = 1/(1-\mu)$.

From a statistical point of view, if we are trying to build a regression model to estimate the vehicle energy consumpiton, then the change in kinetic energy (due to the speed variation) should be the most powerful predictor. This is the fundamental hypothesis of the data-driven analysis presented in the following section.

If the road segment is discretized by time step, then Eq. (4) can be expressed as:

$$\Delta E_{kinetic} = \frac{1}{2} m \cdot \sum_{i=1}^{N-1} \left(v_{i+1}^2 - v_i^2\right) \tag{4-9}$$

where N is the total number of time steps driving on the road segment; and v_i is instantaneous speed (mph). When we consider the positive portion and negative portion separately, then (9) is converted to

$$\Delta E_{kinetic} = \frac{1}{2} m \cdot \sum_{i=1}^{N-1} \max\left(v_{i+1}^2 - v_i^2,\ 0\right) + \frac{1}{2} m \cdot \sum_{i=1}^{N-1} \min\left(v_{i+1}^2 - v_i^2,\ 0\right) \tag{4-10}$$

Since we are estimating the energy consumption per unit distance, we divide Eq. (8) by the distance of the road segment,

$$\frac{E_{tractive}}{L_{link}} \approx \frac{\alpha}{L_{link}} + \beta \cdot \left[\frac{\frac{1}{2} m \cdot \sum_{i=1}^{N-1} \max\left(v_{i+1}^2 - v_i^2, 0\right)}{L_{link}} + \frac{\frac{1}{2} m \cdot \sum_{i=1}^{N-1} \min\left(v_{i+1}^2 - v_i^2, 0\right)}{L_{link}}\right]$$

$$\approx \frac{\alpha}{L_{link}} + \beta \cdot \left[\frac{\frac{1}{2}m \cdot \sum_{i=1}^{N-1} \max(v_{i+1}^2 - v_i^2, 0)}{\sum_{i=1}^{N-1}(d_{i+1} - d_i)} + \frac{\frac{1}{2}m \cdot \sum_{i=1}^{N-1} \min(v_{i+1}^2 - v_i^2, 0)}{\sum_{i=1}^{N-1}(d_{i+1} - d_i)} \right] \quad (4\text{-}11)$$

where d_i is cumulative travel distance up to the *i*-th time step; and $\frac{E_{tractive}}{L_{link}}$ is the energy consumption per unit distance on the road segment, which we call energy consumption rate (ECR). The term, $\frac{\sum_{i=1}^{N-1} \max(v_{i+1}^2 - v_i^2, 0)}{\sum_{i=1}^{N-1}(d_{i+1} - d_i)}$, is the cumulative positive change in kinetic energy rate (PKE), which is first developed by Watson [20] and used as a measure of change in kinetic energy per unit distance due to acceleration. The term, $\frac{\sum_{i=1}^{N-1} \min(v_{i+1}^2 - v_i^2, 0)}{\sum_{i=1}^{N-1}(d_{i+1} - d_i)}$, is newly defined in this study as the cumulative negative change in kinetic energy rate (NKE), which may account for the regenerative braking effect of an EV. Therefore, Eq. (11) can be simplified as:

$$\text{ECR} \approx \frac{\alpha}{L_{link}} + \frac{\beta}{2} \cdot m \cdot (\text{PKE+NKE}) \quad (4\text{-}12)$$

When θ is small, α / L_{link} can be approximated as a constant. So, we can say that the energy consumption rate is (approximately) linearly correlated with PKE and NKE. In other words, PKE and NKE are strong predictors of the link-level EV energy consumpiton rate.

Using the collected EV driving data, PKE and NKE values were calculated on a link-by-link basis. Figure 4-10 and Figure 4-11 illustrate the plots of link-level ECR as a function of PKE and NKE, respectively. It can be seen that there is a clear linear trend between ECR versus PKE or NKE. This implies that PKE and NKE are good indicators of EV energy consumption rate and could be used in EV energy consumption models.

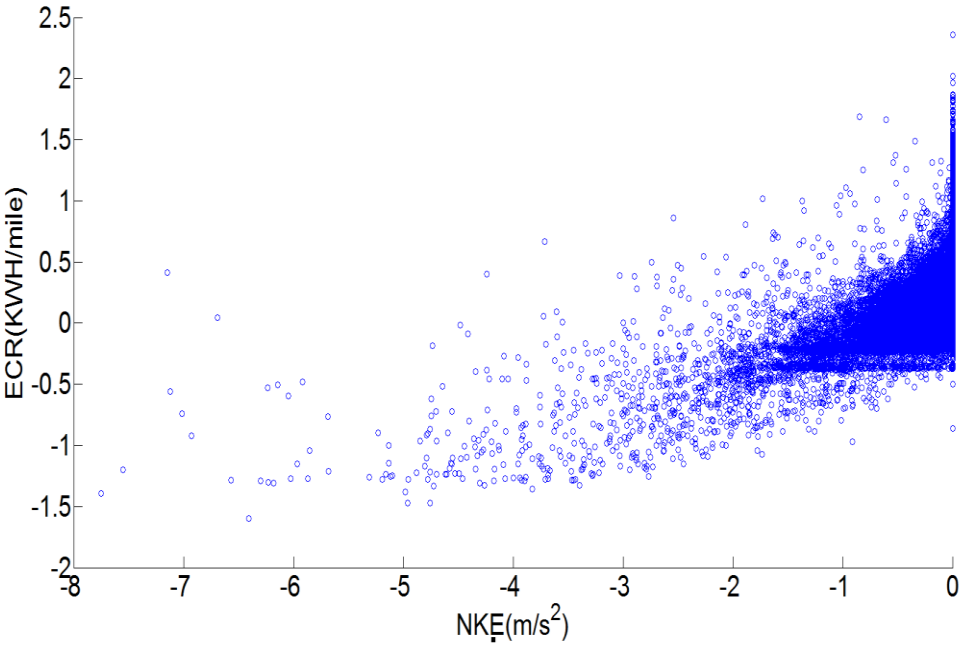

Figure 4-10 ECR vs. NKE.

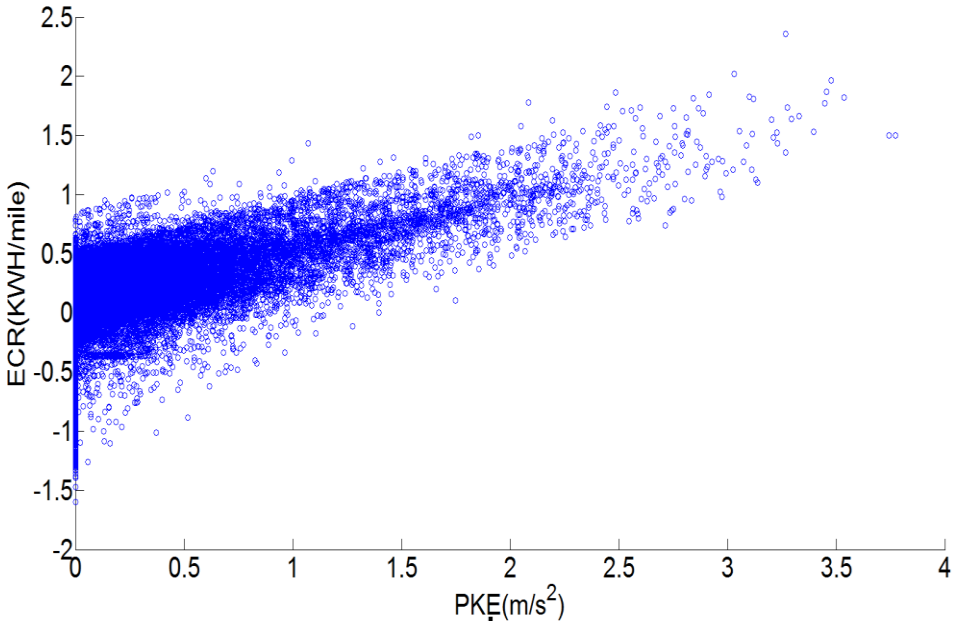

Figure 4-11 ECR vs. PKE.

4.3.2 Regenerative Braking and NKE

As aforementioned, the change in kinetic energy of the vehicle on a road segment is decomposed into PKE and NKE. As shown in Fig. 4-12, NKE is used to measure the negative change in kinetic energy per unit distance due to deceleration, which can be correlated with the

electricity energy gain from EV regenerative braking (RB) on a flat road. This is because the vehicle kinetic energy is converted to electricity through the motor acting as a generator when the vehicle decelerates. Fig. 4-13 shows the electricity flow of EV regenerative braking system.

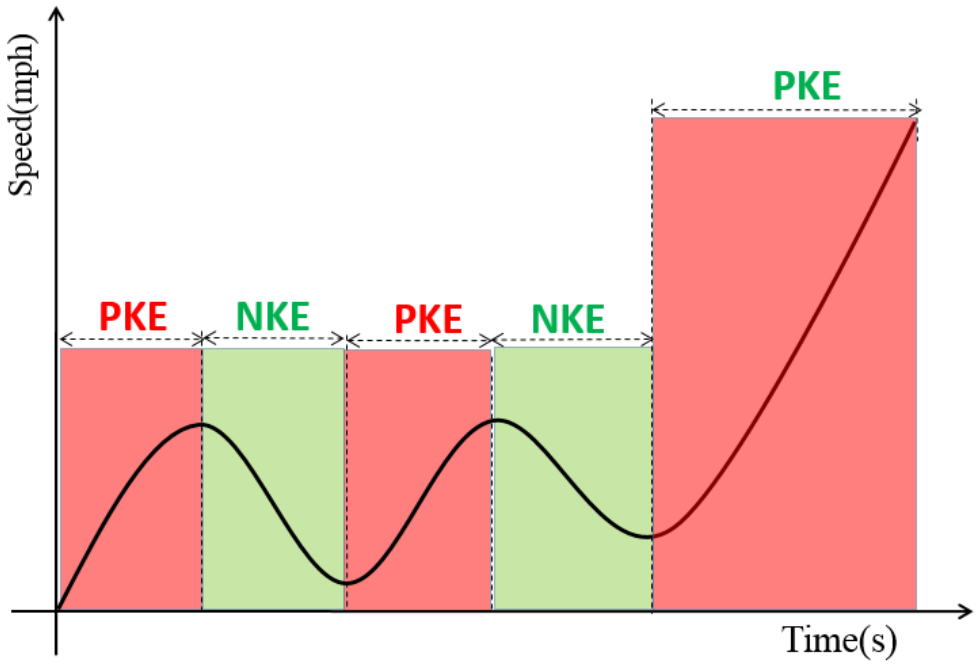

Figure 4-12. PKE and NKE along a trip.

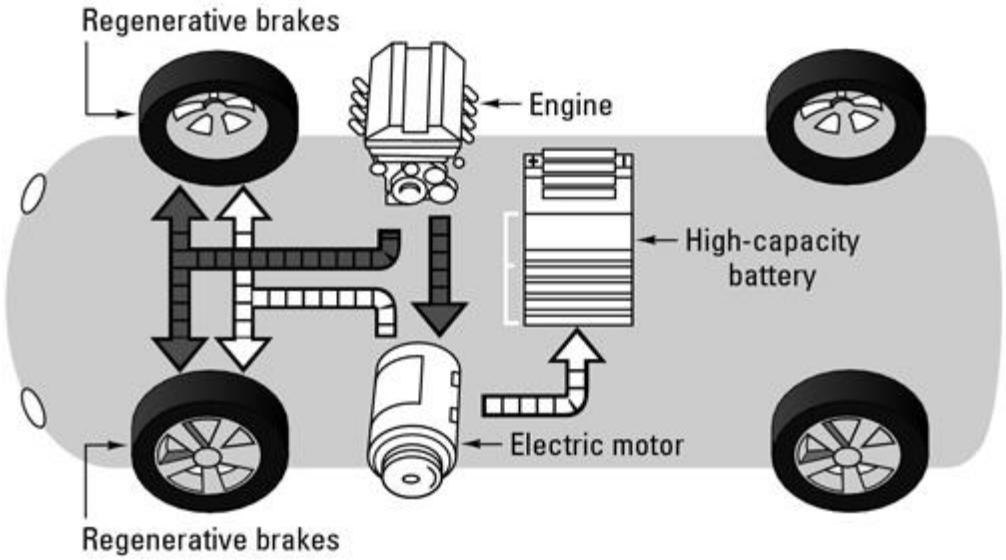

Figure 4-13 Regenerative braking (RB) in EV.(http://www.slideshare.net/)

The energy gains from RB and NKE over different average speeds are plotted in Fig.4-14 and Fig. 4-15, respectively, using the collected field data. As can be seen in these figures, both NKE and energy gain from RB are relatively constant when the average speed is over 30 mph but a surge is observed in both figures under the average speed of 30 mph. These observations indicate that NKE is a good indicator of energy gain from RB.

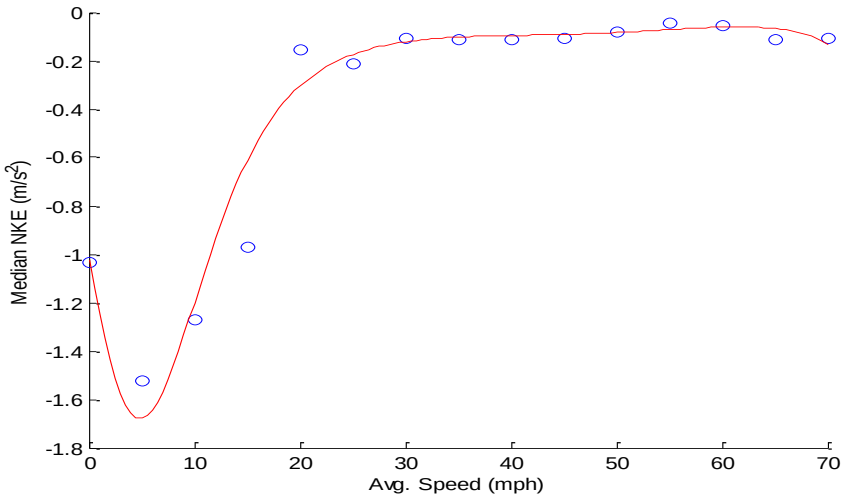

Figure 4-14 Polynomial fit of NKE by average speed.

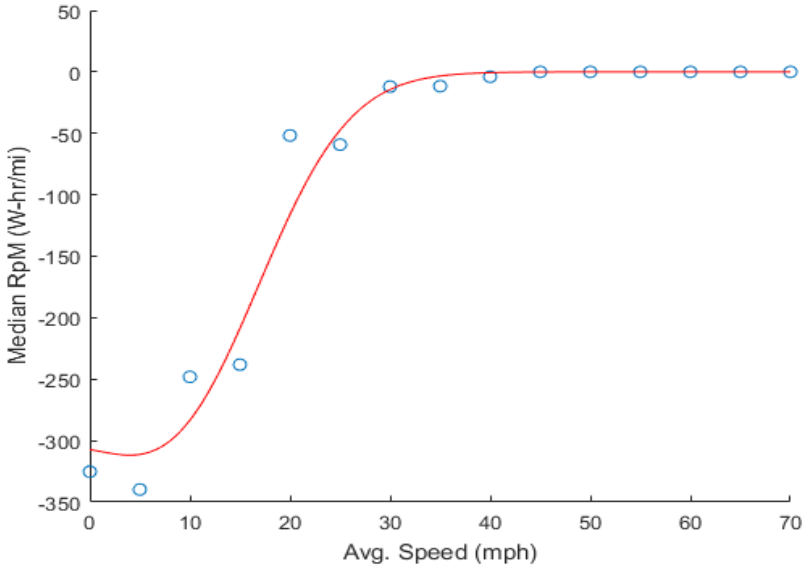

. Figure 4-15 Polynomial fit of collected regenerative power by average speed

4.3.3 Data-driven Energy Consumption Decomposition Analysis

EV energy consumption under real-world congestion

Based on the fundamentals in vehicle dynamics, the instantaneous power of EV is determined by vehicle speed, acceleration and roadway grade. It has been derived in [87] that EV's instantaneous power can be estimated by:

$$P = \frac{rR^2}{(k_a D_d)^2}(ma + kv^2 + f_{rl}mg + mg\,sin\Theta)^2 + v(kv^2 + f_{rl}mg + mg\,sin\Theta) + mav \quad (13)$$

where r is the resistance of the motor conductor; R is the radius of the tire; k_a is the armature constant of the motor; D_d is the magnetic flux; f_{rl} is the rolling resistance constant; a and v are the instantaneous acceleration and velocity; Θ is the road grade; m is the vehicle mass; g is the gravitational acceleration (9.81 m/s^2). From equation (13), we know that the EV instantaneous power is proportional to the 4th order of velocity.

To understand the impact of traffic congestion on EV energy consumption, the relationship between EV energy consumption per unit distance and average vehicle speed on a road link is investigated since average vehicle speed is a good indicator of the level of real-world traffic congestion. We first created boxplots of distance-based ECR vs. average speed (every 5 mph) for different levels of road grade. Figure 4-16 presents the ECR at different speed levels. A 4th order polynomial fit is applied to the median values of ECR by different speed bins:

$$f_k = \sum_{i=0}^{4} \alpha_i \cdot v_k^i \quad (14)$$

where i is the order of polynomial; v_k is (link-level) average vehicle speed (mph); α_i's are regression coefficients; and f_k is (link level) distance-based energy consumption rate (W-hr/mi). The fitted curve is shown in Figure 4-17. Unlike the typical "U-shaped" ECR curve for

gasoline light-duty vehicles found in our previous work [101] as shown in the Fig 4-19, the ECR curve for the test EV displays a “W-shape”. The explanation for this difference is given in the following section.

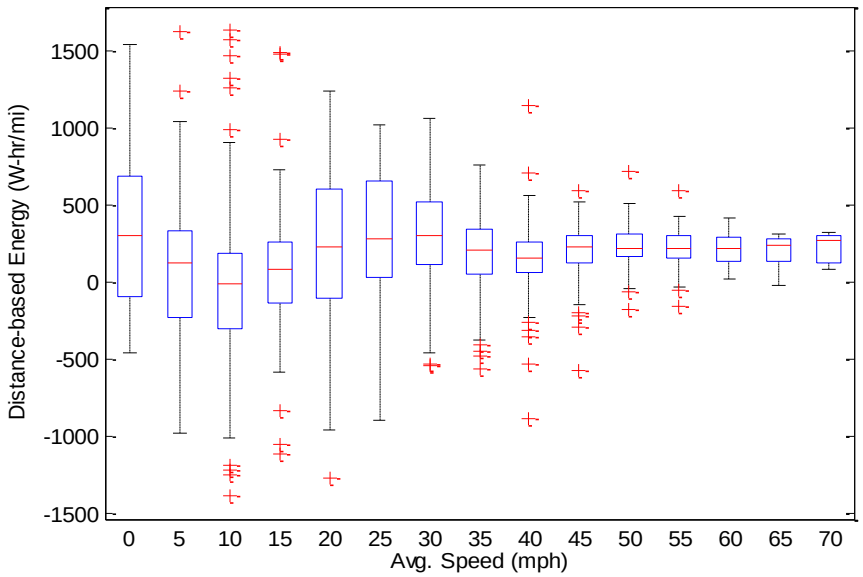

Figure 4-16 Boxplot of ECR for different average speed

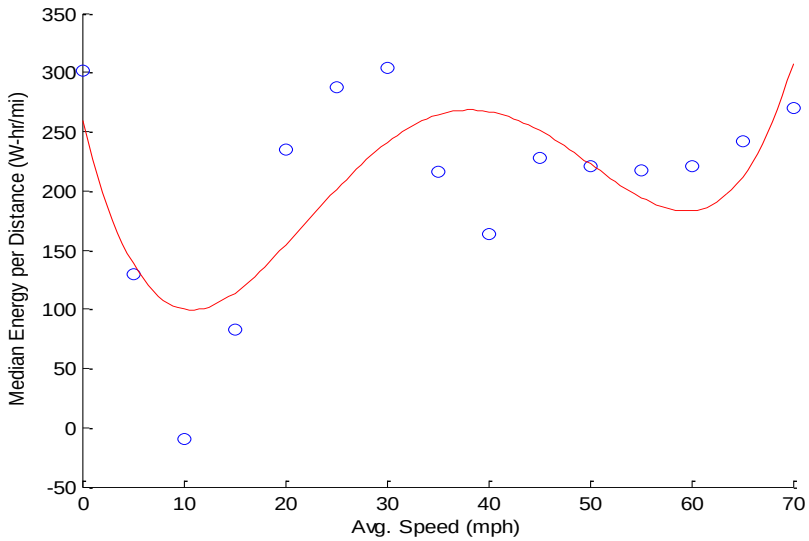

Figure 4-17 Polynomial fit of median ECR by average speed.

As described in the data collection section, to fully investigate the impact of traffic congestion on EV link based energy consumption, EV energy consumption data under different constant speeds were also collected in a controlled environment, where vehicles were running without interaction with other traffic and always kept in a constant or close constant speed. Based on these data, we further compared the EV energy consumption at different constant speeds with that at different average speeds (in traffic). Figure 4-18 shows the fitted ECR curves by speed. As can be seen in the figure, ECR in real traffic with stop-and-go driving is lower than that of constant speed driving when the average speed is less than about 10 mph (region A in Figure 18). This suggests that the test EV is very energy efficient in low-speed driving on urban routes considering the real-world vehicle activity patterns. Region B in Figure 18 shows potential energy savings of the test EV from a smoother traffic flow that can be achieved by different ITS or intelligent vehicle strategies (e.g., speed harmonization). When the average is higher than 60 mph, there is little difference in the ECR due to the lack of traffic congestion in both driving scenarios at high average speeds on freeways. It is also noteworthy that there is an intersection between two curves for EV but no intersection for gasoline light-duty vehicles (See Figure 19). This is mainly due to the regenerative braking that collects power when EVs are decelerating, but the energy is dissipating in the form of heat for gasoline vehicles.

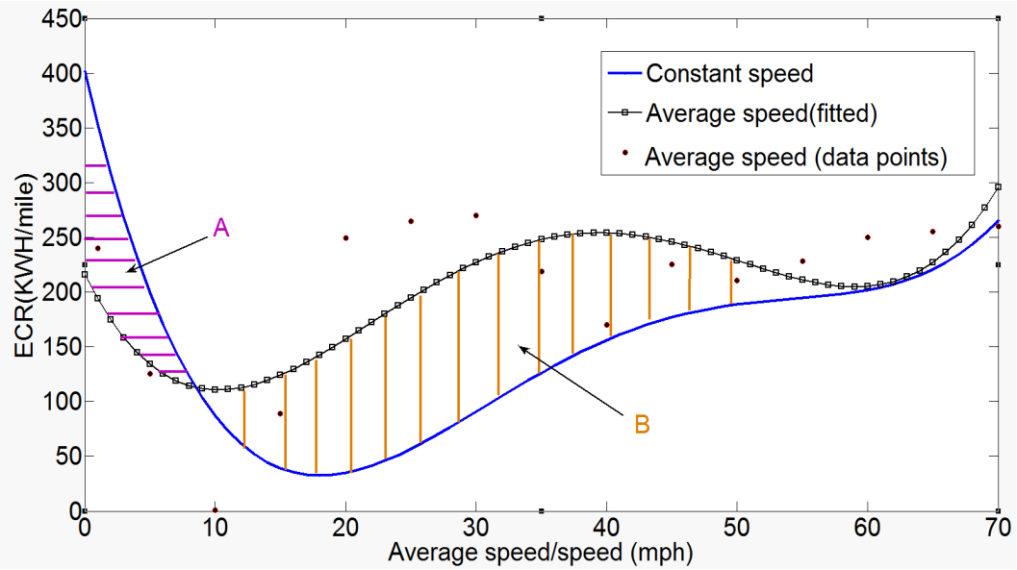

Figure 4-18 ECR by constant speed vs. average speed.

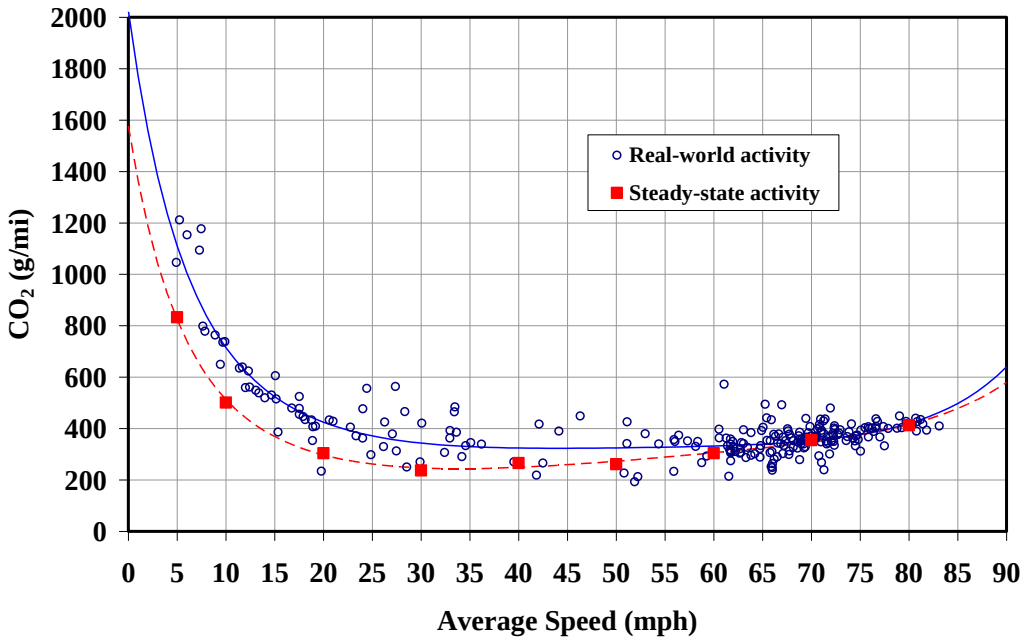

Figure 4-19 ECR by constant speed vs. average speed [101].

4.3.4 Data-Driven Energy Consumption Decomposition

To explain the interesting "W-shaped" relationship between median ECR and average vehicle speed in Figure 17, PKE, NKE, and KE values by different average speeds are further investigated using the collected EV data (see Figure 4-20). Please note that the y axis for PKE

is positive and NKE is negative. As we can see from these three sub figures, the curve in Fig. 4-20c is the sum of curve in Fig. 4-20a and Fig. 4-20b. Therefore, the trend in Fig. 4-20c can be explained by combining the trend in Fig. 4-20a and Fig. 4-20b And the trend in Fig. 4-20c is quite similar to that in Fig.17, which is also a "W" shape (Note: all these 3 figures are fitted separately from raw data, hence they are not likely to be exactly the same). This implies that PKE+NKE is a good indicator for EV energy consumption under real world congestion. In other words, ECR by average speed under real-world congestion can be decomposed by PKE and NKE. This is an evidence for the previously proposed hypothesis presented by Equation. (15) based on fundamental physics.

More specifically, as shown in Figures 4-20b, there is drop in NKE when the average speed is lower than 10 mph, which coincide with the first drop in Figure 4-17 around the average speed of 10 mph. This drop in NKE actually means the increase of collected energy from RB, which is due to the high frequency of stop-and-go in this low speed region. We can also see that PKE deceases after 30 mph. This can be explained by lower speed fluctuation after 25 mph (see Fig.4-16). After 60mph, although the speed fluctuation is still at a low level, but the high speed cruise results in higher power demand and therefore the ECR is increased again as shown in Fig.4-18. In summary, the "W" shape in EV energy consumption comparing to that of gasoline vehicle is mainly due to the NKE drop at the low average speed which results from the regenerative braking.

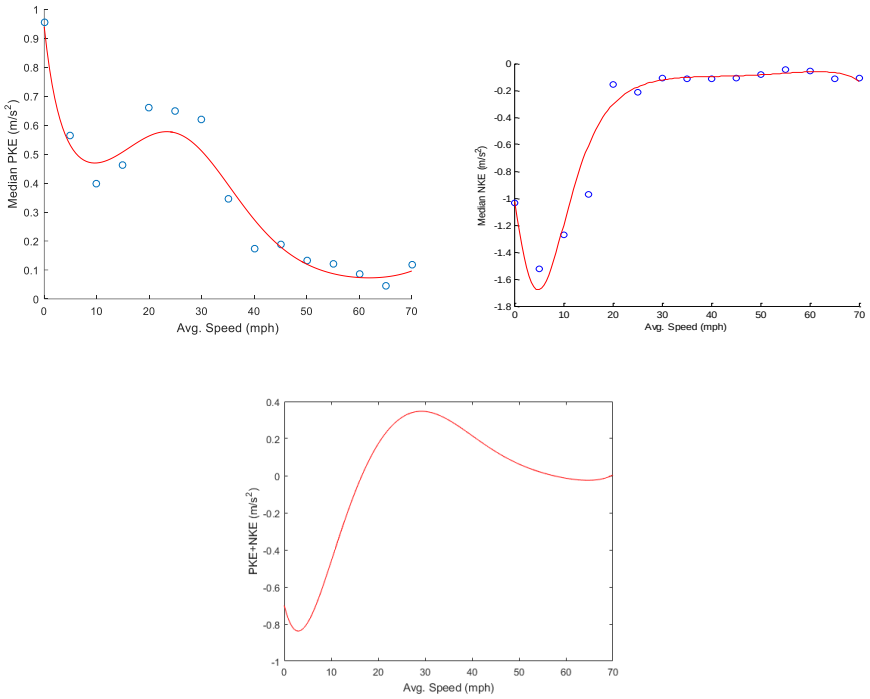

a. PKE b. NKE
c. PKE+NKE

Figure 4-20 Polynomial fit of PKE, NKE and PKE+NKE by average speed.

4.3.5 Feature Selection and Analysis

Principal components analysis for feature selection/analysis

To analyze the importance of different predicting variables for estimating EV link-level energy consumption, and to provide further convincing data-driven evidence for our previous discussions, principal component analysis (PCA) [102] is utilized to numerically study the significance of each variable. PCA is a statistical procedure that uses an orthogonal transformation to convert a set of observations of possibly correlated variables into a set of values of linearly uncorrelated variables called principal components (PCs). Through such transformation, the first principal component normally has the largest possible variance (that is, accounts for as much of the variability in the data as possible), and each succeeding component in turn has the highest variance out of the rest of components. The resulting vectors

are an uncorrelated orthogonal basis set. PCA is sensitive to the relative scaling of the original variables, hence the original values for all variables have been normalized into the same scale.

Suppose $\boldsymbol{X}^T$ =($X_1, X_2 \ldots, X_p$) is an random vector that represents all the predicting variables. p is the number of predicting variables. $\sum$ =Var(**X**) is the $p \times p$ variance-covariance matrix. (λ_i, e_i) for i = 1, ... p are the eigenvalue and the associated eigenvector, and $\lambda_1 \geq \cdots \geq \lambda_p \geq 0$. For p variables, we can construct p PCs, Y_1 ... Y_p , each of which is a linear combination of the original set of variables:

$$Y_1 = \boldsymbol{\alpha}_1^T \boldsymbol{X} = a_{11}X_1 + \ldots + a_{1p}X_p$$

$$Y_2 = \boldsymbol{\alpha}_2^T \boldsymbol{X} = a_{21}X_1 + \ldots + a_{2p}X_p$$

…

$$Y_p = \boldsymbol{\alpha}_p^T \boldsymbol{X} = a_{p1}X_1 + \ldots + a_{pp}X_p$$

then

$$\text{Var}(Y_i) = \boldsymbol{\alpha}_i^T \sum \boldsymbol{\alpha_i}$$

$$\text{Cov}(Y_i, Y_k) = \boldsymbol{\alpha}_i^T \sum \boldsymbol{\alpha_k}$$

All these constructed PCs are orthogonal to each other such that $\|\boldsymbol{\alpha}_i\|^2 = \boldsymbol{\alpha}_i^T \boldsymbol{\alpha}_i = 1$. And a larger weight indicates a greater importance of that variable in a PC. Each PC is obtained by:

$Y_i = \boldsymbol{\alpha}_i^T \boldsymbol{X}$= such that Var($Y_i$)= $\boldsymbol{\alpha}_i^T \boldsymbol{\alpha}_i = max_{\|\boldsymbol{\alpha}\|=1}\, \boldsymbol{\alpha}^T \sum \boldsymbol{\alpha}$ **,** with $\boldsymbol{\alpha}_i^T \sum \boldsymbol{\alpha_j}$ **= 0 for** j=1, …, i-1

Actually, $\boldsymbol{\alpha}_i = \boldsymbol{e}_i$, *for i=1, ..., p* and $Y_i = \boldsymbol{e}_i^T \boldsymbol{X}$ and Var(Y_i) = λ_i.

In this work, we take 7 predicting variables (shown in Table 4-1) as the original variables and conduct the principal components analysis. The following table gives coefficients of all the PCs. It can be observed that NKE and PKE are the first two PCs with the largest variance.

Table 4-1coefficients of principle components

Variables	**PCA coefficients**						
	PC1	*PC2*	*PC3*	*PC4*	*PC5*	*PC6*	*PC7*
Road type	-0.08936	0.180285	0.120264	0.376948	**0.89605**	0.007005	-0.00216
Road grade	-0.00903	0.001795	-0.07008	**0.785232**	-0.13896	7.30E-05	0.000419
Avg. speed	-0.13645	0.42776	**0.99019**	0.011401	-0.4206	0.00016	-0.00017
PKE	0.11785	**0.885204**	0.007689	-0.44944	0.021687	-0.00024	-0.00076
NKE	**0.97950**	-0.03045	0.00941	0.197959	0.019273	-0.00056	0.000278
Acum Acc.[103]	-0.00088	0.001518	0.000231	0.001664	0.004372	-0.42387	**0.905709**
Acum.Dec.[103]	0.00094	-0.00054	-0.00088	-0.00227	-0.00478	**0.905695**	0.423894

The trace of a symmetric matrix is the sum of its eigenvalues $\lambda_1 \geq \cdots \geq \lambda_p$. Thus the total variance is

$$\mathrm{tr}(\sum) = \lambda_1 + \cdots + \lambda_p$$

Since covariance matrix $\sum$ is positive-semidefinite, the total variance is non-negative and the first *k* PCs make up

$$\left(\frac{\lambda_1 + \cdots + \lambda_k}{\lambda_1 + \cdots + \lambda_p} * 100\%\right)$$

of the total variance (in particular, they make up 100% of the total variance when *k*=*p*). As we can see in Fig 4-21, the first two PCs make up over 80% of total variance. This indicates that NKE and PKE are the most significant predicting variables for estimating link-based EV energy consumption.

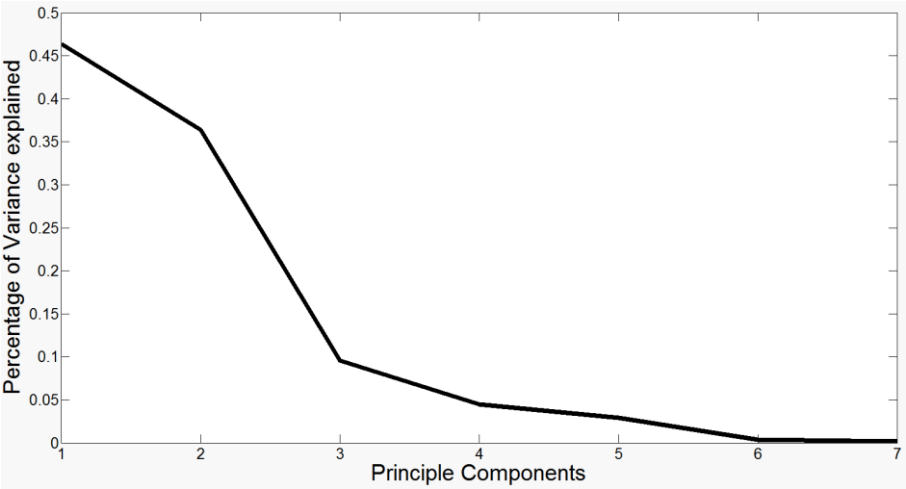

Figure 4-21. Percentage of variance explained by different impact factors.

Decision Tree Analysis for Energy Consumption

Decision tree builds regression or classification on models in the form of a tree structure [105, 106]. It breaks down a dataset into smaller and smaller subsets while an associated decision tree is incrementally developed. The final result is a tree with *leaf nodes* and *branches*. In these tree structures, leaves represent class labels and branches represent conjunctions of features that lead to those class labels. The topmost decision node in a tree which corresponds to the best predictor called root node. Decision trees can handle both categorical and numerical data. Decision trees where the target variable can take continuous values (typically real numbers) are called regression trees. In this work, a regression tree model is used to analyze the energy consumption predicting variables.

There are two important process in building a regression tree. One is the optimal partition of each variable in the continuous range, and the other one is to choose the best variable for splitting the data set at each *leaf node.* In this study, the entropy based information gain is adopted as the criteria for optimally splitting the dataset on different attributes (i.e., predicting variables). And the Gini index [107] is used for choosing the best variable at each *leaf node* to obtain the largest standard deviation reduction.

In regression tree, the continuous variables are first discretized into multiple intervals, and then an optimal partition is selected based on information gain criteria. Given a set of samples *S*, if *S* is partitioned into two intervals *S1* and *S2* using boundary *T*,

Entropy is calculated based on class distribution of the samples in the set. Given *m* classes, the entropy before the partition is

$$Entropy(S) = -\sum_{i=1}^{m} p_i \ log_2(p_i)$$

the entropy after partitioning is:

$$I\ (S,T) = \frac{S_1}{S} Entropy(S_1) + \frac{S_2}{S} \text{Entropy}(S_2)$$

where p_i is the probability of class *i* in *S*. Therefore, the informaton gain is obtained by:

$$Gain(T)=Entropy(S) - I\ (S,T)$$

To select the best attribute for each *leaf node*, the Gini index[25] is used in this study and calculated by

$$\text{Gini}(D)=1-\sum_{j=1}^{n} p_j^2$$

where *D* is the data set which contains examples from *n* classes, p_j is the relative frequecny of class *j* in *D*. If a data set *D* is split on A into two subsets D_1 and D_2 , the Gini index is defined as

$$Gini_{After}(\text{D}) = \frac{D_1}{D} Gini(D_1) + \frac{D_2}{D} \text{Gini}(D_2)$$

The reduction in impurity is

$$\Delta Gini(D)=Gini(D) - Gini_{After}(D)$$

The variable providing the smallest reduction in impurity is chosen to split the node. Figure 4-22 presents the first three layers of the constructed regression tree. The values on the branches

are the optimal split on the predecessor node. It is noted that the most important 2 variables are NKE, PKE. The 3-D plot of ECR on PKE/NKE (Fig. 4-23a) and partition (Fig. 4-23b) based on the decision tree analysis is provided in Fig.4-23. It can be seen that the ECR distribution is partitioned into four major regions. Region A (average 0.02) represents the driving situation where PKE and NKE are both not too high. This region corresponds to the low speed driving scenarios. Also, a larger variation is witnessed in this region, which can be explained by the frequent fluctuation in driving under low (average) speed traffic conditions. Region B (average 0.71) where PKE is high but NKE is low represents the set of driving scenarios when acceleration maneuvers dominate. In contrast to Region B, Region C (average -0.31) is mainly characterized by deceleration maneuvers. Region D (average 0.24) is just in the middle between region B and C. Please note that the boundary between D and C is because of the road grade (cut by -0.014 as shown in Fig 22). And also this boundary does not have to be exactly a straight line but it reflects the basic difference between region C and D.

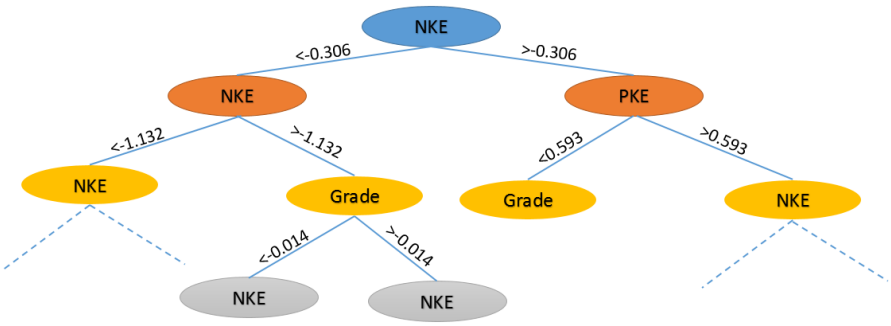

Figure 4-22 Decision tree built from the real-world driving data (top 3 layers)

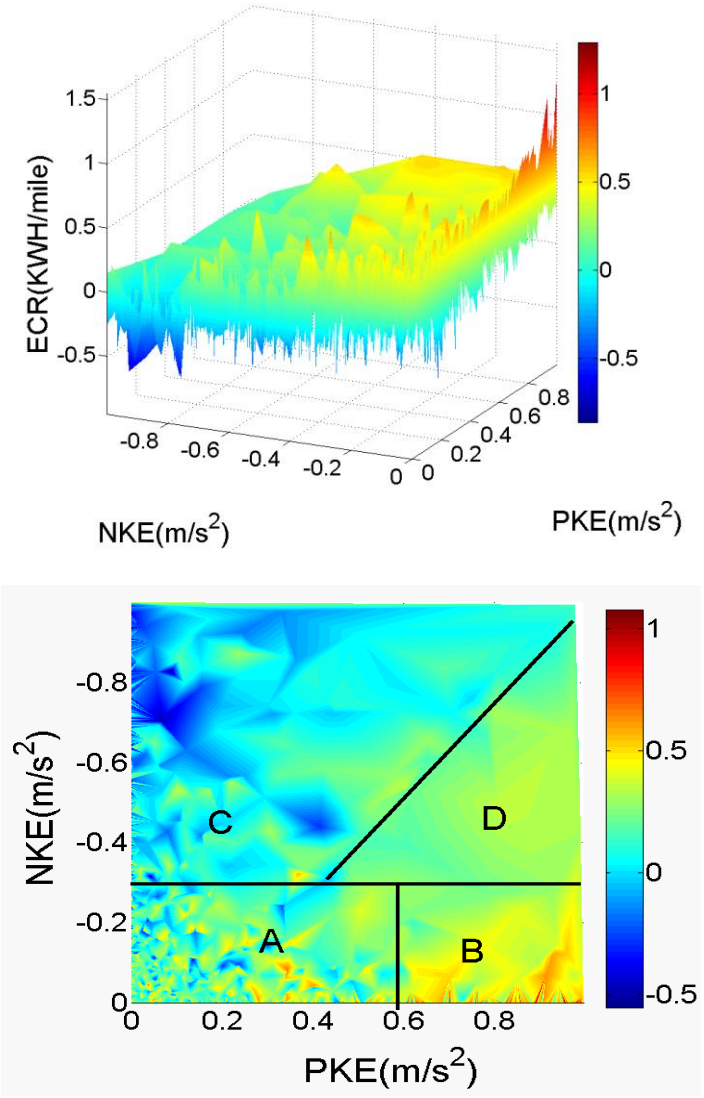

a. 3-D plot of ECR by PKE/NKE b. ECR partition based on decision tree

Figure 4-23 ECR partition based on decision tree analysis

Model Fitting and Comparison

Beyond the abovementioned factor analysis, three different types of link-level EV energy consumption models with different levels of information availability are proposed and compared (see Table 4-2). Specifically, Model type 1 takes the compound factors PKE and NKE as the only predicting variables; Model type 2 uses a 4^{th} order polynomial of average speed. Lastly, Model type 3 uses all the possible raw factors as predictors, such as average

speed, PKE, NKE, road type, road grade, accumulated accelerations and accumulated decelerations. To better capture the different relationship (linear or nonlinear) between the predictors and energy consumption rate, for each type of model, both a regression fitted model and an artificial neural network fitted model are built. Please note that Model type 1 is proposed in this study and model type 2 & 3 are regarded as baseline models to represent the similar existing models that discussed in [16, 24].

Table 4-2 estimation models

Model type	Predictors
1	PKE, NKE
2	Avg. speed (up to 4th order)
3	Avg. speed, Acc.Acc, Acc.Dcc, road grade, road type

The performance of the four models was evaluated based on the estimation error that is defined in terms of symmetric mean absolute percentage error [101], or SMAPE:

$$SMAPE = \frac{\sum_{t=1}^{n}|E_t - A_t|}{\sum_{t=1}^{n}|A_t + E_t|}$$

where n is sample size, which is also the total number of road link that data were collected from; A_t is the actual energy consumption on road link *t*; and E_t is the estimated energy consumption on road link *t*. When building the model, 70% of the data set is used for training and 30% for model testing. For ANN models, 1 hidden layer and 5 hidden neuros are chosen after a parameter tuning process. The details will not be presented here due to space limit. Table 3 summarizes the error statistics, where the best estimation is achieved by type 1a and 1b models with less than 5% of SMAPE, in spite of their simplicity. This result further verifies the findings in previous discussion that PKE and NKE are the most powerful compound indicators of link-level EV energy consumption when link-level typical vehicle speed trajectories are known (or just PKE and NKE is known). A hypothesis is that the EV test driving was conducted

at a relatively flat terrain. The polynomial regression in type 2 model achieves the second best performance (both fall into the error range of 10%) indicating that average speed is also a strong and effective indicator when only link-level average speed is available (e.g., based on measurements from the loop detectors). Type 3 models have the worst performance which is due to the fact that more prediction variables may introduce more noise. In addition, this model in real-world applications may require high-resolution data which are usually not available.

Table 4-3 Estimaton performance

Model type	**Regression**		**Neural Network**	
	R-square	Error	R-square	Error
1	0.8019	4.93%	0.8076	4.97%
2	0.6162	6.94%	0.6099	9.81%
3	0.5909	15.11%	0.5801	12.55%

Model Application and Trip Level Validation

The proposed link-level EV energy consumption estimation model 1 is applied to a crowd-sourcing data based eco-routing system as shown in Fig 4-24. All the EVs equipped with the routing system are connected through the mobile network. For each vehicle, the abovementioned best model (the regression model of Type 1b) is trained with its own driving data collected on different road links using the same technology as described in Section 2. Please note that for each link, a model 1 can be built if the data is available. Once the model is built, the energy consumption on a selected route will be estimated using the estimation model with the crowd sourced PKE and NKE data from other vehicles on the road links at the time when selecting the route.

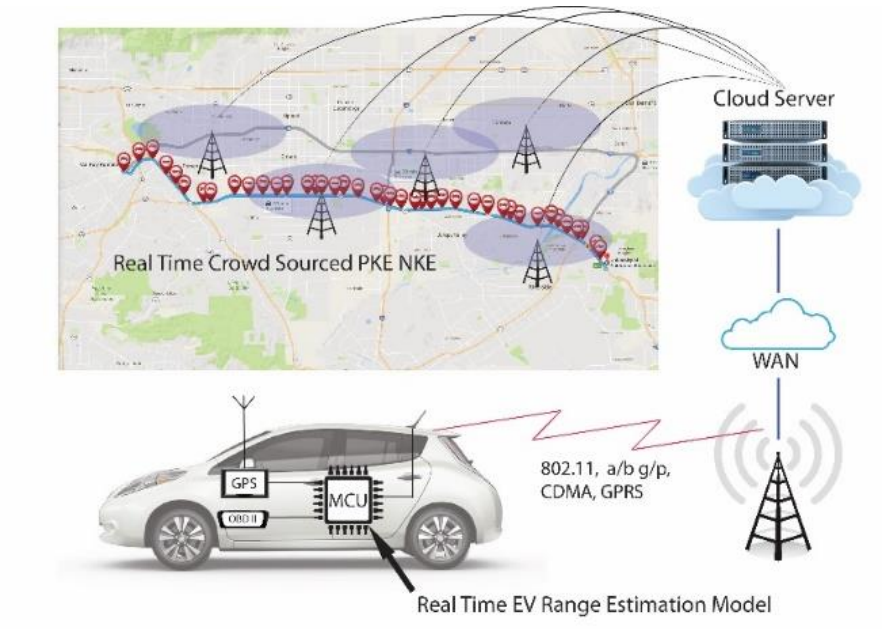

Figure 4-24 crowd-sourced EV link level energy consumption estimation

Therefore, we are also interested in knowing the performance of the proposed models in estimating the total energy consumption of complete trip. The estimated total energy consumption of a trip is simply a sum of estimated energy consumption of all the road segments in that route. Figure 4-25 shows an example trip with the plotted actual energy consumption and estimated energy consumption with regression model of type 1b for each road link. For comparison purpose, results from models with better performance of each type (see Table 4-3) are plotted in Figure 26. It is observed that type 1 is the closest curve to the actual energy consumption.

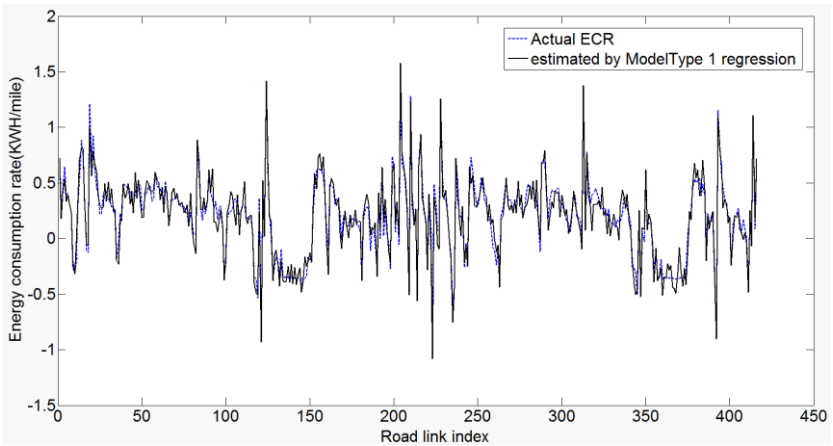

Figure 4-25 comparison between actual energy consumption and estimated

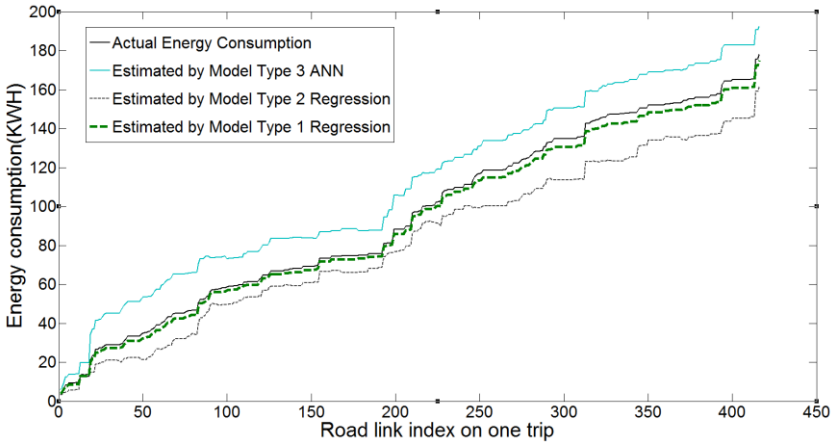

Figure 4-26 Accumulated energy consumption on a trip

4.3.6 Summary and Discussion

In this work, the EV energy consumption on a road link in real-world traffic congestion is first decomposed based on fundamental physics. Then, with the real-world EV driving data, a data-driven energy consumption decomposition analysis is conducted by analyzing two newly constructed compound factors: positive kinetic energy (PKE), and negative kinetic energy (NKE). The NKE is analyzed and related to the regenerative braking power collection characteristics. The energy consumption rate curve along the average speed is constructed and a "W" shape curve is discovered and explained with real-world driving data. An accurate and simple EV energy consumption estimation model is built upon this decomposition and the feature selection analysis also prove the significant effectiveness of these two constructed factors. The comparison to the existing models shows that the proposed model outperforms the others in terms of both accuracy and simplicity. These models can be used to support the energy consumption estimation in eco-routing systems for electric vehicles as well as many other on-board, low cost ecodriving applications. The future work would be focused on applying the proposed model into a ecorouting system and testing the system in real-world driving.

4.4 Microscopic EV Energy Consumption Estimation Model

Besides the macroscopic EV energy consumption estimation model designed in previous section, a microscopic estimation of EV energy consumption using real-world driving condition data (e.g., vehicle speed trajectory) is also critical in evaluating the energy performance of different ecodriving technologies when calculating the second-by-second energy consumption. In this study, a microscopic EV energy consumption estimation model developed in [68] is adopted to calculate the EV energy consumption based on the vehicle speed profiles. This model is designed for 4 different EV driving conditions: accelerating, decelerating, cruising and idling. The final model is presented as follows:

$$ECR = \begin{cases} e^{(\sum_{i=0}^{3}\sum_{j=0}^{3}(l_{i,j}\times v^i\times a^j))} & a > 0 \\ e^{(\sum_{i=0}^{3}\sum_{j=0}^{3}(m_{i,j}\times v^i\times a^j))} & a < 0 \\ e^{(\sum_{i=0}^{3}(n_i\times v^i))} & a = 0, v \neq 0 \\ \overline{const} & a = 0, v = 0 \end{cases} \quad (4\text{-}13)$$

where *ECR* is energy consumption rate (Watt); $l_{i,j}, m_{i,j,}$ and n_i are coefficients for ECR at speed power index *i* (i= 0, 1, 2, 3) and acceleration power index *j* (= 0, 1, 2, 3); *v* is instantaneous speed (km/h); *a* is instantaneous acceleration (m/s^2); $\overline{const}$ is the average energy consumption rate for idling. The coefficients in this model were obtained through training with real-world driving data and can be found in [68].

4.5 Connected Ecodriving Assistance without Considering Driver Error

In this section, a connected EAD assistance system is designed for EV at signalized intersections to achieve the most energy efficient driving. As a baseline system, an open-loop system without considering the driver error is designed for the purpose of comparison. As can be seen in Fig.4-27, a vehicle trajectory planning algorithm (VTPA) is designed for generating an optimal velocity profile based on real-time SPaT information. The calculated real-time

optimal speed is advised to the human driver through an in-vehicle advising display. Then the human driver controls the actual vehicle speed by the gas pedal and brake.

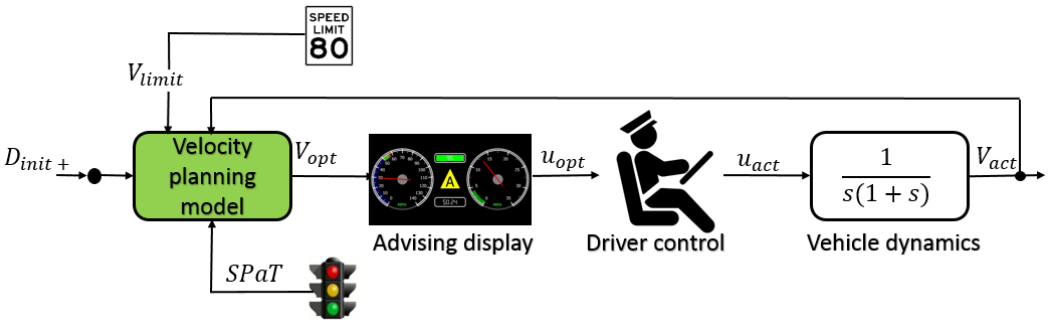

Figure 4-27 Control flowchart of EAD system without considering driver error

As explained in the Fig.4-35, there could be different scenarios for vehicles passing through a signalized intersection. Among all the possible velocity profiles with which a vehicle can safely travel through an intersection, the VTPA can choose the velocity profile that has minimum tractive power requirements, in order to minimize energy consumption. For a given passing scenario, the speed profile to approach and depart from the intersection is calculated by the distance to intersection d, desired time-to-arrival T, and current speed vc, based on the trigonometric model developed in our previous work [134]. For the acceleration, deceleration, or full-stop scenario (i.e. Vehicle 2, 3 or 4), the vehicle speed v at time t is decided by the following equation:

$$v = \begin{cases} v_h - (v_h - v_c) - \cos(mt) & t \in \left[0, \frac{\pi}{2m}\right) \\ v_h - (v_h - v_c) \cdot \frac{m}{n} \cos n(t - \frac{\pi}{2m} + \frac{\pi}{2n}) & t \in \left[\frac{\pi}{2m}, \frac{\pi}{2m} + \frac{\pi}{2n}\right) \\ v_h + (v_h - v_c) \cdot \frac{m}{n} & t \in \left[\frac{\pi}{2m} + \frac{\pi}{2n}, \frac{d}{v_h}\right) \\ v_h + (v_h - v_c) \cdot \cos m(t - \frac{d}{v_h} - \frac{\pi}{2m} + \frac{\pi}{2n}) & t \in \left[\frac{d}{v_h} + \frac{\pi}{2n}, \frac{\pi}{2m} + \frac{\pi}{2n} + \frac{d}{v_h}\right) \\ v_c & t \in \left[\frac{\pi}{2m} + \frac{\pi}{2n} + \frac{d}{v_h}, +\infty\right) \end{cases} \quad (4\text{-}14)$$

where v_c is the current speed, $v_h = d/T$ is the uniform speed; n is the maximum value that satisfies

$$\begin{cases} |n \cdot (v_h - v_c)| \le a_{max} \\ |n \cdot (v_h - v_c)| \le d_{max} \\ |n^2 \cdot (v_h - v_c)| \le jerk_{max} \\ n \ge \frac{\frac{\pi}{2}-1}{T} \end{cases} \quad (4\text{-}15)$$

and

$$m = \frac{-\frac{\pi}{2}n - \sqrt{\left(\frac{\pi}{2}n\right)^2 - 4n^2 \cdot \left[\left(\frac{\pi}{2}-1\right) - T \cdot n\right]}}{2\left[\left(\frac{\pi}{2}-1\right) - T \cdot n\right]} \quad (4\text{-}16)$$

Here parameters m and n determine the shape of the speed profile. They are also the dominant variables to control the energy efficiency of the acceleration and deceleration process. In our previous work [26], results indicated that if m and n satisfy Eq. (2) and (3), then the tractive power (of a generic vehicle model) would be minimized without compromising the driving comfort and acceleration/ deceleration capability. This designed trigonometric model was tested with ICE vehicles in our previous work [26] which has achieved 10-15% fuel savings when crossing the intersections. In this study, it is expected that this model can also help EV improve its fuel efficiency by providing smooth and energy efficient speed trajectory at intersections.

4.6 Connected Ecodriving Assistance with Considering Driver Error

As mentioend in chapter 1, air pollution and climate change impacts associated with the fossil fuel use in transportation have continued to attract public attentions due to its close relation to peoples' everyday life. Current research has tried the following ways to address the issues from vehicle, infrastructure, and human driver perspectives:

1) Building more energy efficient vehicles, which involves creating alternative fuel powered powertrain system (e.g., electric vehicles (EVs)) and designing more efficient powertrain control systems to achieve higher fuel economy, such as the energy management system (EMS) for plug-in hybrid electric vehicles (PHEVs) [111-113]. This could also involve analyzing the unique characteristics of a specific type of powertrain that would greatly impact the energy efficiency of that type of vehicle, e.g., the regenerative braking (RB) for EVs.

2) Taking advantage of transportation infrastructure. In recent years, applying advanced intelligent transportation system technologies to result in more energy efficient driving is one of the most popular research areas, for example, reducing traffic congestion or unnecessary stop-and-go behaviors at signalized intersections in arterials by using vehicle-to-infrastructure wireless communication. It is reported that nearly 7 billion hours of delay and more than 3 billion gallons of fuel were wasted in 2015 due to traffic congestion in the U.S. [114], a significant portion of which is due to getting stuck at traffic signals. Various types of applications are designed to address such issue, for example, Eco-approach and departure system [108] is developed to help vehicles achieve a smooth travel and avoid unnecessary idling by calculating the most energy efficient speed profile to pass through the intersections by obtaining the signal phase and timing information (SPaT) from upcoming traffic signals.

3) Analyzing the impact of human driving behavior on vehicle energy consumption. Driving behavior has been proved to influence the vehicle energy consumption [115]. For example, the unnecessarily aggressive acceleration and decelerations could result in additional energy consumption. Some efforts have been put in training the drivers to have good driving habit through the Ecodriving training programs [115].

In recent years, transportation electrification has been a very active research area. Gradually replacing conventional vehicles with electric vehicles (EVs) is a promising way to reduce fossil fuel consumption and pollutant emissions in the transportation sector, since electricity can be

much cleaner than fossil fuels since it can be converted from the renewable and clean energy, such as solar and wind energy. However, the massive adoption of EVs is impeded by the limited charging infrastructure and limited cruise range per charge. This also usually causes the driver's anxiety which is called "range anxiety" [116]. There have been many efforts to improve the performance of EVs by overcoming technical barriers such as battery technology limitations [117] and charging infrastructure problems [118]. However, very limited amount of effort so far has been focused on how to improve the energy efficiency of the EVs through vehicle connectivity and automaton. Furthermore, there has been no effort to investigate the dynamic interaction between vehicles, infrastructure and human drivers and its impact on the energy efficiency of EV driving.

Toward this end, to fill the research gap and address the above-mentioned issues, in this study, a driver-vehicle-infrastructure cooperative system for EV energy efficient driving is proposed. As an example and demo, a driver-in-the-loop EAD assistance system considering human driver error is designed and tested for EVs which is also compared with an open-loop EAD system not considering human driver error. The designed system is capable of estimating the human driver error and adjusts to the error to mitigate the negative impact of human error and achieve the maximum energy efficiency benefits. Real-world driving data were collected for performance evaluation, by comparing the resulted energy benefits. There are several major contributions of this study;

- A driver-vehicle-infrastructure cooperative system framework for energy efficient driving is proposed.
- A first-of-its-kind EAD assistance system considering driver error is designed for EVs and evaluated with real human driver data.
- The energy benefits of the designed system are evaluated with the real-world driving data and compared with different baseline scenarios.

4.6.1 Overview

Human Factor in Ecodriving Technology

Thus far, most of the current connected ecodriving assistance technologies are based on the assumption that the vehicle is either in full control or that the driver follows the instruction precisely, which is actually hard to realize with human driver control. In our previous study, the energy benefit of an EAD system for ICE vehicles at actuated signal environment reaches 10% [129] but only 2% can be achieved real-world test driving [130]. This decrease in energy benefit is at least partially due to the error when human driver following the instructions. However, to the best of our knowledge there have been very few efforts on building a driver behavior model on following a speed trajectory. A proportional-integral-derivative (PID) function is proposed to simulate such kind of deriver's behavior [131]. The simulation results show 4% of energy savings comparing to the model without considering the human driver error. One possible issue in applying such model is the difficulty in identifying the appropriate proportional, integral and derivative coefficients that reflect different driving habits. In addition, this PID model does not consider the expected human error in the multiple future steps and no optimization is conducted according to the human driver error. To address these issues, this work proposes a Markov chain based driving error estimation model which is able to be adaptive to the changing driving behavior and also estimate the future driver error in multiple time steps. More details are given in the following sections.

Connected Ecodriving Technology for EVs

Despite the abovementioned efforts on connected ecodriving systems for ICE vehicles, very few are focused on designing such driving assistances system for EVs when approaching a signalized intersection to save electricity consumption. [132] applied a dynamic programming (DP)-based model to develop ecodriving systems for EVs along signalized arterials. The

proposed model was tested in the simulation with very limited signal phase conditions. In a recent study [133], the authors developed an EAD system for EVs based on their own EV energy consumption estimation model, where the validation was also conducted in a simulation environment under 4 very simple scenarios with different signal phases. To the best of our knowledge, there has been no research that investigates the ecodriving system for EV with real-world driving data. There is no effort on modeling the human driver error in ecodriving technology for EVs either. The objective of this study is to fill these gaps.

4.6.2 Methodology

Vehicle-Driver-Infrastructure Cooperative System for Energy Efficient Driving

There are various types of impact factors that influence the energy consumption of vehicles, which can be mainly classified into the following categories (see Fig. 4-35.):

- Vehicle-related: many vehicle-related factors could influence the energy consumption, such as the powertrain type (i.e., ICE or EV), powertrain efficiency and vehicle mass etc.
- Driver-related: the driving behavior (e.g., acceleration and deceleration profile) is the major human related impact factor for vehicle energy consumption. This is especially important for EVs due to the unique regenerative braking feature.
- Infrastructure-related: Traffic signal is one of the major infrastructures that would influence vehicle energy consumption due to stop-and-go behavior at signalized intersections.

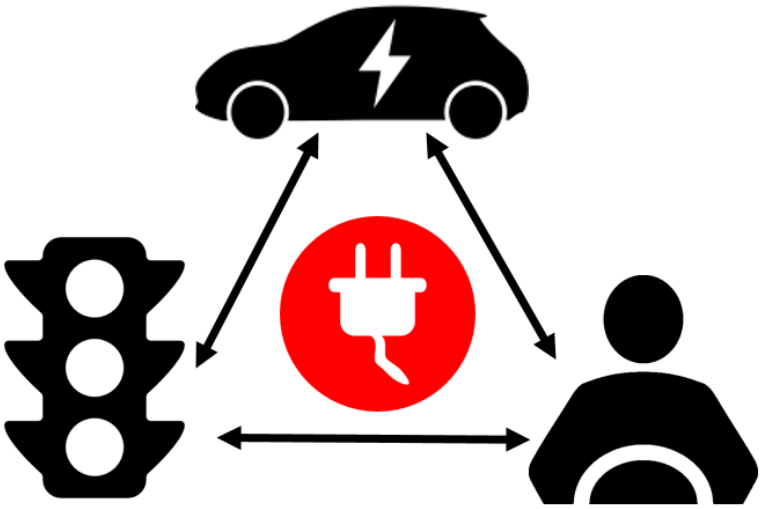

Figure 4-28 Three class of factors that impact EV energy consumption

In order to maximize the energy efficiency of EVs by considering all the impact factors above, a vehicle-driver-infrastructure cooperative system is designed for energy efficient driving (see Fig. 4-36) in the connected vehicle environment.

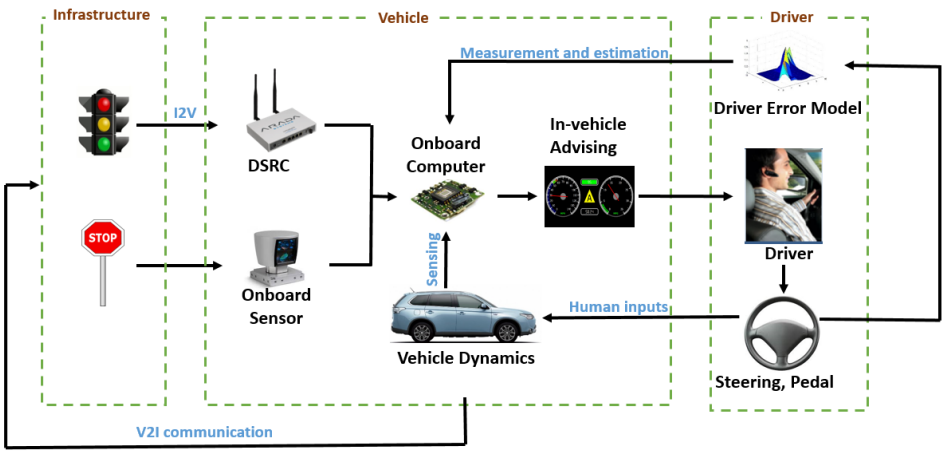

Figure 4-29 A Vehicle-Driver-Infrastructure Cooperative framework for energy efficient driving.

In the connected vehicle environment, a vehicle equipped with wireless communication devices can share its location, speed, heading, and many other data in real time with nearby equipped vehicles and the surrounding infrastructure via wireless communications. Therefore, in the designed cooperative system, the vehicle and infrastructure are tightly integrated by taking

advantage of advanced wireless communications, high accuracy positioning, and onboard sensing technology. In addition, the impact of driving behavior is also integrated into the framework by modeling and estimating the driver error in the in-vehicle advising driving. Human driver is involved in this framework; hence it is designed for driving assistance rather than fully autonomous driving.

In the designed cooperative system, the interaction between every two objects (e.g., between infrastructure and vehicle) are all bidirectional (see Fig.4-35). For example, vehicles can adjust its speed according to the signal phase and timing. The traffic single is also able to adjust its signal phase and timing according to the vehicle states at the intersection (e.g. traffic signal priority). Based on this proposed cooperative system, this study aims at designing a driver-in-the-loop adaptive connected ecodriving assistance system that considering the driver error for electric vehicles. As a baseline for comparison, an open-loop ecodriving assistance system without considering driver error is also designed and discussed.

Driver error modeling with Markov Chain Model

A nonlinear vehicle longitudinal dynamics model [27] is adopted in this work:

$$\dot{x} = v, \tag{4-17a}$$

$$\dot{v} = -\frac{1}{M} C_D \rho_a A_v v^2 - \mu g - g\theta + u_f, \tag{4-17b}$$

$$u_f = u + w \tag{4-17c}$$

where x is position of the vehicle; v is velocity; M is mass; θ is road gradient ($\theta = 0$ in this work); g is acceleration of gravity (i.e., 9.8 m/s^2); u_f is braking or traction force per unit mass (i.e., the acceleration/deceleration generated from vehicle propulsion) and is considered as the sum of actual vehicle control; u is the optimal tractive fore per unit mass suggested by the driving assistance system; w is the error (m/s^2) injected by the human when trying to follow the advised u; $C_D$is drag coefficient; ρ_a is air density; A_v is frontal area of the

vehicle; and μ is rolling friction coefficient. The values of $C_D, \rho_a, A_v,$ and μ can be found in [135].

The driver error in this study is defined as the difference between the actual tractive force per unit mass and the optimal tractive force per unit distance calculated by the VTPA model. And it is generated by human drivers when trying to follow the advised vehicle dynamics displaying on the in-vehicle human-machine interface (HMI) as shown in Fig.4-38.

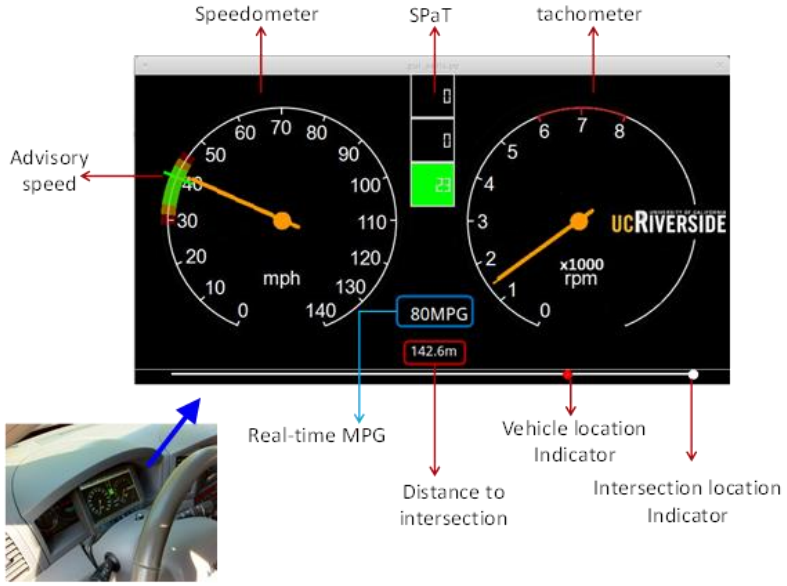

Figure 4-30 HMI interface for in-vehicle advising.

To investigate the human error in a formal way, the error is first discretized into a finite number of states N_e. When we look at the human error along the time step, it can be observed that the human error in the next time step is only depend on the current error and it is driver specific. Inspired by this Markovian property, a Markov chain model is adopted for modeling the human driver error and it can help represent the stochastic behavior of the human driver while tracking the advised command from driving assistance system.

Now the driver error dynamics is model as a Markov chain with a transition probability matrix T_e where its elements τ_{ij} represent the probability of state transition from state *i* to *j*, *i*,*j*

$\leq N_e$(see Fig. 6).

$$\begin{bmatrix} p_{11} & p_{21} & p_{31} & \cdots & p_{N_e 1} \\ p_{12} & p_{22} & p_{31} & \cdots & p_{N_e 1} \\ p_{13} & p_{23} & p_{31} & \cdots & p_{N_e 1} \\ \cdots & \cdots & \cdots & \cdots & \cdots \\ p_{1N_e} & p_{2N_e} & p_{3N_e} & \cdots & p_{N_e N_e} \end{bmatrix} \quad (4\text{-}18)$$

The transition matrix is driver specific and can be obtained from the real-world driving data collected from driving with the designed driving assistance system. Fig.4-39 provides an example on how to obtain the error from the real-world driving data.

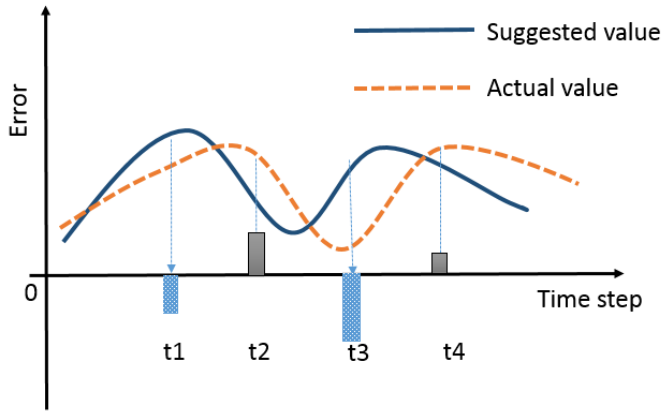

Figure 4-31 Driver error calculation

Closed-driver-in-the-loop EAD considering driver error

By taking into account the abovementioned driver error, a driver-in-the-loop based EAD system is proposed (see Fig.7). In this system, the designed VTPA is integrated with a stochastic model predictive control (SMPC) model developed to calculate the future optimal advising for EV drivers (see Figure 2) based on the estimated human driver error when following the advice, so that the resulted actual vehicle speed (with human inputs) is as close to the actual optimal

vehicle trajectory as possible. For each optimization time horizon, the future human error during that time horizon is estimated based on the learned human error probability transition matrix. From a control system perspective, the human inputted error actually is regarded as a source of disturbances. The receding horizon property of SMPC allows the system to better handle predictable disturbances. The control system diagram is provided in Figure 4-40.

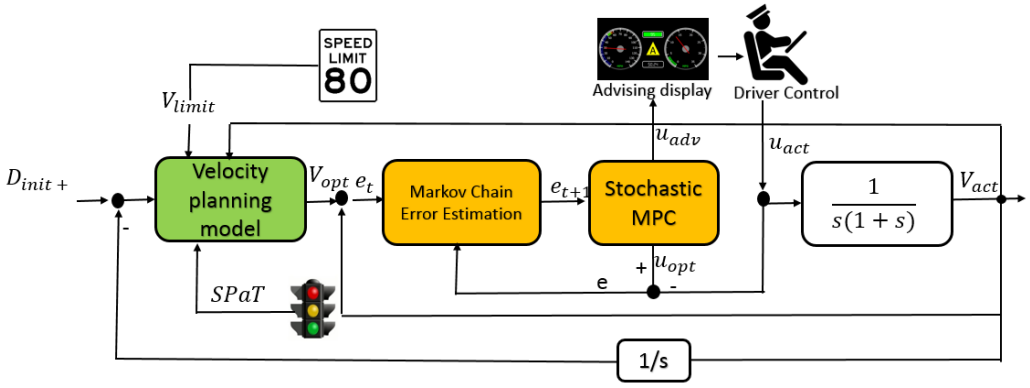

Figure 4-32 Driver-in-the-loop EAD flowchart

The above vehicle dynamics model described in eq. (4) need to be discretized as follows when implementing SMPC:

$$x(t_0 + (k+1)\Delta t) = x(t_0 + k\Delta t) + v(t_0 + k\Delta t)\Delta t, \quad (4-19a)$$

$$v(t_0 + (k+1)\Delta t) = v(t_0 + k\Delta t) + (-\frac{1}{M} C_D \rho_a A_v v(t_0 + k\Delta t)^2 \quad (4-19b)$$
$$- \mu g - g\theta + u_f(t_0 + k\Delta t))\Delta t,$$

where t_0 is starting time, Δt is sampling period, and k is time step. For brevity, we denote $x(t_0 + k\Delta t)$ as $x(k)$, $v(t_0 + k\Delta t)$ as $v(k)$, and $u_f(t_0 + k\Delta t)$ as $u_f(k)$ in the remaining parts of this work.

For each finite time horizon, different trajectory states are possible depending on different human error w at each time step. Therefore, SMPC is used to solve this optimization problem

with the uncertainty of human error during each finite time horizon. A *scenario tree* is developed consisting of different paths from the root node to the leaf nodes. The *root node* is the current state of the error *w* and the *leaf nodes* are the states reached from the current state at the end of the time horizon T. A *scenario is* defined by a path from the *root node* to *leaf nodes* with different *w* values for each time step within that time horizon. For each possible scenarios, p_s is the defined as the probability of its occurrence which is evaluated by the product of the probability of all edges in the path. Figure 4-41 provides an example of a scenario tree when N_e is 3 and only 4 time steps in the horizon:

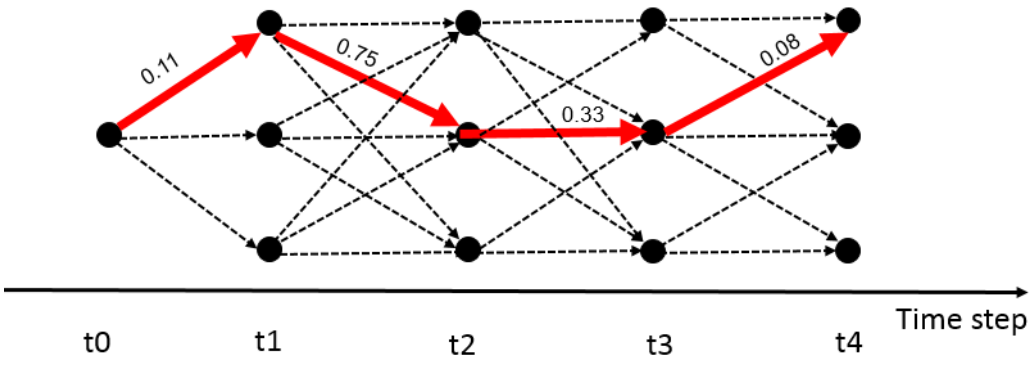

Figure 4-33 Example scenario tree

As seen in Fig.4-41, the probability of occurrence of example scenario path (with red solid arrow) is p=0.11×0.75×0.33×0.08=0.0022. This means this scenario path is not much likely to happen. When the probability of each possible path is obtained, the cost function of the optimization during that finite time horizon is defined as the expectation of total difference between the optimal speed and actual speed along that time horizon:

$$\sum_{s=1}^{N_e} p_s \sum_{K=t}^{t+l} [v(k) - v_r(k)]^2 \qquad (4-20)$$

Therefore, the objective function is defined as the sum of squared differences between the modeled and reference velocities. We also consider box constraints for the velocities,

acceleration/deceleration, and jerk values. In summary, the optimal control problem based on SMPC can be formulated as:

$$\text{argmin}_{u_f} \sum_{s=1}^{N_e} p_s \sum_{K=t}^{t+l} [v(k) - v_r(k)]^2$$

$$\text{subject to} \quad \text{the discritized dynamics } (4-19)$$

$$v_m \le v(k) \le v_M,$$

$$\left|u_f(k)\right| \le u_M,$$

$$\left|u_f(k+1) - u_f(k)\right| \le du_M,$$

where t is current time; l is optimization horizon; $v(\cdot)$ is velocity computed by the SMPC; $v_r(\cdot)$ is reference velocity; v_m is minimum allowable speed, which is set to 0 in this work; v_M is maximum allowable speed (usually the speed limit); u_M is maximum acceleration /deceleration constrained by the vehicle propulsion power; and du_M is the user-defined maximum jerk (mainly for driving comfort). We use 1 second as the time step and the control horizon of the SMPC is tunable and will be discussed later. Note that as the dynamics in Eq. (4) are nonlinear, the optimization problem at every time step of the SMPC is non-convex.

The total number of scenario paths is ${N_e}^l$, for example, if there are 10 level human error (N_e=10) and length of horizon is 10(l=10), the total number of scenario path would be 10^{10}, hence the increase of N_e and l would significantly increase the computation time, to make the solving of this optimization problem more computationally tractable, the Monte Carlo method is adopted to generate a number of realizations of scenario paths, which is shown as in

Algorithm 1: Monte Carlo method

Set the current step as 0, the last time as -1, the future time as $1,2,\cdots l-1,l$, total number of sampling paths as N_{mc}

1. Initialization: human error at last time: $error(-1)$, number of scenario paths N_{mc}
2. for $N_s = 1: N_{mc}$

a. for $t = 1: l-1$

1) generate a random number $r(t)\sim U[0,1]$

2) set $error(t)$ as the j^{th} entry in the error vector if $\sum_{k=1}^{j-1} T_e(error(t-1),k) < r(t) \le \sum_{k=1}^{j} T_e(error(t),k)$

b. end

3. end

Algorithm 1.

To solve the optimization problem in the SMPC, interior point method [28] is adopted:

For simplicity's sake on notations, we use $f(u_f)$ for the objective function $\sum_{k=t}^{t+l}[v(k)-v_r(k)]^2$, $h(u_f)$ for the equality constraints, i.e., the discretized dynamics (3), and $g(u_f)$ for the inequality constraints, i.e.,$v_m \le v(k) \le v_M$, $\left|u_f(k)\right| \le u_M$ and $\left|u_f(k+1)-u_f(k)\right| \le du_M$. So the MPC is converted to

$$\text{argmin}_{u_f} \quad f(u_f),$$

$$\text{subject to} \quad h(u_f) = 0,$$

$$g(u_f) \le 0,$$

Then we use slack variables $s = (s_1, \cdots, s_d)$ to change the inequality constraints into equality constraints, where d is the number of inequality constraints, and use barrier function to approximate the problem as below,

$$\begin{aligned} \text{argmin}_{u_f, s} \quad & f(u_f) - \rho \sum_i \log s_i, \\ \text{subject to} \quad & h(u_f) = 0, \\ & g(u_f) + s = 0, s \geq 0. \end{aligned}$$

As the problem is non-convex due to the nonlinear dynamics of (3), we use a conjugate gradient step with a trust region in [28] to optimize the problem. The basic idea is to minimize a quadratic approximation of the objective function subject to linearized constraints in a trust region.

The Lagrangian of the approximated problem is

$$L = f(u_f) + \sum_i \lambda_i g_i(u_f) + \sum_j \mu_j h_j(u_f),$$

and one of its KKT conditions (see [27] for details) is

$$\nabla_{u_f} L = \nabla_{u_f} f(u_f) + \sum_i \lambda_i \nabla g_i(u_f) + \sum_j \mu_j \nabla h_j(u_f) = 0.$$

Let the step $(\Delta \mathrm{u_f}, \Delta s)$ be taken as the one solve the KKT condition in the least-squares sense, i.e., $(\Delta \mathrm{u_f}, \Delta s)$ is the solution of

$$\begin{aligned} & \min_{\Delta u_f, \Delta s} \nabla f^T \Delta \mathrm{u_f} + \frac{1}{2} \Delta x^T \nabla^2_{u_f u_f} L \Delta \mathrm{u_f} + \rho e^T S^{-1} \Delta s \\ \text{subject to} \quad & g(u_f) + \nabla g(u_f) \Delta \mathrm{u_f} \\ & h(u_f) + \nabla h(u_f) \Delta u_f = 0, \end{aligned}$$

in a trust region $||\Delta u_f||^2 + ||S^{-1}\Delta s||^2 \leq R^2$, where $\nabla^2_{u_f u_f} L$ is the second order partial derivative of the Lagrangian L with respect to u_f, $e = (1,1,\cdots,1)$ whose dimension is the same as s, S is a diagonal matrix whose diagonal entries are those in the vector s, and Λ is a diagonal matrix whose diagonal entries are λ_i.

4.6.3 Simulation and Numerical Analysis

With the collected field driving data described in section 4.2.2, additional simulation and numerical analysis are conducted to validate the performance of the proposed system.

Driver error estimation with real-world driving data

As described in the previous section, the dynamics of human error is modeled as Markov chain. Now with the collected driving data, the probability transition matrix for each of these drivers can be built. In this study, the human error is discretized into the different levels by *[-0.4,-0.3,-0.2,-0.1,0,0.1,0.2,0.3,0.4]*.

There are 9 levels in total. Please note the actual error value would not be those exact 9 values, but we use them to best approximate the actual value. For example, when the error is between -0.1 and 0.1 we use 0 as the estimated error value.

In this work, the human driver error is extracted from the real-world with the method described in Fig.4-39 using the Stage II driving data. The probability transition matrices for each of the 4 drivers are built. For example, the transition matrix for driver 1 is given as follows and the 3-D plot is given in Fig. 4-43.

$$\begin{bmatrix} \mathbf{0.33} & 0.31 & 0.13 & 0.15 & 0.03 & 0 & 0 & 0.05 & 0 \\ 0.12 & \mathbf{0.62} & 0.26 & 0 & 0 & 0 & 0 & 0 & 0 \\ 0.04 & 0.15 & \mathbf{0.60} & 0.15 & 0.03 & 0.02 & 0 & 0.01 & 0 \\ 0.01 & 0.01 & 0.06 & \mathbf{0.53} & 0.37 & 0.02 & 0 & 0 & 0 \\ 0 & 0 & 0 & 0.07 & \mathbf{0.87} & 0.05 & 0 & 0 & 0 \\ 0 & 0 & 0 & 0.07 & 0.60 & \mathbf{0.31} & 0.02 & 0 & 0 \\ 0 & 0 & 0 & 0.06 & 0.90 & 0.24 & \mathbf{0.42} & 0.15 & 0.03 \\ 0 & 0 & 0 & 0 & 0.05 & 0.08 & 0.21 & \mathbf{0.47} & 0.18 \\ 0 & 0 & 0 & 0 & 0 & 0 & 0.10 & 0.35 & \mathbf{0.55} \end{bmatrix}$$

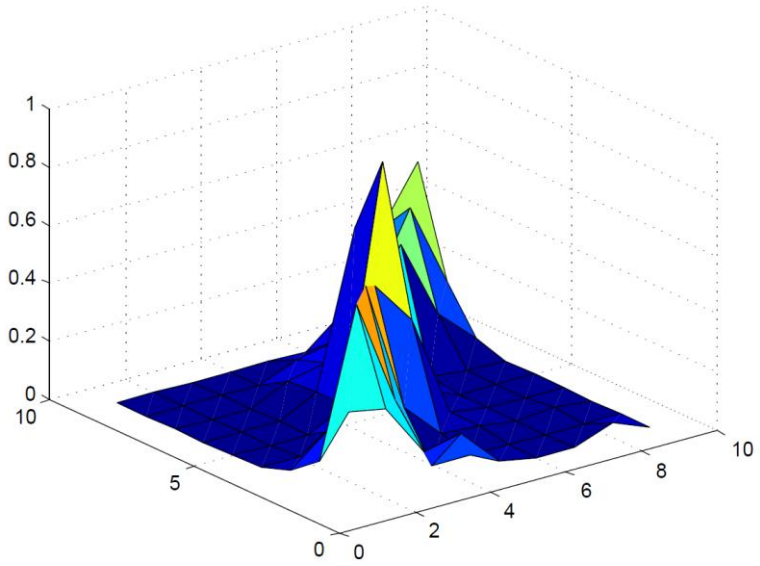

Figure 4-34 3-D plot of probability transition matrix (driver 1)

As can be seen in the transition matrix, the diagonal entries of the matrix are the biggest value for each column, which implies the latency of human driving manipulation. The human error at the immediate next step is most likely to be within the same range of the current error level. It is also noticed that different drivers have different driving behavior or habit, which results in different transition matrix patterns that can be identified by comparing Fig.4-43 and Fig.4-44.

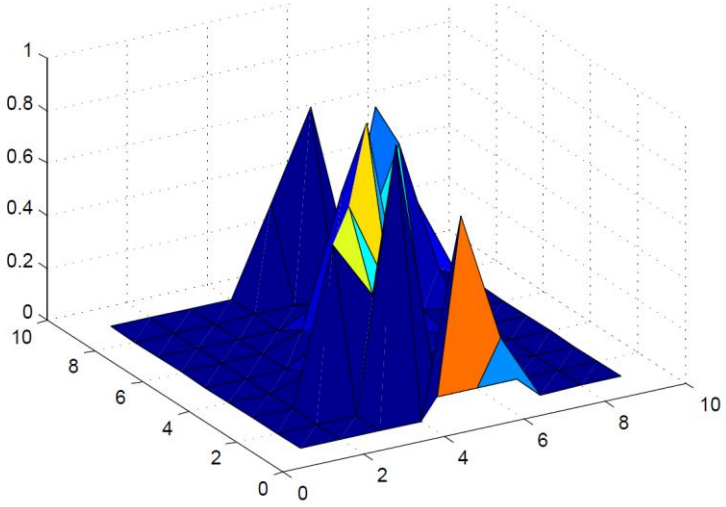

Figure 4-35 3-D plot of probability transition matrix (driver 2)

Simulation of EAD Assistance System Considering Driver Error

In this study, the Driver-in-the-loop EAD assistance system is not implemented in filed driving but simulated with the real-world driving data collected from open-loop EAD assistance system. In the simulation framework as shown in the Fig.4-45, the built human error probability transition matrix is used in two places in the simulation for different purpose. One is used to estimate the human driver error that is input for the SMPC model. Another is used to replace the real human driver who adds in error when trying to follow the advised speed. These two matrix should be from the same driver and we assume the driving habit (represented by the error probability transition matrix) is not significantly changed during the simulation time.

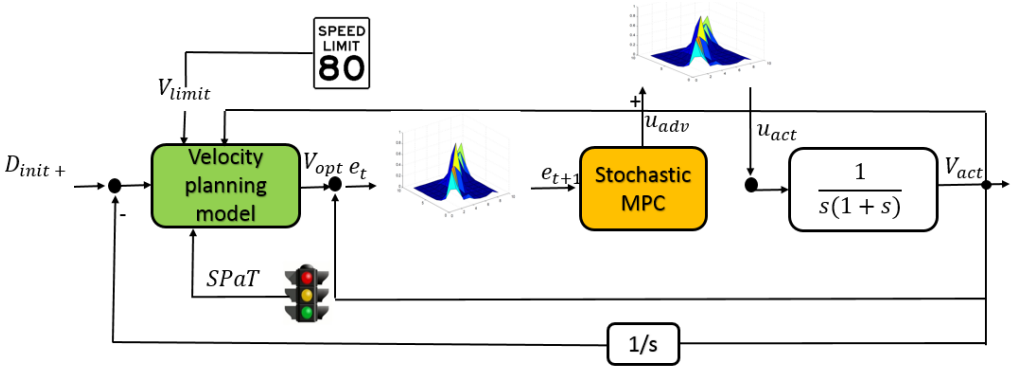

Figure 4-36 Simulation framework

To extensively evaluate the performance of EAD with driver-in-the-loop, the simulation is conducted using the field test driving data for every *entry case* described in the previous section (288 in total), so that the average performance can cover different driving conditions and different drivers. The vehicle speed trajectories obtained from the simulation are compared with that of real-world test driving. For example, the Fig.4-46 provides the vehicle speed trajectory and its reference speed trajectory in *entry case* 11. As we can see in the figure, the reference speed is adjusted or recalculated for 3 times (marked by A, B, and C in the figure) due to the increasing human driving following error. Although with the reference speed adjustment, the final driving speed trajectory is still away from the advised optimal speed due to the unavoidable human error. However, in Fig.4-47, we can see that the speed trajectory by EAD with driver-in-the-loop is overlapped with the calculated optimal speed trajectory for most of the simulation time (using the same initial speed, initial position and entry time). It is also observed that the speed trajectory resulting from EAD with drive-in-the-loop systems is much smoother than that of EAD without (shown in Fig. 48), which is a possible reason of energy saving that will be discussed in the following sections.

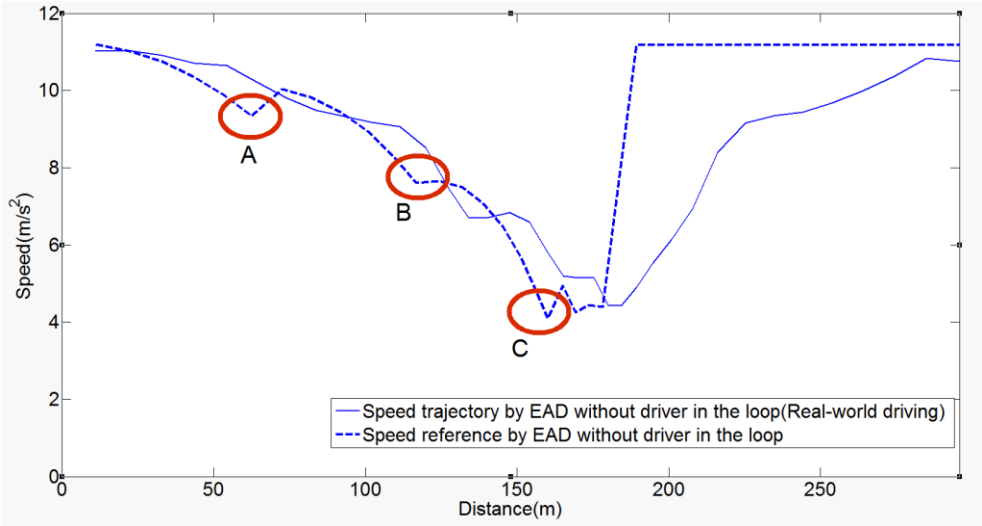

Figure 4-37 Speed trajectory of EAD without driver-in-the-loop (real-world driving by driver 1 in *entry case* 11)

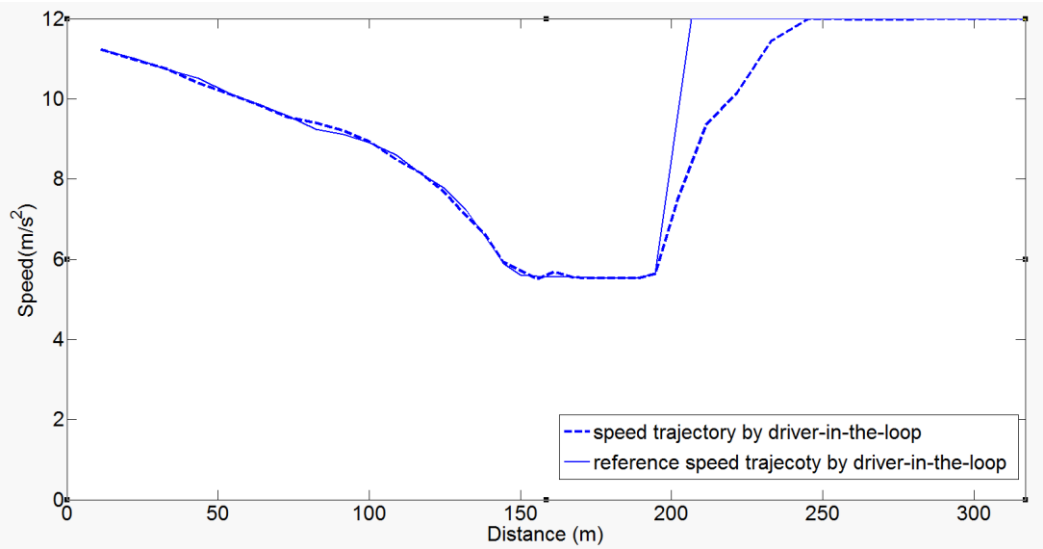

Figure 4-38 Speed trajectory of EAD with driver-in-the-loop (simulation driving)

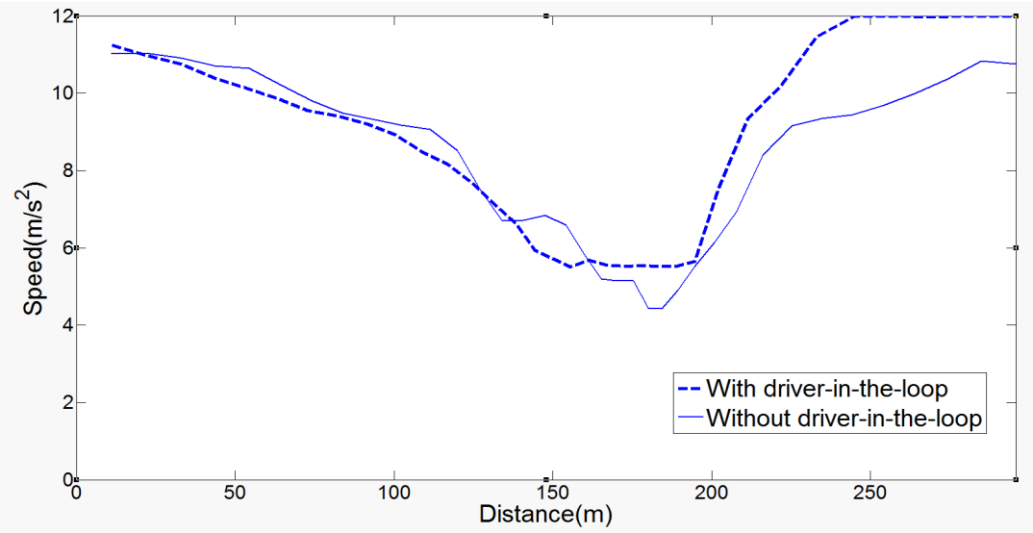

Figure 4-39 Speed trajectory of EAD with/without driver-in-the-loop

Real- time Performance and Parameter Tuning

In the implementation of the proposed SMPC system, to ensure the real-time performance, the optimization of each time horizon should be finished within one-time step (e.g., 1s). In our

study, the running time is recorded on the computing platform used for simulation (with Intel Core i7 3.4GHz, RAM 4G, and 64bit-Matlab 2012). Fig. 16 provides the time consumed for time horizon by different horizon length (For driver 1 and entry case 7, and the total number of sampling paths is 100). As we can see that, more than 1 second time is consumed when horizon length is longer than 10 s, which means the real-time performance is ensured when horizon length is shorter than 10s. It is also noticed that the minimal energy consumption (marked in the Fig.4-49 with a circle) is identified around the horizon length 9 and 10. Therefore, the length of the receding horizon (l) in his study is set as 10.

In addition, another important parameter that can be tuned to maximize the performance of the SMPC based EAD with driver-in-the-loop, is the total number of sampling paths (N_{mc}). In Fig. 4-50 gives the energy consumption by different total numbers of scenario path sampling size and it is observed that the increase of sampling size is not able to improve the performance (i.e., reduce energy consumption). A possible reason is that, the scenario path with very small probability is not likely to be sampled no matter how large the sample size is. Hence we set the sampling size (N_{mc}) is 100, which is marked by a circle in the figure.

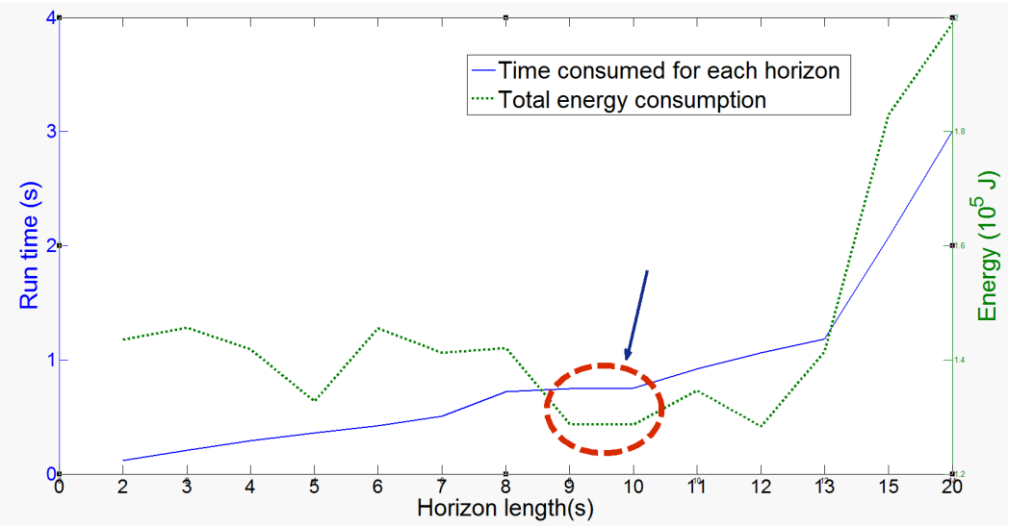

Figure 4-40 Time and energy consumption by different horizon length

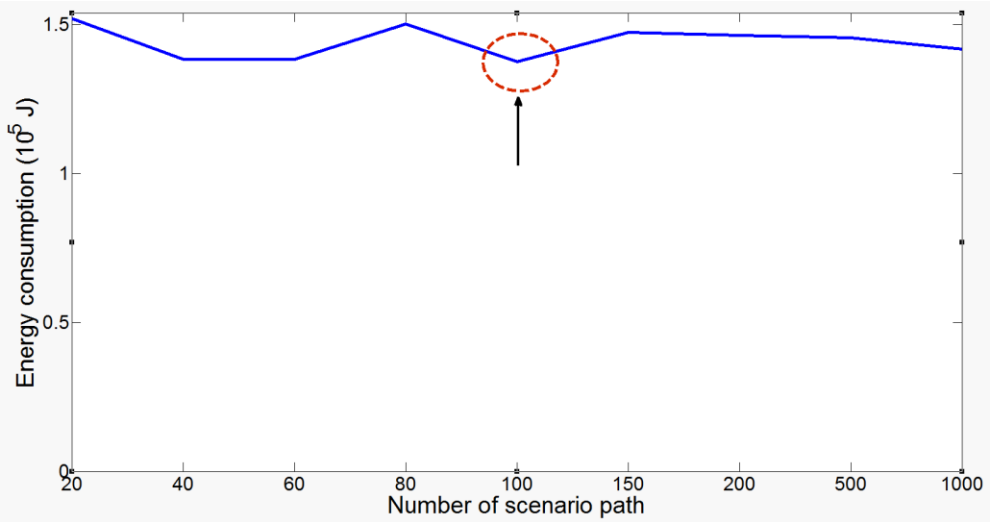

Figure 4-41 Energy consumption by different number of scenario sampling size ($l = 10$)

Energy Savings Analysis

As described in Fig.4-34, there are 4 different *passing scenarios* for a vehicle passing through an intersection. Fig. 4-51 gives the passing scenarios (in different colors) resulting from different stages of technology (for driver 1 with 25mph initial speed). It is observed in Fig.18 that for some *entry cases*, the passing scenario is changed due to the consideration of human drive error in the EAD system. For example, for entry case 1, the driving by EAD with driver-in-the-loop is 4 rather than 3 in EAD without driver-in-the-loop. It shows that a full stop at the intersection is avoided due to the technology improvement, which will potentially reduce the energy consumption.

Signal Phase	Entering Time(s)	Entry Case	Stage I	Stage II	Stage III
Green	27	1	3	3	4
	22	2	3	3	4
	17	3	3	3	4
	12	4	3	3	2
	7	5	1	1	1
	2	6	1	1	1
Red	27	7	1	1	1
	22	8	1	1	1
	17	9	1	1	1
	12	10	4	1	2
	7	11	3	4	4
	2	12	3	3	4

Scenario 1 Scenario 2 Scenario 3 Scenario 4

Figure 4-42 Passing scenario at different entry case

As can be seen in Fig.4-52, the energy savings of Stage III comparing to Stage II is significantly different for different *entry case*. The largest energy saving is at entry case 4 (40.5%) and the speed trajectory is shown in Fig.4-53. The energy saving is due to the passing scenario change from 3 to 2. The complete avoidance of stop-and-go is the main reason of the energy benefit.

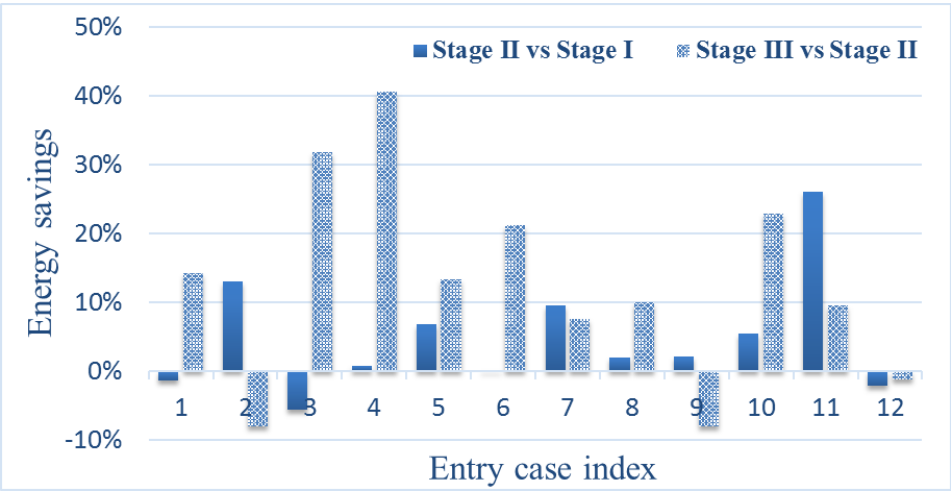

Figure 4-43 Energy savings by different stages and entry case (driver 1)

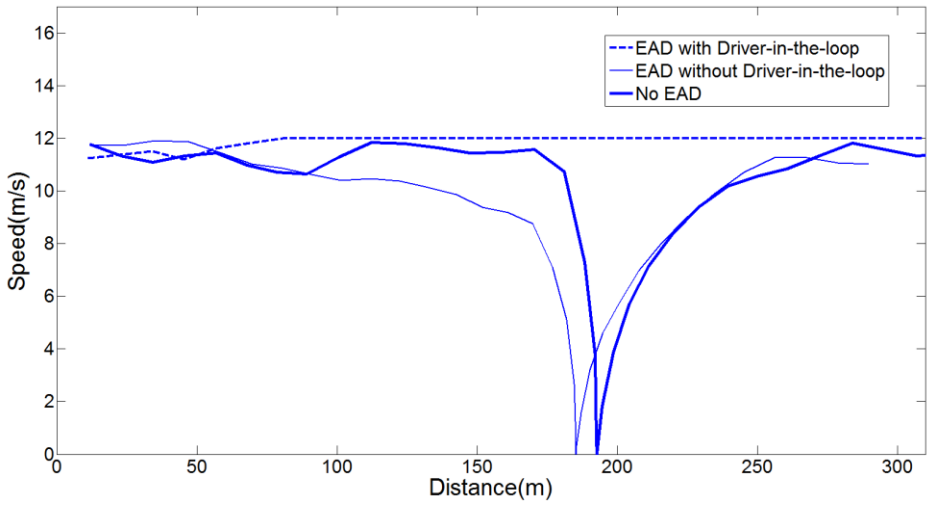

Figure 4-44 Speed trajectory of EAD with/without driver-in-the-loop (case 4)

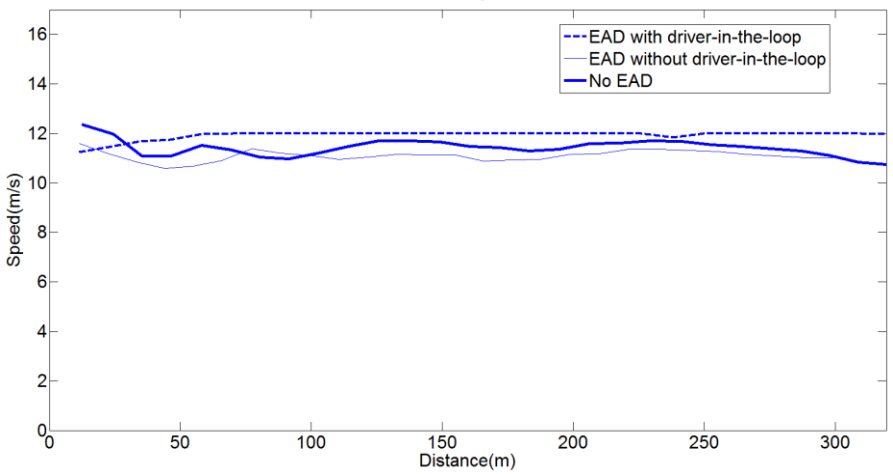

Figure 4-45 Speed trajectory of EAD with/without driver-in-the-loop (entry case 9)

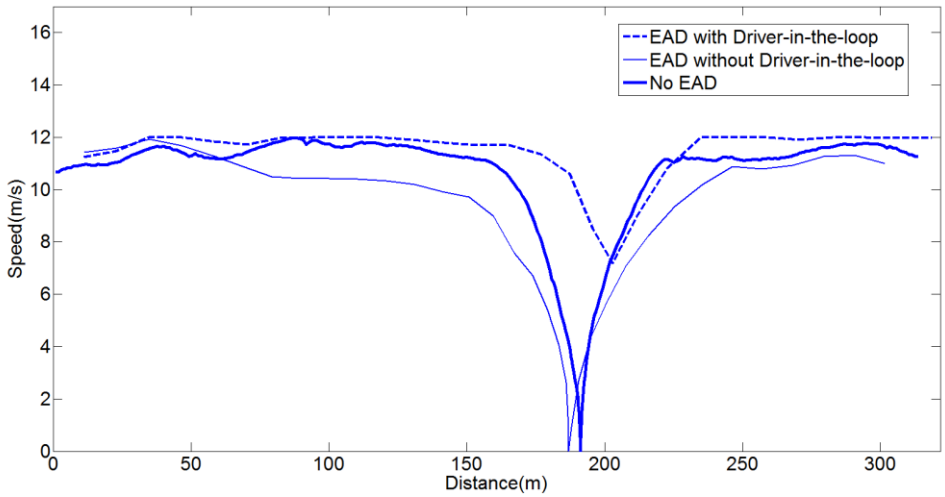

Figure 4-46 Speed trajectory of EAD with/without driver-in-the-loop (entry case 12)

For the *entry case* 9(Fig. 4-54), all the three stages result in *passing scenario 1* , therefore, there would no significant energy savings and it could even a smaller increase of energy consumption (-7.8 %) due to the stochastic property of the SMPC. For *entry case* 12, the energy saving (2.3%) is due to the reduce of acceleration and comparing a full stop for Stage I and II. But this energy saving is smaller comparing to entry case 4 (see Fig.4-55) where the unnecessary deceleration and acceleration is completely avoided. In addition, the energy savings of Stage II comparing to Stage I is also given in Fig.4-52

To obtain a statistical performance evaluation, the collected data of all the test driving (288 in total) are used to calculated the energy savings resulted by different stages of technologies. Table 4-6 gives the statistics of energy savings for different *passing scenario* changes. The change from 3 to 2 or 4 could result in the most part of the energy savings due to the reduced unnecessary acceleration from low speed.

Table 4-4 Scenario-change analysis

Stage	**Scenario Change**	**Energy savings**		
		min	**mean**	**max**
II vs III	3-›2	19.1%	25.7%	40.5%
II vs III	3-›4	9.9%	18.9%	26.7%
II vs III	1-›1	-6.7%	1.3%	10.3%
II vs III	4-›4	-15.5%	1.9%	13.2%

The overall average savings of Stage II vs. Stage I and Stage III vs Stage II are listed in Table 4-7 . The EAD assistance without drive-in-the-loop achieves 12.1% energy savings comparing to the human driving without any EAD assistance. And the EAD assistance with driver-in-the-loop can achieve another 11.7% energy savings comparing to EAD without driver-in-the-loop. It shows that considering human driving errors in driving assistances systems has potential in improving the energy performance of electric vehicles.

Table 4-5 Average Energy and Mobility Improvement

Stage	**Energy benefit (Energy savings)**		
	min	mean	max
III vs II	-8.9%	11.7%	40.5%
II vs I	-14.3%	12.1%	27%

4.6.4 Summary and Discussion

In this study, a driver-vehicle-infrastructure cooperative framework for EV energy efficient driving is proposed. To validate this framework, a EAD assistance system considering human driver error is designed and tested for EVs which is also compared with an open-loop EAD system without driver-in-the-loop. Real-world driving data were collected for performance evaluation, by comparing the resulted energy benefits. The simulation and numerical analysis show that an average of 11.7% energy savings achieved by EAD assistance system considering human driver error. The future work will mainly focus on the real-world implementation of the EAD system with considering the driver error.

4.7 Connected Ecodriving Assistance with Partial Automation

In this dissertation study, to obtain an upper bound of the energy benefit of the EAD assistance system, A EAD assistance with partial automation is designed and evaluated with real-world driving data. In the system, the designed VTPA is integrated with a model predictive control (MPC) scheme to develop a partially automated EAD system for EVs (see Figure 4-28). For

each optimization time horizon of the proposed system, the control objective is to follow the pre-calculated optimal vehicle trajectory as close as possible. In addition, the receding horizon property of MPC allows the system to better handle unpredicted disturbances. The system diagram is provided in Figure 2.

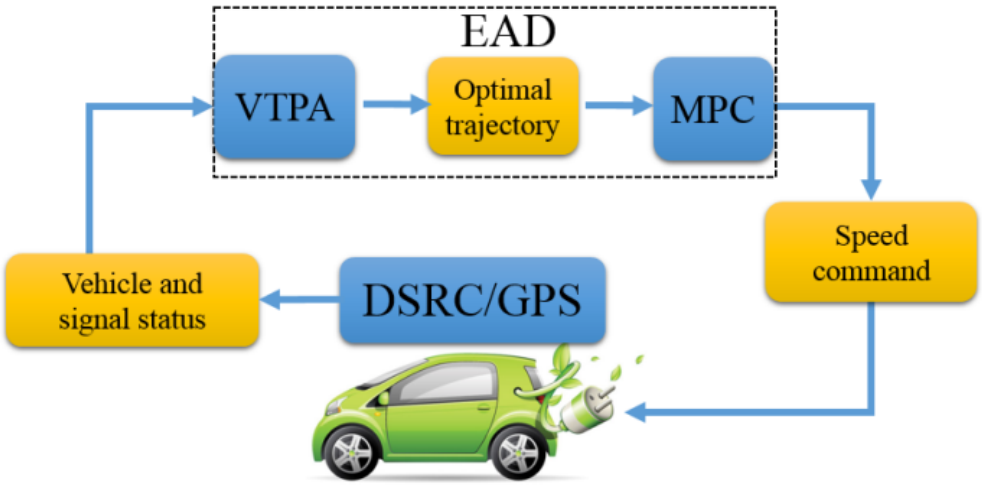

Figure 4-47 The system diagram of MPC-based EAD for EVs.

A nonlinear vehicle dynamics model (longitudinal dynamics) [109] and also its discretized version is adopted in this study (see eq.(4-17) and eq.(4-19)). MPC is designed to follow the optimal vehicle trajectory. Therefore, the objective function is defined as the sum of squared differences between the modeled and reference velocities. We also consider box constraints for the velocities, acceleration/deceleration and jerk values. In summary, the optimal control problem based on MPC can be formulated as:

$$\begin{aligned} \text{argmin}_{u_f} \quad & \sum_{k=t}^{t+l}[v(k) - v_r(k)]^2 , \\ \text{subject to} \quad & \text{the discritized dynamics (3)}, \\ & v_m \le v(k) \le v_M, \\ & \left|u_f(k)\right| \le u_M, \\ & \left|u_f(k+1) - u_f(k)\right| \le du_M, \end{aligned}$$

where t is current time; l is optimization horizon; $v(\cdot)$ is velocity computed by the MPC; $v_r(\cdot)$ is reference velocity; v_m is minimum allowable speed, which is set to 0 in this work; v_M is maximum allowable speed (usually the speed limit); u_M is maximum acceleration /deceleration constrained by the vehicle propulsion power; and du_M is the user-defined maximum jerk (mainly for driving comfort). We use 0.1 second as the time step and the control horizon of the MPC is set to 1 second, which means that there are 10 time steps to optimize for each control horizon. Note that as the dynamics in Eq. (3) are nonlinear, the optimization problem at every time step of the MPC is non-convex.

For the optimization problem in the MPC, we apply the interior point method with conjugate gradient step in the trust region used in the MATLAB command fmincon. In this

part we use $\mathrm{u(k)}$ for $\mathrm{u_f(k)}$ for the simplicity's sake of notations, and u for the vector composed of $\mathrm{u(k)}$. The basic idea of the method is first to change the optimization problem to one with equality constraints with slack variables and barrier functions, then to find a solution to its KKT conditions approximately with linear approximations.

For the optimization problem in the MPC in this paper, after using the slack variables, the objective function becomes

$$\mathrm{J} = [\mathrm{v}(1) - \mathrm{v_r}(1)]^2 + [\mathrm{v}(2) - \mathrm{v_r}(2)]^2 + [\mathrm{v}(3) - \mathrm{v_r}(3)]^2 - \rho \sum_{\mathrm{i}} \mathrm{s_{l,i}},$$

where $\mathrm{s_{l,i}}$ is the slack variables. In the following parts, when we refer to the slack variables for different constraints, we will use $\mathrm{o(k)}, \mathrm{p(k)}, \mathrm{q(k)}, \mathrm{r(k)}, \mathrm{s(k)}, \mathrm{j(k)}$ for different constraints, while when we want to emphasize the slack variables as a whole, we use $\mathrm{s_l}$. Then we change the constraints to affine equality:

$$\mathrm{v(k)} - \mathrm{v_M} + \mathrm{o(k)} = 0,$$

$$\mathrm{v_m} - \mathrm{v(k)} + \mathrm{p(k)} = 0,$$

$$u(k) - u_M + q(k) = 0,$$

$$-u(k) - u_M + r(k) = 0,$$

$$u(k+1) - u(k) - du_M + s(k) = 0,$$

$$u(k) - u(k+1) - du_M + j(k) = 0.$$

Note that the constraints of the dynamics of the car do not appear in these constraints because we will substitute it into the objective function. In this way, we can make the objective function directly dependent on the optimization variables $u(k)$.

To get the KKT conditions of the optimization problem with slack variables, we need first get its Lagrangian, which is as follows:

$L = J + \sum_{k=1}^{3} \lambda_k [v(k) - v_M + o(k)] + \sum_{k=1}^{3} \mu_k [v_m - v(k) + p(k)] + \sum_{k=1}^{3} \alpha_k [u(k) - u_M + q(k)] + \sum_{k=1}^{3} \beta_k [-u(k) - u_M + r(k)] + \sum_{k=0}^{1} \gamma_k [u(k+1) - u(k) - du_M + s(k)] + \sum_{k=0}^{1} \delta_k [u(k) - u(k+1) - du_M + j(k)],$

where $\lambda_k, \mu_k, \alpha_k, \beta_k, \gamma_k, \delta_k$ are the Lagrangian multipliers. For the KKT conditions, we first have that

$$\frac{\partial L}{\partial u(k)} = 0.$$

As L is not quadratic with respect to $u(k)$, $\frac{\partial L}{\partial u(k)}$ is not linear. So we need to do a first-order approximation to it. Then in each step in the optimization problem, we solve indeed the

following quadratic programming problem with conjugate gradient method: Type equation here.

in a trust region $||\Delta u_f||^2 + ||S^{-1}\Delta s||^2 \leq R^2$. Here, Δu and Δs_l are the steps in the optimization

$$\min_{\Delta u, \Delta s_l} \nabla J^T \Delta u + \frac{1}{2}\Delta u^T \nabla^2_{uu} L \Delta u + \rho e^T S_l^{-1} \Delta s_l$$

$$\begin{aligned} \text{Subject to} \quad & v(k) - v_M + o(k) = 0, \\ & -v(k) - v_m + p(k) = 0, \\ & u(k) - u_M + q(k) = 0, \\ & -u(k) - u_M + r(k) = 0, \\ & u(k+1) - u(k) - du_M + s(k) = 0, \\ & u(k) - u(k+1) - du_M + j(k) = 0, \end{aligned}$$

algorithms, $e = (1,1,\cdots,1)$, S_l is a diagonal matrix whose diagonal entries are the slack variables $s_{l,i}$, i.e., $o(k), p(k), q(k), r(k), s(k), j(k)$, Λ is a diagonal matrix whose diagonal entries are the Lagrangian multipliers $\lambda_k, \mu_k, \alpha_k, \beta_k, \gamma_k, \delta_k$. And ∇J is the gradient of J, $\nabla^2_{uu} L$ is the Hessian of L with respect to u. As the mathematical expressions of ∇J and $\nabla^2_{uu} L$ are very complicate, we put them at the end of the paper for readability.

As the problem is not convex due to the nonlinear dynamics of the car, we are not guaranteed to find a global optimal solution. But by setting the initial iteration point such that $J = 0$, we may find a good solution because the initial guess is a global solution to the unconstrained problem.

Energy and Mobility Benefits Analysis

Using the data collected in the field test, the designed EAD system for EVs were evaluated in terms of energy and motility benefits. Besides the Stage I and Stage II technologies described in the section 4.2.2, a new Stage III is defined as following:

Stage III: "MPC-based (partially) automated" driving (MPC). No real-world testing has been conducted in this stage due to the limited resources. Instead, we evaluated the performance of

the designed MPC-based longitudinal control system in a simulation environment developed in Matlab using data collected from the field testing. The optimal speed profile calculated by the VTPA was used as the reference input to the MPC model. The results from this simulation likely represent the upper bound of system performance.

The EV energy consumption model described above was applied to calculate the energy consumption associated with the collected vehicle trajectory data. Figure 4-29 indicates the change in *passing scenarios* due to the application of the EAD system for one of the drivers (Driver 1). For example, in *entry case* 4, Driver 1 passed the intersection with passing scenario 3 (which is the most energy intensive passing scenario) in both stages I and II, but he would have done so with passing scenario 2 in stage III if the proposed MPC-based longitudinal controller has been applied. It is observed that among the 12 *entry case*s of Driver 1, there are more scenario 3 in stage I than that in stage II or stage III due to the lack of recommended driving speed provided to the driver. In stage III, there would have been no passing scenario 3 with the aid of the MPC-based longitudinal controller.

Figure 4-30 and Figure 4-31 show the energy savings and time savings of stage II ("HMI vs. MUD") and stage III ("MPC vs. MUD"), as compared to stage I, for Driver 1 . Figure 6 shows clearly that most of the energy savings happen when the *passing scenarios* changes from scenario 3 to scenario 2 or scenario 4 (i.e., entry cases 3, 4, 5, 6, and 7 shown in Figure 5). The biggest energy saving (45.3%) occurs in *entry case* 4 where the *passing scenario* changes from scenario 3 to scenario 2. The speed profiles for this entry case are given in Figure 8. As shown in the figure, when given the advisory speed profile through HMI, Driver 1 failed to follow it closely at the beginning, resulting in a switch from passing scenario 2 to 3, and therefore, trivial energy savings. For those *entry case*s where the three different stages are in the same *passing scenarios*, the energy savings are not as much and, for some entry cases of stage 2, turn negative because of variations in real-world driving.

Signal Phase	Entering Time(s)	Entry Case	MUD	HMI	MPC
Green	2	1	1	1	1
	7	2	2	2	2
	12	3	3	3	2
	17	4	3	3	2
	22	5	3	3	4
	27	6	3	3	4
Red	2	7	3	4	4
	7	8	4	4	4
	12	9	1	1	1
	17	10	1	1	1
	22	11	1	1	1
	27	12	1	1	1

Scenario 1 Scenario 2 Scenario 3 Scenario 4

Figure 4-48 Changes in passing scenario in different stages (driver 1).

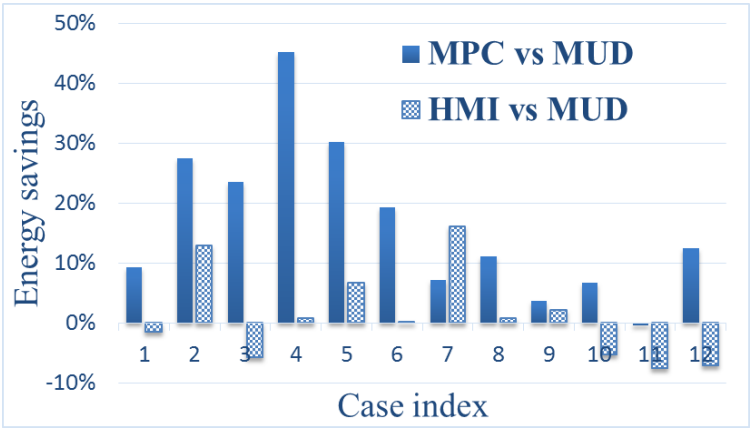

Figure 4-49 Energy savings for different cases (Driver 1).

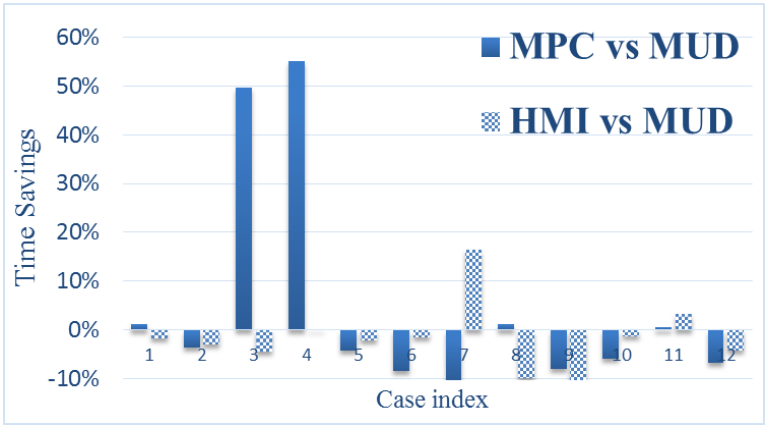

Figure 4-50 Time savings for different scenarios (Driver 1)

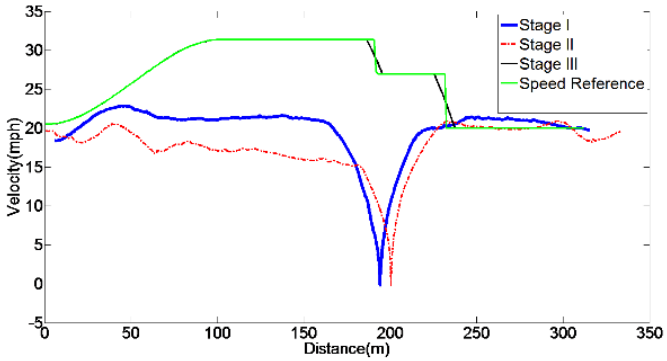

Figure 4-51 Speed versus distance for *entry case* 4 (Driver 1)

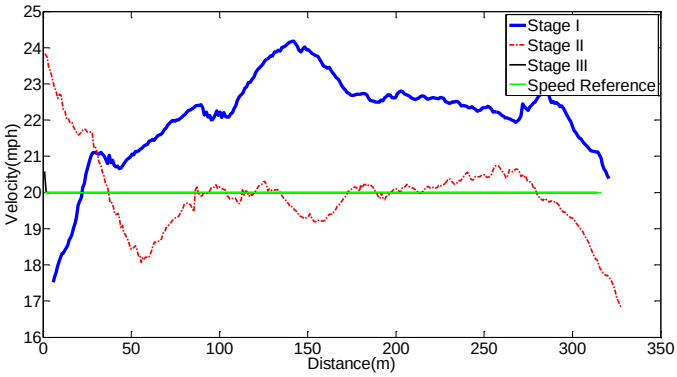

Figure 4-52 Speed versus distance for *entry case* 9 (Driver 1)

From the mobility perspective, it is observed in Figure 4-31 that most of the *entry case*s in stage II and stage III result in minimal time savings or even small time penalties except *entry case* 3 and *entry case* 4 of stage III where the passing scenario is 2. This can be well explained by Figure 4-33 where the speed profile in stage I shows a more aggressive trend (i.e., exceeding the speed limit of 20 mph almost throughout) than either of the other two stages. Although stages II and III have longer travel times in this case, it is because of the uncharacteristic driving in stage 1 rather than the shortcoming of the EAD system.

To further analyze the energy benefits of the designed EAD system, a scenario change analysis was conducted using the driving data of all 4 drivers. The analysis covers all the scenario changes that happened in the field experiment. As shown in Table 4-4, most of the energy savings happen when the passing scenario changes from scenario 3 to scenario 2 or scenario 4

with the assistance of the EAD system. However, when the EAD system cannot change the passing scenario, there is not as much energy saving (on average) or even a negative saving (for scenario 3 between stage I and stage II) due to variations in real-world driving. This may suggest that the information disseminated by the HMI is not effective enough in assisting the manual driving and more comprehensive system design should be conducted to take into consideration the human factors aspect. One possible way to improve the existing system is to disable the display of advisory speed when the system predicts that there will be no change in the passing scenario.

Table 4-6 Scenario-change analysis

Stage	Scenario Change	Energy savings		
		min	mean	max
I vs III	3-›2	13.9%	25.7%	45.3%
I vs III	3-›4	10.3%	19.1%	27.0%
I vs III	1-›1	-16.0%	7.3%	11.3%
I vs III	2-›2	-15.5%	5.9%	10.9%
I vs II	3-›2	2.2%	9.5%	18.3%
I vs II	3-›4	1.2%	3.8%	13.9%
I vs II	1-›1	-6.7%	1.1%	6.3%
I vs II	2-›2	-15.1%	0.9%	5.1%
I vs II	3-›3	-10.3%	-3.1%	7.3%

Finally, the average energy and time savings across all *entry case*s and all drivers were calculated and thus are provided in Table 4-5. It shows that the MPC based EAD system can achieve an average of 21.9% electricity savings along with an average of 10.7% time savings (mostly contributed by *entry case* 3 and *entry case* 4), while the driving assistance system with HMI achieves 12.1% energy savings on average but with compromise of travel time (increase of 3.2%).

Table 4-7. Average Energy and Mobility Improvement

Stage	Energy benefit (Energy savings)			Mobility benefit (Time savings)		
	min	mean	max	min	mean	max
II	-14.3%	12.1%	27%	-13%	-3.2%	17.6%
III	3.7%	21.9%	45.3%	-28.1%	10.7%	55.1%

4.8 Summary of Energy Benefits for Different Technology Stages

In this chapter, 3 different stages of EAD assistance technologies are designed and evaluated for PEVs. They are all compared with the baseline (i.e., Stage I). The definitions for each stage are listed as follows one more time just for clarification:

- Stage I: *Uninformed driving*. In this stage, the driver approached and traveled through the intersection in a normal fashion without guidance or automation, stopping as needed without any guidance. The vehicle is fully controlled by the human driver. This stage is used as lower bound performance technological stage.
- Stage II: *In-vehicle advising driving without considering driver error*. In this stage, the driver was assisted by an open-loop EAD system as described in Fig. 4-37. An enhanced dashboard presenting a recommended range of driving speed is provided (see Figure 4-38). This information can assist the driver to approach and depart the intersection in an environmentally friendly manner while obeying the traffic signal. This driving assistance system does not consider human driver error.
- Stage III: "*In-vehicle advising driving with considering driver error*". At this stage, no real-world testing has been conducted due to the limited resources. Instead, we evaluated the performance of the designed EAD with the driver-in-the-loop system in a simulation environment developed in Matlab using data collected from the field testing of Stage II. The same VTPA model is used to calculate the optimal speed profile as part of the SMPC control model. More details about the simulation are given in the following sections.
- Stage IV: "*Partially automated" driving.* At this stage, an automatic controller was responsible for longitudinal control of the vehicle, allowing it to speed up or slow down while the driver steered for lateral control. The vehicle automatically controlled the brake and throttle based on the calculated eco-friendly velocity profile according to signal state

and distance to the stop-bar.

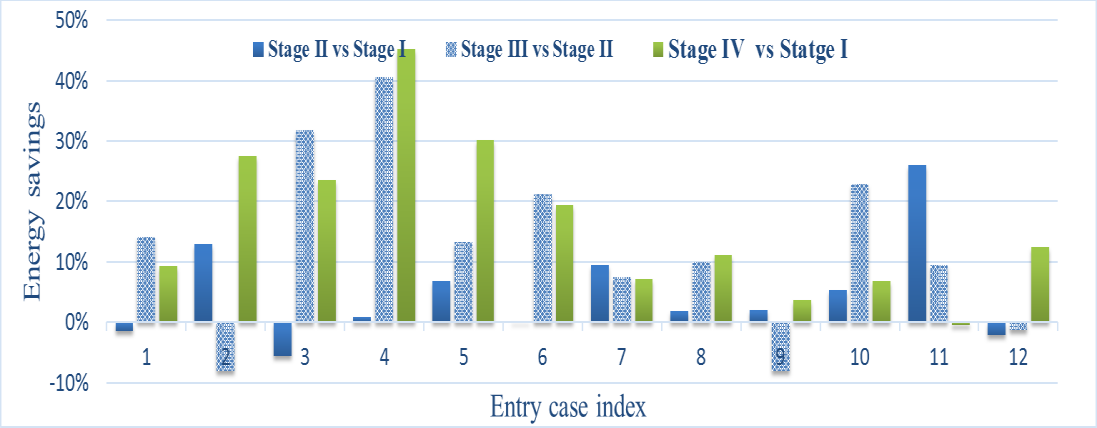

Figure 4-53 Energy benefits for different stages of EAD technologies for *entry case 9*

As discussed in previous sections, the energy benefits are highly dependent on the different *entry cases*. As shown in Fig. 4-53, the energy benefits for different stages of technologies along different entry cases have similar patterns. Most of the energy benefits are identified when the passing scenario changes from 3 to 1 or 2. And for the situations where passing scenarios are not changed, there is no significant energy benefits are identified. Therefore, the main reason of energy consumption reduction is due to the reduction of unnecessary accelerations and decelerations.

Fig 4-54 also provides the average energy benefits of Stage II, II and IV of EAD technologies. It is observed that the consideration of human driver error does improve the EAD driving performance and fully automated driving can reach the upper bound of the EAD system.

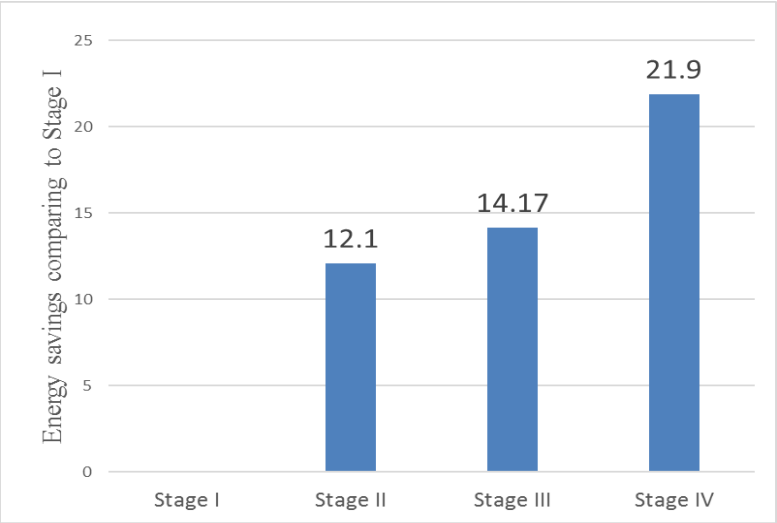

Figure 4-54 Average energy savings for different EAD technologies comparing to driving without EAD

5 Powertrain Operation Optimization: Optimal Power-split Control

5.1 Overview

Air pollution and climate change impacts associated with the use of fossil fuels have motivated the electrification of transportation systems. In the realm of powertrain electrification, groundbreaking changes have been witnessed in the past decade in terms of research and development of hybrid electric vehicles (HEVs) and electric vehicles (EVs) [136]. As a combination of HEVs and EVs, plug-in hybrid electric vehicles (PHEVs) can be plugged into the electrical grid to charge their batteries, thus increasing the use of electricity and achieving even higher overall fuel efficiency, while retaining the internal combustion engine that can be called upon when needed [137].

In comparison to conventional HEVs, the energy management systems (EMS) in PHEVs are significantly more complex due to their extended electric-only propulsion (or extended all-electric range capability) and battery chargeability via external electric power sources. Numerous efforts have been made in developing a variety of EMS for PHEVs [138, 139]. From the control perspective, existing EMS can be roughly classified as rule-based [140] and optimization-based [141]. This is discussed in more detail in Section II.

In spite of all these efforts, most of the existing PHEVs' EMS have one or more of the following limitations:

- Lack of adaptability to real-time information, such as traffic and road grade. This applies to rule-based EMS (either deterministic or using fuzzy logic) whose parameters or criteria have been pre-tuned to favor certain conditions (e.g., specific driving cycles and route elevation profiles) [138]. In addition, most EMS that are based on global optimization off-line assume that the future driving condition is known [137]. Thus far, only a few studies have focused on the development of on-line EMS for PHEVs [142].

- Dependence on accurate (or predicted) trip information that is usually unknown a priori. Many of the existing EMS require at a minimum the trip duration as known or predicted information prior to the trip [143]. Furthermore, it is reported that the performance of EMS is largely dependent on the time span of the trip [143]. There are very few studies analyzing the impacts of trip duration on the performance of EMS for PHEVs.
- Emphasis on a single trip level optimization without considering opportunistic charging between trips. The most critical feature that differentiates PHEVs from conventional HEVs is that PHEVs' batteries can be charged by plugging into an electrical outlet. Most of the existing EMS are designed to work on a trip-by-trip basis. However, taking into account inter-trip charging information can significantly improve the fuel economy of PHEVs [137].

5.1.1 PHEV Modeling

Typically, there are three major types of PHEV powertrain architectures: a) series, b) parallel, and c) power-split (series-parallel). This study is focused on the power-split architecture where the internal combustion engine (ICE) and electric motors can, either alone or together, power the vehicle while the battery pack may be charged simultaneously through the ICE. Different approaches with various levels of complexity have been proposed for modeling PHEV powertrains [144]. However, a complex PHEV model with a large number of states may not be suitable for the optimization of PHEV energy control. A simplified but sufficiently detailed power-split powertrain model has been developed in MATLAB and used in this study. For more details, please refer to [137].

5.1.2 Operation Mode and SOC Profile

During the operation of a PHEV, the SOC may vary with time, depending on how the energy sources work together to provide the propulsion power at each instant. The SOC profile can serve as an indicator of the PHEV' operating modes, i.e., charge sustaining (CS), pure electric vehicle (EV), and charge depleting (CD) modes [138], as shown in Fig. 5-1.

The CS mode occurs when the SOC is maintained at a certain level (usually the lower bound of SOC) by jointly using power from both the battery pack and the ICE. The pure EV mode is when the vehicle is powered by electricity only. The CD mode represents the state when the vehicle is operated using power primarily from the battery pack with supplemental power from the ICE as necessary. In the CD mode, the ICE is turned on if the electric motor is not able to provide enough propulsion power or the battery pack is being charged (even when the SOC is much higher than the lower bound) in order to achieve better fuel economy.

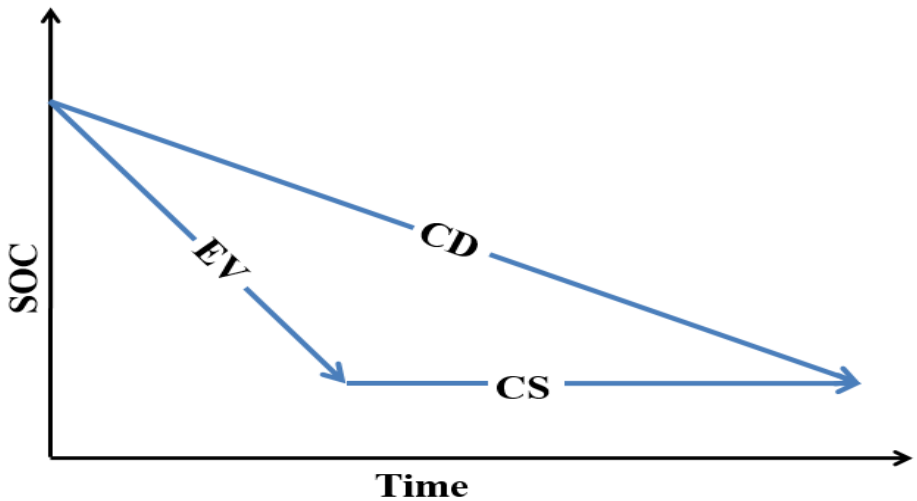

Figure 5-1 Basic operation modes for PHEV.

5.1.3 EMS for PHEVs

The goal of the EMS in a PHEV is to satisfy the propulsion power requirements while maintaining the vehicle's performance in an optimal way. A variety of strategies have been proposed and evaluated in many previous studies [139]. A detailed literature review on EMS for PHEVs is provided in this section. Broadly speaking, the existing EMS for PHEVs can be divided into two major categories:

- Rule-based EMS are fundamental control schemes operating on a set of predefined rules without prior knowledge of the trip. The control decisions are made according to the current vehicle states and power demand only. Such strategies are easily implemented but the resultant operations may be far from being optimal due to not considering future traffic conditions.
- Optimization-based EMS aim at optimizing a predefined cost function according to the driving conditions and behaviors. The cost function may include a variety of vehicle performance metrics, such as fuel consumption and tailpipe emissions.

For Rule-based EMS, deterministic and fuzzy control strategies (e.g., binary control) have been well investigated. For Optimization-based EMS, the strategies can be further divided into three subgroups based on how the optimizations are implemented: 1) off-line strategy which requires a full knowledge of the entire trip beforehand to achieve the global optimal solution; 2) prediction-based strategy or so called real-time control strategy which takes into account predicted future driving conditions (in a rolling horizon manner) and achieves local optimal solutions segment-by-segment. This group of strategies are quite promising due to the rapid advancement and massive deployment of sensing and communication technologies (e.g., GPS) in transportation systems that facilitate the traffic state prediction; and 3) learning-based strategy which is recently emerging owing to the research progress in machine learning techniques. In such a data-driven strategy, a dynamic model is no longer required. Based on massive historical and real-time information, trip characteristics can be learned and the

corresponding optimal control decisions can be made through advanced data mining schemes. This strategy fits very well for commute trips. Figure 5-2 presents a classification tree of EMS for PHEVs and the typical strategies in each category, based on most existing studies.

In addition to the classification above, Table I highlights several important features which help differentiate the aforementioned strategies. Example references are also included in Table 5-1.

Table 5-1 Classification of current literature

	Rule-based	Off-line optimization	Prediction based	Learning based
Optimality	local	global	local	local
Real time	Yes	No	Yes	Yes
SOC control	No	Yes	Yes	No
Need trip duration	No	Yes	Yes	Yes
Example references	[142], [145], [146], [147]	[137], [148], [149], [150] [155], [156], [158]	[151], [152], [154], [159], [161], [162], [163]	[14], [15], [153], [157], [160], [164]

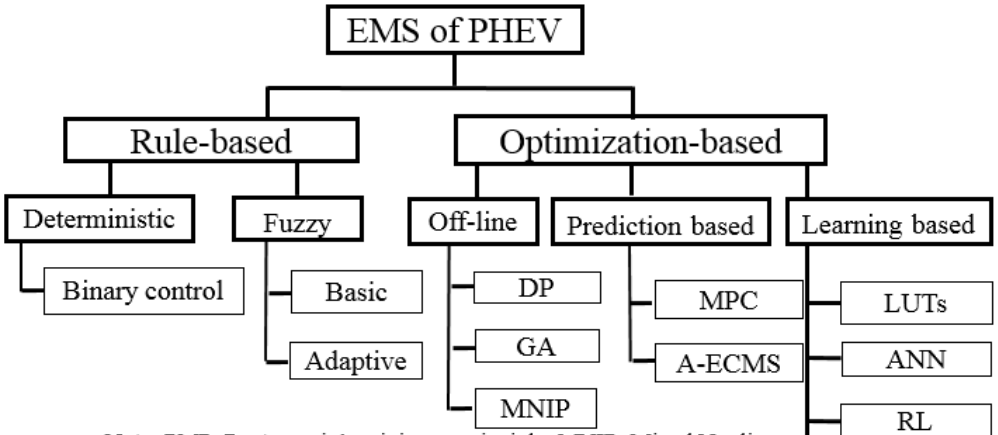

Note: PMP: Pontraysgin's minimum principle; MNIP: Mixed Nonlinear Integer Programming; DP: Dynamic programming QP: Quadratic programming; RL: reinforcement learning; ANN: artificial neural network; LUTs: look-up-tables; MPC: model predictive control; AECMS: Adaptive equivalent consumption minimization strategy

Figure 5-2 Basic classification of EMS for PHEV.

5.1.4 PHEVs' SOC Control

For a power-split PHEV, the optimal energy control is, in principle, equivalent to the optimal SOC control. Most of the existing EMS for PHEVs implicitly integrate SOC into the dynamic model and regard it as a key control variable [157], while only a few studies have explicitly described their SOC control strategies. A SOC reference control strategy is proposed in [154] where a supervisory SOC planning method is designed to pre-calculate an optimal SOC reference curve. The proposed EMS then tries to follow this curve during the trip to achieve the best fuel economy. Another SOC control strategy is proposed in [159] where a probabilistic distribution of trip duration is considered. More recently, machine learning-based SOC control strategies (e.g., [160]) have emerged, where the optimal SOC curves are pre-calculated using historical data and stored in the form of look-up tables for real-time implementation. A common drawback for all these strategies is that accurate trip duration information is required in an either deterministic or probabilistic way. In reality, however, such information is hard to be known ahead of time or may vary significantly due to the uncertainties in traffic conditions. To ensure the practicality of our proposed EMS for PHEVs, we employ a self-adaptive SOC control strategy in this study which does not require any information about the trip duration (or length).

5.2 PHEV Architecture

This chapter describe the PHEV model used in this study. Several approaches with different levels of complexity have been proposed for modeling PHEV vehicle and powertrain. A complex PHEV model with a large number of states may not be suitable for the optimization of PHEV energy control. Therefore, a simplified but sufficiently detailed vehicle and powertrain model was developed in this dissertation study [165]. In general, there are three major PHEV powertrain architectures: a) series, b) parallel, and c) power-split (series-parallel). This study is focused on the power-split one. Figure 5-3 depicts the configuration of a power-

split PHEV, in which three major sub-systems: a) internal combustion engine (ICE), b) planetary gear set (PGS), and c) motor/battery are modeled as described below.

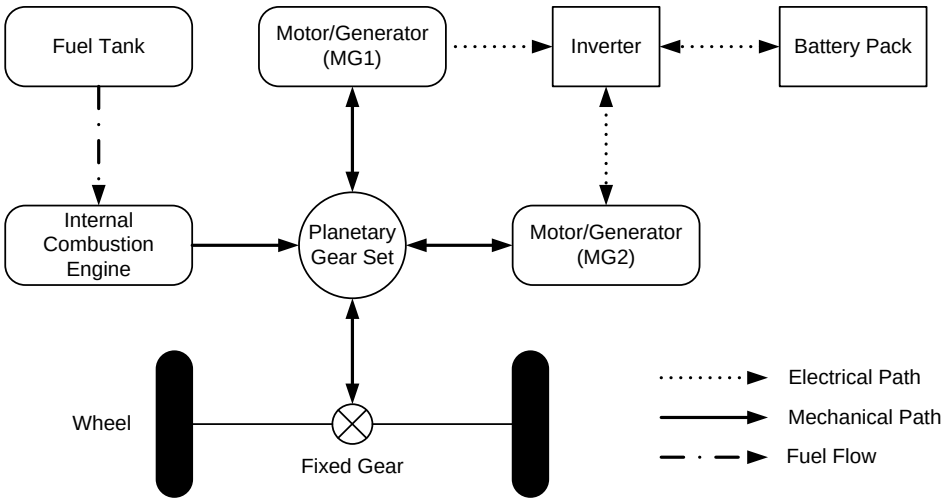

Figure 5-3 Power-split plug-in hybrid electric vehicle configuration.

5.2.1 PHEV Model Parameters

All major parameters and the associated values of the PHEV model used in this study are listed in Table 5-2.

Table 5-2 List of PHEV Model Parameters

Parameters	Value	Unit
Vehicle curb weight	1718	kg
Final drive ratio	3.93	/
Vehicle equivalent mass	1853	kg
Tire radius	0.317	m
No. of teeth on sun gear	30	/
No. of teeth on ring gear	78	/
Gravitational acceleration	9.81	m/s^2
Rolling resistance coefficient (constant term)	0.008	
Rolling resistance coefficient (linear term)	0.00012	s/rad
Air density	1.2041	kg/m^3
Projected frontal area	2.2508	m^2
Aerodynamic drag coefficient	0.26	
Maximum engine power	60	kWatt
Moment of inertia for engine	0.1598	$kg*m^2$
Maximum motor power	50	kWatt
Moment of inertia for motor	0.0302	$kg*m^2$
Maximum generator power	30	kWatt
Moment of inertia for generator	0.0287	$kg*m^2$
Maximum brake torque	2000	N*m
No. of battery cells per module	12	/
No. of battery module	6	/
Nominal open-circuit voltage	3.6	volt
Battery capacity	17	Ah
Minimum state of charge (SOC)	0.2	/

5.3 Problem Formulation, Optimality and Complexity

5.3.1 Proposed On-line EMS Framework for PHEVs

In this dissertation study, we propose an on-line EMS framework for PHEVs, using the receding horizon control structure (see Fig. 5-7). The proposed EMS framework consists of information acquisition (from external sources), prediction, optimization, and power split control. With the receding horizon control, the entire trip is divided into segments or time horizons. As shown in Fig. 5-8, the prediction horizon (N sampling time steps) needs to be longer than the control

horizon (M sampling time steps). Both horizons keep moving forward (in a rolling horizon style) while the system is operating. More specifically, the prediction model is used to predict the power demand at each sampling step (i.e., each second) in the prediction horizon. Then, the optimal ICE power supply for each second during the prediction horizon is calculated with this predicted information.

In each control horizon, the pre-calculated optimal control decisions are inputted into the powertrain control system (e.g., electronic control unit (ECU)) at the required sampling frequency. In this study, we focus on the on-line energy optimization, assuming that the short-term prediction model is available (which is one of our future research topics).

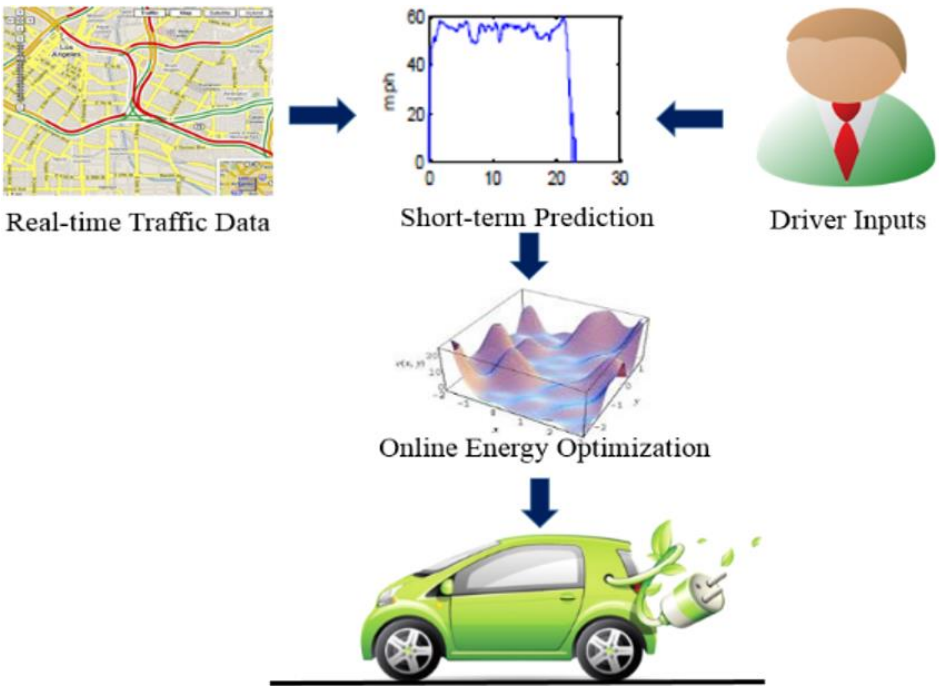

Figure 5-4 Flow chart of the proposed on-line EMS.

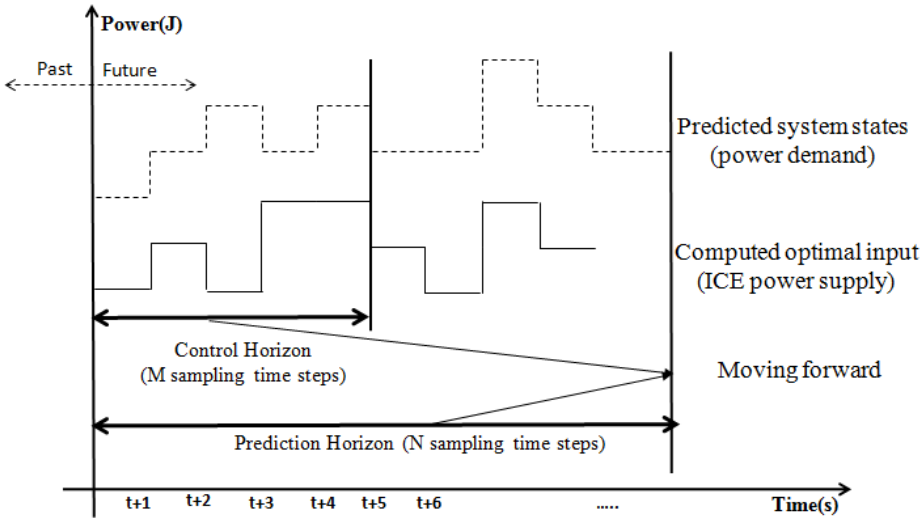

Figure 5-5 Time horizons of prediction and control.

5.3.2 Optimal Power-Split Control Formulation

Mathematically, the optimal (in terms of fuel economy) energy management for PHEVs can be formulated as a nonlinear constrained optimization problem. The objective is to minimize the total fuel consumption by ICE along the entire trip.

$$\begin{cases} \min\left\{\int_0^T h(\omega_e, q_e, t)dt\right\} \\ \text{subject to:} \\ \dot{SOC} = f(SOC, \omega_{MG1}, q_{MG1}, \omega_{MG2}, q_{MG2}) \\ (\omega_e, q_e) = g(\omega_{MG1}, q_{MG1}, \omega_{MG2}, q_{MG2}) \\ SOC_{min} \le SOC \le SOC_{max} \\ \omega_{min} \le \omega_e \le \omega_{max} \\ q_{min} \le q_e \le q_{max} \end{cases} \quad (5\text{-}1)$$

where T is the trip duration; ω_e, q_e are the engine's angular velocity and engine's torque, respectively; $h(\omega_e, Tq_e)$ is ICE fuel consumption model; ω_{MG1}, q_{MG1} are the first motor/generator's angular velocity and torque, respectively; ω_{MG2}, q_{MG2} are the second motor/generator's angular velocity and torque, respectively; $f(SOC, \omega_{MG1}, q_{MG1}, \omega_{MG2}, q_{MG2})$is the battery power consumption model; For more details about the model derivations and equations, please refer to [138].

Such formulation is quite suitable for traditional mathematical optimization methods [148] with high computational complexity. In order to facilitate on-line optimization, we herein discretize the engine power and reformulate the optimization problem represented by (1) as follows:

$$min \sum_{k=1}^{T} \sum_{i=1}^{N} x(k,i)\, P_i^{eng} / \eta_i^{eng} \quad (5\text{-}2)$$

subject to:

$$\sum_{k=1}^{j} f\left(P_k - \sum_{i=1}^{N} x(k,i) P_i^{eng}\right) \le C \quad \forall j = 1, \dots, T \quad (5\text{-}3)$$

$$\sum_{i=1}^{N} x(k,i) = 1 \qquad \forall k \quad (5\text{-}4)$$

$$x(k,i) = \{0,1\} \qquad \forall k, i \quad (5\text{-}5)$$

where N is the number of discretized power level for the engine; k is the time step index; i is the engine power level index; C is the gap of the battery pack's SOC between the initial and the minimum; P_i^{eng} is the i-th discretized level for the engine power and η_i^{eng} is the associated engine efficiency; and P_k is the driving power demand at time step k.

Furthermore, if the change in SOC (ΔSOC) for each possible engine power level at each time step is pre-calculated given the (predicted) power demand, then constraint (3) can be replaced by

$$SOC^{ini} - SOC^{max} \le \sum_{k=1}^{j} x(k,i) \Delta SOC(k,i) \le SOC^{ini} - SOC^{min}$$

$$\forall j = 1, \dots, T \quad (5\text{-}6)$$

where SOC^{ini} is the initial SOC; and SOC^{min} and SOC^{max} are the minimum and maximum SOC, respectively. Therefore, the problem is turned into a combinatory optimization problem whose objective is to select the optimal ICE power level for each time step given the predicted information in order to achieve the highest fuel efficiency for the entire trip. Fig.5-9 gives three

example ICE power output solutions. The solution represented by the blue line has a lower total ICE power consumption (i.e., 40 units) than the red line (i.e., 90 units), while the green line represents an infeasible solution due to the SOC constraint.

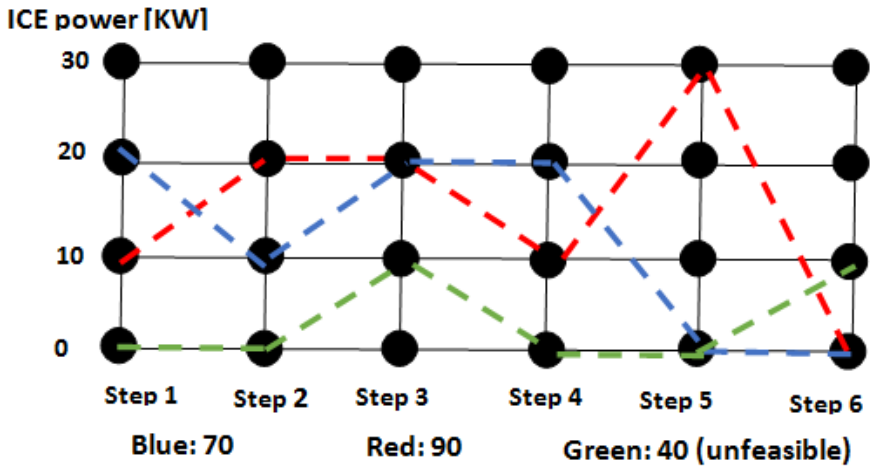

Figure 5-6 Example solutions of power-split control.

5.3.3 Optimality and Complexity

Evolutionary algorithms are stochastic search algorithms which do not guarantee to find the global optima. Hence, in the proposed on-line EMS, the optimal power control for each trip segment is not guaranteed to be found. Moreover, EAs are also population-based iterative algorithms which are usually criticized due to their heavy computational loads [169], especially for real-time applications. Theoretically, time complexity of EAs is worse than $\theta(m^2 * log(m))$ where m is the size of the problem [170]. However, we apply the receding horizon control technique in this study, where the entire trip is divided into small segments. Therefore, the computational load can be significantly reduced since the EA-based optimization is applied only for each small segment rather than the entire trip. In this sense, the proposed framework can be implemented in "real-time", as long as the optimization for the next prediction horizon can be completed in the current control horizon (see Fig. 4). As previously discussed, the rule-

based EMS can run in real-time but the results may be far from being optimal while most of the optimization-based EMS have to operate off-line. Therefore, the proposed on-line EMS would be a well-balanced solution between the real-time performance and optimality.

5.4 SOC Self-Adaptive Control Strategies

5.4.1 SOC Control Strategies

An appropriate SOC control strategy is critical in achieving the optimal fuel economy for PHEVs [171]. In the previously presented problem formulation, the major constraint for SOC is defined by Eq.(6), which means that at any time step the SOC should be within the predefined range (e.g., between 0.2 and 0.8) to avoid damage to the battery pack. However, this constraint only may not be enough to accelerate the search for the optimal solution. Hence, additional constraint(s) on battery use (e.g., reference bound of SOC) should be introduced to improve the on-line EMS. To investigate the effectiveness of different SOC control strategies within the proposed framework, two types of SOC control strategies, i.e., reference control and self-adaptive control, are designed and evaluated in this study.

SOC Reference Control (Known Trip Duration)

When the trip duration is known, a SOC curve can be pre-calculated and used as a reference to control the use of battery power along the trip to achieve optimal fuel consumption. We propose three heuristic SOC references (i.e., lower bounds) in this study (see Fig. 5-10 for example): 1) concave downward; 2) straight line; and 3) concave upward. These SOC minimum bounds are generated based on the given trip duration information by the following equations, respectively:

- Concave downward control: (lower bound 1)

$$SOC_i^{min} = \frac{(SOC_{init} - SOC^{min})}{T-(i*M)} * N + SOC^{init} \quad (5\text{-}7)$$

- Straight line control :(lower bound 2)

$$SOC_i^{min} = \frac{-(SOC_i^{min} - SOC^{min})}{T} \cdot ((i-1) \cdot M + N) + SOC^{init} \quad (5\text{-}8)$$

- Concave upward control :(lower bound 3)

$$SOC_i^{min} = \frac{-(SOC_{i-1}^{end} - SOC^{min})}{T-(i*M)} * N + SOC_{i-1}^{end} \quad (5\text{-}9)$$

where i is the segment index; SOC_i^{min} is the minimum SOC at the end of i-th segment; and SOC_{i-1}^{end} is the SOC at the end of last control horizon. It is self-evident that the concave downward bound (i.e., lower bound 1) is much more restrictive than a concave upward bound (i.e., lower bound 3) in terms of battery energy use at the beginning of the trip.

A major drawback for these reference control strategies is that they assume that the trip duration (i.e., T) is given, or at least can be well estimated beforehand. As mentioned earlier, this assumption may not hold true for many real-world applications. Therefore, a new SOC control strategy without relying on the knowledge of trip duration would be more attractive.

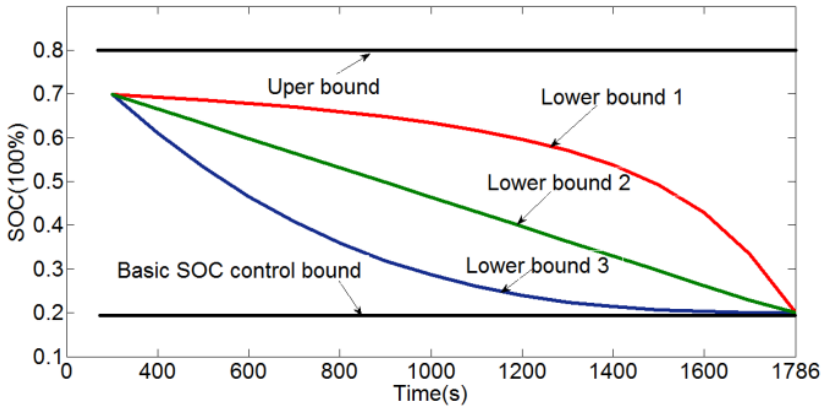

Figure 5-7 SOC reference control bound examples.

SOC Self-Adaptive Control (Unknown Trip Duration)

In this study, we also propose a novel self-adaptive SOC control strategy for real-time optimal charge-depleting control, where trip duration information is not required. Unlike those SOC

reference control strategies which control the use of battery by explicit reference curves, the self-adaptive control strategy controls the battery power utilization implicitly by adopting a new fitness function in place of the one in Eq. (7):

$$f(s) = R_{fuel} + R_{soc} + P' \tag{5-10}$$

where R_{fuel} and R_{soc} are the ranks (in an ascending order) of ICE fuel consumption and SOC decrease, respectively, of an individual candidate solution s in the current population; and P' is the added penalty when the individual s violates the constraints given in Eq.(6). The penalty value is selected to be greater than the population size in order to guarantee that an infeasible solution always has a lower rank (i.e., larger fitness value) than a feasible solution in the ascending order by fitness value. Compared to the fitness function adopted for SOC reference control (see Eq. (7)), this new fitness function tries to achieve a good balance between two conflicting objectives: least fuel consumption and least SOC decrease. For a better understanding of the differences between these two fitness functions, Table 5-3 provides an example of fitness evaluation of the same population. In this case, the population size is 100. As we can see in the table, Individual 2 which has a better balance between fuel consumption and SOC decrease is more favorable than Individual 3 in the ranking by Eq. (11) than that by Eq.(7)

Table 5-3 Example fitness evaluation by different fitness functions

Indiv. Index	Fuel Con.	SOC decrease	R_{fuel}	R_{soc}	Rank by Eq.(7)	Rank by Eq.(11)
1	0.001	0.005(**P**)	5	35	98	140
2	0.010	0.002	25	14	33	**39**
3	0.007	0.003	19	23	**24**	42
4	0.002	0.004(**P**)	7	32	99	139
….	……	……..	…….	……	……..	…….

5.5 Evolutionary Algorithm based Online EMS

5.5.1 EDA-Based On-line EMS Algorithm with SOC Control

Details of the proposed EDA-based on-line EMS algorithm with SOC control are summarized in the ***Algorithm 1*** below. This algorithm is implemented on each prediction horizon (N time steps) within the framework presented in Fig. 5-11 (see the box with red dashed line).

Algorithm 1 EDA-based on-line EMS with SOC control

1: Initialize a random output solution I_{best}(N time steps)
2: $P_{current}$ <= Generate initial population randomly
3: While iteration_number ≤ Max_iterations, do
4: For each individual s in $P_{current}$
5: Calculate fuel consume C_{fuel} using eq. (1).
6: Calculate SOC decrease using eq. (5)
7: Obtain the rank index of s: R_{fuel}
8: Obtain the rank index of s: R_{soc}
9: If SOC reference control is adopted
10 Calculate the lower bound using eqs.(8)(9)(10)
11: If individual s violates eq.(6)
12: P=P_0;//largest fuel consumption in N steps
13: Else
14: P=0;
15: End If
16: Calculate the fitness value for s using eq.(7)
17: Else If SOC self-adaptive control is adopted
18: If individual s violates eq.(6)
19: P'=S
20: Else
21: P'=0;
22: End If
23: Calculate the fitness value for s using eq.(11)
24: End If
25: End For
26: Rank $P_{current}$ in ascending order based on fitness
27: P_{top} <= Select top α% individuals from $P_{current}$
28: E <= Estimate a new distribution from P_{top}
29: P_{new} <= Sample N individuals from built model E
30: Evaluate each individual in P_{new} using line 5 to 14
31: Mix $P_{current}$ and P_{new} to form 2N individuals
32: Rank 2N individuals in ascending order by fitness
33: $P_{current}$<= Select top N individuals
34: Update I_{best} if a better one is identified.
35: Iteration_number ++
36: End While
37: Output I_{best}

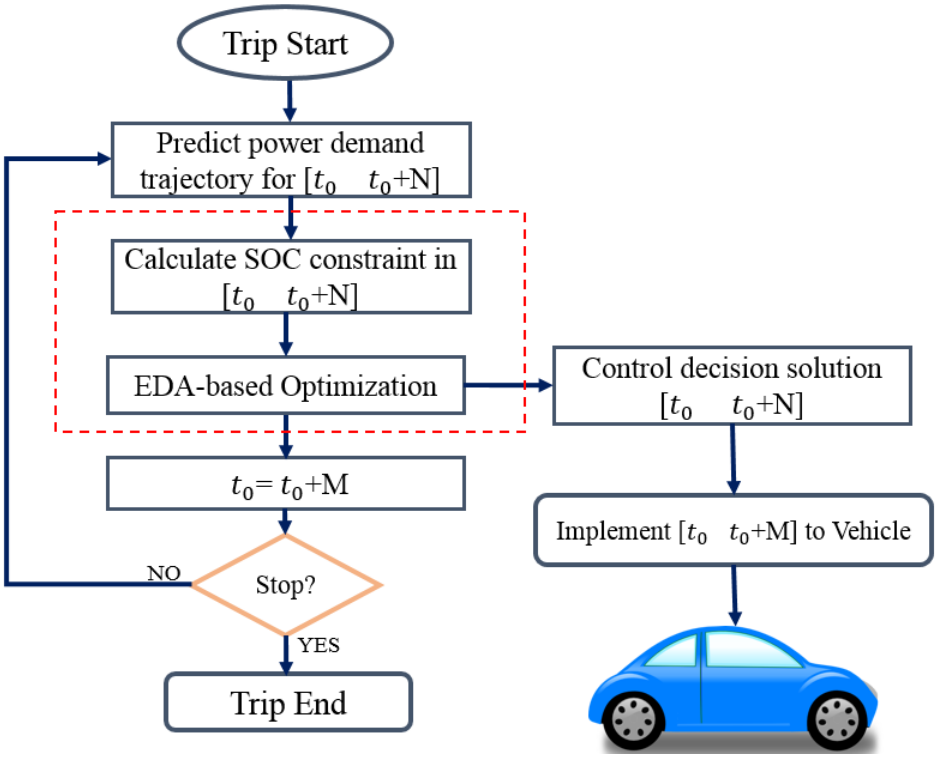

Figure 5-8 EDA-based on-line energy management system.

In the following section, we compare the performance of the proposed self-adaptive SOC control with other SOC control strategies. For convenience, we list the abbreviations of all the involved strategies in Table 5-4.

Table 5-4 Abbreviations of different SOC control strategies compared in this study

SOC control strategies	Abbreviations
Binary control	B-I
Basic SOC control	B-A
Concave downward	C-D
Straight line	S-L
Concave upward	C-U
Self-adaptive SOC control	S-A

5.6 Case Study with Real-world Traffic Data

5.6.1 Synthesized Trip Information

To validate the proposed EMS for PHEVs, we use real-world data collected on January 17th, 2012, along I-210 between I-605 and Day Creek Blvd in San Bernardino, California, as a case study (see Fig. 5-12). Please refer to [138] for more detailed description of data collection and specifications of the power-split PHEV model if interested.

Based on the collected traffic data along with road grade information, second-by-second vehicle velocity trajectory and power demand have been synthesized as described in [138]. As pointed out earlier, it is impractical to have a priori knowledge of the exact vehicle velocity trajectory. In this study, we focus on the development of the optimal power-split control, assuming perfect prediction of vehicle velocity trajectory. Research on improving the prediction of vehicle velocity trajectory in real time is part of our future work.

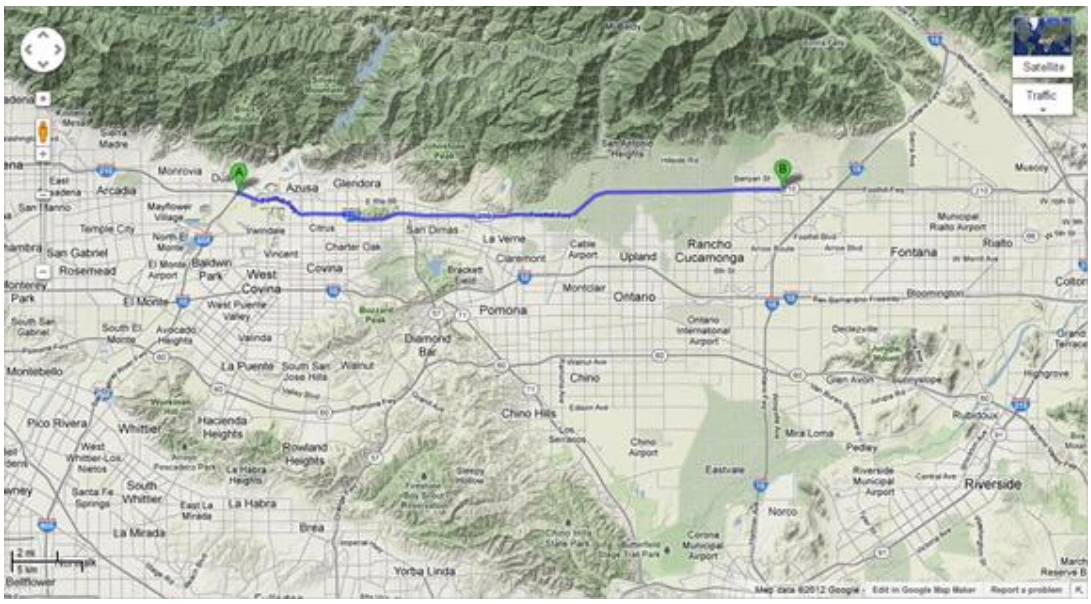

Figure 5-9 Example trip along I-210 in Southern California used for evaluation.

5.6.2 Off-line Optimization for Validation

To justify the selection of EDA as the kernel of the proposed framework, we first test EDA on the full-trip off-line optimization. The results are compared with those obtained from two other popular evolutionary algorithms: genetic algorithm (GA) and particle swarm optimization (PSO). The fitness (i.e., total ICE energy consumption) of EDA-based off-line optimization obtains better fuel economy (0.346 gallons) than the other two (0.364 gallons for GA and 0.377 for PSO, respectively), at the same computational expense (i.e., same population size and same number of iterations) [172]. In addition, the result from EDA is much closer to the global optimum (0.345 gallons in this case) with the difference being less than 1%.

5.6.3 Real-time Performance Analysis and Parameter Tuning

As aforementioned, a necessary condition for on-line implementation of the proposed EMS is that the optimization for the next prediction horizon has to be finished within the current control horizon (see Fig.5-8). In our study, for example, the optimization for a prediction horizon of 50 seconds can be completed within 1.1 seconds (with Intel Core i7 3.4GHz, RAM 4G, and 64bit-Matlab 2012). In addition, one of our previous work [172] has shown that the lengths of prediction horizon and control horizon may significantly affect the algorithm performance. The best combination of these two parameters is found to be N=250 and M=10 in this case.

Unlike the conventional MPC whose optimization has to be implemented along each prediction horizon, our proposed EA based online EMS (see Fig.5-11) can take advantage of the optimal results from previous prediction horizons, which avoids a new optimization starting from scratch and therefore saves a lot of computational overhead. As can be seen in Fig. 5-13, part of the optimal decisions from previous prediction optimization horizon is adopted as the seed for initial population of current prediction horizon optimization. For example, when the control

horizon is 3s and prediction/optimization horizon is N, only 3 control decisions need to be randomly initialized and optimized in the second prediction/optimization horizon. This allows the optimization or search to be much more efficient, compared to the same process over entire prediction horizon. To further validate this computational performance, we designed an EA based MPC (EAMPC) which activates a complete new optimization for each prediction/optimization horizon and compared it with our proposed model. The computation time track in Fig.5-14 shows that for a 50-seconds prediction horizon, the conventional MPC takes around 1.1 seconds for each optimization horizon but our proposed model can take only less than 0.1s to finish the optimization from the second prediction horizon.

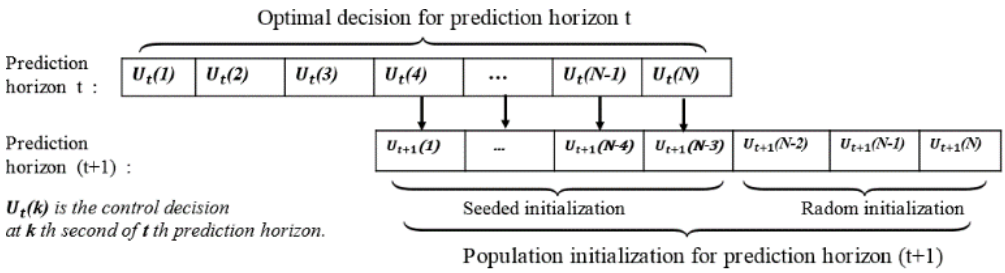

Figure 5-10 Population initialization from the second prediction horizon (i.e., t≥ 2).

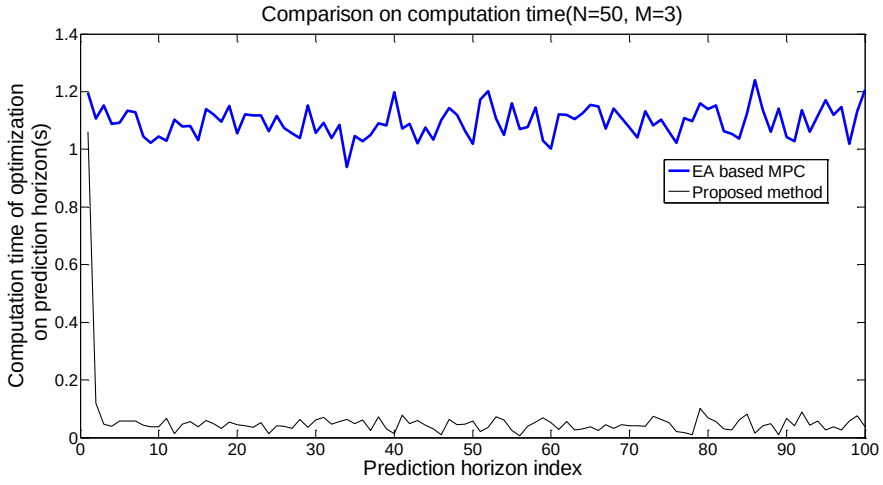

Figure 5-11 Comparison on computation time.

5.6.4 On-line Optimization Performance Comparison

To fully evaluate the performance of the proposed on-line EMS strategies, we compare them to the conventional binary control (implementable in real-time) strategy as well as the off-line global optimal control strategy (with the use of dynamic programming [145]). The comparisons are carried out on both the single trip scenario and multiple trips scenario.

When tested on a single (westbound) trip, the fuel consumption and SOC profiles by different strategies are illustrated in Fig. 5-15. It is shown that the proposed S-A algorithm achieves the lowest fuel consumption (0.3515 gallons) which is only 1.56% worse than that of global optima obtained by the off-line optimization (0.3460 gallons). These results can be explained by the shape of the resultant SOC profiles. For instance, SOC decreases very quickly in the B-I strategy, and reaches the lower bound (i.e., 0.2) at around 1,200 seconds because the use of battery power is always prioritized whenever available. Therefore, ICE has to supply most of the demanded power after 1,200 seconds. This is very similar to the cases of the B-A and C-U strategies where the battery power is also consumed aggressively at the beginning of the trip with very loose constraints. On the other hand, the S-L and C-D strategies perform better since their battery power is used more cautiously along the trip. These findings are consistent with the conclusions of many other studies [159, 171] in that a smoother distribution of battery power usage along the trip would result in higher fuel efficiency.

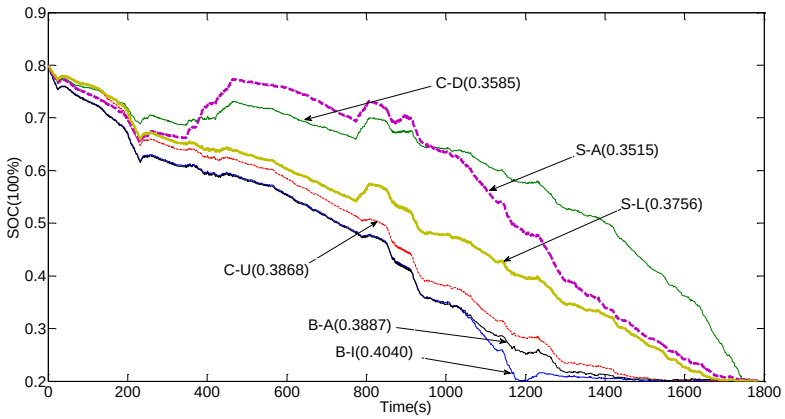

Figure 5-12 SOC trajectories resulted from different control strategies.

In order to know the statistical significance of the different EMS strategies, we test them on 30 randomly selected trip profile data extracted from the same road segment on 12 different days. The results are also compared to the binary control and dynamic programming (D-P) strategies. For the purpose of comparison, we set the fuel consumption obtained by the binary control strategy as the baseline and calculate the percentage of fuel savings achieved by the other EMS strategies. As we can see in Fig. 5-16, the D-P strategy achieves the best fuel savings with an average of 19.4% and the least variance simply because it is an off-line optimization strategy. The proposed S-A strategy achieves an average of 10.7% fuel savings which is higher than all other on-line strategies and consistent with the result of the single trip test. An interesting observation is that the S-L strategy has better average fuel savings (i.e., 9.3%) than the C-D and C-U strategies which is not consistent with the test result of the single trip test. A possible reason is that the C-D strategy performs better on some trips in which the power demand is higher in later stages of the trip but the C-U strategy performs better on the trips in which the power demand is higher in earlier stages. On the other hand, the S-L strategy balances the SOC control between these two types of trip pattern, and therefore has better average performance.

For further validation, the proposed S-A strategy with the best performance is compared with

other existing PHEV EMS strategies that employ short-term prediction. Although these strategies were proposed to handle powertrain models with different fidelity as well as different data set for validation, they all used the binary control strategy as a benchmark (the same as in this work). This provides us a chance to compare all models in a relatively fair manner. The comparison results are listed in table 5-5, which proves that our model achieves the largest improvement of fuel efficiency (with regard to the binary control strategy) but requires less trip information.

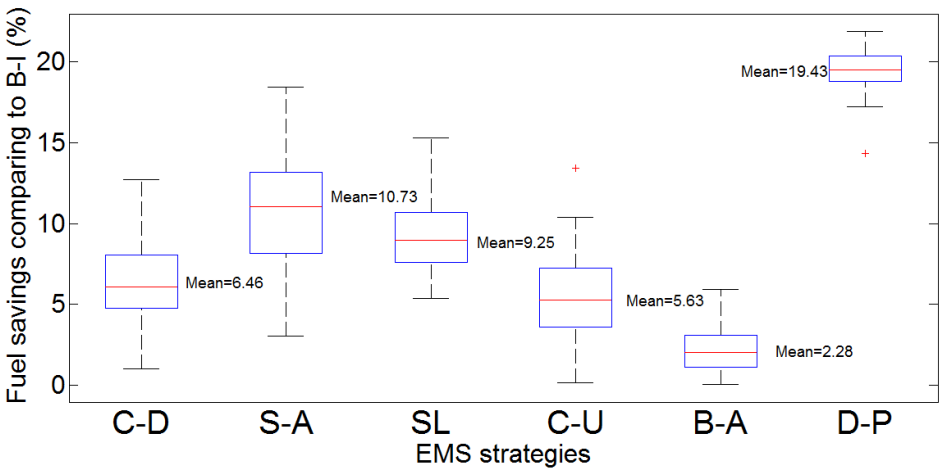

Figure 5-13 Box-plot of fuel savings on 30 trips.

Table 5-5 Comparisons with existing models

EMS model	Year	STP[1]	Trip distance	FE I[2]	Consider Charging?
This work	**2016**	**Yes**	**Unknown**	**10.7%**	**Yes**
EAMPC	**2016**	**Yes**	**Unknown**	**7.9%**	**Yes**
MPC[173]	2014	Yes	Known	8.5%	No
MPC[154]	2015	Yes	Known	6.7%	No
A-ECMS[173]	2014	Yes	Known Known	10.2%	No
A-ECMS[151]	2015	Yes	Known	7.6%	No
DP[174]	2015	Yes	Known	5.8%	No
SDP[3] [175]	2011	Yes		7.7%	No

[1]Short-term prediction; [2]Fuel economy improvement comparing to binary control; [3] Stochastic Dynamic Programming.

Analysis of Trip Duration

In this section, we analyze and compare the effectiveness of the proposed on-line EMS for longer trips. These longer trips are constructed by concatenating multiple trip profiles and the results are shown in Fig. 5-17. As can be observed, the B-I strategy has the best fuel economy when the trip duration is shorter than 1,500 seconds. For these short trips, the PHEV can mostly rely on battery energy. However, as the trip duration becomes longer, especially when longer than 2,500 seconds, the S-A strategy outperforms all the others.

To further explain this finding, the resultant fuel consumption and the corresponding SOC profiles for the longest trip (5,000 seconds) are provided in Fig. 5-18. According to the figure, the S-A strategy has the lowest fuel consumption and its SOC profile is a combination of the CD mode (defined in Fig. 5-1) before 2,000 seconds and the CS mode after 2,000 seconds. This contradicts with most of the existing studies, which report that an optimal fuel economy for the trip can be achieved by operating solely in the CD mode [159]. Here, we present evidence that it is not always the case, and that the CD+CS operation can result in optimal fuel efficiency for long trips. Furthermore, this finding also implies the potential for the proposed S-A strategy to adapt to different trip durations.

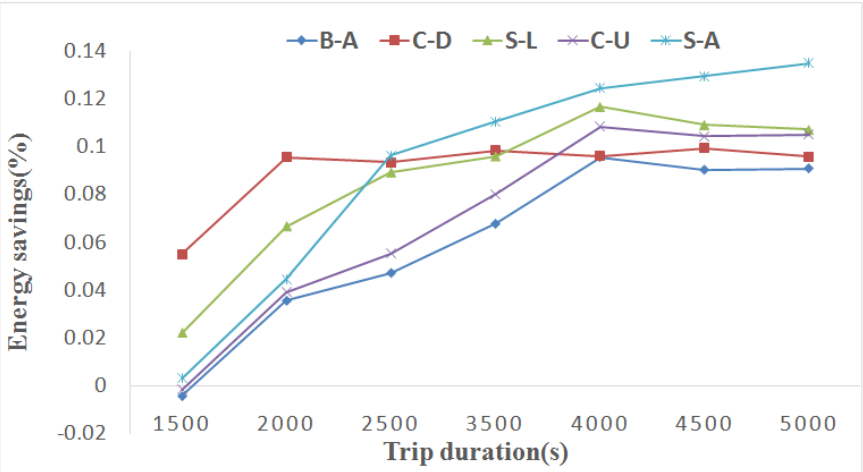

Figure 5-14 Fuel savings for trips with different duration, compared to B-I.

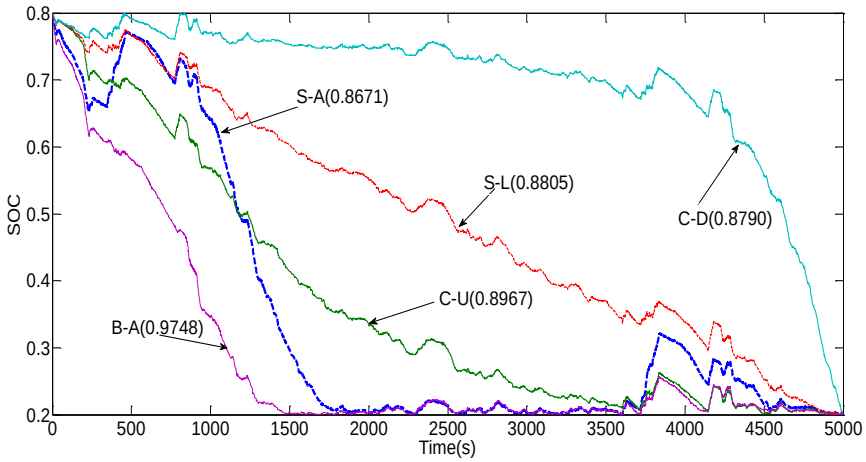

Figure 5-15 Resultant SOC curve when trip duration is 5,000 seconds.

Performance with Charging Opportunity

Considering the plug-in capability of PHEVs, we evaluate the performance of the proposed strategies at the tour level. More specifically, we consider the commute trips of the case study as a tour and assume that there is a charging opportunity (to a full charge) between the end of the westbound trip and the beginning of the eastbound trip. We then compare the different SOC control strategies under the following two scenarios:

1) Scenario I: The proposed EMS with a priori knowledge of the charging opportunity;
2) Scenario II: The proposed EMS without a priori knowledge of the charging opportunity. In this case, a conservative strategy is applied by assuming that there is no charging station available in between the trips.

The results are illustrated in Fig.5-19. They show that the knowledge of the charging opportunity information has great influence on the resultant SOC profiles for the deterministic SOC reference control strategies but no influence on the SOC self-adaptive control strategy.

Table 5-6 presents the increased fuel consumption due to the lack of knowledge of the charging opportunity prior to the tour. As shown in the table, the C-D, S-L, and C-U strategies all have 13% or more increase in fuel consumption if the charging opportunity information is unknown, while the B-I and S-A strategies are not affected because the trip duration is not considered in their decision-making process. These findings further emphasize the advantage of the proposed SOC self-adaptive control strategy in terms of robustness to the level of knowledge about charging availability.

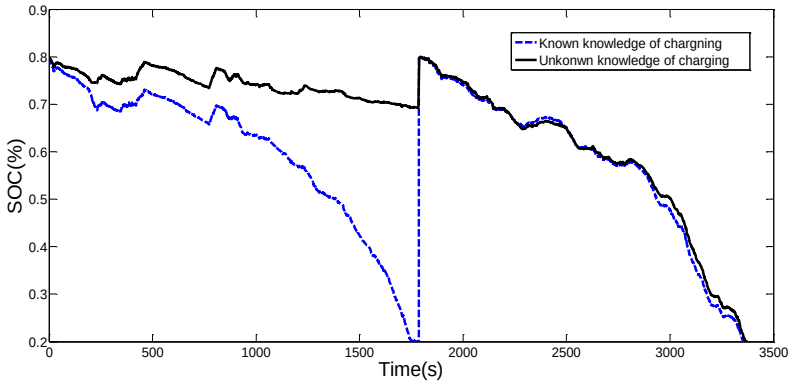

a. C-D

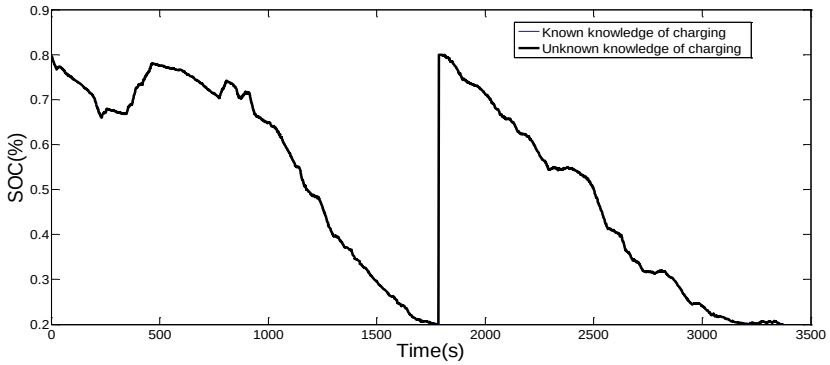

b. S-A

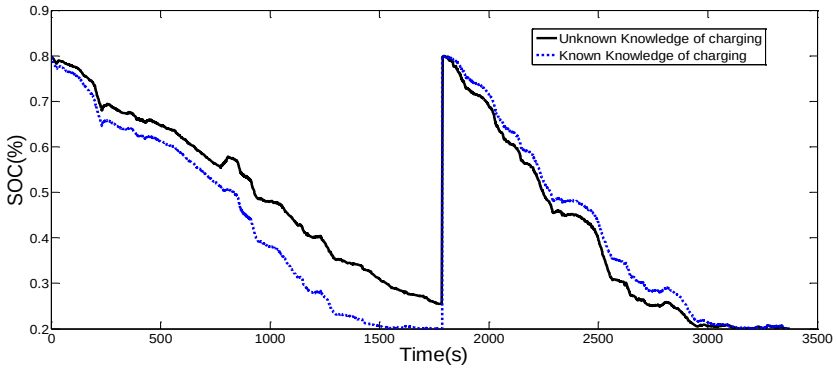

c. C-U

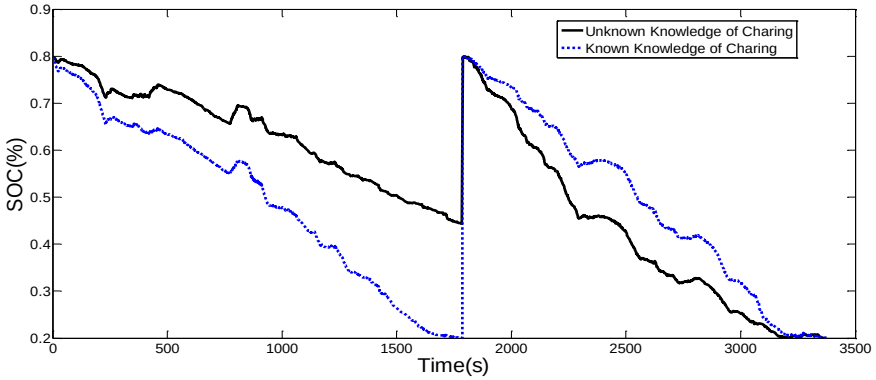

d. S-L

Figure 5-16 SOC track with known or unknown charging opportunity.

Table 5-6 Increased fuel consumption

Control strategy	Known (gal)	Unknown (gal)	Increased fuel consumption
B-I	0.9748	0.9748	00.0%
B-A	0.7109	0.7543	06.1%
C-D	0.6729	0.8439	25.1%
S-L	0.6809	0.7853	15.0%
C-U	0.7066	0.8034	13.0%
S-A	0.6681	0.6681	00.0%

5.7 Summary and Discussion

For the EA based EMS, the proposed framework applies the self-adaptive strategy to the control of the vehicle's state-of-charge (SOC) in a rolling horizon manner for the purpose of real-time implementation. The control of the vehicle's SOC is formulated as a combinatory optimization problem that can be efficiently solved by the estimation distribution algorithm (EDA). The proposed energy management system is comprehensively evaluated using a number of trip profiles extracted from real-world traffic data. The results show that the self-adaptive control strategy used in the proposed system statistically outperforms the conventional binary control strategy with an average of 10.7% fuel savings. The sensitivity analysis reveals that the optimal prediction horizon window of the proposed energy management system is 250 seconds, which requires 5.8 seconds of computation time in our study case. This amount of time is much less than the optimal control horizon window of 10 seconds, which confirms the feasibility of real-time implementation. Another important advantage of the proposed energy management system is that, unlike other existing systems, it does not require a priori knowledge about the trip duration. This allows the proposed system to be robust against real-world uncertainties, such as unexpected traffic congestion that increases the trip duration significantly, and changes in inter-trip charging availability.

6 Co-optimization of Vehicle Dynamics and Powertrain Operations

6.1 Overview

The existing research work reviewed in previous sections shows that vehicle fuel efficiency can be improved at least from two different perspectives: vehicle dynamics and powertrain control The majority of exiting studies are only focused on one of them. Very few researchers have conducted research on the combined optimization of vehicle dynamics and powertrain operation. In one of our previous work [207], a power-based longitudinal control algorithm with co-optimization of vehicle dynamics and powertrain operations for internal combustion engine (ICE) vehicles was proposed and tested. The system took into account the vehicle's brake specific fuel consumption (BSFC) map, roadway grade, downstream traffic conditions, and traffic signal status of the upcoming intersection in the calculation of an optimal speed profile in terms of energy savings and emissions reduction. Hu et al. [208] recently developed an ecodriving assistance system for hybrid electric vehicles (HEV) on rolling terrains. The system was capable of optimizing the powertrain operations of HEVs by taking advantage of the information obtained via connected vehicle technology, but neither traffic signal information nor different vehicle automaton levels are considered. Thus far, to the best of authors' knowledge, no existing work has been focused on designing an integrated and connected ecodriving system for PHEVs with co-optimization of vehicle dynamics and powertrain operations.

To address this gap, an innovative ecodriving system with co-optimization of VD&PT for PHEVs is developed in this study. The proposed system combines the functionality of Eco-approach and departure system at signalized intersections and online EMS system for PHEVs, which can significantly boost the fuel efficiency of PHEVs for urban driving. The designed system is implemented in two different stages: in-vehicle advising stage and automatic

longitudinal control stage. The results are compared to the baseline scenario which is manual driving without any assistance system. The major contributions of this chapter are:

a. A first-of-its-kind integrated ecodriving system for PHEVs is designed to improve fuel efficiency.
b. The performance of the designed system is extensively validated and tested with real-world driving data at different levels of vehicle automation.

6.2 Integrated Co-optimization Framework

In this work, the next generation connected Ecodriving system is proposed to assist the energy-efficient driving of PHEVs in an urban environment (e.g., along signalized corridors) through the co-optimization of vehicle dynamics and powertrain operation. Theoretically, the objective of the co-optimization is the to minimize the total fuel consumption of PHEV along a trip considering all the factors that influence the vehicle energy consumption. As shown in Fig.6-2, the inputs into the co-optimization model are the real-time traffic condition and downstream traffic signal information that obtained through cellular network or vehicle-and-infrastructure (V2I/I2V) wireless communications. The output of the system. The outputs are the optimal powertrain operations strategy and finally the resulted vehicle speed trajectory.

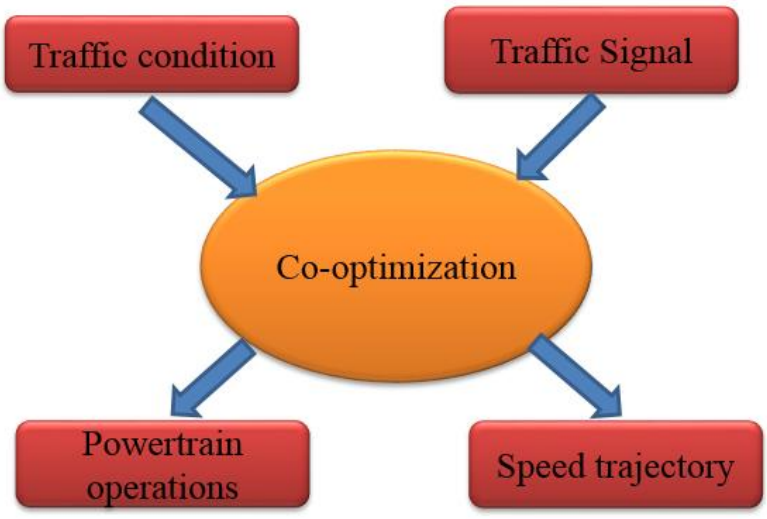

Figure 6-1 Flowchart of co-optimization system

Mathematically, the co-optimization of vehicle dynamics and powertrain operations for PHEVs is formulated as a nonlinear constrained optimization problem. The ICE power supply at each time step is optimized to minimize the total fuel consumption by ICE of a PHEV along the entire trip by taking advantage of the real-time data that obtained or predicted within the connected vehicle environment. The formulation of this co-optimization is given as:

Assumption:

- Hybrid PHEVs
- Consider longitudinal velocity (v_t) only
- Focus on fuel consumption only
- No grade information is in consideration
- Without loss of generality, t starts from 0
- The vehicle will not back up

$$\min_{\omega,\tau} \int_t \frac{P_{eng}\left(\omega_{eng}(t),\tau_{eng}(t)\right)}{\eta_{eng}\left(\omega_{eng}(t),\tau_{eng}(t)\right)} \tag{6-1}$$

subject to

(Power Related):

$$P_{eng}\left(\omega_{eng}(t),\tau_{eng}(t)\right) = P_{tr}(v(t);\boldsymbol{A}) - P_{batt}\left(\omega_{MG1}(t),\tau_{MG1}(t),\omega_{MG2}(t),\tau_{MG2}(t)\right) \qquad \forall t$$

(Travel Distance Related):

$$\int_t v(t) = \int_t \Upsilon\left(\omega_{eng}(t),\omega_{MG1}(t),\omega_{MG2}(t);\boldsymbol{B}\right) = L_0$$

(Boundary Related):

$$\begin{cases} \omega_{(\cdot)}^{min} \le \omega_{(\cdot)}(t) \le \omega_{(\cdot)}^{max} \\ \tau_{(\cdot)}^{min} \le \tau_{(\cdot)}(t) \le \tau_{(\cdot)}^{max} \\ P_{eng}^{min} \le P_{eng}(t) \le P_{eng}^{max} \\ P_{batt}^{min} \le P_{batt}(t) \le P_{batt}^{max} \\ 0 \le v(t) \le v^{max} \\ SOC^{min} \le SOC(t) \le SOC^{max} \end{cases} \quad \forall t$$

(Initial Conditions Related)

v_0, L_0, and SOC_0 are given.

where ***A*** and ***B*** are vectors of parameters associated with tractive power (e.g., vehicle mass, frontal area) and mechanical transmission (e.g., gear ratio, final drive ratio).

6.3 Bi-level Approximation of Co-optimization

In this work. a bi-level optimization is designed to solve and obtain the optimal or near optimal solution of above formulated optimization problem. As shown in Fig.6-3, the optimal speed trajectory is calculated by the onboard system based on the obtained information and then advised to the driver through the in-vehicle display for PHEVs with level 0 of automation. If there is level 1 or above vehicle automation level, the optimal longitudinal speed trajectory can be fed into the vehicle control system without human intervention. The real-time traffic data and signal information can be obtained through cellular network or vehicle-and-infrastructure (V2I/I2V) wireless communications. With this information, the future vehicle speed trajectory can be obtained in two different ways: 1) based on the downstream traffic condition when there is no near intersection; and 2) based on the signal phase and timing information when approaching a signalized intersection.

Besides the vehicle dynamics optimization through vehicle trajectory planning, the powertrain optimization is also included in the designed system.

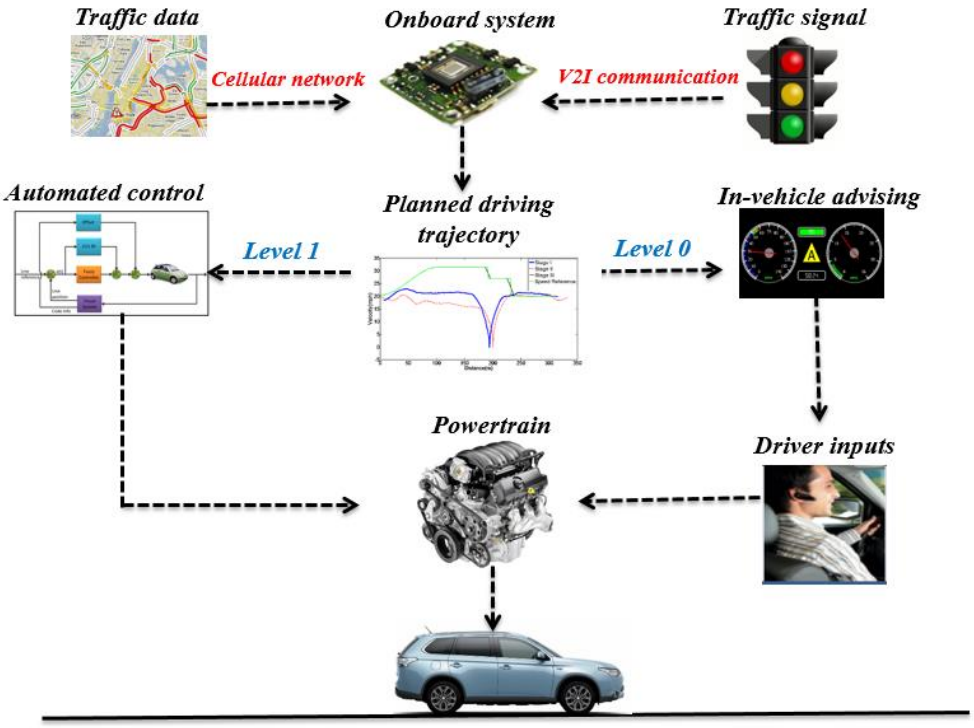

Figure 6-2 Framework of the proposed Connected Ecodriving assistance system.

As shown in Fig 6-4, the whole system is implemented in a receding horizon framework. For each N (seconds) step horizon, the future vehicle trajectory is calculated by the vehicle trajectory planning subsystem, and then the optimal powertrain operation is calculated with the given optimal speed trajectory. Finally, only a portion of the calculated optimal powertrain operations (M seconds) are implemented and another calculation for the next N seconds starts immediately. In such time horizon receding framework, the OEMS are implemented in real time.

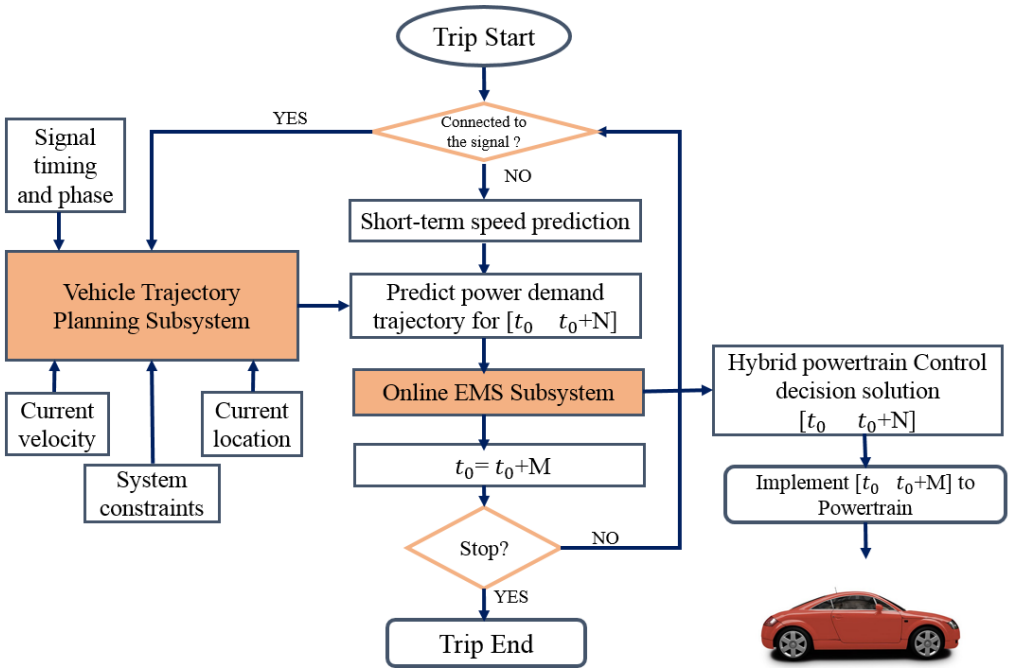

Figure 6-3 Flowchart of connected Ecodriving system with co-optimization.

6.4 Vehicle Dynamics Optimization: Connected Ecodriving

In connected vehicle environment, vehicle dynamics (e.g., velocity profile) can be optimized to achieve energy-efficient driving styles using the information through connectivity. In this chapter, the similar connected ecodriving systems described in chapter 4 are adopted to achieve the vehicle dynamics optimization. Three different technology stages are used to represent different level of vehicle dynamics optimization, which includes Uninformed human driving, human driving with EAD assistance not considering driver error and EAD assistance with automatic longitudinal control. For more details, please refer to chapter 4.

6.5 Powertrain Operation Optimization: Online Energy Management System

Beside the vehicle dynamics optimization in connected vehicle environment, the operations of powertrain can also be optimized, especially for PHEVs. The optimal (in terms of fuel economy)

energy management for PHEVs can be formulated as a nonlinear constrained optimization problem. The objective is to minimize the total fuel consumption by ICE along the entire trip given the required power.

$$min \int_0^T fuel(\omega_e, \tau_e) dt \tag{6-2}$$

subject to

$$\begin{cases} \dot{SOC} = f(P_{tr}, SOC, \omega_{MG1}, \tau_{MG1}, \omega_{MG2}, \tau_{MG2}) \\ g(\omega_e, \tau_e, \omega_{MG1}, \tau_{MG1}, \omega_{MG2}, \tau_{MG2}) = 0 \\ SOC^{min} \le SOC \le SOC^{max} \\ \omega_{(\cdot)}^{min} \le \omega_{(\cdot)} \le \omega_{(\cdot)}^{max} \\ \tau_{(\cdot)}^{min} \le \tau_{(\cdot)} \le \tau_{(\cdot)}^{max} \end{cases} \tag{6-3}$$

where T is the trip duration; ω_e, τ_e are the engine's angular velocity and engine's torque, respectively; $fuel(\omega_e, \tau_e)$ is ICE fuel consumption model which is a function of ω_e and τ_e; ω_{MG1}, τ_{MG1} are the first motor/generator's angular velocity and torque, respectively; ω_{MG2}, τ_{MG2} are the second motor/generator's angular velocity and torque, respectively(see Fig.1b); $f(P_{tr}, SOC, \omega_{MG1}, \tau_{MG1}, \omega_{MG2}, \tau_{MG2})$ models the battery power consumption which is related to the tractive power P_{tr}, state-of-charge (SOC), and key parameters (i.e., speeds and torques) of ICE and motors; $g(\omega_e, \tau_e, \omega_{MG1}, \tau_{MG1}, \omega_{MG2}, \tau_{MG2}) = 0$ represents the coupling relationship among ICE and motors. For more details about the model derivations and equations, please refer to our previous work in [189].

Such formulation is suitable for traditional mathematical optimization methods with high computational complexity, which is difficultly to be implemented in real-time. In order to facilitate on-line optimization, we herein discretize the engine power and reformulate the optimization problem represented by (4) as follows:

$$\min \sum_{k=1}^{T} \sum_{i=1}^{N} x(k,i)\, P_e(i)/\eta_e(i) \tag{6-4}$$

subject to:

$$\sum_{k=1}^{j} f\left(P_{tr}(k) - \sum_{i=1}^{N} x(k,i) P_e(i)\right) \le C \quad \forall j = 1, \dots, T \tag{6-5}$$

$$\sum_{i=1}^{N} x(k,i) = 1 \qquad \forall k \tag{6-6}$$

$$x(k,i) = \{0,1\} \qquad \forall k, i \tag{6-7}$$

where N is the number of discretized power level for the engine; k is the time step index; i is the engine power level index; C is the gap of the battery pack's SOC between the initial and the minimum; $P_e(i)$ is the i-th discretized level for the engine power and $\eta_e(i)$ is the associated engine efficiency; and $P_{tr}(k)$ is the tractive power demand at time step. $x(k,i)$ is a binary function which gives either 1 or 0.

Furthermore, if the change in SOC (ΔSOC) for each possible engine power level at each time step is pre-calculated given the (predicted) power demand, then constraint (7) can be replaced by

$$SOC^{ini} - SOC^{max} \leq \sum_{k=1}^{j} x(k,i)\Delta SOC(k,i) \leq SOC^{ini} - SOC^{min}$$

$$\forall j = 1, \dots, T \qquad (6\text{-}8)$$

where SOC^{ini} is the initial SOC; and SOC^{min} and SOC^{max} are the minimum and maximum SOC, respectively. Therefore, the problem is turned into a combinatory optimization problem whose objective is to select the optimal ICE power level for each time step given the predicted information in order to achieve the highest fuel efficiency for the entire trip. Ideally, the optimization can be performed for the entire trip by assuming the entire trip information is known as a priori. In practice, however, it is too challenging to accurately know the entire trip information before the trip due to the expected uncertainty. Therefore, an online energy management systems (OEMS) is usually more practical.

In our pervious study [187,190], different versions of online energy management system (OEMS) for PHEVs have been proposed and tested. In this work, we designed a similar estimation distribution algorithm based OEMS for PHEVs, using the receding horizon control structure (see Fig. 6-6). With the receding horizon control, the entire trip is divided into segments or time horizons. As shown in Fig. 6-6, the prediction horizon (N sampling time steps) needs to be longer than the control horizon (M sampling time steps). Both horizons keep moving forward (in a rolling horizon style) while the system is operating. More specifically, the prediction model is used to predict the power demand at each sampling step (e.g., each second) in the prediction horizon. Then, the optimal ICE power supply for each second during the prediction horizon is calculated with this predicted information.

In each control horizon, the pre-calculated optimal control decisions are fed into the powertrain control system (e.g., electronic control unit or ECU) at the required sampling frequency. In this study, when the vehicle is connected to the signal controller by V2I communication, the future driving trajectory is obtained by the above mentioned VTP model. Otherwise, we assume that the short-term prediction model is available (which is out of the scope this study) and the focus of this subsystem is on-line power-split optimization.

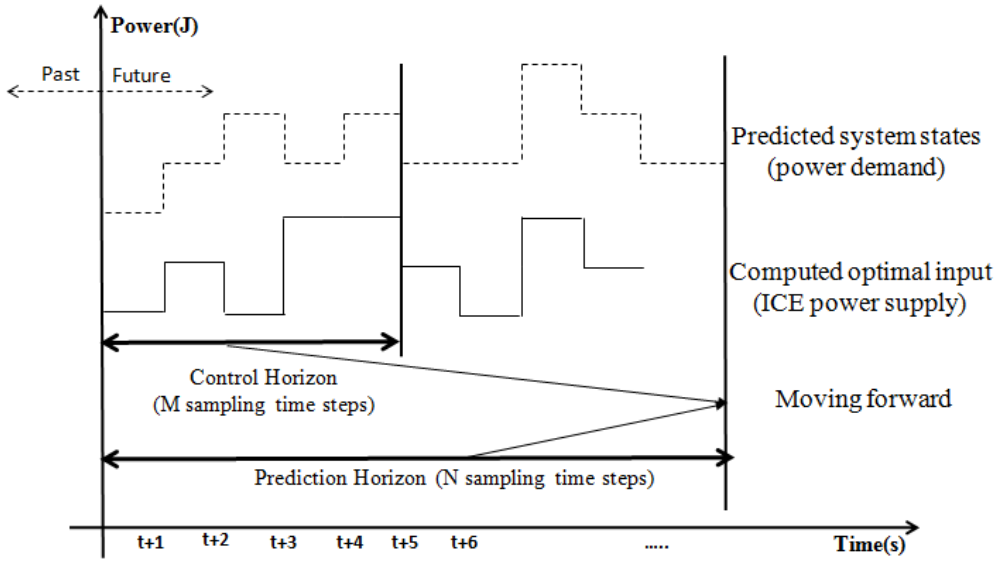

Figure 6-4 Time horizons of prediction and control.

In this study, for performance comparison, the basic and most common Binary control strategy is used as the baseline EMS model. In Binary control strategy, engine power can be used only when the battery power is not able to satisfy the power demand or the SOC lower bound is reached.

6.6 Trip Data Synthesis

To comprehensively evaluate the energy saving performance of the proposed system, the real-world driving data collected in the GlidePath project [209] under different automation level (or different stages of EAD) of driving assistance system at the Turner-Fairbank Highway Research Center (TFHRC) in McLean, Virginia, were used in this study. For more information about the data set ,please refer to section 4.2.2.

6.7 Urban Route Synthesis

It is noted that the spatial span of each run for the aforementioned EAD testing is only about 306 meters, which is too short to obtain tangible drop in State-of-charge (SOC) of a PHEV (less than 0.01). To address this issue, we propose a methodology to synthesize trips along a signalized corridor with multiple intersections (e.g., 24 intersections in this study), using the field test data from each run (as described in the previous subsection) as well as certain driving cycle which should satisfy at least the following conditions:

1) It is a (truncated) standard driving cycle widely accepted by public, e.g., a driving schedule (https://www.epa.gov/vehicle-and-fuel-emissions-testing/dynamometer-drive-schedules) accepted in emissions test by U.S. Environmental Protection Agency.
2) The speed limit and average speed are consistent with the field test data (e.g., the speed limit is 25 mph for the field test).
3) The (truncated) standard driving cycle covers a speed range wide enough to accommodate the variations in the entry speeds (at 190 m before the stop-bar) and exit speeds (at 116 m after the stop-bar) of all trips.

In this study, the truncated Urban Dynamometer Driving Schedule or UDDS (shown in Fig. 6-9 (a)) was selected to concatenate the test data from each run. It should be pointed out the truncated UDDS starts and ends at 0 mph, resulting in additional stop(s) in the synthesized trajectories between intersections. To avoid the occurrence of these stop(s), we only used the portion above the dash-line in Fig. 6-9 (a) for trajectory synthesis. In addition, we shuffled the sequence of each run (at intersections) randomly to generate multiple trajectories for evaluation and comparison in a statistical manner. Fig. 6-9 (b) presents an example of synthesized trajectory along a segment of the hypothetical corridor in this study.

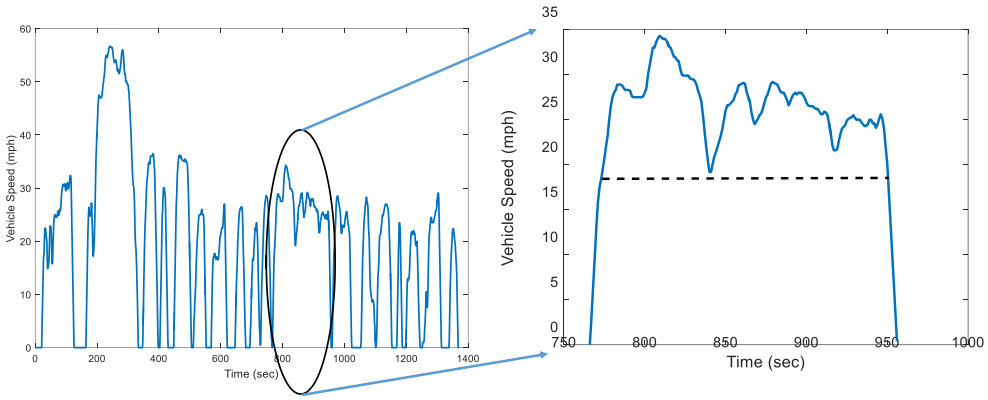

(a) The selected UDDS driving schedule and the truncated portion (zoomed in on the right)

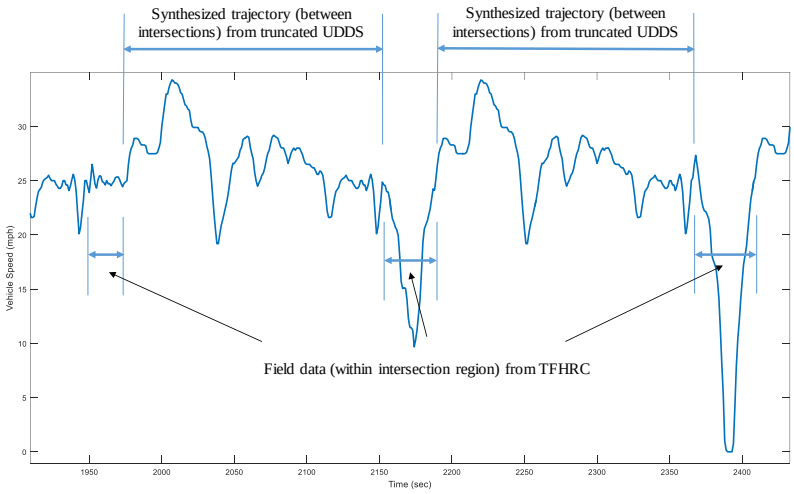

(b) An example of synthesized along the hypothetical corridor

Figure 6-5 Urban driving trajectory synthesis.

6.8 Performance Evaluation and Analysis

6.8.1 Technology Scenarios Matrix

To fully investigate the environment benefits from different options on two major fuel efficiency improvement directions: 1) vehicle dynamics optimization; and 2) powertrain control optimization, the proposed integrated connected ecodriving system in Figure 4 is implemented

by different combination of EAD stages (i.e., MUD, HMI and AUTO) and EMS control modes (i.e., Binary control mode and OEMS mode). We call each of these technique combinations a "technology scenario". The details for each of these technology scenarios are provided in the following scenario matrix (see Fig., 6-10)

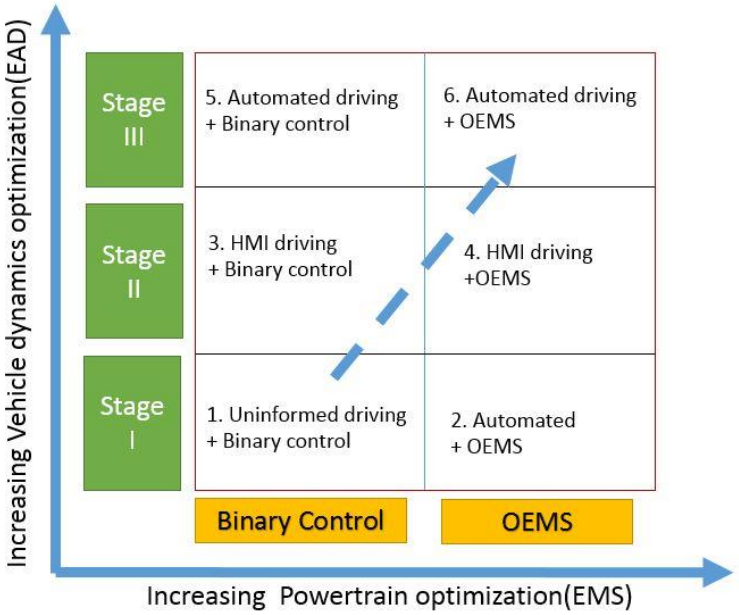

Figure 6-6 . Technology scenario matrix for comparison.

6.8.2 Evaluation of Short-trip at Signalized Intersections

The proposed system is first evaluated at the intersections only. Vehicle trajectories when passing through the intersections are selected from the real-world driving data, to calculate the energy consumptions in different scenarios as described in Fig. 6-10. Due to the testing driving facility limitation (190 m upstream and 116 m downstream), the trajectory within this road segment is very short (30 seconds on average). The energy consumption is not quite demanding if looking at these short trips alone. Hence when the initial SOC is high enough, the PHEV would only use electricity without consuming fuels. As can be seen in Fig. 6-11 (a) and 6-11(b), there is no fuel consumption difference between OEMS and Binary control mode when the

initial SOC is higher than 0.205 (in the case of the minimum SOC being 0.2), because the battery stored energy is enough to satisfy all the power demand when travelling through the intersection. Therefore, in this study, in order to investigate the difference in energy consumption resulting from different EMS models within the intersection region, the initial SOC has to be selected at a very low level such as 0.205.

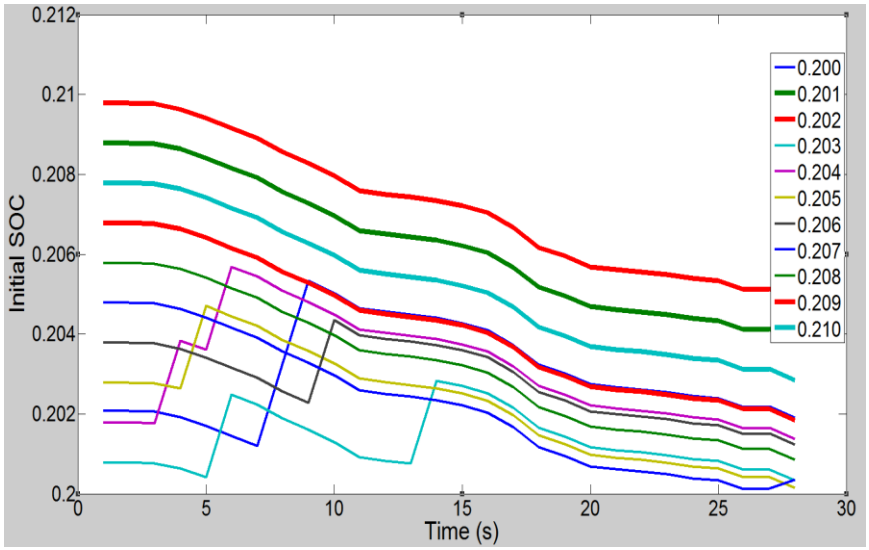

(a) Resulted SOC track for different initial SOC

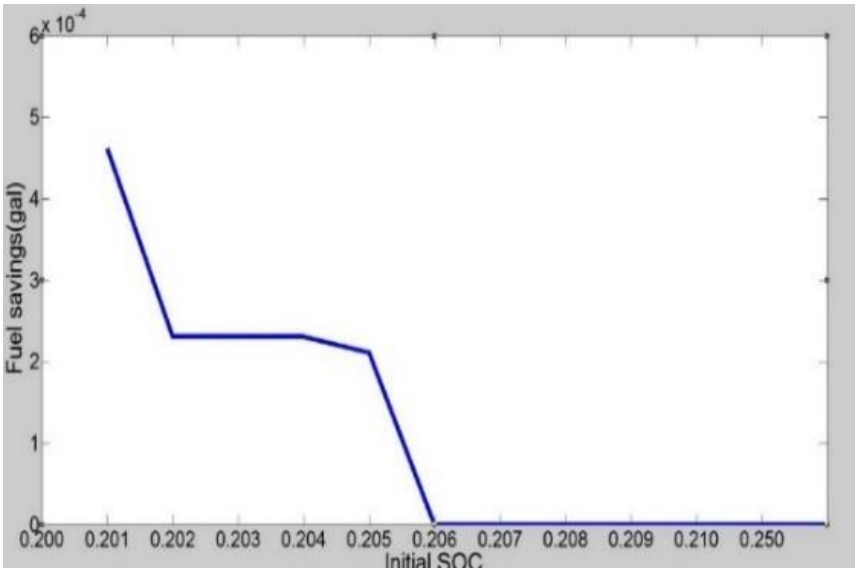

(b) Fuel savings comparing to Binary control mode

Figure 6-7 Initial SOC analysis for drive 1 on stage II and entry case 9.

The field driving data described in previous section are used for quantifying the fuel savings due to different technology scenarios. Table 6-1 indicates that higher fuel savings can be achieved from the optimization of powertrain operation than the optimization of vehicle dynamics. Compared to the baseline technology scenario (i.e., uninformed manual driving with binary EMS control), the technology scenario with OEMS and Stage III EAD (i.e., AUTO) achieves the highest fuel savings (89.73%). In other words, almost 90% of the fuels can be saved due to the co-optimization of vehicle dynamics and powertrain operation when traveling through the intersections.

Table 6-1 Fuel consumptions for different technology scenarios and its saving percentage

	Binary control	**OEMS**
Stage III	0.001053(-37.51%)	0.000173(-89.73%)
Stage II	0.001190(-29.38%)	0.000231(-86.29%)
Stage I	0.001685(baseline)	0.000288(-82.91%)

In order to get better understanding of how the aforementioned energy savings are achieved, more detailed information of an example trip by Driver 1 with OEMS is provided in Fig. 6-12. As can be seen in the figure, the speed profiles of case 6 by different EAD stages show that the passing scenario changes from 3 to 2 (defined in Fig. 2) with the assistance of automatic longitudinal control (i.e., stage III), resulting in significant fuel savings by avoiding the stop-and-go behaviors in Stage I and II. However, for entry case 9, there is no passing scenario change between different EAD stages, so no significant fuel savings can be achieved.

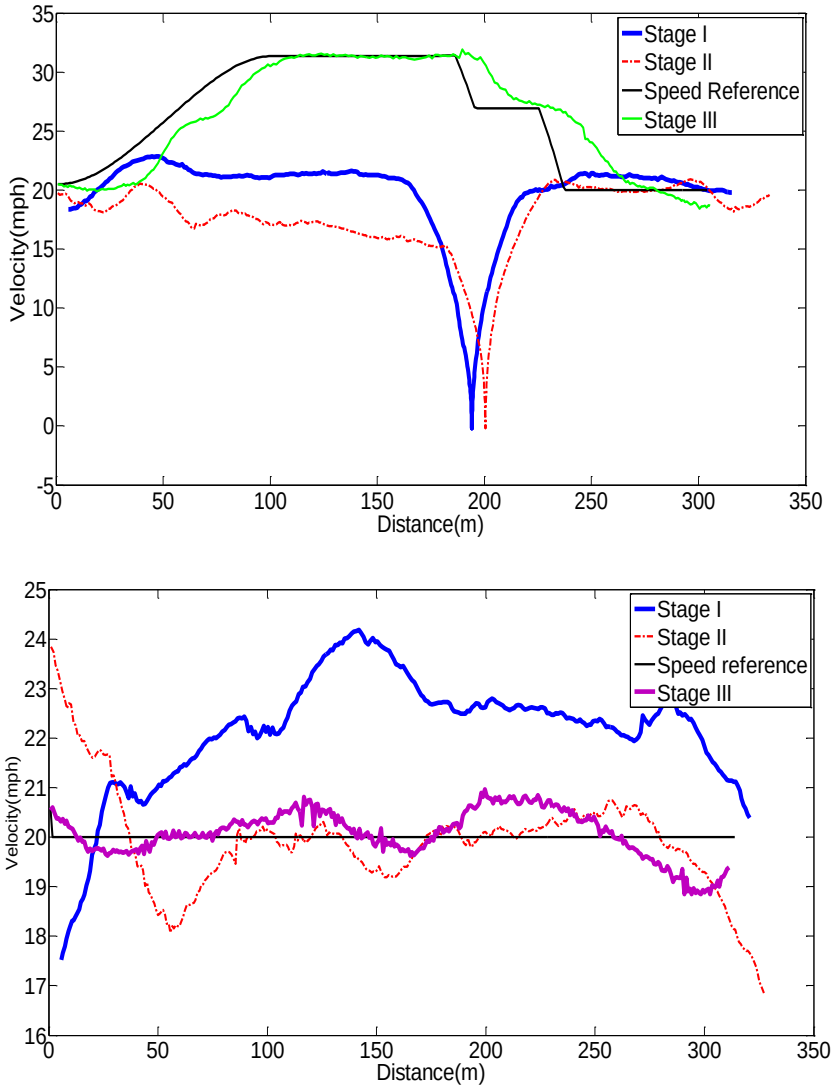

Figure 6-8 Speed versus distance for entry case 6 and case 9 (Driver 1).

6.8.3 Evaluation of Synthesized Long-trips on Urban Route

The synthesized trip data as described in Section 4.2 are adopted to further investigate the fuel savings for a relatively long urban trip which includes driving cycles within the intersection regions (as collected in the field) and between intersections (generated from the truncated UDDS as shown in Fig.6-9). The effective range of different technology combinations are given in the Fig. 6-13. EAD only works at interaction area but OEMS is always on along the entire trip. The resultant SOC profiles for different technology scenarios of an example synthesized

trip are presented in Fig.6-14 (a). It is observed that all the technology scenarios with OEMS result in more conservative consumption of battery power at the beginning of the trips and are able to achieve more fuel savings. In this study, we synthesized totally 6 synthesized trips for evaluation of fuel savings. As shown in Fig. 6-14(b), the EAD system (even with automatic longitudinal control) is not able to achieve very significant energy savings because the driving cycles within the intersection regions only account for a small portion of the entire trip (around 10%). The Co-optimization of vehicle dynamics and powertrain operation can save 23.59% of fuel on average for the synthesized urban driving trips.

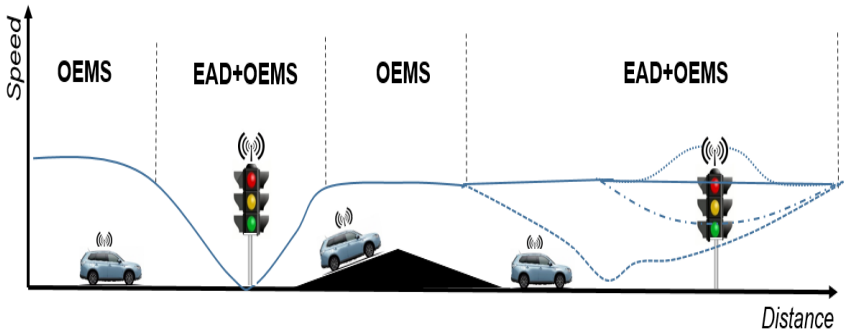

Figure 6-9 Effective range of different technologies

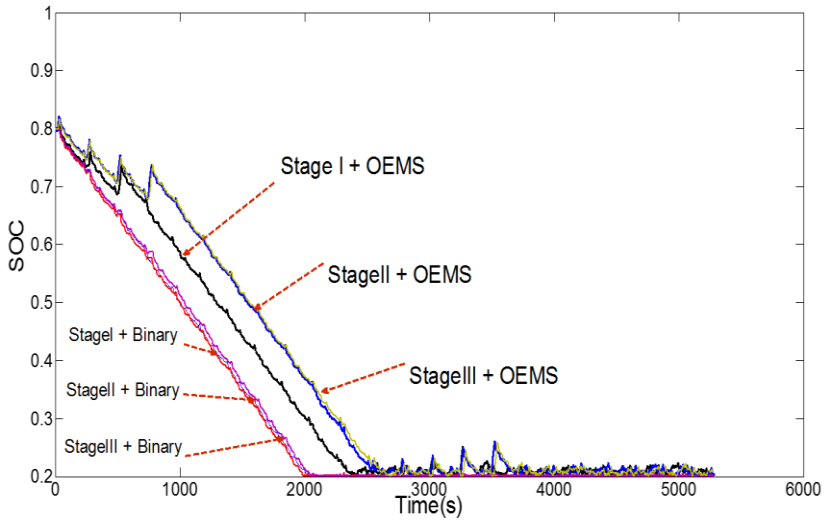

(a) SOC tracks of an example synthesized trip by different technology scenarios.

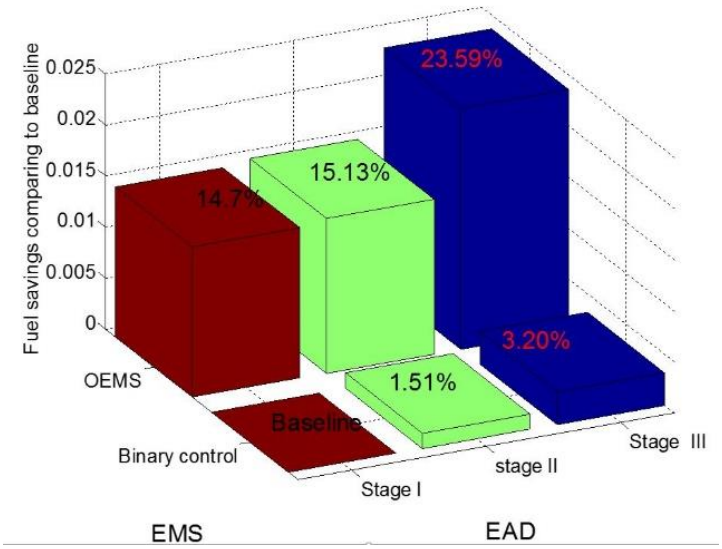

b. Average fuel savings for 6 synthesized trips by different technology scenarios
Figure 6-10 Fuel savings on hypothetical corridor.

6.9 Summary and Discussion

In this study, an integrated connected ecodriving assistance system with co-optimization of vehicle dynamics and powertrain operation for PHEVs was designed and evaluated extensively. The real-world driving data with different ecodriving stages were collected and used for comprehensive performance evaluations. The numerical analysis shows that the combination of automatic longitudinal control and online EMS for PHEVs can achieve almost 90% fuel savings for driving within the intersection region, compared to the baseline (i.e., uninformed manual driving with binary mode EMS). In addition, around 24% of fuel savings can be achieved on synthesized urban trips where the portion (in travel distance) within the intersections account for 10% of the entire trip. The future work will be focused on the further testing and evaluation of the proposed co-optimization system.

7 Data-driven Autonomous Learning for Energy Efficiency Improvement

In previous chapters, the improvement of PEV energy efficiency is achieved by optimizing both vehicle dynamics and powertrain operations. All the optimizations (either vehicle dynamics or powertrain operations) are based on the predicted future traffic condition. In this chapter, another possible way of improving PEV energy efficiency is proposed and discussed. It is machine learning based strategy which is capable of learning the optimal control strategy or optimal operations from historical driving data. It does not rely on any predicted future driving conditions but only learning from the driving recorded from the past. In addition, the previous optimization based method requires a rigid mathematical model that can be used to formulate the optimization problem. For example, the online EMS proposed in chapter 5 is built based on a very precise PHEV model. However, learning based model is data-driven and model-free. It does not need any predefined model anymore and built solely on data.

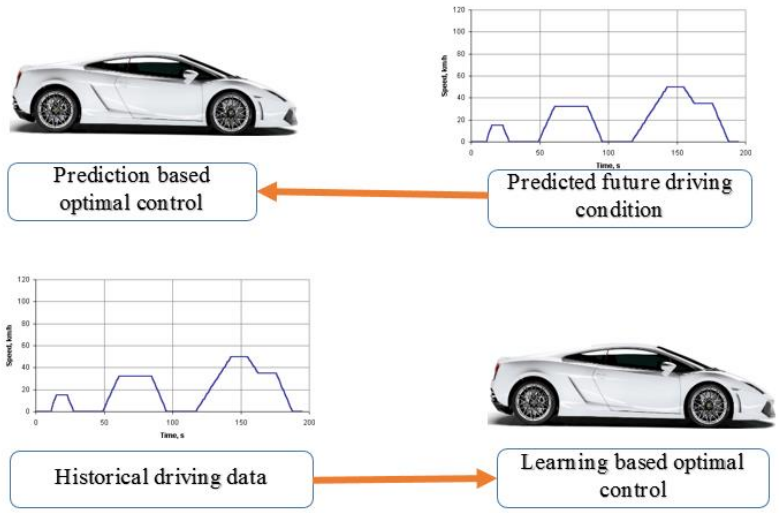

Figure 7-1 Comparison of optimization based model and learning based model

7.1 From Optimization to Learning

As mentioned in chapter 5, the energy management system (EMS) is at the heart of PHEV fuel economy, whose functionality is to control the power streams from both the internal combustion engine (ICE) and the battery pack, based on vehicle and engine operating conditions. In the past decade, a large variety of EMS implementations have been developed for PHEVs, whose control strategies may be well categorized into two major classes as shown in Figure 7-2:

a) rule-based strategies which rely on a set of simple rules without a priori knowledge of driving conditions. Such strategies make control decisions based on instant conditions only and are easily implemented, but their solutions are often far from being optimal due to the lack of consideration of variations in trip characteristics and prevailing traffic conditions; and

b) optimization-based strategies which are aimed at optimizing some predefined cost function according to the driving conditions and vehicle's dynamics. The selected cost function is usually related to the fuel consumption or tailpipe emissions. Based on how the optimization is implemented, such strategies can be further divided into two groups: 1) off-line optimization which requires a full knowledge of the entire trip to achieve the global optimal solution; and 2) short-term prediction-based optimization which takes into account the predicted driving conditions in the near future and achieves local optimal solutions segment by segment within an entire trip. However, major drawbacks of these strategies include: 1) heavy dependence on the a priori knowledge of future driving conditions; and 2) high computational costs that are difficult to implement in real-time.

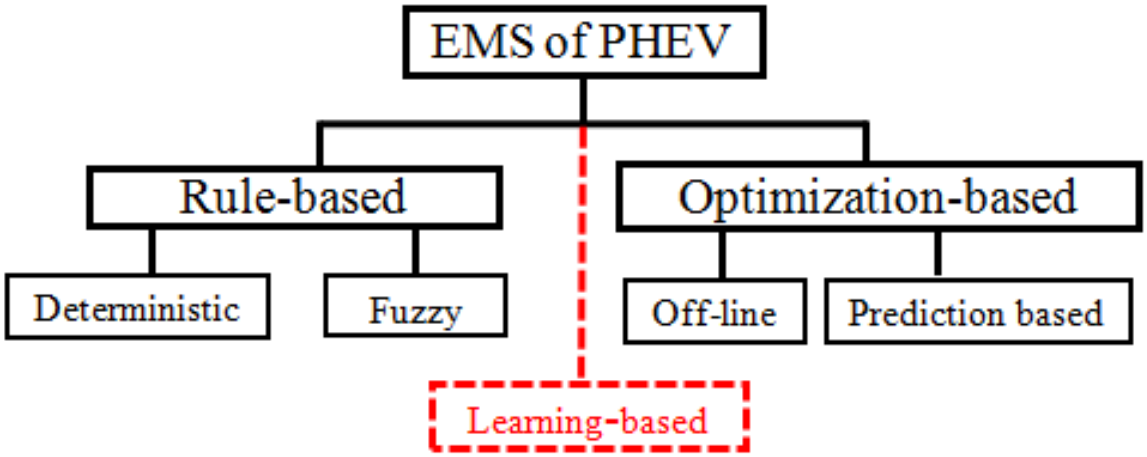

Figure 7-2 Taxonomy of current EMS.

As discussed above, there is a trade-off between the real-time performance and optimality in the energy management for PHEVs. More specifically, rule-based methods can be easily implemented in real time but are far from being optimal while optimization-based methods are able to achieve optimal solutions but are difficult to implement in real time. To achieve a good balance in between, reinforcement learning (RL) has recently attracted researchers' attention. Liu et al. proposed the first and only existing RL-based EMS for PHEVs which outperforms the rule-based controller with respect to the defined reward function but is worse in terms of fuel consumption without considering charging opportunity in the model.

In this chapter, a novel model-free RL-based real-time EMS of PHEVs is proposed and evaluated, which is capable of simultaneously controlling and learning the optimal power split operations in real-time. The proposed model is theoretically derived from dynamic programming (DP) formulations and compared to DP in the computational complexity perspective. There are three major features which distinguish it from existing methods:

- the proposed model can be implemented in real-time without any prediction efforts, since the control decisions are made only upon the current system state. The control decisions also considered for the entire trip information by learning the optimal or near-optimal

control decisions from historical driving behavior. Therefore, it achieves a good balance between real-time performance and energy saving optimality;

- the proposed model is a data-driven model which does not need any PHEV model information once it is well trained since all the decision variables can be observed and are not calculated using any vehicle powertrain models (these details are described in the following sections);
- compared to existing RL-based EMS implementations, the proposed strategy considers charging opportunities along the way (a key distinguishing feature of PHEVs as compared with HEVs). This proposed method represents a new class of models that could be a good supplement to the current methodology taxonomy as shown in Figure 7-2.

7.2 Problem Formulation

In chapter 5.3, the PHEV energy management (i.e., power-split) is formulated as a mixed integer optimization problem. In this chapter, the optimization problem is reformulated as dynamic programming problem as follows:

The above optimization problem can be solved by dynamic programming (DP), since it satisfies the Bellman's Principle of Optimality. Let s ϵ S be the state vector of the system, and a ϵ A the decision variable. The optimization problem can be converted into the following single equation given the initial state s_0 and the decisions a_t for each time step t.

$$\min_{a_t \epsilon A} E\left\{\sum_{t=0}^{T-1} \beta^t g(s_t, s_{t+1}) | s_0 = s\right\} \qquad (7-1)$$

where β is a discount factor and β ϵ (0,1). And it can be solved by recursively calculating:

$$J(s_t) = \min_{a_t \epsilon A} E\left\{\sum_{t=0}^{T-1} g(s_t, s_{t+1}) + \beta J(s_{t+1}) | s_t = s\right\}, for\ t = T-1, T-2, \dots, 0. \quad (7-2)$$

Where T is the time duration; g(.) is a one-step cost function; J(s) is the true value function associated with state s . Eq. (7-2) is also often noted as the Bellman's equation. In the case of PHEV energy management, s_t can be defined as a combination of vehicle states, such as the current SOC level and the remaining time to the destination, which is discussed in the following sections. a_t can be defined as the ICE power supply at each time step.

It is well known that the high computational cost of Eq. (7-2) is always the barrier that impedes its real-world application, although it is a very simple and descriptive definition. It could be computationally intractable even for a small-scale problem (in terms of state space and time span). The major reason is that the algorithm has to loop over the entire state space to evaluate the optimal decision for every single step. Another obvious drawback in the real-world application of DP is that it requires the availability of the full information of the optimization problem. In our case, it means the power demand along the entire trip should be known prior to the trip, which is always impossible in practice.

7.3 Reinforcement Learning

To address the above issues, approximate dynamic programming (ADP) has been proposed (23). The major contribution of ADP is that it significantly reduces the state space by introducing an approximate value function $\hat{J}(s_t, p_t)$ where p_t is a parameter vector. By replacing this approximate value function, Eq. (7-2) can be reformulated as:

$$\hat{J}(s_t) = \min_{a_t \epsilon A} E\left\{\sum_{t=0}^{T-1} g(s_t, s_{t+1}) + \beta \hat{J}(s_{t+1}, p_t)\right\}, for\ t = 0,1, \dots, T-1 \quad (7-3)$$

Now the optimal decision can be calculated at each time step t by

$$a_t = arg\min_{a_t \epsilon A} E\left\{\sum_{t=0}^{T-1} g(s_t, s_{t+1}) + \beta \hat{J}(s_{t+1}, p_t)\right\}, \quad (7-4)$$

The calculation of Eq. (7-4) now only relies on the current system state s_t, which substantially reduces the computational requirement of Eq. (7-2) to polynomial time in terms of the number of the state variables, rather than being exponential to the size of state space. In addition, the value iteration that solves the DP problem becomes forward into time, rather than being backward in Eq. (7-2). In the case of PHEV energy management, this is actually a bonus since the predicted state (e.g. power demand) at the end of the time horizon is much less reliable compared to that at the beginning of the time horizon.

In principle, the value approximate function can be learned by tuning and updating the parameter vector p_t upon the addition of each observation on state transitions. The Reinforcement Learning (RL) is an effective tool for this purpose. The specific learning technique employed in this study is temporal-difference learning (TD-Learning), which is originally proposed by Sutton to approximate the long-term future cost as a function of current states. The details about the implementation of the algorithm are presented in the following sections.

7.4 Reinforcement Learning based EMS

In this study, a TD-learning strategy is adopted for the reinforcement learning problem. An action-value function: Q(s, a) is defined as the expected total reward for the future receipt starting from that state. This function is to estimate "how good" it is to perform a given action in a given state in terms of the expected return. More specifically, we define $Q^{\pi}(s, a)$ as the

value of taking action a in state s under a control policy π (i.e. a map that maps the optimal action to a system state), which is also the expected return starting from s, taking the action a, and thereafter following policy π:

$$Q^{\pi}(s,a)=E_{\pi}\{\sum_{k=1}^{\infty}\gamma^{k}*r(s_{t+k},a_{t+k})|s_t=s,a_t=a\} \quad (7\text{-}5)$$

where s_t is the state at time step t; γ is a discount factor in (0, 1) to guarantee the convergence; $r(s_{t+k},a_{t+k})$ is the immediate reward based on the state s and action a at a given time step (t+k). The ultimate goal of reinforcement learning is to identify the optimal control policy that maximizes the above action-value function for all the state-action pairs.

Comparing to the formulations defined by Eq (7-2) and (7-3), the policy π is the ultimate decision for each time step along the entire time horizon. The reward function $r(s_{t+k},a_{t+k})$ here is g(.) in eq (7-2). The action-value function (i.e., Q(s,a)) is actually an instantiation of the approximate value function $\hat{J}(s_t)$. So, it is not difficult to understand that the DP formulas are the basis for a reinforcement learning problem.

Conceptually, a RL system consists of two basic components: a learning agent and an environment. The learning agent interacts continuously with the environment in the following manner: at each time step, the learning agent receives an observation on the environment state. The learning agent then chooses an action which is subsequently input to the environment. The environment then moves to a new state due to the action, and the reward associated with the transition is calculated and fed back to the learning agent. Along with each state transition, the agent receives an immediate reward and these rewards are used to form a control policy that maps the current state to the best control action upon that state. At each time step, the agent makes the decision based on its control policy. Ultimately, the optimal policy can guide the learning agent to take the best series of actions in order to maximize the cumulated reward over time that can be learned after sufficient training. A graphical illustration of the learning system is given in Figure 7-3. The definition of the environmental states, actions and reward are

provided as following:

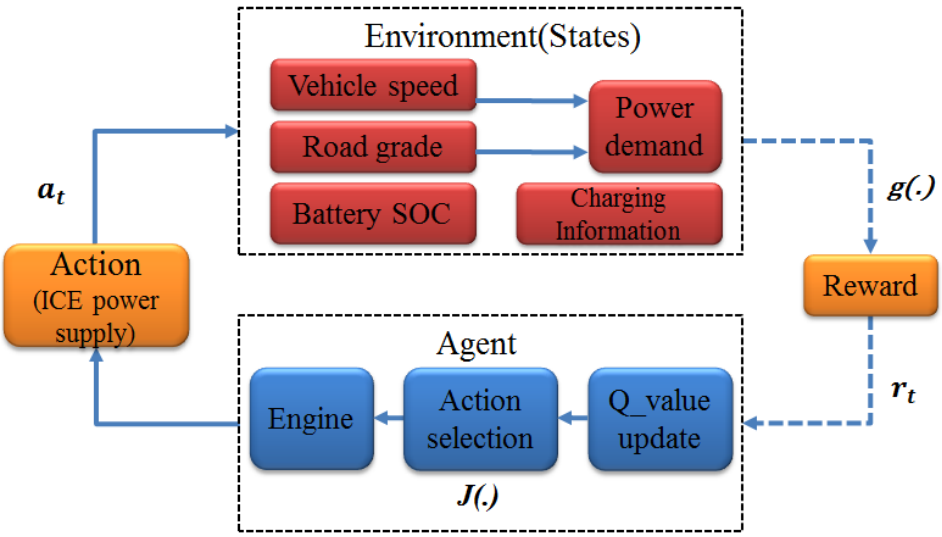

Figure 7-3 Graphical illustration of reinforcement learning system.

7.4.1 Action & Environmental States

In this study, we define the discretized ICE power supply level (i.e. P_i^{eng}) as the only action the learning agent can take. The environment states include any other system parameters that could influence the decision of engine power supply. Herein we define a 5-dimensional state space for the environment, including the vehicle velocity (v_{veh}), road grade (g_{road}), percentage of remaining time to destination (t_{togo}), the battery pack's state-of-charge (b_{soc}), the available charging gain (c_g) of the selected charging station:

$$S=\Big\{s=\left[v_{veh},\ g_{road}, t_{togo}, b_{soc}, c_g\right]^T | v_{veh}\epsilon V_{veh},$$

$$g_{road}\epsilon G_{road}, t_{togo}\epsilon T_{togo}, b_{soc}\epsilon B_{soc}, c_c\epsilon C_g\Big\}$$

where V_{veh} is the set of discretized vehicle speed level; G_{road} is the set of discretized road grade levels; P_{brk} is the discretized level of power collected from regenerative braking (note: this power is negative compared to power demand). The minimum and maximum value of

vehicle velocity, road grade, and regenerative braking power can be estimated from the historical data of commuting trips which will be elaborated in the following section. B_{soc} is the set of battery state-of-charge (SOC) levels between the lower bound (e.g., 20%) and upper bound (e.g., 80%); T_{togo} is the percentage (10% ~ 90%) of remaining time out of the entire trip duration, which is calculated based on the remaining distance to destination. C_g is the set of discretized charging gain (e.g., 30%, 60%) of the selected charger. This charging gain represents the availability of the charger which may be a function of the charging time and charging rate and is assumed to be known beforehand. It is noteworthy that all the states can be measured and updated in real-time as the vehicle is running. Figure 7-4 shows all the real-time environmental states.

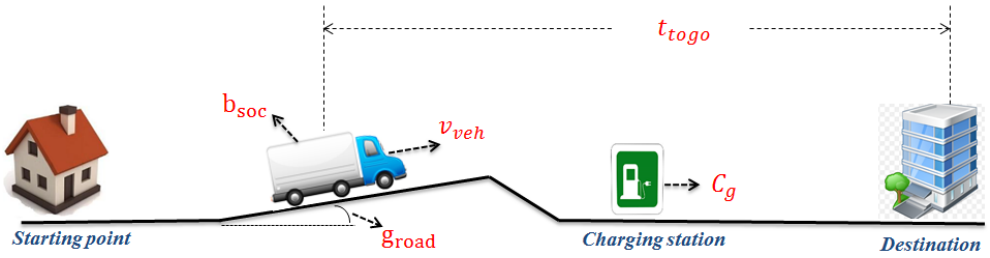

Figure 7-4 Illustration of environment states along a trip.

7.4.2 Reward Initialization

The definition of reward is dependent upon the control objective which is to minimize the fuel cost while satisfying the power demand requirement. Hence, we define the reciprocal of the resultant ICE power consumption at each time step as the immediate reward. A penalty term is also included to penalize the situation where the SOC is beyond the predefined SOC boundaries. Immediate reward is calculated by the following equations:

$$r_{ss'}^{a}=\begin{cases} \frac{1}{P_{ICE}} & if\ P_{ICE}\neq 0\ and\ 0.2\leq SOC\leq 0.8 \\ \frac{1}{P_{ICE}+P} & if\ P_{ICE}\neq 0\ and(SOC\leq 0.2\ or\ SOC\geq 0.8) \\ \frac{2}{Min_{P_{ICE}}} & if\ P_{ICE}=0\ and\ 0.2\leq SOC\leq 0.8 \\ \frac{1}{2*P} & if\ P_{ICE}=0\ and(SOC\leq 0.2\ or\ SOC\geq 0.8) \end{cases} \quad (7\text{-}6)$$

where $r_{ss'}^{a}$ is the immediate reward when state changes from s to s' by taking action a; P_{ICE} is the ICE power supply; P is the penalty value and is set as the maximum power supply from ICE in this study; Min_P_{ICE} is the minimum nonzero value of ICE power supply. This definition guarantees that the minimum ICE power supply (action) which satisfies the power demand as well as SOC constraints can have the largest numerical reward. A good initialization of reward is also critical for the quick convergence of the proposed algorithm. In this case, the optimal or near optimal results of typical trips obtained from simulation are used as the initial seeds. These optimal or near optimal results are deemed as the control decisions made by "good drivers" from historical driving. In order to obtain a large number of such good results for algorithm training, an evolutionary algorithm (EA) is adopted for the off-line full-trip optimization since EA can provide multiple solutions for one single run. These solutions are of different quality which may well represent different level of driving proficiency in the real world situation.

7.4.3 Q-value Update and Action Selection

In the algorithm, a Q value, denoted by Q(s, a), is associated with each possible state-action pair (s, a). Hence there is a Q table which is kept updating during the learning process and can be interpreted as the optimal control policy that the learning agent is trying to learn. At each time step, the action is selected upon this table after it is updated. The details of the algorithmic process are given in the following pseudo code:

Algorithm RL based PHEV EMS algorithm

Inputs: Initialization 6-D Q(s, a) table; Discount factor γ=0.5; Learning rate α=0.5; Exploration probability ε ϵ(0,1); Vehicle power demand profile P_d (N time steps)

Outputs: Q(s, a) array; Control decisions P_d (T time steps)

1: Initialize Q(s, a) arbitrarily
2: for each time step t=1:T
3: Observe current s_t $(v_{veh},\ g_{road}, t_{togo}, b_{soc}, C_g)$
4: Choose action a_t for the current state s_t:
5: temp=random(0,1);
6: if temp <= ε
7: $a_t = \arg\max_{a \epsilon A}\{ Q(s_t, a)\}$
8: else
9: a_t= randomly choose an action;
10: end
11: Take action a_t, observe next state s_{t+1} (P_{t+1}, SOC_{t+1})
12: if SOC_{t+1}<0.2
13: Switch into Charging-Sustaining mode;
14: Give big penalty to r_t according to Eq. (10)
15: else
16: Calculate reward r_t according to Eq. (10)
17: end
18: Update $Q(s_t, a_t)$ with following value:
19: $Q(s_t, a_t)+\alpha\{r_t + \gamma * \max_{a_{t+1}}\{ Q(s_{t+1}, a_{t+1})\} - Q(s_t, a_t)\}$
20: end

7.5 Validation with Real-world Driving Cycles

The proposed model is then evaluated with real-world data in two different scenarios: one without charging opportunities and the other with charging opportunities. The data set is described in section 6.6.1

7.5.1 Model without Charging Opportunity (trip level)

To validate the proposed strategy, the model without considering charging opportunity is first trained and tested with trips where there is no charging opportunity within the trip. Data for multiple westbound trips described in (21) are used for training. Although it has been proven that Q-learning is guaranteed to converge mathematically, an experimental analysis of convergence is conducted in this study. In the experiment, the trip data for the first six days are concatenated one by one to form a single training cycle. The proposed model is trained with

repeated training cycles. At the end of each training cycle, the trained model is tested with the 7th day trip and the fuel consumption is recorded in the following Figure 7-5. In addition, the training with or without good initialization using simulated optimal or near optimal solution are also compared. As we can see in the figure, there is a clear convergence in fuel consumption for both cases. However, the initialization with simulated optimal or near optimal solutions help achieve a faster convergence.

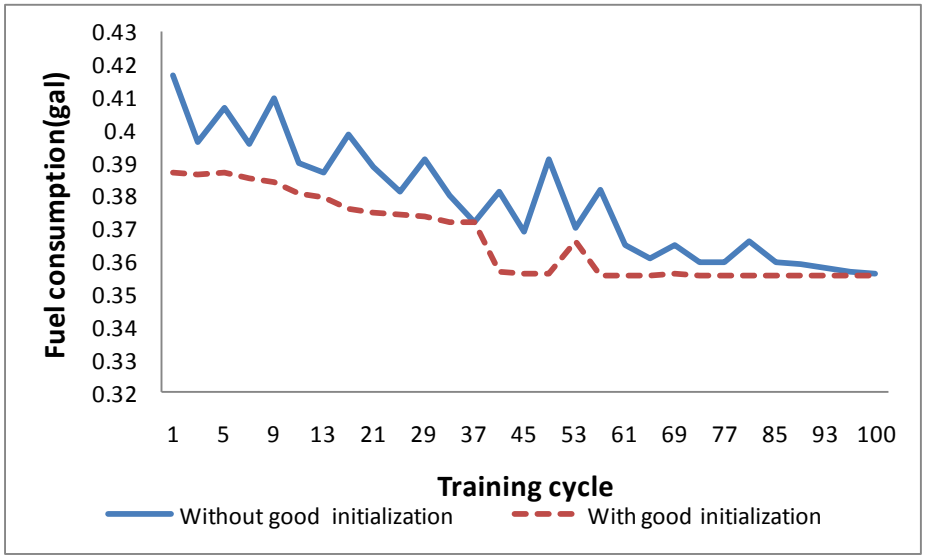

Figure 7-5 Convergence Analysis (ε =0.7; γ=0.5; α=0.5).

As previously described, the selected state space is 5-dimensional and the action space has 1 dimension. Therefore the Q(s, a) table is 6-dimensional. Figure 7-6 shows the 4-D slice diagram of the learned Q(s, a) table in which different color grids represent different numerical reward values (e.g., blue color means lower values) and 3 slices on the (ICE power supply, power demand) space are given at three different SOC levels: 1, 6 and 12 (i.e., 20%, 50%, and 80%). Please note that the road grade and vehicle speed are implicitly aggregated into power demand. The dimension of remaining time is not indicated in the figure. As can be observed in each slice, when the power demand is not so high (e.g., below level 5), action level 1 or 2 is usually the most appropriate because the least ICE power is consumed. When the power demand becomes higher, the range of the feasible action levels gets wider also. In such cases, lower

levels of ICE power supply may not be enough to satisfy the power demand and the resultant SOC level could be lower than 0.2, resulting in a penalty defined in Eq. (17). It is also noted that when SOC level is high, it is less likely the higher ICE power supply level would be chosen to satisfy the same power demand. This is because when the vehicle battery SOC is high, the ICE power is not likely to be used aggressively.

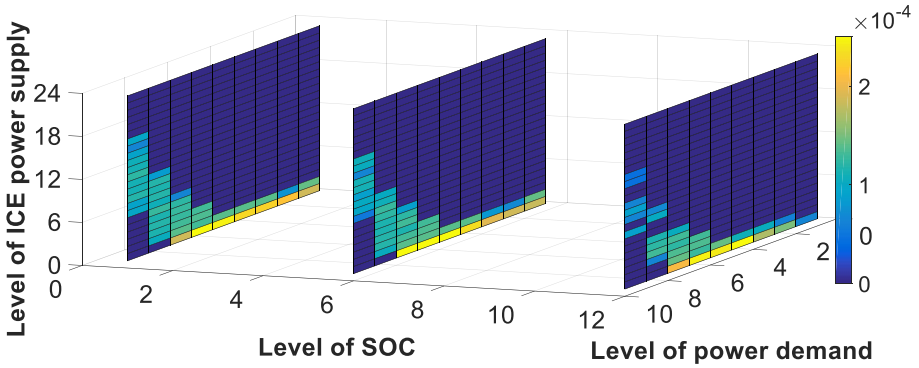

Figure 7-6 4-D slice diagram of the learned Q table.

As discussed in the previous sections, an exploration-exploitation strategy is adopted for the action selection process to avoid premature convergence. The action with the biggest Q value has a probability of 1-ε to be selected. Hence the value of ε may significantly affect the performance of the proposed method. To evaluate such impacts, a sensitively analysis of ε is carried out and illustrated in Figure 8. It can be observed that both the fuel consumption and the resultant SOC curves are very close to those of the binary mode control if the value of ε is small. A possible explanation is that a small ε value indicates a large probability to select the most aggressive action with the biggest Q value (or the lowest levels of ICE power supply). Therefore, the battery power is consumed drastically as it is with the binary mode control. However, if the value of ε is too large (e.g., >0.8), the battery power is utilized too conservatively where the final SOC is far away from the lower bound, resulting in much greater fuel consumption. It is found that the best value of ε in this study is around 0.7, which ensures the SOC curve is quite close to the global optimal solution obtained by the off-line DP strategy. With this best ε value, the fuel consumption is 0.3559 gallon, which is 11.9% less than that of

the binary mode control and only 2.86% more than that of DP strategy as shown in Figure 7-7. This also implies that an adaptive strategy for determining exploration rate along the trip could be a useful. Figure 7-8(a) shows a linearly decreasing control of ε along the trip. A smaller ε is preferred at the later stage of the trip because SOC is low and the battery power should be consumed more conservatively. With this adaptive strategy for ε(see Fig. 7-8(a)), the proposed mode could also achieve a good solution with 0.3570 gallon of fuel consumption, which is 11.7% less than binary control shown in Figure 7-7.

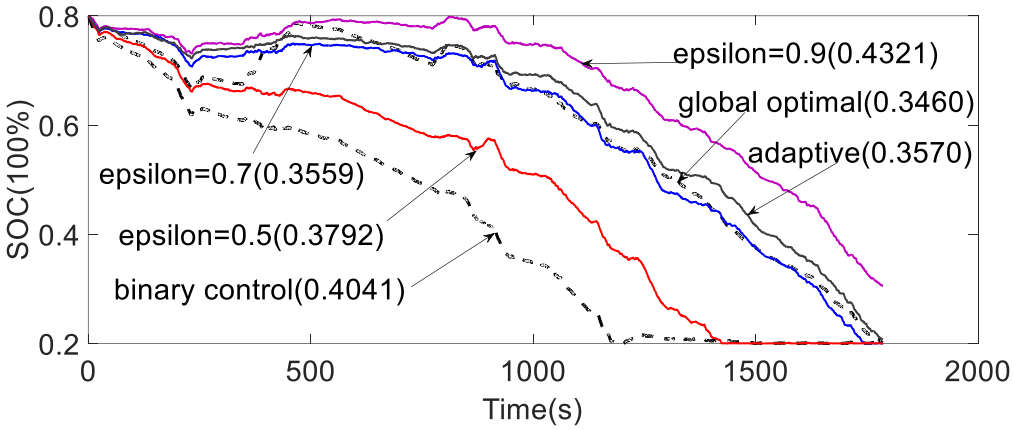

Figure 7-7 Fig. 22. Fuel consumption in gallon (bracketed values) and SOC curves by different exploration probabilities.

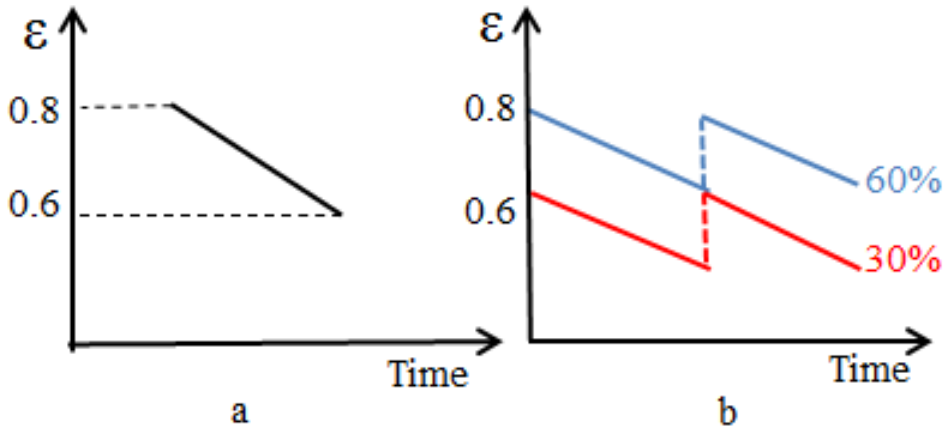

Figure 7-8 Fig. 23. (a) Linear adaptive control of ε; (b) Linear adaptive control of ε with charging opportunity.

7.5.2 Model with Charging Opportunity (tour level)

The most distinctive characteristics of PHEVs from HEVs is that PHEV can be externally charged whenever a charging opportunity is available. To further evaluate the impacts due to charging availability, we include this information in the proposed model as a decision variable. For simplicity, the charging opportunity is quantified by the gain in the battery's SOC, which may be a function of available charging time and charging rate. Data for a typical tour is constructed by combining a round trip between the origin and destination. We assume there is a charger in the working place (west-most point in the map) and the available charging gain has only two levels: 30% and 60%. In this case, a corresponding adaptive strategy of ε is also used as shown in Figure 7-8(b). The rationale behind this adaptive strategy is that battery power should be used less conservatively (i.e., higher ε value) after charging, and/or when C_g is higher.

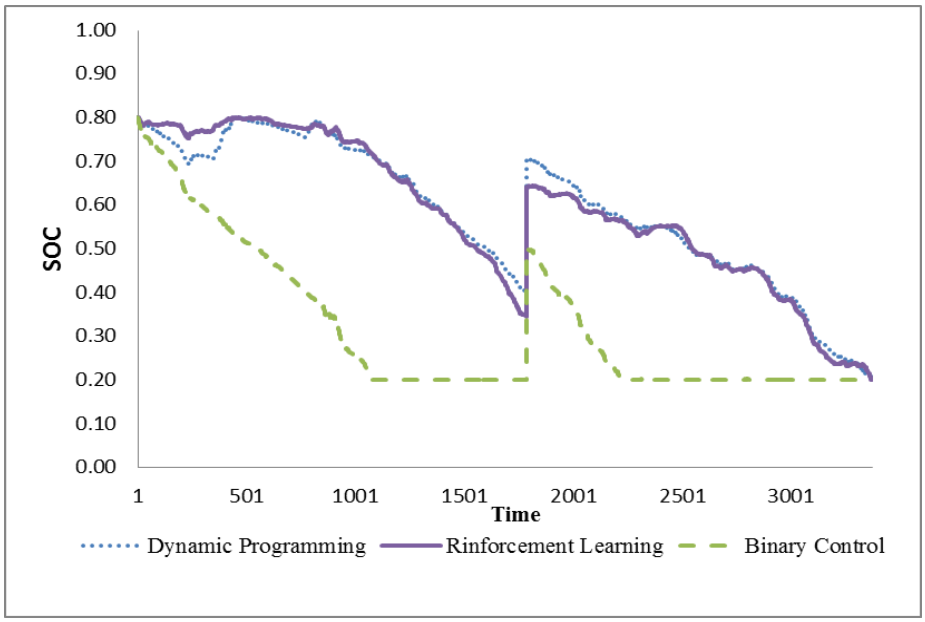

Figure 7-9 Optimal results when available charging gain is 0.3 (C_g=0.3)

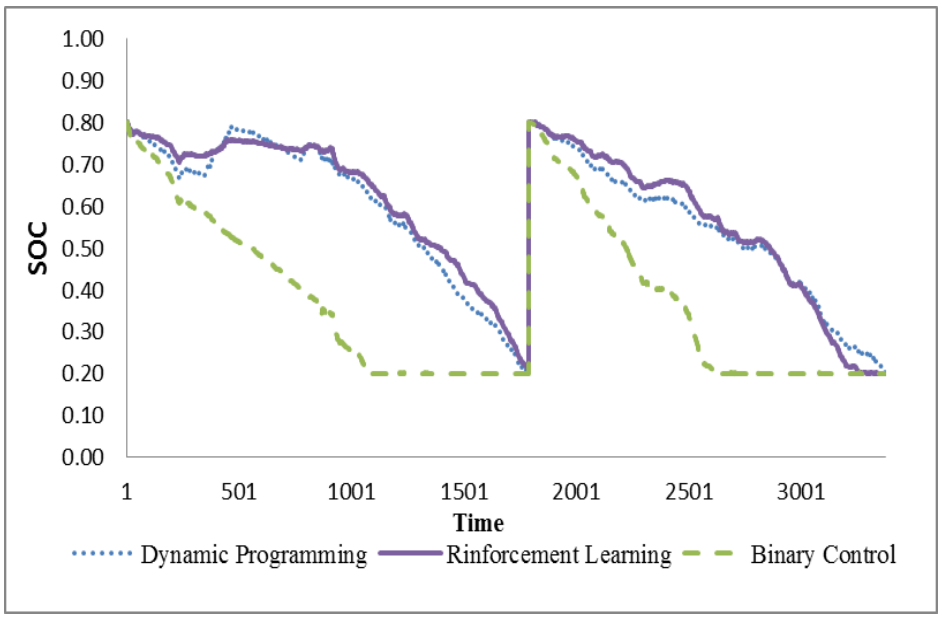

Figure 7-10 Optimal results when available charging gain is 0.6 (C_g=0.6)

The obtained optimal results are shown in Figure 7-9 and Figure 7-10. As we can see in both figures, the resultant SOC curves are much closer to the global optimal solutions obtained by DP than binary control. To obtain a statistical significance of the performance, the proposed model is tested with 30 different trips by randomly combining two trips and assume a charging station in between with a random C_g (randomly choose from 30% and 60%). By taking binary control as baseline, the reduced fuel consumption is given in the following Figure 7-11. As we can see in the figure, RL model achieves an average of 7.9% fuel savings. It seems that having more information results in lower fuel savings which is counterintuitive. The reason is that the inclusion of additional information or state variable to the model exponentially increases the search space of the problem, which thereby increases the difficulty of learning the optimal solution. And also more uncertainty is introduced to the learning process due to the errors within the added information, which degrades the quality of the best solution the model can achieve.

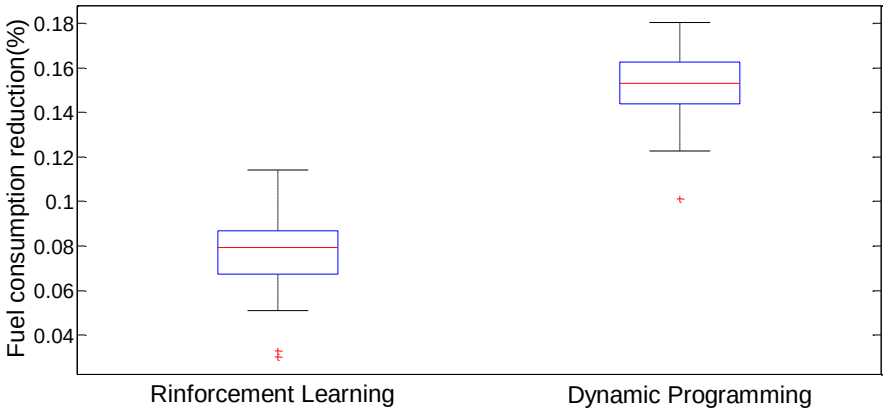

Figure 7-11 Fuel consumption reduction compared to binary control.

8 Conclusions and Future Work

8.1 Conclusions

This dissertation research work provides solutions for improving PEV energy efficiency in real-world driving by taking the synergies from the following functional components or aspect: vehicle dynamics optimization, powertrain operations, co-optimizations and the autonomous learning strategy. Hence the conclusions drawn for each aspect are listed as follows:

- *Vehicle dynamics Optimization*

  In chapter 4, three different connected ecodriving assistance system are designed and tested with real-world driving data: EAD system without driver-in-the-loop, EAD system with driver-in-the-loop and partially automated EAD system (i.e., automatic longitudinal control). The numerical analysis with real-world driving data collected from U.S. DOT Turner-Fairbank Highway Research Center (TFHRC) shows that the EAD system without driver-in-the-loop can achieve 12.1% energy efficiency improvement on average comparing to human driving without any EAD assistance; EAD system with driver-in-the-loop is able to achieve additional 11.7% energy savings comparing to that without driver-in-the-loop; and partially automated EAD assistance system can achieve 21.9% energy savings on average comparing to human driving without any EAD assistance.

  These results prove that the optimization of vehicle dynamics is able to improve the energy efficiency of PEVs. Furthermore, the consideration of human driver can also help improve PEV driving efficiency.

- *Powertrain operation optimization*:

  In chapter 5, a framework of on-line energy management system for plug-in hybrid electric vehicles is developed. The framework applies the self-adaptive strategy to control the

vehicle's state-of-charge (SOC) in a rolling horizon manner for the purpose of real-time implementation. The control of the vehicle's SOC is formulated as a combinatory optimization problem that can be efficiently solved by the estimation distribution algorithm (EDA). The proposed energy management system is comprehensively evaluated using a number of trip profiles extracted from real-world traffic data. The results show that the self-adaptive control strategy used in the proposed system statistically outperforms the conventional binary control strategy with an average of 10.7% fuel savings. In addition, the real-time performance analysis shows that the proposed mode is very computationally efficient and can be implemented in real-time by taking the advantage of evolutionary optimization. Another important advantage of the proposed energy management system is that, unlike other existing optimization based EMS systems, it does not require a priori knowledge about the trip duration. This allows the proposed system to be robust against real-world uncertainties, such as unexpected traffic congestion that increases the trip duration significantly, and changes in inter-trip charging availability.

- *Co-optimization*

  In chapter 6, an integrated connected Ecodriving assistance system with co-optimization of vehicle dynamics and powertrain operation for PHEVs was designed and evaluated extensively. The real-world driving data with different Ecodriving stages were collected and used for comprehensive performance evaluations. The numerical analysis shows that the combination of automatic longitudinal control and online EMS for PHEVs can achieve almost 90% fuel savings for driving within the intersection region, compared to the baseline (i.e., uninformed manual driving with binary mode EMS). In addition, around 24% of fuel savings can be achieved on synthesized urban trips where the portion (in travel distance) within the intersections account for 10% of the entire trip. These results indicate that

augmented energy benefits can be achieved by the joint consideration of vehicle dynamics and powertrain operations.

- *Autonomous learning for improving energy efficiency*

  In chapter 7, a data-driven reinforcement learning based real-time energy management system for PHEVs is proposed, which is capable of simultaneously controlling and learning the optimal power split operation. The proposed EMS model is tested with trip data (i.e., multiple speed profiles) synthesized from real-world traffic measurements. Numerical analyses show that a near-optimal solution can be obtained in real time when the autonomous learning model is well trained with historical driving cycles. For the study cases, the proposed autonomous learning model can achieve better fuel economy than the binary mode strategy by about 12% and 8% at the trip level and tour level (with charging opportunity), respectively. It is indicated that when the prediction of future driving conditions is not reliable or even available, autonomous learning based model can be used to learn the optimal (or near optimal) control strategies from historical driving data to improve PEV energy efficiency.

8.2 Selected Publications, Patent and Media Coverage

There are total 16 manuscripts are finished during this dissertation study period, including 10 published, 4 submitted and 2 accepted (as of 12/8/2016). There will be another two manuscripts under preparation but not finished by the time of this dissertation is filed. All the details on these manuscripts are listed in Table 8-1:

Table 8-1 Publications status (***By 12/08/2016***)

Authorship	Type	Publisher	Total Number
First Author	Journal published (3)	IEEE transaction of Intelligent Transportation System	1
		ASCE Journal of Transpiration Engineering	1
		Journal of Transportation Research Board (TRR)	1
	Conference published (5)	IEEE Conference of Intelligent Transportation System (ITSC)	2
		IEEE Conference of Intelligent Vehicles (IV)	1
		Automated Vehicle Symposium (AVS) (poster)	1
		ACM Genetic and Evolutionary Computation Conference	1
	Finished/ Submitted (4)	IEEE Transactions of Intelligent Vehicles	1
		Transportation Research Part D	1
		Applied Energy	1
		IEEE Transactions of Intelligent Transportation System	1
Co-author	Conference published (4)	IEEE International conference on Connected Vehicles(ICCVE)	2
		Annual Meeting of Transportation Research Board	2
Manuscripts in preparation		Deep Reinforcement Learning based Fuel efficiency learning	1
		Swarm Intelligence based Multi-vehicle Learning	1

1) **Xuewei Qi**; Guoyuan Wu; Boriboonsomsin, K.; Barth, M.J., "A Novel Blended Real-Time Energy Management Strategy for Plug-in Hybrid Electric Vehicle Commute Trips," in Intelligent Transportation Systems (ITSC), 2015 IEEE 18th International Conference on , vol., no., pp.1002-1007, 15-18 Sept. 2015

2) **Xuewei Qi**; Guoyuan Wu; Boriboonsomsin, K.; Barth, M.J.; Jeffery Gonder, "Data-Driven Reinforcement Learning-Based Real-Time Energy Management System for Plug-in Hybrid Electric Vehicles" Transportation Research Record (Journal of Transportation Research Board),vol,2572,pp. 1-8,2016. DOI: 10.3141/2572-01

3) **Xuewei Qi**; Guoyuan Wu; Boriboonsomsin, K.; Barth, M.J., "Evolutionary algorithm based on-line PHEV energy management system with self-adaptive SOC control," in Intelligent Vehicles Symposium (IV), 2015 IEEE , vol., no., pp.425-430, June 28 2015-July 1 2015doi: 10.1109/IVS.2015.7225722

4) **Xuewei Qi**, Guoyuan, Wu, Matthew, Barth. "An on-line intelligent energy management strategy for Plug-in Hybrid Electric Vehicles" Proceedings of IEEE conference of Intelligent Transportation System, 2014, Qindao.

5) **Xuewei Qi**, Guoyuan, Wu, Matthew, Barth." Development and Evaluation of an Evolutionary Algorithm-Based On-Line Energy Management System for Plug-In Hybrid Electric Vehicles" accepted and in press by IEEE transections of Intelligent Transportation System.

6) **Xuewei Qi,** Wu, G., Boriboonsomsin, K., and Barth, M. (2015). "Empirical Study of Lane-Changing Characteristics on High-Occupancy-Vehicle Facilities with Different Types of Access Control Based on Aerial Survey Data." ASCE Journal of Transportation Engineering, 10.1061/(ASCE)TE.1943-5436.0000803 , 04015034.

7) **Xuewei Qi,** Guoyuan, Wu, Matthew, Barth. "Comparative Study of Lane Changing Characteristics on Different Types of HOV Facility Using Smoothed Aerial Photo Data" Proceedings of Transportation Research Board Annual Meeting 2015, Washington D.C..

8) G. Wu, D. Kari, **Xuewei Qi**, K. Boriboonsomsin and M. J. Barth, "Developing and evaluating an eco-speed harmonization strategy for connected vehicles," 2015 International Conference on Connected Vehicles and Expo (ICCVE), Shenzhen, China, 2015, pp. 373-378.doi: 10.1109/ICCVE.2015.16Y.

9) Chen, S. Young, **Xuewei Qi** and J. Gonder, "Estimate of fuel consumption and GHG emission impact from an automated mobility district," 2015 International Conference on Connected Vehicles and Expo (ICCVE), Shenzhen, China, 2015, pp. 271-278. doi: 10.1109/ICCVE.2015.32

10) **Xuewei Qi**; Guoyuan Wu; Boriboonsomsin, K.; Barth, M.J., "Data-driven Decomposition and Estimation of Link-level Energy consumption of Electric Vehicles Considering Real-world Traffic Conditions," submitted to Transportation Research Part D.

11) **Xuewei Qi**; Guoyuan Wu; Boriboonsomsin, K.; Barth, M.J., "Estimating Energy and Mobility Benefits from Eco-approach/Departure System for Electric Vehicles" submitted to Applied Energy

12) **Xuewei Qi** Guoyuan Wu and Matthew Barth, "Next Generation Connected Ecodriving System for PHEVs: Co-optimization of Vehicle Dynamics and Powertrain Operations" submitted to IEEE Transections of Intelligent Vehicles

13) **Xuewei Qi** Guoyuan Wu and Matthew Barth," Driver-vehicle-infrastructure Cooperative System: Adaptive Connected Ecodriving Considering Human Driver Error" submitted to IEEE transections of Intelligent Vehicles.

14) **Xuewei Qi,** Matthew Barth, Guoyuan Wu, and Kanok Boriboonsomsin. 2016. Intelligent On-Line Energy Management System for Plug-in Hybrid Electric Vehicles based on Evolutionary Algorithm. In *Proceedings of the 2016 on Genetic and Evolutionary Computation Conference Companion* (GECCO '16 Companion), Tobias Friedrich (Ed.). ACM, New York, NY, USA, 167-168.

15) Fei Ye**,** Peng Hao, **Xuewei Qi**; Guoyuan Wu; Boriboonsomsin, K.; Barth, M.J., "Prediction-based Eco-Approach and Departure Strategy in Congested Urban Traffic" accepted Transportation Research Board Annual Meeting 2017, Washington D.C..

16) Chao Wang**,** Peng Hao, **Xuewei Qi**; Guoyuan Wu; Boriboonsomsin, K.; Barth, M.J., "Intersection and Stop Bar Positon Extraction from Crowdsourcing GPS Trajectories Data" accepted Transportation Research Board Annual Meeting 2017, Washington D.C..

8.3 Patent & Media Coverage

The designed Data-driven EMS for PHEV described in Chapter 7 has been filed in a patent application before its publication by the commercialization office of UC Riverside. Several major auto manufactures (e.g., Honda) have contacted the authors and inquiry about the possibility of commercialization of this invention.

Since its publication early this year, more than 10 major science and technology websites and journals have made a coverage for this invention, some of them are listed below and also in Fig. 8-1:

IEEE

http://spectrum.ieee.org/cars-that-think/transportation/advanced-cars/hybrid-car-system-learns-fuel-efficiency

Science Daily

https://www.sciencedaily.com/releases/2016/02/160209132051.htm

UCR Today

http://ucrtoday.ucr.edu/34819

Automotive Industries

http://www.ai-online.com/Adv/Previous/show_issue.php?id=6895&search=true#sthash.TJy9naah.Uf1ubVng.dpbs

IEEE.org | IEEE *Xplore* Digital Library

IEEE SPECTRUM

Follow on:

Engineering Topics | Special Reports | Blogs

Cars That Think | Transportation | Advanced Cars

Hybrid Car System Learns Fuel Efficiency

By Jeremy Hsu
Posted 16 Feb 2016 | 22:00 GMT

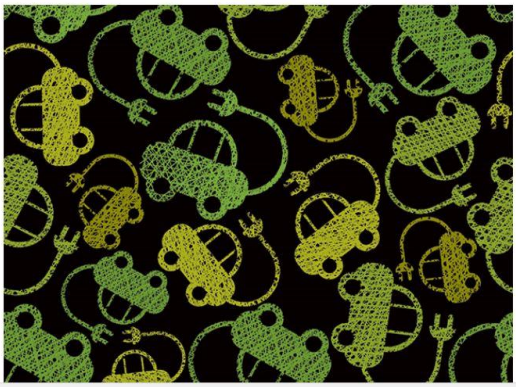

ScienceDaily

Your source for the latest research news

Mobile | Follow

Breaking News: Mapping Neural

S_D Health | Tech | Enviro | Society | Quirky | Store

Science News *from research organizations*

Getting more miles from plug-in hybrids

Smart energy management systems can improve plug-in hybrid efficiency by 12 percent

Date: February 9, 2016

Source: University of California - Riverside

Summary: Plug-in hybrid electric vehicles (PHEVs) can reduce fuel consumption and greenhouse gas emissions compared to their gas-only counterparts. Researchers have taken the technology one step further, demonstrating how to improve the efficiency of current PHEVs by almost 12 percent.

Share:

RELATED TOPICS

Matter & Energy

- Energy Technology
- Batteries

Earth & Climate

- Energy and the Environment

FULL STORY

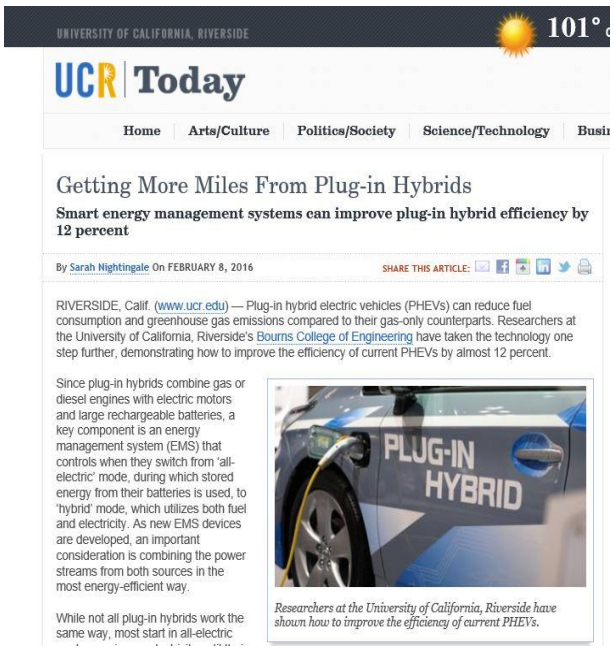

Figure 8-1 Media coverage of this dissertation research work

8.4 Future Research Directions

This dissertation work provides a very complete technological framework for improving PEV energy efficiency in real-world driving from the following perspectives: vehicle dynamics optimization, powertrain operations, co-optimizations and the autonomous learning strategy. There is still much valuable future work can be done for each of these functional components that proposed in this dissertation. All the future work is inspired by the results and findings that achieved by this dissertation work. The potential future research directions are listed as follows:

- *Vehicle dynamics optimization*:

  The future work on this part will be focused on the field testing driving of partially automated EAD driving for EVs (MPC based) and EAD with driver-in-the-loop (SMPC based) for EVs; In addition, the VTPA will be further improved by considering more EV

exclusive characteristics. The EAD system will also be extended to Eco-ACC that will also work and provide optimal speed trajectory to achieve maxim energy efficiency outside the intersections range.

- *Powertrain operation optimization*:

  The proposed several different energy management systems in this dissertation are all for one single vehicle optimization., The future work on this part will be focused on the extension of the single vehicle optimization model to multi-vehicle optimization model in connected vehicle environment. For example, the current single PHEV EMS mode can be extended into multi-PHEV EMS in a fleet level. The objective of such system would be a cooperative optimization of all the PHEVs within a fleet. The energy efficiency is expected to be further improved with the help of this multi-vehicle exchange and cooperation.

- *Co-optimization*:

  In this part, the current dissertation study uses a bi-level optimization to best approximate the co-optimization of the vehicle dynamics and powertrain operations for PHEVs, this can be further improved by proposing another formulation of the problem to provide more optimal solution, although the current results are quite promising.

- *Autonomous learning for improving energy efficiency*

  The future work derived from this dissertation study will be mainly involved in this part. The proposed model in this dissertation is reinforcement learning based autonomous learning system for single vehicle. There are two major directions for further improving the

performance of the autonomous learning system: One is from extending the current single vehicle based autonomous learning to a multi-vehicle cooperative learning framework that accommodate the collaborative learning behavior among all the connected vehicles. There is one manuscript is in preparation on this topic.The other one is proposing deep learning based mode to replace the current reinforcement learning based model so that the learning ability is significantly improved. There is one manuscript is in preparation on this topic.

Bibliography

[1] U.S. energy information administration, Monthly Energy Review (March 2015), Table 2.1 Available at: http://www.eia.gov/Energyexplained/?page=us_energy_transportation

[2] U.S. Environmental Protection Agency (EPA). Inventory of U.S. Greenhouse Gas Emissions and Sinks: 1990 – 2014. Final report, April, 2016.

[3] S. G. Wirasingha and A. Emadi. "Classification and Review of Control Strategies for Plug-In Hybrid Electric Vehicles". IEEE Transactions on Vehicular Technology, Vol.60, No.1, January 2011, pp. 111 – 122

[4] A. Panday and H. O. Bansal. "A Review of Optimal Energy Management Strategies for Hybrid Electric Vehicle". International Journal of Vehicular Technology, 2014, p. 19.

[5] D. Schrank, B. Eisele, T. Lomax and J. Bak.2015 Urban Mobility scorecard. http://d2dtl5nnlpfr0r.cloudfront.net/tti.tamu.edu/documents/mobility-scorecard-2015.pdf

[6] M. Barth, S. Mandava, K. Boriboonsomsin and H. Xia, "Dynamic Ecodriving for arterial corridors," Integrated and Sustainable Transportation System (FISTS), 2011 IEEE Forum on, Vienna, 2011, pp. 182-188.

[7] R. Zhang and E. Yao, "Ecodriving at signalised intersections for electric vehicles," in *IET Intelligent Transport Systems*, vol. 9, no. 5, pp. 488-497, 6 2015.

[8] US DOT, 2010. Transportation's Role in Reducing U.S. Greenhouse Gas Emissions Volume 1: Synthesis Report, Report to Congress, U.S. Department of Transportation.

[9] Skerlos, S.J., Winebrake, J.J., 2010. Targeting plug-in hybrid electric vehicle policies to increase social benefits. Energy Policy 38 (2), 705–708.

[10] Canis, B. (2011). Battery manufacturing for hybrid and electric vehicles: policy issues. Congressional research service. <http://nepinstitute.org/get/CRS_Reports/CRS_Energy/Energy_Efficiency_and_Conservation/Batteries_for_Hybrid_and_Elec_Vehicles.pdf> (Accessed April 10, 2013).

[11] Elkind, E.N., 2012. Electric drive by '25: how California can catalyze mass adoption of electric vehicles by 2025, workshop by UCLA Law/Berkeley Law,<http://www.law.berkeley.edu/files/ccelp/Electric_Drive_by_25-2.pdf> (Accessed April 22, 2013).

[12] Axsen, J., Kurani, K.S., Burke, A., 2010. Are batteries ready for plug-in hybrid buyers? Transport Policy 17, 173–182.

[13] Morrowa, K., Karnerb, D., Francfortc, J., 2008. U.S. Department of Energy Vehicle Technologies Program – Advanced Vehicle Testing Activity Plug-in Hybrid Electric Vehicle: Charging Infrastructure Review, Final Report: INL/EXT-08-15058, Battelle Energy Alliance, Contract No. 58517.

[14] Steven Lavrenz & Konstantina Gkritza (2013) Environmental and Energy Impacts of Automated Electric Highway Systems, Journal of Intelligent Transportation Systems: Technology, Planning, and Operations, 17:3, pp 221-232.

[15] G. Wu, K. Boriboonsomsin, M. Barth (2014) "Development and Evaluation of an Intelligent Energy Management Strategy for Plug-in Hybrid Electric Vehicles", in press, IEEE Transactions on Intelligent Transportation Systems.

[16] U.S. Environmental Protection Agency, U.S. Greenhouse Gas Inventory Report: 1990-2013, see http://www.epa.gov/climatechange/ghgemissions/usinventoryreport.html, 2015.

[17] U.S. Department of Transportation, Intelligent Transportation Systems Joint Program Office, National ITS Architecture, see http://www.iteris.com/itsarch/, accessed May 2015.

[18] M. Barth, K. Boriboonsomsin, "Real-World Carbon Dioxide Impacts of Traffic Congestion", Transportation Research Record: Journal of the Transportation Research Board, V. 2058, pp. 163-171.

[19] U.S. Department of Transportation, Federal Highway Administration Exploratory Advanced Research Program, see http://www.fhwa.dot.gov/advancedresearch, 2015.

[20] V. Milanes, S. E. Shladover, J. Spring, C. Nowakowski, H. Kawazoe, M. Nakamura, "Cooperative Adaptive Cruise Control in Real Traffic Situations", IEEE Transactions on Intelligent Transportation Systems, Vol. 15, No. 1, pp. 296-305.

[21] P. Hao, G. Wu, K. Boriboonsomsin, M. Barth, "Developing a Framework of Eco-Approach and Departure Application for Actuated Signal Control", IEEE Intelligent Vehicles Symposium, 2015 (accepted).

[22] U.S. Department of Transportation, University Transportation Centers Program, see http://www.rita.dot.gov/utc/home, 2015.

[23] National Center for Sustainable Transportation, see http://ncst.ucdavis.edu/, 2015.

[24] Mid-Atlantic Transportation Sustainability Center, see http://www.matsutc.org/, 2015.

[25] D. Kari, G. Wu, and M. Barth, "Eco-Friendly Freight Signal Priority Using Connected Vehicle Technology: A Multi-Agent Systems Approach", Proceedings of the 2014 IEEE Symposium on Intelligent Vehicles, Dearborn, Michigan, June, 2014.

[26] K. Ahn, H. Rakha, "Ecolane Applications", Transportation Research Record: Journal of the Transportation Research Board, V. 2427, No. 1, pp.41-53.

[27] U.S. Department of Transportation, Applications for the Environment: Real-Time Information Synthesis (AERIS) Research Program, see http://www.its.dot.gov/aeris/, 2015.

[28] Virginia Tech Transportation Institute, see http://www.its.dot.gov/aeris/pdf/EcoDriving.pdf, 2011.

[29] Calmar Telematics, see http://ntl.bts.gov/lib/46000/46100/46187/FINAL_PKG_FHWA-JPO-12-051.pdf, 2012.

[30] Virginia Tech Transportation Institute, see http://www.its.dot.gov/aeris/pdf/EcoDriving.pdf, 2011.

[31] University of California, Riverside, see http://ntl.bts.gov/lib/45000/45600/45636/FINAL_PKG_FHWA-JPO-12-042_V3.pdf, 2011.

[32] University of Buffalo, see http://www.civil.buffalo.edu/research/research-areas/area:transportation-systems-engineering/section:projects/project:an-evaluation-of-likely-environmental-benefits-of-lowest-fuel-consumption-route-guidance-in-the-buffalo-niagara-metropolitan-area/, 2014.

[33] H. Xia, K. Boriboonsomsin, M. Barth, "Dynamic Ecodriving for Signalized Arterial Corridors and Its Indirect Network-Wide Energy/Emissions Benefits", Journal of Intelligent Transportation System: Technology, Planning, and Operations, Vol 17, Issue 1.

[34] U.S. Department of Transportation, AERIS-Applications for the Environment: Real-Time Information Synthesis: Eco-Signal Operations Modeling Report, publication number FHWA-JPO-14-185, see http://ntl.bts.gov/lib/54000/54900/54930/Eco-Signal_Operations_Modeling_Report_-_Final_508_-_012615.pdf, 2014.

[35] U.S. Department of Transportation, AERIS-Applications for the Environment: Real-Time Information Synthesis: Eco-Lanes Operational Scenario Modeling Report, publication number FHWA-JPO-14-186, see http://ntl.bts.gov/lib/54000/54900/54929/Eco-Lanes_Modeling_Report_-_Final_508_-_012615.pdf, 2014.

[36] EU Working Group for Clean and Efficient Mobility, see http://www.imobilitysupport.eu/library/imobility-forum/working-groups/active/ict-for-clean-and-efficient-mobility/reports-4/2332-wg4cem-final-report-131308

[37] Cooperative mobility systems and services for energy efficiency, see http://www.ecomove-project.eu/, 2015.

[38] ECOSTAND: Joint EU - Japan - US task force on the development of a standard methodology for determining the impacts of ITS on energy efficiency and CO2 emissions, see http://www.ecostand-project.eu/, 2015.

[39] EU Compass4D research project, see http://www.compass4d.eu/, 2015.

[40] Co-operative Systems for Sustainable Mobility and Energy Efficiency, see http://www.cosmo-project.eu/, 2015.

[41] Co-operative Networked Concept for Emission Responsive Traffic Operations, see http://www.traffictechnologytoday.com/news.php?NewsID=27116, 2014.

[42] A Decision Support System for Reducing CO2 and Black Carbon Emissions by Adaptive Traffic Management, see http://carbotraf.eu/, 2014.

[43] Assessment Methodologies for ICT in multimodal transport from User Behaviour to CO2 reduction, see http://www.amitran.eu/, 2015.

[44] Cooperative Advanced Driver Assistance System for Green Cars, see http://www.transport-research.info/web/projects/project_details.cfm?id=44395, 2015.

[45] *Liden, Daniel.* "What Is a Driverless Car?". *WiseGeek*. Retrieved 11 October 2013.

[46] *Kelly, Heather (30 October 2012).* "Self-driving cars now legal in California". *CNN*. Retrieved 11 October 2013.

[47] *Thrun, Sebastian (2010).* "Toward Robotic Cars". *Communications of the ACM. 53 (4): 99–106.* doi:10.1145/1721654.1721679.

[48] *Gehrig, Stefan K.; Stein, Fridtjof J. (1999). Dead reckoning and cartography using stereo vision for an autonomous car. IEEE/RSJ International Conference on Intelligent Robots and Systems. Kyongju. pp. 1507–1512.* doi:10.1109/IROS.1999.811692. ISBN 0-7803-5184-3.

[49] *Lassa, Todd (January 2013).* "The Beginning of the End of Driving". Motor Trend. Retrieved 1 September 2014.

[50] European Roadmap Smart Systems for Automated Driving, European Technology Platform on Smart Systems Integration (EPoSS), 2015.

[51] Zhu, Wentao; Miao, Jun; Hu, Jiangbi; Qing, Laiyun (2014-03-27). "Vehicle detection in driving simulation using extreme learning machine". Neurocomputing. 128: 160–165. doi:10.1016/j.neucom.2013.05.052.

[52] Antsaklis, Panos J.; Passino, Kevin M.; Wang, S.J. (1991). "An Introduction to Autonomous Control Systems" (PDF). IEEE Control Systems. 11 (4): 5–13. doi:10.1109/37.88585.

[53] Wood, S. P.; Chang, J.; Healy, T.; Wood, J. "The potential regulatory challenges of increasingly autonomous motor vehicles.". 52nd Santa Clara Law Review. 4 (9): 1423–1502.

[54] "AdaptIVe system classification and glossary on Automated driving" (PDF).

[55] NHTSA, 2013, http://www.nhtsa.gov/About-NHTSA/Press-Releases/U.S.-Department-of-Transportation-Releases-Policy-on-Automated-Vehicle-Development

[56] David B. Sandalow, ed. (2009). Plug-In Electric Vehicles: What Role for Washington? (1st. ed.). The Brookings Institution. pp. 2–5. ISBN 978-0-8157-0305-1. See definition on pp. 2.

[57] "Plug-in Electric Vehicles (PEVs)". Center for Sustainable Energy, California. Retrieved 2010-03-31.

[58] "Electric Vehicles: Turning Buzz into Reality". European Automobile Manufacturers Association. 2010-02-09. Retrieved 2010-04-23.

[59] Xu, G., Li, W., Xu, K., Song, Z., 2011. An intelligent regenerative braking strategy for electric vehicles. Energies 4, 1461–1477.

[60] Knowles, M., Scott, H., Baglee, D., 2012. The effect of driving style on electric vehicle performance, economy and perception. Int. J. Electric Hybrid Veh. 4 (3),228–247.

[61] Gao, Y.M., Chen, L.P., Ehsani, M., 1999. Investigation of the effectiveness of regenerative braking for EV and HEV. SAE Trans. 108, 3184–3190.
[62] Wardrop, J.G., 1952. Some theoretical aspects of road traffic research. Proc. Inst. Civil Eng. II (1), 325–378.
[63] Sheffi, Y., 1984. Urban Transportation Networks: Equilibrium Analysis with Mathematical Programming Methods. Prentice-Hall Inc, Englewood Cliffs, NJ.
[64] Ericsson, E., Larsson, H., Brundell-Freij, K., 2006. Optimizing route choice for lowest fuel consumption – potential effects of a new driver support tool. Transport. Res. C Emer. Technol. 14 (6), 369–383.

[65] M. Barth, S. Mandava, K. Boriboonsomsin and H. Xia, "Dynamic Ecodriving for arterial corridors," *Integrated and Sustainable Transportation System (FISTS), 2011 IEEE Forum on*, Vienna, 2011, pp. 182-188.

[66] H. Xia *et al*., "Field operational testing of ECO-approach technology at a fixed-time signalized intersection," *2012 15th International IEEE Conference on Intelligent Transportation Systems*, Anchorage, AK, 2012, pp. 188-193.

[67] R. Zhang and E. Yao, "Ecodriving at signalised intersections for electric vehicles," in *IET Intelligent Transport Systems*, vol. 9, no. 5, pp. 488-497, 6 2015.

[68] Xinkai Wu, David Freese, Alfredo Cabrera, William A. Kitch, Electric vehicles' energy consumption measurement and estimation, Transportation Research Part D: Transport and Environment, Volume 34, January 2015, Pages 52-67,

[69] A. Diaz Alvarez, F. Serradilla Garcia, J. E. Naranjo, J. J. Anaya and F. Jimenez, "Modeling the Driving Behavior of Electric Vehicles Using Smartphones and Neural Networks," in *IEEE Intelligent Transportation Systems Magazine*, vol. 6, no. 3, pp. 44-53, Fall 2014.

[70] Estimating energy consumption based on microscopic driving parameters for electric vehicle. Transportation Research Record Journal of the Transportation Research Board 2454(-1):84-91 · November 2014

[71] Microscopic Driving Parameters-Based Energy-Saving Effect Analysis under Different Electric Vehicle Penetration, Advances in Mechanical Engineering 2013:1-8 · December 2012

[72] R. Abousleiman and O. Rawashdeh, "A Bellman-Ford approach to energy efficient routing of electric vehicles," *Transportation Electrification Conference and Expo (ITEC), 2015 IEEE*, Dearborn, MI, 2015, pp. 1-4.

[73] Zonggen Yi, Peter H. Bauer. "Sensitivity Analysis of Environmental Factors for Electric Vehicles Energy Consumption." Vehicle Power and Propulsion Conference (VPPC). IEEE, 2015.

[74] J. Felipe, J. C. Amarillo, J. E. Naranjo, F. Serradilla and A. Díaz, "Energy Consumption Estimation in Electric Vehicles Considering Driving Style," *2015 IEEE 18th International Conference on Intelligent Transportation Systems*, Las Palmas, 2015, pp. 101-106.

[75] Energy Consumption Prediction for Electric Vehicles Based on Real-World Data. Energies 8(8):8573-8593 · August 2015

[76] Rui Zhang, Enjian Yao, Electric vehicles' energy consumption estimation with real driving condition data, Transportation Research Part D: Transport and Environment, Volume 41, December 2015, Pages 177-187.

[77] F. Flehmig, A. Sardari, U. Fischer and A. Wagner, "Energy optimal Adaptive Cruise Control during following of other vehicles," *2015 IEEE Intelligent Vehicles Symposium (IV)*, Seoul, 2015, pp. 724-729

[78] R. Frank, G. Castignani, R. Schmitz and T. Engel, "A novel Ecodriving application to reduce energy consumption of electric vehicles," 2013 International Conference on Connected Vehicles and Expo (ICCVE), Las Vegas, NV, 2013, pp. 283-288.

[79] S. Koehler, A. Viehl, O. Bringmann and W. Rosenstiel, "Improved energy efficiency and vehicle dynamics for battery electric vehicles through torque vectoring control," *2015 IEEE Intelligent Vehicles Symposium (IV)*, Seoul, 2015, pp. 749-754.

[80] M. Miyatake, M. Kuriyama and Y. Takeda, "Theoretical study on Ecodriving technique for an Electric Vehicle considering traffic signals," *Power Electronics and Drive Systems (PEDS), 2011 IEEE Ninth International Conference on*, Singapore, 2011, pp. 733-738.

[81] R. Zhang and E. Yao, "Ecodriving at signalised intersections for electric vehicles," in *IET Intelligent Transport Systems*, vol. 9, no. 5, pp. 488-497, 6 2015.

[82] M. S. Kamal, M. Mukai, J. Murata, and T. Kawabe, "Model predictive control of vehicles on urban roads for improved fuel economy," IEEE Transactions on Control Systems Technology, vol. 21, no. 3, pp. 831–841, 2013.

[83] R. Zhang and E. Yao, "Ecodriving at signalized intersections for electric vehicles," in IET Intelligent Transport Systems, vol. 9, no. 5, pp. 488-497, 6 2015.

[84] Rui Zhang, Enjian Yao, Electric vehicles' energy consumption estimation with real driving condition data, Transportation Research Part D: Transport and Environment, Volume 41, December 2015, Pages 177-187, ISSN 1361-9209,

[85] R. Abousleiman and O. Rawashdeh, "A Bellman-Ford approach to energy efficient routing of electric vehicles," Transportation Electrification Conference and Expo (ITEC), 2015 IEEE, Dearborn, MI, 2015, pp. 1-4.

[86] Zonggen Yi, Peter H. Bauer. "Sensitivity Analysis of Environmental Factors for Electric Vehicles Energy Consumption." Vehicle Power and Propulsion Conference (VPPC). IEEE, 2015.

[87] Xinkai Wu, David Freese, Alfredo Cabrera, William A. Kitch, Electric vehicles' energy consumption measurement and estimation, Transportation Research Part D: Transport and Environment, Volume 34, January 2015, Pages 52-67,

[88] J. Felipe, J. C. Amarillo, J. E. Naranjo, F. Serradilla and A. Díaz, "Energy Consumption Estimation in Electric Vehicles Considering Driving Style," 2015 IEEE 18th International Conference on Intelligent Transportation Systems, Las Palmas, 2015, pp. 101-106.

[89] Energy Consumption Prediction for Electric Vehicles Based on Real-World Data. Energies 8(8):8573-8593 · August 2015

[90] A. Diaz Alvarez, F. Serradilla Garcia, J. E. Naranjo, J. J. Anaya and F. Jimenez, "Modeling the Driving Behavior of Electric Vehicles Using Smartphones and Neural Networks," in IEEE Intelligent Transportation Systems Magazine, vol. 6, no. 3, pp. 44-53, Fall 2014.

[91] N. Chang, and J. Hong, "Power consumption characterization, modeling and estimation of electric vehicles," 2014 IEEE/ACM International Conference on Computer-Aided Design (ICCAD), San Jose, CA, 2014, pp. 175-182.
[92] X. Zhou, J. Huang, W. Lv and D. Li, "Fuel Consumption Estimates Based on Driving Pattern Recognition," Green Computing and Communications (GreenCom), 2013 IEEE and Internet of Things (iThings/CPSCom), IEEE International Conference on and IEEE Cyber, Physical and Social Computing, Beijing, 2013, pp. 496-503.
[93] Fouad Baouche, Rochdi Trigui, Nour Eddin El Faouzi, Romain Billot. "Energy Consumption Assessment For Electric Vehicles". International symposium on recent advances in transport modeling, Apr 2013, Australie. 5 p., 2013.
[94] Enjian Yao, Meijing Yang, "Estimating energy consumption based on microscopic driving parameters for electric vehicle." Transportation Research Record Journal of the Transportation Research Board 2454(-1):84-91 · November 2014
[95] Enjian Yao, Zhifeng Lang, "Microscopic Driving Parameters-Based Energy-Saving Effect Analysis under Different Electric Vehicle Penetration," Advances in Mechanical Engineering 2013:1-8 · December 2012
[96] Yao, E.; Yang, Z.; Song, Y.; Zuo, T. Comparison of electric vehicle's energy consumption factors for different road types. Discret. Dyn. Nat. Soc. 2013, 2013, 328757:1–328757:7.
[97] R. Shankar and J. Marco, "Method for estimating the energy consumption of electric vehicles and plug-in hybrid electric vehicles under real-world driving conditions," in IET Intelligent Transport Systems, vol. 7, no. 1, pp. 138-150, March 2013
[98] Billings, S.A. (2013) "Nonlinear System Identification: NARMAX Methods in the Time, Frequency, and Spatio-Temporal Domains". Wiley
[99] K. Holmberg, P. Andersson and L. Erdemir (2012) "Global energy consumption due to friction in passenger cars", Tribology International 47, pp. 221 – 234
[100] Watson, H. C. et al. (1982). "Development of the Melbourne Peak Cycle." Paper #82148, SAE of Australia
[101] Barth, M. and K. Boriboonsomsin (2008). "Real-World CO2 Impacts of Traffic Congestion", Transportation Research Record No. 2058, pp 163-171, Transportation Research Board, National Academy of Science.
[102] Armstrong, J. S. (1985). "Long-range Forecasting: From Crystal Ball to Computer." 2nd. ed. Wiley.
[103] Hemmerle, Peter, Hermanns, Gerhard, "Macroscopic Consumption Matrix for On-line Energy-efficient Route Guidance , Proceedings of Transportation Research Record 2014. Washington D.C.
[104] S. Grubwinkler, T. Brunner and M. Lienkamp, "Range Prediction for EVs via Crowd-Sourcing," 2014 IEEE Vehicle Power and Propulsion Conference (VPPC), Coimbra, 2014, pp. 1-6.
[105] Quinlan, J. (1992). Learning with continuous classes. Proceedings of the 5th Australian Joint Conference On Artificial Intelligence, 343–348.
[106] Quinlan, J. (1993). Combining instance-based and model-based learning. Proceedings of the Tenth International Conference on Machine Learning, 236–243.
[107] (CART)Breiman, Leo; Friedman, J. H.; Olshen, R. A.; Stone, C. J. (1984). Classification and regression trees. Monterey, CA: Wadsworth & Brooks/Cole Advanced Books & Software. ISBN 978-0-412-04841-8.
[108] M. Barth, S. Mandava, K. Boriboonsomsin and H. Xia, "Dynamic Ecodriving for arterial corridors," Integrated and Sustainable Transportation System (FISTS), 2011 IEEE Forum on, Vienna, 2011, pp. 182-188.

[109] M. S. Kamal, M. Mukai, J. Murata, and T. Kawabe, “Model predictive control of vehicles on urban roads for improved fuel economy,” IEEE Transactions on Control Systems Technology, vol. 21, no. 3, pp. 831–841, 2013.

[110] R. Zhang and E. Yao, "Ecodriving at signalised intersections for electric vehicles," in IET Intelligent Transport Systems, vol. 9, no. 5, pp. 488-497, 6 2015.

[111] X. Qi; G. Wu; K, Boriboonsomsin; M.J. Barth, "An on-line energy management strategy for plug-in hybrid electric vehicles using an Estimation Distribution Algorithm," Intelligent Transportation Systems (ITSC), 2014 IEEE 17th International Conference on , vol., no., pp.2480,2485, 8-11 Oct. 2014.

[112] X. Qi, Guoyuan Wu, Kanok Boriboonsomsin, Matthew J. Barth, Jeffrey Gonder. Data-Driven Reinforcement Learning–Based Real-Time Energy Management System for Plug-In Hybrid Electric Vehicles. Transportation Research Record: Journal of the Transportation Research Board, 2016; 2572: 1 DOI: 10.3141/2572-01

[113] X. Qi, G. Wu, K. Boriboonsomsin and M. J. Barth, "A Novel Blended Real-Time Energy Management Strategy for Plug-in Hybrid Electric Vehicle Commute Trips," 2015 IEEE 18th International Conference on Intelligent Transportation Systems, Las Palmas, 2015, pp. 1002-1007.

[114] D. Schrank, B. Eisele, T. Lomax and J. Bak.2015 Urban Mobility scorecard.http://d2dtl5nnlpfr0r.cloudfront.net/tti.tamu.edu/documents/mobility-scorecard-2015.pdf

[115] Qiu Jin, K. Boriboonsomsin and M. J. Barth, “Energy and Emissions Benefits of a Real-Time Driving Speed Advisory System for Heavy-Duty Trucks”, Proceedings of Annual Meeting of Transportation Research Board, 2016, Washington D.C.

[116] M. Faraj and O. Basir, "Range anxiety reduction in battery-powered vehicles," 2016 IEEE Transportation Electrification Conference and Expo (ITEC), Dearborn, MI, 2016, pp. 1-6

[117] Axsen, J., Kurani, K.S., Burke, A., 2010. Are batteries ready for plug-in hybrid buyers? Transport Policy 17, 173–182.

[118] Morrowa, K., Karnerb, D., Francfortc, J., 2008. U.S. Department of Energy Vehicle Technologies Program – Advanced Vehicle Testing Activity Plug-in Hybrid Electric Vehicle: Charging Infrastructure Review, Final Report: INL/EXT-08-15058, Battelle Energy Alliance, Contract No. 58517

[119] European Commission (EC), “eCoMove – Cooperative Mobility Systems and Services for Energy Efficiency,” http://www.ecomove-project.eu/.

[120] European Union (EU), “Compass4D – One Step Closer to C-ITS Deployment in Cities,” http://www.compass4d.eu/.

[121] U.S. Department of Transportation (USDOT), “Applications for the Environment: Real-Time Information Synthesis (AERIS),” http://www.its.dot.gov/aeris/.

[122] U.S. Department of Transportation (USDOT), "AERIS Concept of Operations and Modeling Workshop," Washington D. C., March 26 – 27, 2013

[123] B. Asadi, and A. Vahidi. "Predictive Cruise Control: Utilizing Upcoming Traffic Signal Information for Improving Fuel Economy and Reducing Trip Time", IEEE Transactions on Control Systems Technology, 19(3):707–714, 2011

[124] G. De Nunzio, C. Canudas De Wit, P. Moulin, and D. Di Domenico, "Ecodriving in Urban Traffic Networks using Traffic Signal Information," The 52nd IEEE Conference on Decision and Control, Florence, Italy, Dec. 2013.

[125] M. Seredynski, B. Dorronsoro, and D. Khadraoui, "Comparison of Green Light Optimal Speed Advisory (GLOSA) Approaches," The 16th IEEE Conference on Intelligent Transportation Systems (ITSC), 2013, pp. 2187–2192

[126] R. Kamalanathsharma, and H. Rakha, "Agent-Based Simulation of Eco-Speed Controlled Vehicles at Signalized Intersections," Transportation Research Record, No. 2427, 2014, pp. 1 – 12

[127] Z. Chen, Y. Zhang, J. Lv, and Y. Zou, "Model for Optimization of Ecodriving at Signalized Intersections," Transportation Research Record, No. 2427, 2014, pp. 54 – 62

[128] Hao, P., Wu, G., Boriboonsomsin, K., & Barth, M. (2015). Developing a framework of eco-approach and departure application for actuated signal control. Proceedings of 2015 IEEE Intelligent Vehicles Symposium (IV), 796-801.

[129] Hao, P., Wu, G., Boriboonsomsin, K., & Barth, M. (2016). Eco-Approach and Departure application for actuated signals in real-world traffic. Accepted by the 96th Annual Meeting of Transportation Research Board, Washington, DC.

[130] X. Xiang, K. Zhou, W. B. Zhang, W. Qin and Q. Mao, "A Closed-Loop Speed Advisory Model With Driver's Behavior Adaptability for Ecodriving," in IEEE Transactions on Intelligent Transportation Systems, vol. 16, no. 6, pp. 3313-3324, Dec. 2015.

[131] M. Miyatake, M. Kuriyama and Y. Takeda, "Theoretical study on Ecodriving technique for an Electric Vehicle considering traffic signals," Power Electronics and Drive Systems (PEDS), 2011 IEEE Ninth International Conference on, Singapore, 2011, pp. 733-738.

[132] R. Zhang and E. Yao, "Ecodriving at signalised intersections for electric vehicles," in IET Intelligent Transport Systems, vol. 9, no. 5, pp. 488-497, 6 2015.

[133] H. Xia, K. Boriboonsomsin, M. Barth, "Dynamic Ecodriving for Signalized Arterial Corridors and Its Indirect Network-Wide Energy/Emissions Benefits", Journal of Intelligent Transportation Systems: Technology, Planning, and Operations, 17(1), 2013, pp. 31 – 41

[134] M. S. Kamal, M. Mukai, J. Murata, and T. Kawabe, "Model predictive control of vehicles on urban roads for improved fuel economy," IEEE Transactions on Control Systems Technology, vol. 21, no. 3, pp. 831–841, 2013.

[135] Richard H. Byrd, Mary E. Hribar, and Jorge Nocedal, "An Interior Point Algorithm for Large-Scale Nonlinear Programming," SIAM Journal on Optimization, vol. 9, no. 4, pp. 877-900, 1999.

[136] U. S. Department of Transportation. Accessed on January 5th, 2015. http://www.its.dot.gov/research/vehicle_electrification_smartgrid.htm

[137] G. Wu, K. Boriboonsomsin, M. Barth. “Development and Evaluation of an Intelligent Energy-Management Strategy for Plug-in Hybrid Electric Vehicles”. IEEE Transactions on Intelligent Transportation Systems, Vol.15, No.3, June 2014, pp. 1091 – 1100

[138] S. G. Wirasingha and A. Emadi. “Classification and Review of Control Strategies for Plug-In Hybrid Electric Vehicles”. IEEE Transactions on Vehicular Technology, Vol.60, No.1, January 2011, pp. 111 – 122

[139] A. Panday and H. O. Bansal. “A Review of Optimal Energy Management Strategies for Hybrid Electric Vehicle”. International Journal of Vehicular Technology, 2014, p. 19

[140] H. Banvait, S. Sohel and Y. Chen. “A Rule-Based Energy Management Strategy for Plug-In Hybrid Electric Vehicle (PHEV)”. Proceedings of American Control Conference, St. Louis, MO, June 2009, pp. 3938 – 3943,2009.

[141] Q. Gong and Y. Li. “Trip Based Optimal Power Management of Plug-In Hybrid Electric Vehicles Using Gas-Kinetic Traffic Flow Model”. Proceedings of American Control Conference, Seattle, WA, June 2008, pp. 3225 – 3230,2008.

[142] L. Tribiloli, M Barbielri, R. Capata, E.Sciubba,E.Jannelli and G.Bella. “A real time energy management strategy for plug-in hybrid electric vehicles based on optimal control theory”, Energy Procedia 45(2014) 949-958.

[143] Cong Hou, Liangfei Xu, Hewu Wang, Minggao Ouyang, Huei Peng, Energy management of plug-in hybrid electric vehicles with unknown trip length, Journal of the Franklin Institute, Volume 352, Issue 2, February 2015, Pages 500-518,

[144] Mahyar Vajedi; Maryyeh Chehrehsaz; Nasser L. Azad, Intelligent power management of plug-in hybrid electric vehicles, part I: real-time optimum SOC trajectory builder Int. J. of Electric and Hybrid Vehicles, 2014 Vol.6, No.1, pp.46 – 67.

[145] Denis, N.; Dubois, M.R.; Desrochers, A., "Fuzzy-based blended control for the energy management of a parallel plug-in hybrid electric vehicle," Intelligent Transport Systems, IET , vol.9, no.1, pp.30,37, 2 2015.

[146] Wang X., He, H. Sun, F., Sun, X., Tang,H., “Comparative Study on Different Energy Management Strategies for Plug-In Hybrid Electric Vehicles” Energies, 6, 5656-5675,2013.

[147] Wu Jian, "Fuzzy energy management strategy for plug-in hev based on driving cycle modeling," Control Conference (CCC), 2014 33rd Chinese , vol., no., pp.4472,4476, 28-30 July 2014

[148] Tribioli, L.; Onori, S., "Analysis of energy management strategies in plug-in hybrid electric vehicles: Application to the GM Chevrolet Volt," American Control Conference (ACC), 2013 , vol., no., pp.5966,5971, 17-19 June 2013

[149] Hai Yu; Ming Kuang; McGee, R., "Trip-Oriented Energy Management Control Strategy for Plug-In Hybrid Electric Vehicles," Control Systems Technology, IEEE Transactions on , vol.22, no.4, pp.1323,1336, July 2014

[150] Qiuming Gong; Yaoyu Li; Zhong-Ren Peng, "Trip based optimal power management of plug-in hybrid electric vehicles using gas-kinetic traffic flow model," American Control Conference, 2008 , vol., no., pp.3225,3230, 11-13 June 2008

[151] Feng, T.; Yang, L.; Gu, Q.; Hu, Y.; Yan, T.; Yan, B., "A supervisory control strategy for plug-in hybrid electric vehicles based on energy demand prediction and route preview," Vehicular Technology, IEEE Transactions on , vol.PP, no.99, pp.1,1, Januay, 2015

[152] Larsson, V.; Johannesson Mårdh, L.; Egardt, B.; Karlsson, S., "Commuter Route Optimized Energy Management of Hybrid Electric Vehicles," Intelligent Transportation Systems, IEEE Transactions on , vol.15, no.3, pp.1145,1154, June 2014

[153] Liu, Chang; Murphey, Yi Lu, "Power management for Plug-in Hybrid Electric Vehicles using Reinforcement Learning with trip information," Transportation Electrification Conference and Expo (ITEC), 2014 IEEE , vol., no., pp.1,6, 15-18 June 2014

[154] C. Sun, S. J. Moura, X. Hu, J. K. Hedrick and F. Sun, "Dynamic Traffic Feedback Data Enabled Energy Management in Plug-in Hybrid Electric Vehicles," in IEEE Transactions on Control Systems Technology, vol. 23, no. 3, pp. 1075-1086, May 2015.

[155] M. P. O'Keefe and T. Markel, "Dynamic programming applied to investigate energy management strategies for a plug-in HEV," National Renewable Energy Laboratory, Golden, CO, Report No. NREL/CP-540-40376, 2006.

[156] Zheng Chen, Chris Chunting Mi, Rui Xiong, Jun Xu, Chenwen You, Energy management of a power-split plug-in hybrid electric vehicle based on genetic algorithm and quadratic programming, Journal of Power Sources, Volume 248, 15 February 2014, Pages 416-426.

[157] Xiao Lin; Banvait, H.; Anwar, S.; Yaobin Chen, "Optimal energy management for a plug-in hybrid electric vehicle: Real-time controller," American Control Conference (ACC), 2010 , vol., no., pp.5037,5042, June 30 2010-July 2 2010

[158] Qiuming Gong; Yaoyu Li; Zhong-Ren Peng, "Trip based optimal power management of plug-in hybrid electric vehicles using gas-kinetic traffic flow model," American Control Conference, 2008 , vol., no., pp.3225,3230, 11-13 June 2008

[159] Cong Hou, Liangfei Xu, Hewu Wang, Minggao Ouyang, Huei Peng, Energy management of plug-in hybrid electric vehicles with unknown trip length, Journal of the Franklin Institute, Volume 352, Issue 2, February 2015, Pages 500-518,

[160] Mahyar Vajedi; Maryyeh Chehrehsaz; Nasser L. Azad, Intelligent power management of plug-in hybrid electric vehicles, part I: real-time optimum SOC trajectory builder Int. J. of Electric and Hybrid Vehicles, 2014 Vol.6, No.1, pp.46 – 67.

[161] M. Vajedi, A. Taghavipour, N. L. Azad and J. McPhee, "A comparative analysis of route-based power management strategies for real-time application in plug-in hybrid

electric vehicles," American Control Conference (ACC), 2014, Portland, OR, 2014, pp. 2612-2617.

[162] Zeyu Chen, Weiguo Liu, Ying Yang, and Weiqiang Chen, "Online Energy Management of Plug-In Hybrid Electric Vehicles for Prolongation of All-Electric Range Based on Dynamic Programming," Mathematical Problems in Engineering, vol. 2015, Article ID 368769, 11 pages, 2015.

[163] S. J. Moura, H. K. Fathy, D. S. Callaway and J. L. Stein, "A Stochastic Optimal Control Approach for Power Management in Plug-In Hybrid Electric Vehicles," in IEEE Transactions on Control Systems Technology, vol. 19, no. 3, pp. 545-555, May 2011.

[164] Xuewei Qi, Guoyuan Wu, Kanok Boriboonsomsin, Matthew J. Barth, Jeffrey Gonder. Data-Driven Reinforcement Learning–Based Real-Time Energy Management System for Plug-In Hybrid Electric Vehicles. Transportation Research Record: Journal of the Transportation Research Board, 2016; 2572: 1 DOI: 10.3141/2572-01

[165] Guoyuan Wu, UCTC working paper http://www.uctc.net/research/papers/UCTC-FR-2012-09.pdf 2015

[166] Kolmanovsky, I., M. Nieuwstadt, and J. Sun. Optimization of Complex Powertrain Systems for Fuel Economy and Emissions. Proceedings of IEEE International Conference on Control Applications, Hawaii, 1999

[167] Argonne National Laboratory. AUTONOMIE, http://www.autonomie.net/. Accessed on February 16th, 2012.

[168] MathWorks. MATLAB R2010b, 2011.

[169] A.E. Eiben, Introduction to Evolutionary Computing, Springer, 2007.

[170] Pietro S. Oliveto04, Jun He, Xin Yao, Time Complexity of Evolutionary Algorithms for Combinatorial Optimization: A Decade of Results (3), International Journey of Automation and Computation, 281-293, July 2007

[171] D. Kum "Modeling and Optimal Control of Parallel HEVs and Plug-in HEVs for Multiple Objectives". Ph.D. dissertation. University of Michigan, 2010.

[172] X. Qi; G. Wu; K, Boriboonsomsin; M.J. Barth, "An on-line energy management strategy for plug-in hybrid electric vehicles using an Estimation Distribution Algorithm," Intelligent Transportation Systems (ITSC), 2014 IEEE 17th International Conference on , vol., no., pp.2480,2485, 8-11 Oct. 2014.

[173] M. Vajedi, A. Taghavipour, N. L. Azad and J. McPhee, "A comparative analysis of route-based power management strategies for real-time application in plug-in hybrid electric vehicles," American Control Conference (ACC), 2014, Portland, OR, 2014, pp. 2612-2617.

[174] Zeyu Chen, Weiguo Liu, Ying Yang, and Weiqiang Chen, "Online Energy Management of Plug-In Hybrid Electric Vehicles for Prolongation of All-Electric Range Based on Dynamic Programming," Mathematical Problems in Engineering, vol. 2015, Article ID 368769, 11 pages, 2015.

[175] S. J. Moura, H. K. Fathy, D. S. Callaway and J. L. Stein, "A Stochastic Optimal Control Approach for Power Management in Plug-In Hybrid Electric Vehicles," in IEEE Transactions on Control Systems Technology, vol. 19, no. 3, pp. 545-555, May 2011.

[176] Henry A. Bonges III, Anne C. Lusk, Addressing electric vehicle (EV) sales and range anxiety through parking layout, policy and regulation, Transportation Research Part A: Policy and Practice, Volume 83, January 2016, Pages 63-73, ISSN 0965-8564, http://dx.doi.org/10.1016/j.tra.2015.09.011.

[177] X. Qi, G. Wu, K. Boriboonsomsin and M. J. Barth, "A Novel Blended Real-Time Energy Management Strategy for Plug-in Hybrid Electric Vehicle Commute Trips," 2015 IEEE 18th International Conference on Intelligent Transportation Systems, Las Palmas, 2015, pp. 1002-1007.

[178] Xuewei Qi; Guoyuan Wu; Boriboonsomsin, K.; Barth, M.J.; Jeffery Gonder, "Data-Driven Reinforcement Learning-Based Real-Time Energy Management System for Plug-in Hybrid Electric Vehicles" Transportation Research Record (Journal of Transportation Research Board),vol,2572,pp. 1-8,2016. DOI: 10.3141/2572-01

[179] S. G. Wirasingha and A. Emadi. "Classification and Review of Control Strategies for Plug-In Hybrid Electric Vehicles". IEEE Transactions on Vehicular Technology, Vol.60, No.1, January 2011, pp. 111 – 122

[180] A. Panday and H. O. Bansal. "A Review of Optimal Energy Management Strategies for Hybrid Electric Vehicle". International Journal of Vehicular Technology, 2014, p. 19.

[181] D. Schrank, B. Eisele, T. Lomax and J. Bak.2015 Urban Mobility scorecard. http://d2dtl5nnlpfr0r.cloudfront.net/tti.tamu.edu/documents/mobility-scorecard-2015.pdf

[182] M. Barth, S. Mandava, K. Boriboonsomsin and H. Xia, "Dynamic Ecodriving for arterial corridors," Integrated and Sustainable Transportation System (FISTS), 2011 IEEE Forum on, Vienna, 2011, pp. 182-188.

[183] L. Tribiloli, M Barbielri, R. Capata, E.Sciubba,E.Jannelli and G.Bella. A real time energy management strategy for plug-in hybrid electric vehicles based on optimal control theory,Energy Procedia 45(2014) 949-958.

[184] Denis, N.; Dubois, M.R.; Desrochers, A., Fuzzy-based blended control for the energy management of a parallel plug-in hybrid electric vehicle, Intelligent Transport Systems, IET , vol.9, no.1, pp.30,37, 2 2015

[185] Wang X., He, H. Sun, F., Sun, X., Tang,H., Comparative Study on Different Energy Management Strategies for Plug-In Hybrid Electric Vehicles, Energies 2013, 6, 5656-5675

[186] Wu J., Fuzzy energy management strategy for plug-in hev based on driving cycle modeling, Control Conference (CCC), 2014 33rd Chinese , vol., no., pp.4472,4476, 28-30 July 2014

[187] X. Qi, G. Wu, K. Boriboonsomsin and M. J. Barth, "Evolutionary algorithm based on-line PHEV energy management system with self-adaptive SOC control," 2015 IEEE Intelligent Vehicles Symposium (IV), Seoul, 2015, pp. 425-430. doi: 10.1109/IVS.2015.7225722

[188] Feng, T.; Yang, L.; Gu, Q.; Hu, Y.; Yan, T.; Yan, B., A supervisory control strategy for PHEVs based on energy demand prediction and route preview, Vehicular Technology, IEEE Transactions on , vol.PP, no.99, pp.1,1

[189] Wu, K. Boriboonsomsin and M. J. Barth, "Development and Evaluation of an Intelligent Energy-Management Strategy for Plug-in Hybrid Electric Vehicles," in IEEE Transactions on Intelligent Transportation Systems, vol. 15, no. 3, pp. 1091-1100, June 2014.

[190] Xuewei Qi; Guoyuan Wu; Boriboonsomsin, K.; Barth, M.J., An on-line energy management strategy for plug-in hybrid electric vehicles using an Estimation Distribution Algorithm, Intelligent Transportation Systems (ITSC), 2014 IEEE 17th International Conference on , vol., no., pp.2480,2485, 8-11 Oct. 2014

[191] M. P. O'Keefe and T. Markel, Dynamic programming applied to investigate energy management strategies for a plug-in HEV, National Renewable Energy Laboratory, Golden, CO, Report No. NREL/CP-540-40376, 2006.

[192] Cong Hou, Liangfei Xu, Hewu Wang, Minggao Ouyang, Huei Peng, Energy management of plug-in hybrid electric vehicles with unknown trip length, Journal of the Franklin Institute, Volume 352, Issue 2, February 2015, Pages 500-518,

[193] U.S. Department of Transportation, "Applications for the Environment: Real-Time Information Synthesis (AERIS)", http://www.its.dot.gov/aeris/. June 2016.

[194] The Compass4D project. http://www.compass4d.eu/. June 2016.

[195] European Commission (EC), "eCoMove – Cooperative Mobility Systems and Services for Energy Efficiency", http://www.ecomove-project.eu/. June 2016.

[196] M. Li, K. Boriboonsomsin, G. Wu, W. Zhang, and M. J. Barth, "Traffic Energy and Emission Reductions at Signalized Intersections: A Study of the Benefits of Advanced Driver Information", International Journal of ITS Research, June 2009.

[197] B. Asadi, and A. Vahidi, "Predictive Use of Traffic Signal State for Fuel Saving". 12th IFAC Symposium on Transportation Systems Redondo Beach, CA, USA, September, 2009.

[198] B. Asadi, and A. Vahidi, "Predictive Cruise Control: Utilizing Upcoming Traffic Signal Information for Improving Fuel Economy and Reducing Trip Time". IEEE Transactions on Control System Technology, 2010.

[199] H. Rakha, R. K. Kamalanathsharma, "Ecodriving at Signalized Intersections Using V2I Communication". The 14th IEEE Conference on Intelligent Transportation Systems (ITSC), Washington, D.C., USA. October 5 – 7, 2011

[200] G. De Nunzio, C. C. de Wit, P. Moulin, D. Di Domenico, "Ecodriving in Urban Traffic Networks using Traffic Signal Information". The 52nd IEEE Conference on Decision

[201] H. Xia, K. Boriboonsomsin, M. Barth, "Dynamic Ecodriving for Signalized Arterial Corridors and Its Indirect Network-Wide Energy/Emissions Benefits", Journal of

Intelligent Transportation Systems: Technology, Planning, and Operations, 17(1), 2013, pp. 31 – 41

[202] H. Xia, K. Boriboonsomsin, F. Schweizer, A. Winckler, K. Zhou, WB. Zhang, M. Barth, "Field Operational Testing of ECO-Approach Technology at a Fixed-Time Signalized Intersection", Proceedings of the IEEE 2012 Intelligent Transportation Systems Conference, Anchorage, AK, September 2012, 6 pp.

[203] P. Hao, G. Wu, K. Boriboonsomsin, M. Barth. "Developing a Framework of Eco-Approach and Departure Application for Actuated Signal Control". IEEE on Intelligent Vehicles Symposium, Seoul, Korea. June, 2015

[204] P. Hao, G. Wu, K. Boriboonsomsin, M. Barth. "Preliminary Evaluation of Field Testing on Eco-Approach and Departure (EAD) Application for Actuated Signals", ICCVE 2015, Shenzhen, China. Oct. 2015.

[205] X. He, H. Liu, X. Liu, "Optimal vehicle speed trajectory on a signalized arterial with consideration of queue", Transp. Res. C, Emerging Technol., vol. 61, pp. 106-120, Dec. 2015.

[206] H. Xia, G. Wu, K. Boriboonsomsin, M. Barth, "Development and Evaluation of an Enhanced Eco-Approach Traffic Signal Application for Connected Vehicles", The 16th IEEE Conference on Intelligent Transportation Systems (ITSC), The Hague, Netherlands, October 6 – 9, 2013

[207] Q. Jin; G. Wu; K. Boriboonsomsin; M. J. Barth, "Power-Based Optimal Longitudinal Control for a Connected Ecodriving System," in IEEE Transactions on Intelligent Transportation Systems , vol.PP, no.99, pp.1-11. doi: 10.1109/TITS.2016.2535439

[208] J. Hu, Y. Shao, Z. Sun, M. Wang, Joe Bared, Peter Huang, Integrated optimal Ecodriving on rolling terrain for hybrid electric vehicle with vehicle-infrastructure communication, Transportation Research Part C: Emerging Technologies, Volume 68, July 2016, Pages 228-244,

[209] Wu, G., Barth, M., Boriboonsomsin, K., and Altan, O. (2015). "GlidePath: Eco-Friendly Automated Approach and Departure at Signalized Intersections." Automated Vehicle Symposium 2015